

# IMPROVING MUTUAL INFORMATION ESTIMATION WITH ANNEALED AND ENERGY-BASED BOUNDS

Rob Brekelmans<sup>\*,1</sup>

Sicong Huang<sup>\*,2,3</sup>

Marzyeh Ghassemi<sup>2,4</sup>

Greg Ver Steeg<sup>1</sup>

Roger Grosse<sup>2,3</sup>

Alireza Makhzani<sup>2,3</sup>

<sup>1</sup> Information Sciences Institute, University of Southern California

<sup>2</sup> Vector Institute <sup>3</sup> University of Toronto <sup>4</sup> MIT EECS / IMES / CSAIL

## ABSTRACT

Mutual information (MI) is a fundamental quantity in information theory and machine learning. However, direct estimation of MI is intractable, even if the true joint probability density for the variables of interest is known, as it involves estimating a potentially high-dimensional log partition function. In this work, we present a unifying view of existing MI bounds from the perspective of importance sampling, and propose three novel bounds based on this approach. Since accurate estimation of MI without density information requires a sample size exponential in the true MI, we assume either a single marginal or the full joint density information is known. In settings where the full joint density is available, we propose Multi-Sample Annealed Importance Sampling (AIS) bounds on MI, which we demonstrate can tightly estimate large values of MI in our experiments. In settings where only a single marginal distribution is known, we propose *Generalized IWAE* (GIWAE) and MINE-AIS bounds. Our GIWAE bound unifies variational and contrastive bounds in a single framework that generalizes INFONCE, IWAE, and Barber-Agakov bounds. Our MINE-AIS method improves upon existing energy-based methods such as MINE-DV and MINE-F by directly optimizing a tighter lower bound on MI. MINE-AIS uses MCMC sampling to estimate gradients for training and Multi-Sample AIS for evaluating the bound. Our methods are particularly suitable for evaluating MI in deep generative models, since explicit forms of the marginal or joint densities are often available. We evaluate our bounds on estimating the MI of VAEs and GANs trained on the MNIST and CIFAR datasets, and showcase significant gains over existing bounds in these challenging settings with high ground truth MI.

## 1 INTRODUCTION

Mutual information (MI) is among the most general measures of dependence between two random variables. Among many other applications in machine learning, mutual information has been used for both training (Alemi et al., 2017, 2018; Chen et al., 2016; Zhao et al., 2018) and evaluating (Alemi & Fischer, 2018; Huang et al., 2020) generative models. Furthermore, recent success in neural network function approximation has encouraged a wave of variational or contrastive methods for MI estimation from samples alone (Belghazi et al., 2018; van den Oord et al., 2018; Poole et al., 2019). However, McAllester & Stratos (2020) have shown that for any estimator that uses direct sampling from the product of marginals and does not have access to the analytical form of at least one marginal distribution, exponential sample complexity in the true MI is required to obtain a high confidence lower bound. This is particularly concerning in applications such as representation learning and generative modeling where we expect the MI to be large. In light of these limitations, we primarily consider settings where a single marginal or the full joint distribution are available. Even in these

<sup>\*</sup>Equal Contribution. Correspondence to brekelma@usc.edu; {huang, makhzani}@cs.toronto.edu. A shorter version appeared in the International Conference on Learning Representations (ICLR) 2022, available here.

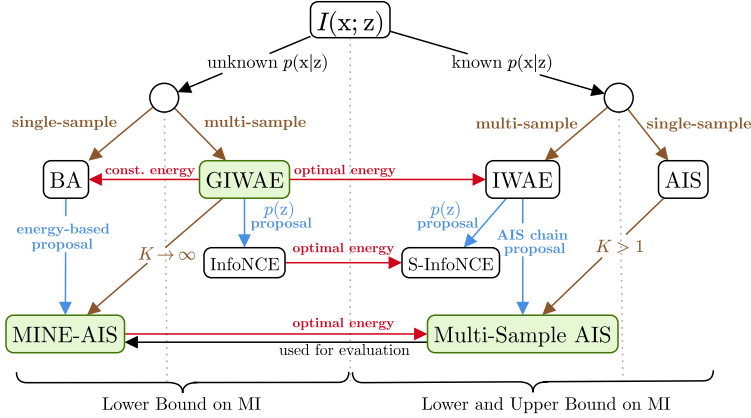


Figure 1: Schematic of various MI bounds discussed in this paper. Green shading indicates our contributions, while columns and gold labels indicate single- or multi-sample bounds. Blue arrows indicate special cases using the indicated proposal distribution. Several bounds with unknown  $p(\mathbf{x}|\mathbf{z})$  use learned energy or critic functions, where the optimal critic function reflects the true  $p(\mathbf{x}|\mathbf{z})$ . Relationships based on critic functions are indicated by red arrows. Bounds with unknown  $p(\mathbf{x}|\mathbf{z})$  provide only lower bounds on MI, while we obtain both upper and lower bounds with known  $p(\mathbf{x}|\mathbf{z})$ . All bounds require a single known marginal  $p(\mathbf{z})$  for evaluation, apart from (Structured) INFO-NCE.

cases, evaluating MI can be challenging due to the need to estimate a potentially high-dimensional log partition function.

In this work, we view MI estimation from the perspective of importance sampling, which sheds light on the limitations of existing estimators and motivates our search for improved proposal distributions using Markov Chain Monte Carlo (MCMC). Using a general approach for constructing extended state space bounds on MI, we combine insights from the importance-weighted autoencoder (IWAE) (Burda et al., 2016; Sobolev & Vetrov, 2019) and annealed importance sampling (AIS) (Neal, 2001) to propose *Multi-Sample* AIS bounds in Sec. 3. We empirically show that this approach can tightly estimate large values of MI when the full joint distribution is known.

Our importance sampling perspective also suggests improvements upon several existing energy-based lower bounds on MI, where our proposed methods only assume access to joint samples for optimization, but require a single marginal distribution for evaluation. In Sec. 2.4, we propose *Generalized* IWAE (GIWAE), which generalizes both IWAE and INFO-NCE (van den Oord et al., 2018; Poole et al., 2019) and highlights how variational learning can complement multi-sample contrastive estimation to improve MI lower bounds.

Finally, in Sec. 4, we propose MINE-AIS, which optimizes a tighter lower bound than Mutual Information Neural Estimation (MINE) (Belghazi et al., 2018) using a stable energy-based training procedure. We denote this bound as the *Implicit Barber Agakov Lower bound* (IBAL), and demonstrate that it corresponds to the infinite-sample limit of the GIWAE lower bound. However, our training scheme involves only a single ‘negative’ contrastive sample obtained using MCMC. MINE-AIS then uses Multi-Sample AIS to evaluate a lower bound on MI for a given energy function and known marginal, and shows notable improvement over existing variational bounds in the challenging setting of MI estimation for deep generative models.

## 1.1 PROBLEM SETTING

The mutual information between two random variables  $\mathbf{x}$  and  $\mathbf{z}$  with joint distribution  $p(\mathbf{x}, \mathbf{z})$  is

$$I(\mathbf{x}; \mathbf{z}) = \mathbb{E}_{p(\mathbf{x}, \mathbf{z})} \left[ \log \frac{p(\mathbf{x}, \mathbf{z})}{p(\mathbf{x})p(\mathbf{z})} \right] = H(\mathbf{x}) - H(\mathbf{x}|\mathbf{z}) = \mathbb{E}_{p(\mathbf{x}, \mathbf{z})} [\log p(\mathbf{x}|\mathbf{z})] - \mathbb{E}_{p(\mathbf{x})} [\log p(\mathbf{x})], \quad (1)$$

where  $H(\mathbf{x}|\mathbf{z})$  denotes the conditional entropy  $-\mathbb{E}_{p(\mathbf{x}, \mathbf{z})} \log p(\mathbf{x}|\mathbf{z})$ . We primarily focus on bounds which assume either a single marginal distribution or the full joint distribution are available. A natural setting where the full joint distribution is available is estimating MI in deep generative models between the latent variables, with a known prior  $\mathbf{z} \sim p(\mathbf{z})$ , and data  $\mathbf{x} \sim p(\mathbf{x})$  simulated from the model

(Alemi & Fischer, 2018).<sup>1</sup> Settings where only a single marginal is available appear, for example, in simulation-based inference (Cranmer et al., 2020), where information about input parameters  $\theta$  is known and a simulator can generate  $\mathbf{x}$  for a given  $\theta$ , but the likelihood  $p(\mathbf{x}|\theta)$  is intractable.

While sampling from the posterior  $p(\mathbf{z}|\mathbf{x})$  for an arbitrary  $\mathbf{x}$  is often intractable, we can obtain a single posterior sample for  $\mathbf{x} \sim p(\mathbf{x})$  in cases where samples from the joint distribution  $p(\mathbf{x})p(\mathbf{z}|\mathbf{x})$  are available. Throughout this paper, we will refer to bounds which involve only a single posterior sample as *practical*, and those involving multiple posterior samples as *impractical*.

When the conditional  $p(\mathbf{x}|\mathbf{z})$  is tractable to sample and evaluate, simple Monte Carlo sampling provides an unbiased, low variance estimate of the conditional entropy term in Eq. (1). In this case, the difficulty of MI estimation reduces to estimating the log partition function, for which importance sampling (IS) based methods are among the most well studied and successful solutions.

## 2 UNIFYING MUTUAL INFORMATION BOUNDS VIA IMPORTANCE SAMPLING

In this section, we present a unified view of mutual information estimation from the perspective of importance sampling, which yields new insights into existing bounds and will provide the foundation for our contributions in Sec. 3 and Sec. 4.

### 2.1 A GENERAL APPROACH FOR EXTENDED STATE SPACE IMPORTANCE SAMPLING BOUNDS

Throughout this paper, we use extended state space importance sampling (Finke, 2015; Domke & Sheldon, 2018) to derive lower and upper bounds on the log partition function, which translate to bounds on MI with known  $p(\mathbf{x}|\mathbf{z})$  as in Sec. 1.1. This general approach provides a probabilistic interpretation of existing MI bounds and will suggest novel extensions in later sections (see App. A).

In particular, we construct proposal  $q_{\text{PROP}}(\mathbf{z}_{\text{ext}}|\mathbf{x})$  and target  $p_{\text{TGT}}(\mathbf{x}, \mathbf{z}_{\text{ext}})$  distributions over an extended state space, such that the normalization constant of  $p_{\text{TGT}}(\mathbf{x}, \mathbf{z}_{\text{ext}})$  is  $\mathcal{Z}_{\text{TGT}} = \int p_{\text{TGT}}(\mathbf{x}, \mathbf{z}_{\text{ext}})d\mathbf{z}_{\text{ext}} = p(\mathbf{x})$  and the normalization constant of  $q_{\text{PROP}}(\mathbf{x}, \mathbf{z}_{\text{ext}})$  is  $\mathcal{Z}_{\text{PROP}} = 1$ . Taking expectations of the log importance weight  $\log p_{\text{TGT}}(\mathbf{x}, \mathbf{z}_{\text{ext}})/q_{\text{PROP}}(\mathbf{z}_{\text{ext}}|\mathbf{x})$  under the proposal and target, respectively, we obtain lower and upper bounds on the log partition function

$$\underbrace{\mathbb{E}_{q_{\text{PROP}}(\mathbf{z}_{\text{ext}}|\mathbf{x})} \left[ \log \frac{p_{\text{TGT}}(\mathbf{x}, \mathbf{z}_{\text{ext}})}{q_{\text{PROP}}(\mathbf{z}_{\text{ext}}|\mathbf{x})} \right]}_{\text{ELBO}(\mathbf{x}; q_{\text{PROP}}, p_{\text{TGT}})} \leq \log p(\mathbf{x}) \leq \underbrace{\mathbb{E}_{p_{\text{TGT}}(\mathbf{x}, \mathbf{z}_{\text{ext}})} \left[ \log \frac{p_{\text{TGT}}(\mathbf{x}, \mathbf{z}_{\text{ext}})}{q_{\text{PROP}}(\mathbf{z}_{\text{ext}}|\mathbf{x})} \right]}_{\text{EUBO}(\mathbf{x}; q_{\text{PROP}}, p_{\text{TGT}})}. \quad (2)$$

These bounds correspond to extended state space versions of the Evidence Lower Bound (ELBO) and Evidence Upper Bound (EUBO), respectively. In particular, the gap in the lower bound is the forward KL divergence, with  $\log p(\mathbf{x}) = \text{ELBO}(\mathbf{x}; q_{\text{PROP}}, p_{\text{TGT}}) + D_{\text{KL}}[q_{\text{PROP}}(\mathbf{z}_{\text{ext}}|\mathbf{x})||p_{\text{TGT}}(\mathbf{z}_{\text{ext}}|\mathbf{x})]$  and the gap in the upper bound equal to the reverse KL divergence  $\log p(\mathbf{x}) = \text{EUBO}(\mathbf{x}; q_{\text{PROP}}, p_{\text{TGT}}) - D_{\text{KL}}[p_{\text{TGT}}(\mathbf{z}_{\text{ext}}|\mathbf{x})||q_{\text{PROP}}(\mathbf{z}_{\text{ext}}|\mathbf{x})]$ .

### 2.2 BARBER-AGAKOV LOWER AND UPPER BOUNDS

As a first example, consider the standard  $\text{ELBO}(\mathbf{x}; q_{\theta})$  and  $\text{EUBO}(\mathbf{x}; q_{\theta})$  bounds, which are derived from simple importance sampling using a variational distribution  $q_{\theta}(\mathbf{z}|\mathbf{x})$  and  $\mathbf{z}_{\text{ext}} = \mathbf{z}$  in Eq. (2). Plugging these lower and upper bounds on  $\log p(\mathbf{x})$  into Eq. (1), we obtain upper and lower bounds on MI as

$$I_{\text{BAL}}(q_{\theta}) := \mathbb{E}_{p(\mathbf{x}, \mathbf{z})} \left[ \log \frac{q_{\theta}(\mathbf{z}|\mathbf{x})}{p(\mathbf{z})} \right] \leq I(\mathbf{x}; \mathbf{z}) \leq \mathbb{E}_{p(\mathbf{x})q_{\theta}(\mathbf{z}|\mathbf{x})} \left[ \log \frac{q_{\theta}(\mathbf{z}|\mathbf{x})}{p(\mathbf{x}, \mathbf{z})} \right] - H(\mathbf{x}|\mathbf{z}) =: I_{\text{BAU}}(q_{\theta}). \quad (3)$$

The left hand side of Eq. (3) is the well-known Barber-Agakov (BA) bound (Barber & Agakov, 2003), which has a gap of  $\mathbb{E}_{p(\mathbf{x})}[D_{\text{KL}}[p(\mathbf{z}|\mathbf{x})||q_{\theta}(\mathbf{z}|\mathbf{x})]]$ . We refer to the right hand side as the BA upper bound  $I_{\text{BAU}}(q_{\theta})$ , with a gap of  $\mathbb{E}_{p(\mathbf{x})}[D_{\text{KL}}[q_{\theta}(\mathbf{z}|\mathbf{x})||p(\mathbf{z}|\mathbf{x})]]$ . In contrast to  $I_{\text{BAU}}(q_{\theta})$ , note that  $I_{\text{BAL}}(q_{\theta})$  does not require access to the conditional density  $p(\mathbf{x}|\mathbf{z})$  to evaluate the bound.

<sup>1</sup>An alternative, ‘‘encoding’’ MI between the real data and the latent code is often of interest (see App. N), but cannot be directly estimated using our methods due to the unavailability of  $p_d(\mathbf{x})$  or  $q(\mathbf{z}) = \int p_d(\mathbf{x})q(\mathbf{z}|\mathbf{x})d\mathbf{x}$ .

### 2.3 IMPORTANCE WEIGHTED AUTOENCODER LOWER AND UPPER BOUNDS

The IWAE lower and upper bounds on  $\log p(\mathbf{x})$  (Burda et al., 2016; Sobolev & Vetrov, 2019) improve upon simple importance sampling by extending the state space using multiple samples  $\mathbf{z}_{\text{ext}} = \mathbf{z}^{(1:K)}$  (Domke & Sheldon, 2018). Consider a proposal  $q_{\text{PROP}}^{\text{IWAE}}(\mathbf{z}^{(1:K)}|\mathbf{x})$  with  $K$  independent samples from a given variational distribution  $q_{\theta}(\mathbf{z}|\mathbf{x})$ . The extended state space target  $p_{\text{TGT}}^{\text{IWAE}}(\mathbf{z}^{(1:K)}|\mathbf{x})$  is a mixture distribution involving a single sample from the posterior  $p(\mathbf{z}|\mathbf{x})$  or joint  $p(\mathbf{x}, \mathbf{z})$  distribution and  $K - 1$  samples from  $q_{\theta}(\mathbf{z}|\mathbf{x})$

$$q_{\text{PROP}}^{\text{IWAE}}(\mathbf{z}^{(1:K)}|\mathbf{x}) := \prod_{s=1}^K q_{\theta}(\mathbf{z}^{(s)}|\mathbf{x}), \quad p_{\text{TGT}}^{\text{IWAE}}(\mathbf{x}, \mathbf{z}^{(1:K)}) := \frac{1}{K} \sum_{s=1}^K p(\mathbf{x}, \mathbf{z}^{(s)}) \prod_{\substack{k=1 \\ k \neq s}}^K q_{\theta}(\mathbf{z}^{(k)}|\mathbf{x}). \quad (4)$$

As in Sec. 2.1, taking the expectation of the log importance weight  $\log \frac{p_{\text{TGT}}^{\text{IWAE}}(\mathbf{x}, \mathbf{z}^{(1:K)})}{q_{\text{PROP}}^{\text{IWAE}}(\mathbf{z}^{(1:K)}|\mathbf{x})}$  under the proposal and target, respectively, yields the IWAE lower (Burda et al., 2016) and upper (Sobolev & Vetrov, 2019) bounds on  $\log p(\mathbf{x})$ ,

$$\underbrace{\mathbb{E}_{\prod_{k=1}^K q_{\theta}(\mathbf{z}^{(k)}|\mathbf{x})} \left[ \log \frac{1}{K} \sum_{i=1}^K \frac{p(\mathbf{x}, \mathbf{z}^{(i)})}{q_{\theta}(\mathbf{z}^{(i)}|\mathbf{x})} \right]}_{\text{ELBO}_{\text{IWAE}}(\mathbf{x}; q_{\theta}, K)} \leq \log p(\mathbf{x}) \leq \underbrace{\mathbb{E}_{p(\mathbf{z}^{(1)}|\mathbf{x}) \prod_{k=2}^K q_{\theta}(\mathbf{z}^{(k)}|\mathbf{x})} \left[ \log \frac{1}{K} \sum_{i=1}^K \frac{p(\mathbf{x}, \mathbf{z}^{(i)})}{q_{\theta}(\mathbf{z}^{(i)}|\mathbf{x})} \right]}_{\text{EUBO}_{\text{IWAE}}(\mathbf{x}; q_{\theta}, K)}. \quad (5)$$

See App. B for derivations. For simplicity of notation, we assume  $s = 1$  and  $\mathbf{z}^{(1)} \sim p(\mathbf{z}|\mathbf{x})$  when writing the expectation in  $\text{EUBO}_{\text{IWAE}}(q_{\theta}, K)$ , due to invariance of Eq. (4) to permutation of the indices.

As for the standard ELBO and EUBO, the gaps in the lower and upper bounds are  $D_{KL}[q_{\text{PROP}}^{\text{IWAE}}(\mathbf{z}^{(1:K)}|\mathbf{x})||p_{\text{TGT}}^{\text{IWAE}}(\mathbf{z}^{(1:K)}|\mathbf{x})]$  and  $D_{KL}[p_{\text{TGT}}^{\text{IWAE}}(\mathbf{z}^{(1:K)}|\mathbf{x})||q_{\text{PROP}}^{\text{IWAE}}(\mathbf{z}^{(1:K)}|\mathbf{x})]$ , respectively. With known  $p(\mathbf{x}|\mathbf{z})$ , the lower and upper bounds on  $\log p(\mathbf{x})$  translate to upper and lower bounds on MI,  $I_{\text{IWAE}_U}(q_{\theta}, K)$  and  $I_{\text{IWAE}_L}(q_{\theta}, K)$ , as in Sec. 1.1.

**Complexity in K** While it is well-known that increasing  $K$  leads to tighter IWAE bounds (Burda et al., 2016; Sobolev & Vetrov, 2019), we explicitly characterize the improvement of multi-sample IWAE bounds over the single-sample ELBO or EUBO in the following proposition.

This proposition lays the foundation for similar results throughout the paper. In particular, any bound which involves expectations under a mixture of one ‘positive’ sample and  $K - 1$  ‘negative’ samples, such as  $\text{EUBO}_{\text{IWAE}}(\mathbf{x}; q_{\theta}, K)$  in Eq. (5) or (7), will be limited to logarithmic improvement in  $K$ .

**Proposition 2.1** (Improvement of IWAE with Increasing  $K$ ). *Let  $p_{\text{TGT}}^{\text{IWAE}}(s|\mathbf{x}, \mathbf{z}^{(1:K)}) = \frac{p(\mathbf{x}, \mathbf{z}^{(s)})}{q_{\theta}(\mathbf{z}^{(s)}|\mathbf{x})} / \sum_{k=1}^K \frac{p(\mathbf{x}, \mathbf{z}^{(k)})}{q_{\theta}(\mathbf{z}^{(k)}|\mathbf{x})}$  denote the normalized importance weights and  $\mathcal{U}(s)$  indicate the uniform distribution over  $K$  discrete values. Then, we can characterize the improvement of  $\text{ELBO}_{\text{IWAE}}(\mathbf{x}; q_{\theta}, K)$  and  $\text{EUBO}_{\text{IWAE}}(\mathbf{x}; q_{\theta}, K)$  over  $\text{ELBO}(\mathbf{x}; q_{\theta})$  and  $\text{EUBO}(\mathbf{x}; q_{\theta})$  using KL divergences, as follows*

$$\text{ELBO}_{\text{IWAE}}(\mathbf{x}; q_{\theta}, K) = \text{ELBO}(\mathbf{x}; q_{\theta}) + \underbrace{\mathbb{E}_{q_{\text{PROP}}^{\text{IWAE}}(\mathbf{z}^{(1:K)}|\mathbf{x})} \left[ D_{\text{KL}}[\mathcal{U}(s)||p_{\text{TGT}}^{\text{IWAE}}(s|\mathbf{z}^{(1:K)}, \mathbf{x})] \right]}_{0 \leq \text{KL of uniform from SNIS weights} \leq D_{\text{KL}}[q_{\theta}(\mathbf{z}|\mathbf{x})||p(\mathbf{z}|\mathbf{x})]}, \quad (6)$$

$$\text{EUBO}_{\text{IWAE}}(\mathbf{x}; q_{\theta}, K) = \text{EUBO}(\mathbf{x}; q_{\theta}) - \underbrace{\mathbb{E}_{p_{\text{TGT}}^{\text{IWAE}}(\mathbf{z}^{(1:K)}|\mathbf{x})} \left[ D_{\text{KL}}[p_{\text{TGT}}^{\text{IWAE}}(s|\mathbf{z}^{(1:K)}, \mathbf{x})||\mathcal{U}(s)] \right]}_{0 \leq \text{KL of SNIS weights from uniform} \leq \log K}. \quad (7)$$

Prop. 2.1 demonstrates that the improvement of the IWAE log partition function bounds over its single-sample counterparts is larger for more non-uniform SNIS weights. Notably, the improvement of  $\text{EUBO}_{\text{IWAE}}(\mathbf{x}; q_{\theta}, K)$  over the single-sample  $\text{EUBO}(\mathbf{x}; q_{\theta})$  is limited by  $\log K$ . Translating Prop. 2.1 to the IWAE bounds on MI yields the following corollary.

**Corollary 2.2.** *IWAE bounds on MI improve upon the BA bounds with the following relationships:*

$$I_{\text{BA}_L}(q_{\theta}) \leq I_{\text{IWAE}_L}(q_{\theta}, K) \leq I_{\text{BA}_L}(q_{\theta}) + \log K, \quad I_{\text{IWAE}_U}(q_{\theta}, K) \leq I_{\text{BA}_U}(q_{\theta}). \quad (8)$$

**Cor. 2.2** shows that, in order to obtain a tight bound on MI, the IWAE lower bound requires exponential sample complexity in  $\mathbb{E}_{p(\mathbf{x})} [D_{\text{KL}}[p(\mathbf{z}|\mathbf{x})\|q_\theta(\mathbf{z}|\mathbf{x})]]$ , which is the gap of either  $I_{\text{EUBO}}(\mathbf{x}; q_\theta)$  or  $I_{\text{BAL}}(q_\theta)$ . Although  $\text{ELBO}_{\text{IWAE}}(\mathbf{x}; q_\theta, K)$  and  $I_{\text{IWAE}_U}(q_\theta, K)$  are not limited to logarithmic improvement with increasing  $K$ , it has been argued that the same exponential sample complexity,  $K \propto \exp(D_{\text{KL}}[p(\mathbf{z}|\mathbf{x})\|q_\theta(\mathbf{z}|\mathbf{x})])$ , is required to achieve tight importance sampling bounds (see [App. B.4](#), [Chatterjee et al. \(2018\)](#)). These observations motivate our improved AIS proposals in [Sec. 3](#), which achieve *linear* bias reduction in the number of intermediate distributions  $T$  used to bridge between  $q_\theta(\mathbf{z}|\mathbf{x})$  and  $p(\mathbf{z}|\mathbf{x})$ .

**Relationship with Structured InfoNCE** We can recognize the Structured INFONCE upper and lower bounds ([App. B.5](#), [Poole et al. \(2019\)](#)) as corresponding to the standard IWAE bounds, with known  $p(\mathbf{x}|\mathbf{z})$  and the marginal  $p(\mathbf{z})$  used in place of the variational distribution  $q_\theta(\mathbf{z}|\mathbf{x})$ . In other words, we have  $I_{\text{S-INFONCE}_L}(K) = I_{\text{IWAE}_L}(p(\mathbf{z}), K)$  and  $I_{\text{S-INFONCE}_U}(K) = I_{\text{IWAE}_U}(p(\mathbf{z}), K)$ .

## 2.4 GENERALIZED IWAE

In the previous section, we have seen that IWAE improves upon BA using multiple samples. However, IWAE leverages knowledge of the full joint density  $p(\mathbf{x}, \mathbf{z})$ , whereas evaluating the BA lower bound only requires access to the marginal  $p(\mathbf{z})$ . In this section, we consider a family of *Generalized* IWAE (GIWAE) lower bounds, which use a contrastive critic function  $T_\phi(\mathbf{x}, \mathbf{z})$  to achieve similar multi-sample improvement as IWAE without access to  $p(\mathbf{x}, \mathbf{z})$ . While similar bounds appear in ([Lawson et al., 2019](#); [Sobolev, 2019](#)), we provide empirical validation for MI estimation ([Sec. 5.3](#)), and discuss theoretical connections with IWAE and our proposed MINE-AIS method ([Sec. 4](#)).

To derive a probabilistic interpretation for GIWAE, our starting point is to further extend the state space of the IWAE target distribution in [Eq. \(4\)](#), using a uniform index variable  $\mathcal{U}(s) = \frac{1}{K} \forall s$  that specifies which sample  $\mathbf{z}^{(k)}$  is drawn from the posterior  $p(\mathbf{z}|\mathbf{x})$ . This leads to the following joint distribution over  $(\mathbf{x}, \mathbf{z}^{(1:K)}, s)$  and posterior over the index variable  $s$ ,

$$p_{\text{TGT}}^{\text{GIWAE}}(\mathbf{x}, \mathbf{z}^{(1:K)}, s) := \frac{1}{K} p(\mathbf{x}, \mathbf{z}^{(s)}) \prod_{\substack{k=1 \\ k \neq s}}^K q_\theta(\mathbf{z}^{(k)}|\mathbf{x}), \text{ resulting in } p_{\text{TGT}}^{\text{GIWAE}}(s|\mathbf{x}, \mathbf{z}^{(1:K)}) = \frac{\frac{p(\mathbf{x}, \mathbf{z}^{(s)})}{q_\theta(\mathbf{z}^{(s)}|\mathbf{x})}}{\sum_{k=1}^K \frac{p(\mathbf{x}, \mathbf{z}^{(k)})}{q_\theta(\mathbf{z}^{(k)}|\mathbf{x})}}. \quad (9)$$

Note that marginalization over  $s$  in  $p_{\text{TGT}}^{\text{GIWAE}}(\mathbf{z}^{(1:K)}, s|\mathbf{x})$  leads to the IWAE target distribution  $p_{\text{TGT}}^{\text{IWAE}}(\mathbf{z}^{(1:K)}|\mathbf{x})$  in [Eq. \(4\)](#). The posterior  $p_{\text{TGT}}^{\text{GIWAE}}(s|\mathbf{x}, \mathbf{z}^{(1:K)})$  over the index variable  $s$ , which infers the positive sample drawn from  $p(\mathbf{z}|\mathbf{x})$  given a set of samples  $\mathbf{z}^{(1:K)}$ , corresponds to the normalized importance weights.

For the GIWAE extended state space proposal distribution, we consider a categorical index variable  $q_{\text{PROP}}^{\text{GIWAE}}(s|\mathbf{z}^{(1:K)}, \mathbf{x})$  drawn according to *variational* SNIS weights, which are calculated using a learned critic or negative energy function  $T_\phi(\mathbf{x}, \mathbf{z})$

$$q_{\text{PROP}}^{\text{GIWAE}}(\mathbf{z}^{(1:K)}, s|\mathbf{x}) := \left( \prod_{k=1}^K q_\theta(\mathbf{z}^{(k)}|\mathbf{x}) \right) q_{\text{PROP}}^{\text{GIWAE}}(s|\mathbf{z}^{(1:K)}, \mathbf{x}), \text{ where } q_{\text{PROP}}^{\text{GIWAE}}(s|\mathbf{z}^{(1:K)}, \mathbf{x}) := \frac{e^{T_\phi(\mathbf{x}, \mathbf{z}^{(s)})}}{\sum_{k=1}^K e^{T_\phi(\mathbf{x}, \mathbf{z}^{(k)})}}. \quad (10)$$

We can view the SNIS distribution  $q_{\text{PROP}}^{\text{GIWAE}}(s|\mathbf{z}^{(1:K)}, \mathbf{x})$  as performing variational inference of the posterior  $p_{\text{TGT}}^{\text{GIWAE}}(s|\mathbf{x}, \mathbf{z}^{(1:K)})$ . We will show in [Prop. 2.3](#) that the optimal GIWAE critic function is  $T^*(\mathbf{x}, \mathbf{z}) = \log \frac{p(\mathbf{x}, \mathbf{z})}{q_\theta(\mathbf{z}|\mathbf{x})} + c(\mathbf{x})$ , in which case [Eq. \(9\)-\(10\)](#) recover the IWAE probabilistic interpretation from [Domke & Sheldon \(2018\)](#) (see [App. B.1](#)).

We focus on the upper bound on  $\log p(\mathbf{x})$ , obtained by taking the expected log importance ratio under  $p_{\text{TGT}}^{\text{GIWAE}}(\mathbf{z}^{(1:K)}, s|\mathbf{x})$  as in [Sec. 2.1](#).<sup>2</sup> We write the corresponding GIWAE lower bound on MI as

$$I_{\text{GIWAE}_L}(q_\theta, T_\phi, K) = \underbrace{\mathbb{E}_{p(\mathbf{x}, \mathbf{z})} \left[ \log \frac{q_\theta(\mathbf{z}|\mathbf{x})}{p(\mathbf{z})} \right]}_{I_{\text{BAL}}(q_\theta)} + \underbrace{\mathbb{E}_{p(\mathbf{x})p(\mathbf{z}^{(1)}|\mathbf{x}) \prod_{k=2}^K q_\theta(\mathbf{z}^{(k)}|\mathbf{x})} \left[ \log \frac{e^{T_\phi(\mathbf{x}, \mathbf{z}^{(1)})}}{\frac{1}{K} \sum_{i=1}^K e^{T_\phi(\mathbf{x}, \mathbf{z}^{(i)})}} \right]}_{\text{contrastive term} \leq \log K}. \quad (11)$$

<sup>2</sup>We consider  $\text{ELBO}_{\text{GIWAE}}(\mathbf{x}; q_\theta, T_\phi, K)$  in [App. C.2](#). For MI estimation, the corresponding upper bound is always inferior to  $I_{\text{IWAE}_U}(q_\theta, K)$ , since known  $p(\mathbf{x}|\mathbf{z})$  is needed to evaluate  $H(\mathbf{x}|\mathbf{z})$ . See [Cor. 2.4](#) and [App. C.2](#).



We see that the GIWAE lower bound decomposes into the sum of two terms, where the first is the BA variational lower bound for  $q_\theta(\mathbf{z}|\mathbf{x})$  and the second is a contrastive term which distinguishes negative samples from  $q_\theta(\mathbf{z}|\mathbf{x})$  and positive samples from  $p(\mathbf{z}|\mathbf{x})$ . Similarly to BA, GIWAE requires access to the analytical form of  $p(\mathbf{z})$  to *evaluate* the bound on MI. However, if the goal is to *optimize* mutual information, both the BA and GIWAE lower bounds can be used even if no marginal distribution is available. See App. N for more detailed discussion.

**Relationship with BA** Choosing constant  $T_\phi(\mathbf{x}, \mathbf{z}) = c$  means that the second term in GIWAE vanishes, so that we have  $I_{\text{GIWAE}_L}(q, T_\phi = c, K) = I_{\text{BA}_L}(q_\theta)$  for all  $K$ . Similarly, the single sample  $I_{\text{GIWAE}_L}(q, T_\phi, K = 1)$  equals the BA lower bound for all  $T_\phi(\mathbf{x}, \mathbf{z})$ .

**Relationship with InfoNCE** When the prior  $p(\mathbf{z})$  is used in place of  $q_\theta(\mathbf{z}|\mathbf{x})$ , we can recognize the second term in Eq. (11) as the INFONCE contrastive lower bound (van den Oord et al., 2018; Poole et al., 2019), with  $I_{\text{INFONCE}_L}(T_\phi, K) = I_{\text{GIWAE}_L}(p(\mathbf{z}), T_\phi, K)$ . From this perspective, the GIWAE lower bound highlights how variational learning can complement contrastive bounds to improve MI estimation beyond the known  $\log K$  limitations of INFONCE (van den Oord et al. (2018), Eq. (15)). However, using the prior as the proposal in INFONCE does allow the critic function to admit a bi-linear implementation  $T_\phi(\mathbf{x}, \mathbf{z}) = f_{\phi_x}(\mathbf{x})^\top f_{\phi_z}(\mathbf{z})$ , which requires only  $N + K$  forward passes instead of  $NK$  for GIWAE, where  $N$  is the batch size and  $K$  is the total number of positive and negative samples.

**Relationship with IWAE** The following proposition characterizes the relationship between the GIWAE lower bound in Eq. (11) and the IWAE lower bound on MI from Sec. 2.3.

**Proposition 2.3** (Improvement of IWAE over GIWAE). *For a given  $q_\theta(\mathbf{z}|\mathbf{x})$ , the IWAE lower bound on MI is tighter than the GIWAE lower bound for any  $T_\phi(\mathbf{x}, \mathbf{z})$ . Their difference is the average KL divergence between the normalized importance weights  $p_{\text{TGT}}^{\text{GIWAE}}(s|\mathbf{z}^{(1:K)}, \mathbf{x})$  and the variational distribution  $q_{\text{PROP}}^{\text{GIWAE}}(s|\mathbf{z}^{(1:K)}, \mathbf{x})$  in Eq. (10),*

$$I_{\text{IWAE}_L}(q_\theta, K) = I_{\text{GIWAE}_L}(q_\theta, T_\phi, K) + \mathbb{E}_{p(\mathbf{x})p_{\text{TGT}}^{\text{IWAE}}(\mathbf{z}^{(1:K)}|\mathbf{x})} \left[ D_{\text{KL}}[p_{\text{TGT}}^{\text{GIWAE}}(s|\mathbf{z}^{(1:K)}, \mathbf{x}) \| q_{\text{PROP}}^{\text{GIWAE}}(s|\mathbf{z}^{(1:K)}, \mathbf{x})] \right].$$

**Corollary 2.4** (Optimal GIWAE Critic Function yields IWAE). *For a given  $q_\theta(\mathbf{z}|\mathbf{x})$  and  $K > 1$ , the optimal GIWAE critic function is equal to the true log importance weight up to an arbitrary constant:  $T^*(\mathbf{x}, \mathbf{z}) = \log \frac{p(\mathbf{x}, \mathbf{z})}{q_\theta(\mathbf{z}|\mathbf{x})} + c(\mathbf{x})$ . With this choice of  $T^*(\mathbf{x}, \mathbf{z})$ , we have*

$$I_{\text{GIWAE}_L}(q_\theta, T^*, K) = I_{\text{IWAE}_L}(q_\theta, K). \quad (12)$$

**Corollary 2.5** (Logarithmic Improvement of GIWAE). *Suppose the critic function  $T_\phi(\mathbf{x}, \mathbf{z})$  is parameterized by  $\phi$ , and  $\exists \phi_0$  s.t.  $\forall (\mathbf{x}, \mathbf{z}), T_{\phi_0}(\mathbf{x}, \mathbf{z}) = \text{const}$ . For a given  $q_\theta(\mathbf{z}|\mathbf{x})$ , let  $T_{\phi^*}(\mathbf{x}, \mathbf{z})$  denote the critic function that maximizes the GIWAE lower bound. Using Cor. 2.2 and Cor. 2.4, we have*

$$I_{\text{BA}_L}(q_\theta) \leq I_{\text{GIWAE}_L}(q_\theta, T_{\phi^*}, K) \leq I_{\text{IWAE}_L}(q_\theta, K) \leq I_{\text{BA}_L}(q_\theta) + \log K. \quad (13)$$

See App. C.4-C.5 for proofs. Note that Prop. 2.1, which relates the IWAE and BA lower bounds, can be seen as a special case of Prop. 2.3, since  $I_{\text{BA}_L}(q_\theta)$  is a special case of GIWAE. Cor. 2.4 shows that when the full joint density  $p(\mathbf{x}, \mathbf{z})$  is available, IWAE is always preferable to GIWAE. Finally, Eq. (11) suggests a similar decomposition of  $I_{\text{IWAE}_L}(q_\theta, K)$  into a BA term and a contrastive term (see App. B.3)

$$I_{\text{IWAE}_L}(q_\theta, K) = \underbrace{\mathbb{E}_{p(\mathbf{x}, \mathbf{z})} \left[ \log \frac{q_\theta(\mathbf{z}|\mathbf{x})}{p(\mathbf{z})} \right]}_{I_{\text{BA}}(q)} + \underbrace{\mathbb{E}_{p(\mathbf{x})p(\mathbf{z}^{(1)}|\mathbf{x}) \prod_{k=2}^K q_\theta(\mathbf{z}^{(k)}|\mathbf{x})} \left[ \log \frac{\frac{p(\mathbf{x}, \mathbf{z}^{(1)})}{q_\theta(\mathbf{z}^{(1)}|\mathbf{x})}}{\frac{1}{K} \sum_{i=1}^K \frac{p(\mathbf{x}, \mathbf{z}^{(k)})}{q_\theta(\mathbf{z}^{(k)}|\mathbf{x})}} \right]}_{0 \leq \text{contrastive term} \leq \log K}. \quad (14)$$

**Relationship with Structured InfoNCE** INFONCE and Structured INFONCE are special cases of GIWAE and IWAE, respectively, which use  $p(\mathbf{z})$  as the variational distribution. Since  $I_{\text{BA}_L}(p(\mathbf{z})) = 0$ , Cor. 2.5 suggests the following relationship

$$0 \leq I_{\text{INFONCE}_L}(T_\phi, K) \leq I_{\text{S-INFONCE}_L}(K) \leq \log K. \quad (15)$$

From the GIWAE perspective, we can interpret the  $\log K$  limitations of (Structured) INFONCE as arising from the  $\log K$  improvement results for  $I_{\text{GIWAE}_L}(q_\theta, T_\phi, K)$  and  $I_{\text{IWAE}_L}(q_\theta, K)$  in Cor. 2.5.

### 3 MULTI-SAMPLE AIS BOUNDS FOR ESTIMATING MUTUAL INFORMATION

AIS (Neal, 2001) is considered the gold standard for obtaining unbiased and low variance estimates of the partition function, while Bidirectional Monte Carlo (BDMC) (Grosse et al., 2015, 2016) provides lower and upper bounds on the log partition function using forward and reverse AIS chains. In this section, we propose various *Multi-Sample* AIS bounds, which highlight that extending the state space over multiple samples, as in IWAE, is complementary to extending the state space over intermediate distributions as in AIS. Our approach includes BDMC bounds as special cases, and we obtain a novel upper bound which can match or improve upon the performance of BDMC. We derive novel probabilistic interpretations of Multi-Sample AIS bounds which, perhaps surprisingly, suggest that the practical sampling schemes used in BDMC do not correspond to the same probabilistic interpretation.

We present our Multi-Sample AIS bounds of  $\log p(\mathbf{x})$  within the context of estimating the generative mutual information (Alemi & Fischer, 2018), as in Sec. 1.1. However, our methods are equally applicable for other applications, including evaluating the marginal likelihood (Wu et al., 2017; Grosse et al., 2015) or rate-distortion curve (Huang et al., 2020) of generative models.

We first review background on AIS, before describing Multi-Sample AIS log partition function bounds in Sec. 3.2 and 3.3. For all bounds in this section, we assume that *both* the true marginal  $p(\mathbf{z})$  and conditional  $p(\mathbf{x}|\mathbf{z})$  densities are known.

#### 3.1 ANNEALED IMPORTANCE SAMPLING BACKGROUND

AIS (Neal, 2001) constructs a sequence of intermediate distributions  $\{\pi_t(\mathbf{z})\}_{t=0}^T$ , which bridge between a normalized initial distribution  $\pi_0(\mathbf{z}|\mathbf{x})$  and target distribution  $\pi_T(\mathbf{z}|\mathbf{x}) = p(\mathbf{z}|\mathbf{x})$ . The target has an unnormalized density  $\pi_T(\mathbf{x}, \mathbf{z}) = p(\mathbf{x}, \mathbf{z})$  and normalizing constant  $\mathcal{Z}_T(\mathbf{x}) = p(\mathbf{x})$ . A common choice for intermediate distributions is the geometric path parameterized by  $\{\beta_t\}_{t=0}^T$ :

$$\pi_t(\mathbf{z}|\mathbf{x}) := \frac{\pi_0(\mathbf{z}|\mathbf{x})^{1-\beta_t} \pi_T(\mathbf{x}, \mathbf{z})^{\beta_t}}{\mathcal{Z}_t(\mathbf{x})}, \quad \text{where} \quad \mathcal{Z}_t(\mathbf{x}) := \int \pi_0(\mathbf{z}|\mathbf{x})^{1-\beta_t} \pi_T(\mathbf{x}, \mathbf{z})^{\beta_t} d\mathbf{z}. \quad (16)$$

In the probabilistic interpretation of AIS, we consider an extended state space proposal  $q_{\text{PROP}}^{\text{AIS}}(\mathbf{z}_{0:T}|\mathbf{x})$ , obtained by sampling from the initial  $\pi_0(\mathbf{z}|\mathbf{x})$  and constructing transitions  $\mathcal{T}_t(\mathbf{z}_t|\mathbf{z}_{t-1})$  which leave  $\pi_{t-1}(\mathbf{z}|\mathbf{x})$  invariant. The target distribution  $p_{\text{TGT}}^{\text{AIS}}(\mathbf{z}_{0:T}|\mathbf{x})$  is given by running the reverse transitions  $\tilde{\mathcal{T}}_t(\mathbf{z}_{t-1}|\mathbf{z}_t)$  starting from a target or posterior sample  $\pi_T(\mathbf{z}|\mathbf{x})$ , as shown in Fig. 2,

$$q_{\text{PROP}}^{\text{AIS}}(\mathbf{z}_{0:T}|\mathbf{x}) := \pi_0(\mathbf{z}_0|\mathbf{x}) \prod_{t=1}^T \mathcal{T}_t(\mathbf{z}_t|\mathbf{z}_{t-1}), \quad p_{\text{TGT}}^{\text{AIS}}(\mathbf{x}, \mathbf{z}_{0:T}) := \pi_T(\mathbf{x}, \mathbf{z}_T) \prod_{t=1}^T \tilde{\mathcal{T}}_t(\mathbf{z}_{t-1}|\mathbf{z}_t). \quad (17)$$

As in Sec. 2.1, taking expectations of the log importance weights under the proposal and target yields a lower and upper bound on the log partition function  $\log p(\mathbf{x})$

$$\underbrace{\mathbb{E}_{\mathbf{z}_{0:T} \sim q_{\text{PROP}}^{\text{AIS}}} \left[ \log \frac{p_{\text{TGT}}^{\text{AIS}}(\mathbf{x}, \mathbf{z}_{0:T})}{q_{\text{PROP}}^{\text{AIS}}(\mathbf{z}_{0:T}|\mathbf{x})} \right]}_{\text{ELBO}_{\text{AIS}}(\mathbf{x}; \pi_0, T)} \leq \log p(\mathbf{x}) \leq \underbrace{\mathbb{E}_{\mathbf{z}_{0:T} \sim p_{\text{TGT}}^{\text{AIS}}} \left[ \log \frac{p_{\text{TGT}}^{\text{AIS}}(\mathbf{x}, \mathbf{z}_{0:T})}{q_{\text{PROP}}^{\text{AIS}}(\mathbf{z}_{0:T}|\mathbf{x})} \right]}_{\text{EUBO}_{\text{AIS}}(\mathbf{x}; \pi_0, T)}. \quad (18)$$

These single-chain lower and upper bounds translate to upper and lower bounds on MI,  $I_{\text{AIS}_U}(\pi_0, T)$  and  $I_{\text{AIS}_L}(\pi_0, T)$ , which were suggested for MI estimation in the blog post of Sobolev (2019). See App. E for detailed derivations.

To characterize the bias reduction for AIS with increasing  $T$ , we prove the following proposition.

**Proposition 3.1** (Complexity in  $T$ ). *Assuming perfect transitions and a geometric annealing path with linearly-spaced  $\{\beta_t\}_{t=1}^T$ , the gap of the AIS upper and lower bounds (Eq. (18)) reduces linearly with increasing  $T$ ,*

$$\text{EUBO}_{\text{AIS}}(\mathbf{x}; \pi_0, T) - \text{ELBO}_{\text{AIS}}(\mathbf{x}; \pi_0, T) = \frac{1}{T} \left( D_{\text{KL}}[\pi_T(\mathbf{z}|\mathbf{x})||\pi_0(\mathbf{z}|\mathbf{x})] + D_{\text{KL}}[\pi_0(\mathbf{z}|\mathbf{x})||\pi_T(\mathbf{z}|\mathbf{x})] \right). \quad (19)$$

See App. D.1 for a proof. Our proposition generalizes Thm. 1 of Grosse et al. (2013), which holds for the case of  $T \rightarrow \infty$  instead of finite  $T$  as above. In our experiments in Sec. 5, we will find that this linear bias reduction in  $T$  is crucial for achieving tight MI estimation when both  $p(\mathbf{z})$  and  $p(\mathbf{x}|\mathbf{z})$  are known. We can further tighten the single-sample AIS bounds with multiple annealing chains ( $K > 1$ ) using two different approaches, which we present in the following sections.

	IWAE	Single-Sample AIS	Independent Multi-Sample AIS	Independent Reverse Multi-Sample AIS	Coupled Reverse Multi-Sample AIS
Practical?	✓	✓	✓	✗	✓
Target EUBO $I_{LB}$					
Proposal ELBO $I_{UB}$					

Figure 2: Extended state-space probabilistic interpretations of Multi-Sample AIS bounds. Forward chains are colored in blue, and backward chains are colored in red. Note that ELBOs and EUBOs are obtained by taking the expectation of the log unnormalized importance weights  $\log p_{\text{TGT}}(\cdot)/q_{\text{PROP}}(\cdot)$  under either the proposal or target distribution, and can then be translated to MI bounds.

### 3.2 INDEPENDENT MULTI-SAMPLE AIS BOUNDS

In our first approach, *Independent Multi-Sample AIS* (IM-AIS), we construct an extended state space proposal by running  $K$  independent AIS forward chains  $\mathbf{z}_{0:T}^{(k)} \sim q_{\text{PROP}}^{\text{AIS}}$  in parallel. Similarly to the IWAE upper bound (Eq. (5)), the extended state space target involves selecting an index  $s$  uniformly at random, and running a backward AIS chain  $\mathbf{z}_{0:T}^{(s)} \sim p_{\text{TGT}}^{\text{AIS}}$  starting from a true posterior sample  $\mathbf{z}_T \sim p(\mathbf{z}|\mathbf{x})$ . The remaining  $K-1$  samples are obtained by running forward AIS chains, as visualized in Fig. 2

$$q_{\text{PROP}}^{\text{IM-AIS}}(\mathbf{z}_{0:T}^{(1:K)}|\mathbf{x}) := \prod_{k=1}^K q_{\text{PROP}}^{\text{AIS}}(\mathbf{z}_{0:T}^{(k)}|\mathbf{x}), \quad p_{\text{TGT}}^{\text{IM-AIS}}(\mathbf{x}, \mathbf{z}_{0:T}^{(1:K)}) := \frac{1}{K} \sum_{s=1}^K p_{\text{TGT}}^{\text{AIS}}(\mathbf{x}, \mathbf{z}_{0:T}^{(s)}) \prod_{\substack{k=1 \\ k \neq s}}^K q_{\text{PROP}}^{\text{AIS}}(\mathbf{z}_{0:T}^{(k)}|\mathbf{x}), \quad (20)$$

where  $q_{\text{PROP}}^{\text{AIS}}$  and  $p_{\text{TGT}}^{\text{AIS}}$  were defined in Eq. (17). Note that sampling from the extended state space target distribution is *practical*, as it only requires one sample from the true posterior distribution.

Taking the expectation of the log unnormalized density ratio under the proposal and target yields lower and upper bounds on  $\log p(\mathbf{x})$ , respectively,

$$\underbrace{\mathbb{E}_{\mathbf{z}_{0:T}^{(1:K)} \sim q_{\text{PROP}}^{\text{AIS}}} \left[ \log \frac{1}{K} \sum_{k=1}^K \frac{p_{\text{TGT}}^{\text{AIS}}(\mathbf{x}, \mathbf{z}_{0:T}^{(k)})}{q_{\text{PROP}}^{\text{AIS}}(\mathbf{z}_{0:T}^{(k)}|\mathbf{x})} \right]}_{\text{ELBO}_{\text{IM-AIS}}(\mathbf{x}; \pi_0, K, T)} \leq \log p(\mathbf{x}) \leq \underbrace{\mathbb{E}_{\substack{\mathbf{z}_{0:T}^{(1)} \sim p_{\text{TGT}}^{\text{AIS}} \\ \mathbf{z}_{0:T}^{(2:K)} \sim q_{\text{PROP}}^{\text{AIS}}}} \left[ \log \frac{1}{K} \sum_{k=1}^K \frac{p_{\text{TGT}}^{\text{AIS}}(\mathbf{x}, \mathbf{z}_{0:T}^{(k)})}{q_{\text{PROP}}^{\text{AIS}}(\mathbf{z}_{0:T}^{(k)}|\mathbf{x})} \right]}_{\text{EUBO}_{\text{IM-AIS}}(\mathbf{x}; \pi_0, K, T)}. \quad (21)$$

which again have KL divergences as the gap in their bounds. Independent Multi-Sample AIS reduces to IWAE for  $T = 1$ , and reduces to single-sample AIS for  $K = 1$ . Both the upper and lower bounds become tight as  $K \rightarrow \infty$  or  $T \rightarrow \infty$ . The IM-AIS upper and lower bounds on  $\log p(\mathbf{x})$  translate to lower and upper bounds on MI, respectively, as in Sec. 1.1.

Since Independent Multi-Sample AIS can be interpreted as IWAE with an AIS proposal, we can use similar arguments as (Burda et al., 2016; Sobolev & Vetrov, 2019) to show that the multi-sample bounds are tighter than their single-sample counterparts. In App. E.3, we show a similar result to Prop. 2.1, which characterizes the improvement of Independent Multi-Sample AIS with increasing  $K$ . In particular, the lower bound on MI is limited to logarithmic improvement over single-sample AIS, with  $I_{\text{IM-AIS}_L}(\pi_0, K, T) \leq I_{\text{AIS}_L}(\pi_0, T) + \log K$ .

### 3.3 COUPLED REVERSE MULTI-SAMPLE AIS BOUNDS

We can exchange the role of the forward and backward annealing chains in Independent Multi-Sample AIS to obtain alternative bounds on the log partition function. We define *Independent Reverse Multi-Sample AIS* (IR-AIS) using the following proposal and target distribution, as shown in Fig. 2

$$q_{\text{PROP}}^{\text{IR-AIS}}(\mathbf{x}, \mathbf{z}_{0:T}^{(1:K)}) := \frac{1}{K} \sum_{s=1}^K q_{\text{PROP}}^{\text{AIS}}(\mathbf{z}_{0:T}^{(s)}|\mathbf{x}) \prod_{\substack{k=1 \\ k \neq s}}^K p_{\text{TGT}}^{\text{AIS}}(\mathbf{x}, \mathbf{z}_{0:T}^{(k)}), \quad p_{\text{TGT}}^{\text{IR-AIS}}(\mathbf{x}, \mathbf{z}_{0:T}^{(1:K)}) := \prod_{k=1}^K p_{\text{TGT}}^{\text{AIS}}(\mathbf{x}, \mathbf{z}_{0:T}^{(k)}).$$



We use a similar approach as in [Sec. 2.1](#) to derive lower and upper bounds on  $\log p(\mathbf{x})$  and MI from these proposal and target distributions in [App. G](#). Just as Independent Multi-Sample AIS extends IWAE using an AIS proposal, we can view Independent Reverse Multi-Sample AIS as an extension of *Reverse* IWAE, which we introduce in [App. F](#). However, these bounds will be impractical in most settings since both the proposal and target distributions require multiple true posterior samples.

To address this impracticality, we propose *Coupled* Reverse Multi-Sample AIS (CR-AIS), which uses backward annealing chains but requires only a *single* posterior sample. In particular, the extended state space target distribution in [Fig. 2](#) initializes  $K$  backward chains from a single  $\mathbf{z}_T \sim \pi_T(\mathbf{z}|\mathbf{x})$ , with remaining transitions denoted by  $p_{\text{TGT}}^{\text{AIS}}(\mathbf{z}_{0:T-1}|\mathbf{z}_T)$ , since they are identical to standard AIS,

$$p_{\text{TGT}}^{\text{CR-AIS}}(\mathbf{x}, \mathbf{z}_{0:T-1}^{(1:K)}, \mathbf{z}_T) := \pi_T(\mathbf{x}, \mathbf{z}_T) \prod_{k=1}^K p_{\text{TGT}}^{\text{AIS}}(\mathbf{z}_{0:T-1}^{(k)}|\mathbf{z}_T, \mathbf{x}). \quad (22)$$

The extended state space proposal is obtained by selecting an index  $s$  uniformly at random and running a single forward AIS chain. We then run  $K - 1$  backward chains, all starting from the last state of the selected forward chain, as visualized in [Fig. 2](#),

$$q_{\text{PROP}}^{\text{CR-AIS}}(\mathbf{z}_{0:T-1}^{(1:K)}, \mathbf{z}_T|\mathbf{x}) := \frac{1}{K} \sum_{s=1}^K q_{\text{PROP}}^{\text{AIS}}(\mathbf{z}_{0:T-1}^{(s)}, \mathbf{z}_T|\mathbf{x}) \prod_{\substack{k=1 \\ k \neq s}}^K p_{\text{TGT}}^{\text{AIS}}(\mathbf{z}_{0:T-1}^{(k)}|\mathbf{z}_T, \mathbf{x}). \quad (23)$$

Taking the expected log ratio under the proposal and target yields lower and upper bounds on  $\log p(\mathbf{x})$ ,

$$\underbrace{-\mathbb{E}_{\substack{\mathbf{z}_{0:T-1}^{(1)}, \mathbf{z}_T \sim q_{\text{PROP}}^{\text{AIS}}(\mathbf{z}_{0:T-1}|\mathbf{x}) \\ \mathbf{z}_{0:T-1}^{(2:K)} \sim p_{\text{TGT}}^{\text{AIS}}(\mathbf{z}_{0:T-1}|\mathbf{z}_T, \mathbf{x})}} \left[ \log \frac{1}{K} \sum_{k=1}^K \frac{q_{\text{PROP}}^{\text{AIS}}(\cdot)}{p_{\text{TGT}}^{\text{AIS}}(\cdot)} \right]}_{\text{ELBO}_{\text{CR-AIS}}(\mathbf{x}; \pi_0, K, T)} \leq \log p(\mathbf{x}) \leq \underbrace{-\mathbb{E}_{\substack{\mathbf{z}_T \sim \pi_T(\mathbf{z}_T|\mathbf{x}) \\ \mathbf{z}_{0:T-1}^{(1:K)} \sim p_{\text{TGT}}^{\text{AIS}}(\mathbf{z}_{0:T-1}|\mathbf{z}_T, \mathbf{x})}} \left[ \log \frac{1}{K} \sum_{k=1}^K \frac{q_{\text{PROP}}^{\text{AIS}}(\cdot)}{p_{\text{TGT}}^{\text{AIS}}(\cdot)} \right]}_{\text{EUBO}_{\text{CR-AIS}}(\mathbf{x}; \pi_0, K, T)}.$$

We show in [App. H.2](#) that Coupled Reverse Multi-Sample AIS bounds get tighter with increasing  $K$ . In [App. H.3](#), we also show that the Coupled Reverse Multi-Sample AIS *upper* bound on MI is limited to logarithmic improvement over single-sample AIS, with  $I_{\text{CR-AIS}_U}(\pi_0, K, T) \geq I_{\text{AIS}_U}(\pi_0, T) - \log K$ .

### 3.4 DISCUSSION

**Relationship with BDMC** Bidirectional Monte Carlo (BDMC) ([Grosse et al., 2015, 2016](#)) was the first to propose multi-sample log partition bounds using AIS chains. In particular, the multi-sample BDMC lower and upper bounds ([Grosse et al., 2015, 2016](#)) on the log partition function correspond to the lower bound of Independent Multi-Sample AIS and upper bound of Coupled Reverse Multi-Sample AIS, respectively. Our probabilistic interpretations provide novel perspective on these existing BDMC bounds. Perhaps surprisingly, we found that the multi-sample BDMC lower bound ([Fig. 2](#) Col. 4, Row 4) and upper bound ([Fig. 2](#) Col. 6, Row 3) do not arise from the same probabilistic interpretation (i.e. are not in the same row in [Fig. 2](#)). In other words, the gap in their log partition function bounds do not correspond to the forward and reverse KL divergences between the same pair of extended state space proposal and target distributions. We experimentally compare all Multi-Sample AIS bounds, including BDMC, in [Sec. 5.1](#) and provide recommendations for which bounds to use in practice.

**Effect of  $K$  and  $T$**  Our Independent and Coupled Reverse Multi-Sample AIS approaches both inherit the linear bias reduction of single-sample AIS in [Prop. 3.1](#), although this computation must be done in serial fashion. While increasing  $K$  involves parallel computation, its bias reduction is often only *logarithmic*, as we have shown for  $I_{\text{IWAE}_L}(q_\theta, K)$  ([Cor. 2.2](#)),  $I_{\text{IM-AIS}_L}(\pi_0, K, T)$  ([App. E.3 Prop. E.2](#)), and  $I_{\text{CR-AIS}_U}(\pi_0, K, T)$  ([App. H.3 Prop. H.2](#)). Based on these arguments, we recommend increasing  $K$  until computation can no longer be parallelized on given hardware and allocating all remaining resources to increasing  $T$ .

## 4 MINE-AIS ESTIMATION OF MUTUAL INFORMATION

In this section, we present energy-based bounds which are designed for settings where the true conditional density  $p(\mathbf{x}|\mathbf{z})$  is unknown. We first review MINE ([Belghazi et al., 2018](#)) in [Sec. 4.1](#), and

present probabilistic interpretations which allow us to derive *Generalized* MINE lower bounds with a variational  $q_\theta(\mathbf{z}|\mathbf{x})$  as the base distribution instead of the marginal  $p(\mathbf{z})$ . Our main contribution in this section is the MINE-AIS method, which optimizes a tighter lower bound on MI than the Generalized MINE lower bound and extends Multi-Sample AIS evaluation to the case where  $p(\mathbf{x}|\mathbf{z})$  is unknown.

#### 4.1 GENERALIZED MUTUAL INFORMATION NEURAL ESTIMATION

To derive a probabilistic interpretation for MINE (Belghazi et al., 2018), consider an energy based approximation to the joint distribution  $p(\mathbf{x}, \mathbf{z})$ . To extend MINE, we consider a general base variational distribution  $q_\theta(\mathbf{z}|\mathbf{x})$  in place of the marginal  $p(\mathbf{z})$

$$\pi_{\theta,\phi}(\mathbf{x}, \mathbf{z}) := \frac{1}{\mathcal{Z}_{\theta,\phi}} p(\mathbf{x}) q_\theta(\mathbf{z}|\mathbf{x}) e^{T_\phi(\mathbf{x}, \mathbf{z})}, \quad \text{where } \mathcal{Z}_{\theta,\phi} = \mathbb{E}_{p(\mathbf{x}) q_\theta(\mathbf{z}|\mathbf{x})} \left[ e^{T_\phi(\mathbf{x}, \mathbf{z})} \right], \quad (24)$$

where  $T_\phi(\mathbf{x}, \mathbf{z})$  is the negative energy function and the partition function  $\mathcal{Z}_{\theta,\phi}$  integrates over both  $\mathbf{x}$  and  $\mathbf{z}$ . Subtracting a joint KL divergence  $D_{\text{KL}}[p(\mathbf{x}, \mathbf{z}) || \pi_{\theta,\phi}(\mathbf{x}, \mathbf{z})]$  from  $I(\mathbf{x}; \mathbf{z})$ , we obtain the *Generalized* MINE-DV lower bound on MI

$$I(\mathbf{x}; \mathbf{z}) \geq I_{\text{GMINE-DV}}(q_\theta, T_\phi) := \underbrace{\mathbb{E}_{p(\mathbf{x}, \mathbf{z})} \left[ \log \frac{q_\theta(\mathbf{z}|\mathbf{x})}{p(\mathbf{z})} \right]}_{I_{\text{BAL}}(q_\theta)} + \underbrace{\mathbb{E}_{p(\mathbf{x}, \mathbf{z})} [T_\phi(\mathbf{x}, \mathbf{z})] - \log \mathbb{E}_{p(\mathbf{x}) q_\theta(\mathbf{z}|\mathbf{x})} \left[ e^{T_\phi(\mathbf{x}, \mathbf{z})} \right]}_{\text{contrastive term}}. \quad (25)$$

Note that the standard MINE-DV lower bound (Belghazi et al., 2018) corresponds to Generalized MINE-DV using the prior  $p(\mathbf{z})$  as the proposal,  $I_{\text{MINE-DV}}(T_\phi) = I_{\text{GMINE-DV}}(p(\mathbf{z}), T_\phi)$ . In App. K.3, we interpret the contrastive term in Eq. (25) as arising from the dual representation of the KL divergence  $D_{\text{KL}}[p(\mathbf{x}, \mathbf{z}) || p(\mathbf{x}) q_\theta(\mathbf{z}|\mathbf{x})]$ .

The Generalized MINE-F bound is a looser lower bound than Generalized MINE-DV, which can be derived from Eq. (25) using the inequality  $\log u \leq \frac{u}{e}$ ,

$$I_{\text{GMINE-DV}}(q_\theta, T_\phi) \geq I_{\text{GMINE-F}}(q_\theta, T_\phi) := \mathbb{E}_{p(\mathbf{x}, \mathbf{z})} \left[ \log \frac{q_\theta(\mathbf{z}|\mathbf{x})}{p(\mathbf{z})} \right] + \mathbb{E}_{p(\mathbf{x}, \mathbf{z})} [T_\phi(\mathbf{x}, \mathbf{z})] - \mathbb{E}_{p(\mathbf{x}) q_\theta(\mathbf{z}|\mathbf{x})} \left[ e^{T_\phi(\mathbf{x}, \mathbf{z})} - 1 \right].$$

Generalized MINE-F reduces to standard MINE-F when the base distribution is the prior, with  $I_{\text{MINE-F}}(T_\phi) = I_{\text{GMINE-F}}(p(\mathbf{z}), T_\phi)$ . We provide a probabilistic interpretation of Generalized MINE-F in App. J.3, and a conjugate duality interpretation in App. K.4.

Despite the intractability of the log partition function term  $\log \mathcal{Z}_{\theta,\phi}$  in Eq. (25), Belghazi et al. (2018) use direct sampling inside the logarithm for training  $T_\phi$ . Our MINE-AIS method will both improve the training and evaluation schemes of (Generalized) MINE and optimize a tighter lower bound.

#### 4.2 MINE-AIS ESTIMATION OF MUTUAL INFORMATION

In this section, we present MINE-AIS, which is inspired by Generalized MINE but optimizes a tighter lower bound on MI that involves an intractable log partition function. We show in Prop. L.2 that this bound corresponds to the limiting behavior of the GIWAE lower bound as  $K \rightarrow \infty$ . However, we present a qualitatively different training scheme inspired by contrastive divergence learning of energy-based models (Hinton, 2002) in Sec. 4.2.1. In Sec. 4.2.2, we use Multi-Sample AIS to evaluate the intractable log partition function, and show that MINE-AIS reduces to the methods in Sec. 3 for the optimal critic function or known  $p(\mathbf{x}|\mathbf{z})$ .

To begin, we consider a flexible energy-based distribution  $\pi_{\theta,\phi}(\mathbf{z}|\mathbf{x})$  as an approximation to the posterior  $p(\mathbf{z}|\mathbf{x})$  (Poole et al., 2019; Arbel et al., 2021)

$$\pi_{\theta,\phi}(\mathbf{z}|\mathbf{x}) := \frac{1}{\mathcal{Z}_{\theta,\phi}(\mathbf{x})} q_\theta(\mathbf{z}|\mathbf{x}) e^{T_\phi(\mathbf{x}, \mathbf{z})}, \quad \text{where } \mathcal{Z}_{\theta,\phi}(\mathbf{x}) = \mathbb{E}_{q_\theta(\mathbf{z}|\mathbf{x})} \left[ e^{T_\phi(\mathbf{x}, \mathbf{z})} \right], \quad (26)$$

where  $q_\theta(\mathbf{z}|\mathbf{x})$  is a base variational distribution which can be tractably sampled from and evaluated and  $T_\phi(\mathbf{x}, \mathbf{z})$  is the negative energy or critic function.

Plugging  $\pi_{\theta,\phi}(\mathbf{z}|\mathbf{x})$  into the BA lower bound, we denote the resulting bound as the *Implicit Barber-Agakov Lower bound* (IBAL). We use the term ‘‘implicit’’, since it is often difficult to explicitly

evaluate the IBAL due to the intractable log partition function term. After simplifying in [App. J.1](#),

$$\begin{aligned}
I(\mathbf{x}; \mathbf{z}) &\geq \text{IBAL}(q_\theta, T_\phi) := I_{\text{BAL}}(\pi_{\theta, \phi}) = \mathbb{E}_{p(\mathbf{x}, \mathbf{z})} \left[ \log \frac{q_\theta(\mathbf{z}|\mathbf{x})}{p(\mathbf{z})} \right] + \mathbb{E}_{p(\mathbf{x}, \mathbf{z})} [T_\phi(\mathbf{x}, \mathbf{z})] - \mathbb{E}_{p(\mathbf{x})} [\log \mathcal{Z}_{\phi, \theta}(\mathbf{x})] \\
&= \underbrace{\mathbb{E}_{p(\mathbf{x}, \mathbf{z})} \left[ \log \frac{q_\theta(\mathbf{z}|\mathbf{x})}{p(\mathbf{z})} \right]}_{I_{\text{BAL}}(q_\theta)} + \underbrace{\mathbb{E}_{p(\mathbf{x}, \mathbf{z})} \left[ \log \frac{e^{T_\phi(\mathbf{x}, \mathbf{z})}}{\mathbb{E}_{q_\theta(\mathbf{z}|\mathbf{x})} [e^{T_\phi(\mathbf{x}, \mathbf{z})}]} \right]}_{\text{contrastive term} \leq \mathbb{E}_{p(\mathbf{x})} [D_{\text{KL}}[p(\mathbf{z}|\mathbf{x})||q_\theta(\mathbf{z}|\mathbf{x})]]}, \quad (27)
\end{aligned}$$

where the gap of the IBAL is  $\mathbb{E}_{p(\mathbf{x})} [D_{\text{KL}}[p(\mathbf{z}|\mathbf{x})||\pi_{\theta, \phi}(\mathbf{z}|\mathbf{x})]]$ . Note that the IBAL generalizes the Unnormalized Barber-Agakov bound from [Poole et al. \(2019\)](#), with  $I_{\text{UBA}}(T_\phi) = \text{IBAL}(p(\mathbf{z}), T_\phi)$ .

**Proposition 4.1.** *For a given  $q_\theta(\mathbf{z}|\mathbf{x})$ , the optimal IBAL critic function equals the log importance weights up to a constant  $T^*(\mathbf{x}, \mathbf{z}) = \log \frac{p(\mathbf{x}, \mathbf{z})}{q_\theta(\mathbf{z}|\mathbf{x})} + c(\mathbf{x})$ . For this  $T^*$ , we have  $\text{IBAL}(q_\theta, T^*) = I(\mathbf{x}; \mathbf{z})$ .*

**Relationship with MINE**  $\text{IBAL}(q_\theta, T_\phi)$  provides a tighter lower bound than Generalized MINE, as we discuss in detail in [App. J](#) and summarize in [Fig. 8](#). In particular, we have

$$I(\mathbf{x}; \mathbf{z}) \geq \text{IBAL}(q_\theta, T_\phi) \geq I_{\text{GMINE-DV}}(q_\theta, T_\phi) \geq I_{\text{GMINE-F}}(q_\theta, T_\phi). \quad (28)$$

Our MINE-AIS method will optimize and evaluate the intractable IBAL directly.

**Relationship with GIWAE** The IBAL lower bound resembles the GIWAE lower bound in that both improve upon the BA variational bound using a contrastive term. Further, [Prop. 4.1](#) and [Cor. 2.4](#) show that, in both cases, the optimal critic function equals the true log importance weights plus a constant. The following proposition shows that  $\text{IBAL}(q_\theta, T_\phi)$  can be viewed the limiting behavior of the GIWAE lower bound as  $K \rightarrow \infty$ .

**Proposition 4.2** (IBAL as Limiting Behavior of GIWAE). *For given  $q_\theta(\mathbf{z}|\mathbf{x})$  and  $T_\phi(\mathbf{x}, \mathbf{z})$ , we have*

$$\lim_{K \rightarrow \infty} I_{\text{GIWAE}_L}(q_\theta, T_\phi, K) = \text{IBAL}(q_\theta, T_\phi). \quad (29)$$

See [App. L.2](#) for proof. To gain intuition for [Prop. L.2](#), we consider a closely related result involving the *marginal SNIS distribution* of GIWAE  $q_{\text{PROP}}^{\text{GIWAE}}(\mathbf{z}|\mathbf{x}; K)$ , which results from sampling  $K$  times from  $q_\theta(\mathbf{z}|\mathbf{x})$  and returning the sample in index  $s \sim q_{\text{PROP}}^{\text{GIWAE}}(s|\mathbf{x}, \mathbf{z}^{(1:K)}) \propto e^{T_\phi(\mathbf{x}, \mathbf{z}^{(s)})}$ . In [App. L.3](#), we show that in the limit as  $K \rightarrow \infty$ , the marginal SNIS distribution of GIWAE matches the MINE-AIS energy-based posterior  $\pi_{\theta, \phi}(\mathbf{z}|\mathbf{x}) \propto q_\theta(\mathbf{z}|\mathbf{x})e^{T_\phi(\mathbf{x}, \mathbf{z})}$ . In both cases, the energy or critic function ‘modulates’ the base distribution  $q_\theta(\mathbf{z}|\mathbf{x})$  to better approximate the true posterior.

The contrastive term in the GIWAE bound is tractable, as it only requires a single posterior sample and  $K - 1$  samples from the base distribution. As shown in [Cor. 2.4](#), this limits the improvement of  $I_{\text{GIWAE}_L}(q_\theta, T)$  over  $I_{\text{BAL}}(q_\theta)$  to  $\log K$  nats, even for the optimal critic function. By contrast, in the following proposition we show that the contrastive term in  $\text{IBAL}(q_\theta, T_\phi)$  is expressive enough to potentially close the gap in the BA bound. This improved contrastive term comes at the cost of tractability, as  $\text{IBAL}(q_\theta, T_\phi)$  involves an intractable log partition function  $\log \mathbb{E}_{q_\theta(\mathbf{z}|\mathbf{x})} [e^{T_\phi(\mathbf{x}, \mathbf{z})}]$ .

**Proposition 4.3.** *Suppose the critic function  $T_\phi(\mathbf{x}, \mathbf{z})$  is parameterized by  $\phi$ , and that  $\exists \phi_0$  s.t.  $T_{\phi_0}(\mathbf{x}, \mathbf{z}) = \text{const}$ . For a given  $q_\theta(\mathbf{z}|\mathbf{x})$ , let  $T_{\phi^*}(\mathbf{x}, \mathbf{z})$  denote the critic function that maximizes  $\text{IBAL}(q_\theta, T_\phi)$ . Then,*

$$I_{\text{BAL}}(q_\theta) \leq \text{IBAL}(q_\theta, T_{\phi^*}) \leq I(\mathbf{x}; \mathbf{z}) = I_{\text{BAL}}(q_\theta) + \mathbb{E}_{p(\mathbf{x})} [D_{\text{KL}}[p(\mathbf{z}|\mathbf{x})||q_\theta(\mathbf{z}|\mathbf{x})]]. \quad (30)$$

*In particular, the contrastive term in [Eq. \(27\)](#) is upper bounded by  $\mathbb{E}_{p(\mathbf{x})} [D_{\text{KL}}[p(\mathbf{z}|\mathbf{x})||q_\theta(\mathbf{z}|\mathbf{x})]]$ .*

See [App. L.1](#) for proof. In the following sections, we present our MINE-AIS method, which overcomes the intractability of  $\text{IBAL}(q_\theta, T_\phi)$  using an MCMC-based training scheme and AIS-based evaluation.

#### 4.2.1 ENERGY-BASED TRAINING OF THE IBAL

Although the log partition function  $\log \mathcal{Z}_{\theta, \phi}(\mathbf{x})$  in the IBAL is intractable to evaluate, we only require an unbiased estimator of its gradient for training. Differentiating [Eq. \(27\)](#) with respect to the

parameters  $\theta$  and  $\phi$  of the variational and energy function, respectively, we obtain

$$\frac{\partial}{\partial \theta} \text{IBAL}(q_\theta, T_\phi) = \mathbb{E}_{p(\mathbf{x}, \mathbf{z})} \left[ \frac{\partial}{\partial \theta} \log q_\theta(\mathbf{z}|\mathbf{x}) \right] - \mathbb{E}_{p(\mathbf{x})\pi_{\theta, \phi}(\mathbf{z}|\mathbf{x})} \left[ \frac{\partial}{\partial \theta} \log q_\theta(\mathbf{z}|\mathbf{x}) \right]. \quad (31)$$

$$\frac{\partial}{\partial \phi} \text{IBAL}(q_\theta, T_\phi) = \mathbb{E}_{p(\mathbf{x}, \mathbf{z})} \left[ \frac{\partial}{\partial \phi} T_\phi(\mathbf{x}, \mathbf{z}) \right] - \mathbb{E}_{p(\mathbf{x})\pi_{\theta, \phi}(\mathbf{z}|\mathbf{x})} \left[ \frac{\partial}{\partial \phi} T_\phi(\mathbf{x}, \mathbf{z}) \right]. \quad (32)$$

Eq. (31) indicates that in order to maximize the IBAL as a function of  $\theta$  and  $\phi$ , we need to increase the value of the energy function  $T_\phi$  or score function  $\log q_\theta(\mathbf{z}|\mathbf{x})$  on the *real* samples of the true joint  $p(\mathbf{x}, \mathbf{z})$  and decrease the value on *fake* samples from the approximate  $p(\mathbf{x})\pi_{\theta, \phi}(\mathbf{z}|\mathbf{x})$ . However, as is common in training energy-based models, it is difficult to draw samples from  $\pi_{\theta, \phi}$ .

In order to sample from  $\pi_{\theta, \phi}(\mathbf{z}|\mathbf{x})$ , a natural approach is to initialize MCMC chains from a sample of the base distribution  $q_\theta(\mathbf{z}|\mathbf{x})$ , using Hamiltonian Monte Carlo (HMC) transition kernels (Neal, 2011), for example. However, we may require infeasibly long MCMC chains when the base distribution is far from desired energy-based model  $\pi_{\theta, \phi}(\mathbf{z}|\mathbf{x})$ . Instead, we can choose to initialize the chains from the true posterior sample  $\mathbf{z} \sim p(\mathbf{z}|\mathbf{x})$  for a simulated data point  $\mathbf{x} \sim p(\mathbf{x})$ . Letting  $\mathcal{T}_{1:M}$  indicate the composition of  $M$  transition steps, the approximate energy function gradient becomes

$$\frac{\partial}{\partial \phi} \text{IBAL}(q_\theta, T_\phi) \approx \mathbb{E}_{p(\mathbf{x}, \mathbf{z})} \left[ \frac{\partial}{\partial \phi} T_\phi(\mathbf{x}, \mathbf{z}) \right] - \mathbb{E}_{p(\mathbf{x}, \mathbf{z}_0)\mathcal{T}_{1:M}(\mathbf{z}|\mathbf{z}_0, \mathbf{x})} \left[ \frac{\partial}{\partial \phi} T_\phi(\mathbf{x}, \mathbf{z}) \right], \quad (33)$$

We can use an identical modification for the gradient with respect to  $\theta$ .

This initialization greatly reduces the computational cost and variance of the estimated gradient and enables training energy functions in high dimensional latent spaces, as shown in our experiments. This approach is in spirit similar to Contrastive Divergence learning of energy-based models (Hinton, 2002), where one starts an MCMC chain from the true data distribution to obtain a lower variance gradient estimate.

#### 4.2.2 MULTI-SAMPLE AIS EVALUATION OF THE IBAL

After learning an critic function using our improved MINE-AIS training scheme, we still need to evaluate the IBAL lower bound on MI. Although we have an unbiased, low variance estimate for  $\mathbb{E}_{p(\mathbf{x}, \mathbf{z})} [T_\phi(\mathbf{x}, \mathbf{z})]$ , the log partition function  $\log \mathcal{Z}_{\theta, \phi}(\mathbf{x})$  is intractable. We use our Multi-Sample AIS bounds from Sec. 3 to provide both an upper bound and approximate lower bound on  $\text{IBAL}(q_\theta, T_\phi)$ .

**Multi-Sample AIS upper bound on IBAL.** We first consider estimating a lower bound on the log partition function  $\log \mathcal{Z}_{\theta, \phi}(\mathbf{x})$  of  $\pi_{\theta, \phi}(\mathbf{z}|\mathbf{x}) = \frac{1}{\mathcal{Z}_{\theta, \phi}(\mathbf{x})} q_\theta(\mathbf{z}|\mathbf{x}) e^{T_\phi(\mathbf{x}, \mathbf{z})}$ . In order to do so, we can use a Multi-Sample AIS lower bound with a base distribution  $q_\theta(\mathbf{z}|\mathbf{x})$ , intermediate distributions  $\pi_t(\mathbf{z}|\mathbf{x}) \propto q_\theta(\mathbf{z}|\mathbf{x}) e^{\beta_t T_\phi(\mathbf{x}, \mathbf{z})}$ , and final distribution  $\pi_{\theta, \phi}(\mathbf{z}|\mathbf{x})$  at  $\beta_T = 1$ . This yields a stochastic lower bound on  $\log \mathcal{Z}_{\theta, \phi}(\mathbf{x})$ , which translates to a stochastic upper bound for estimating  $\text{IBAL}(q_\theta, T_\phi)$ .

**Multi-Sample AIS approximate lower bound on IBAL.** In order to obtain a lower bound on IBAL and preserve a lower bound on  $I(\mathbf{x}; \mathbf{z})$ , we would like to estimate an upper bound on  $\log \mathcal{Z}_{\theta, \phi}(\mathbf{x})$  using Multi-Sample AIS. However, note that this requires true samples from  $\pi_{\theta, \phi}(\mathbf{z}|\mathbf{x})$  to initialize backward chains. Since these samples are unavailable, we argue in App. M.1 Prop. M.1 that, under mild conditions, Multi-Sample AIS can preserve an approximate upper bound on  $\log \mathcal{Z}_{\theta, \phi}(\mathbf{x})$  and lower bound on  $\text{IBAL}(q_\theta, T_\phi)$  by initializing reverse chains from the true posterior  $p(\mathbf{z}|\mathbf{x})$  instead of  $\pi_{\theta, \phi}(\mathbf{z}|\mathbf{x})$ . With the optimal critic function, we have  $\pi_{\theta, \phi}(\mathbf{z}|\mathbf{x}) = p(\mathbf{z}|\mathbf{x})$ , and our approximate lower bound becomes a true stochastic lower bound on  $\text{IBAL}(q_\theta, T_\phi^*) = I(\mathbf{x}; \mathbf{z})$ .

If the full joint density  $p(\mathbf{x}, \mathbf{z})$  is known, the MINE-AIS upper bound and approximate lower bound on  $\text{IBAL}(q_\theta, T_\phi)$  reduce to the Multi-Sample AIS upper and lower bounds on  $I(\mathbf{x}; \mathbf{z})$ .

## 5 EXPERIMENTS

In this section, we evaluate our proposed Multi-Sample AIS, MINE-AIS, and GIWAE bounds for estimating the mutual information of deep generative models such as VAEs and GANs trained on MNIST and CIFAR datasets. We chose deep generative models as they reflect complex relationships

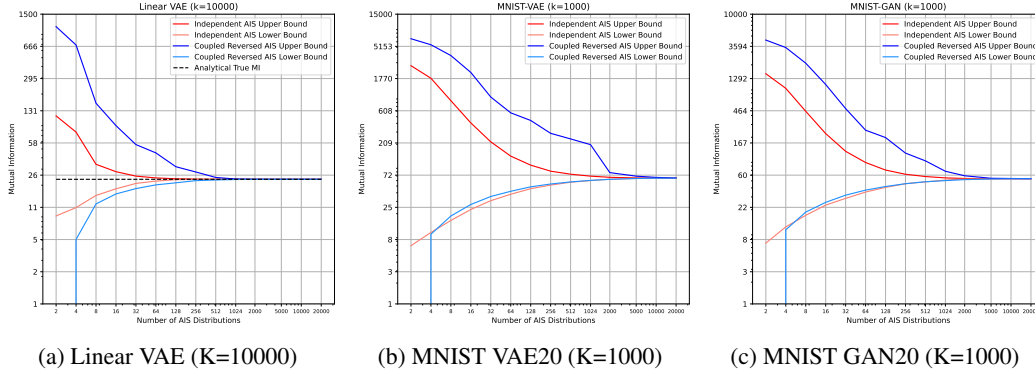


Figure 3: Comparing Multi-Sample AIS sandwich bounds for varying number of AIS distributions.

between latent variables and high-dimensional images, and allow comparison across methods with different assumptions.

We first compare our various Multi-Sample AIS bounds in [Sec. 5.1](#) with the goal of making recommendations for which bound to use in practice. We then compare Multi-Sample AIS and IWAE bounds in [Sec. 5.2](#) for estimating large ground truth values of MI. We will show that Multi-Sample AIS can tightly bound the ground truth MI, assuming access to the true  $p(\mathbf{x}|\mathbf{z})$ . This ground truth information is valuable for evaluating the bias of our energy-based lower bounds, including GIWAE and MINE-AIS, which are applicable even when  $p(\mathbf{x}|\mathbf{z})$  is unknown. We provide a detailed comparison of these energy-based MI bounds in [Sec. 5.3](#). We describe experimental details and link to our publicly available code in [App. O](#).

### 5.1 COMPARISON OF MULTI-SAMPLE AIS BOUNDS

In [Fig. 3](#), we compare the performance of our various Multi-Sample AIS bounds for MI estimation of a Linear VAE with 10 latent variables and random weights, and VAE and GAN models with 20 latent variables trained on MNIST. We provide more extensive results in [App. I](#).

To obtain an upper bound on MI, we recommend using the Independent Multi-Sample AIS ELBO for log partition function estimation. This corresponds to the forward direction of BDMC and achieves the best performance in all cases. This upper bound uses independent samples and is not limited to  $\log K$  improvement, in contrast to the Coupled Reverse Multi-Sample AIS upper bound on MI ([Prop. H.2](#)).

The results are less conclusive for the Multi-Sample AIS lower bounds on MI, where either the Independent Multi-Sample AIS EUBO or Coupled Reverse AIS EUBO may be preferable for log partition function estimation. Recall that these bounds have different sources of stochasticity that provide improvement over single-chain AIS. The stochasticity in the Independent Multi-Sample AIS lower bound on MI comes from  $K - 1$  independent negative forward chains which, by [App. E.3 Prop. E.2](#), can only lead to  $\log K$  improvement over single-sample AIS. However, these gains are easily attained for low values of  $T$ . For example, with two total AIS distributions, which corresponds to simple importance sampling with  $\pi_0(\mathbf{z}) = p(\mathbf{z})$ , the Independent Multi-Sample AIS lower bound on MI reduces to Structured INFO-NCE and saturates to  $\log K$ . This may be useful for quickly estimating values of MI at a similar order of magnitude as  $\log K$ .

The stochasticity in the Coupled Reverse AIS lower bound on MI is induced by MCMC transitions in  $K$  coupled backward chains. While this does not formally limit the improvement over single-sample AIS, we see in [Fig. 3](#) that at least moderate values of  $T$  may be needed to match or marginally improve upon Independent Multi-Sample AIS. These observations suggest that the preferred lower bounds on MI may vary based on the scale of the true MI and the amount of computation available.

### 5.2 MULTI-SAMPLE AIS ESTIMATION OF MUTUAL INFORMATION

We compare Multi-Sample AIS MI estimation against IWAE, since both methods assume the full joint distribution is available. For the initial distribution of AIS or variational distribution of IWAE, we can use any distribution that is tractable to sample and evaluate. We experiment using both the prior  $p(\mathbf{z})$  and a learned Gaussian  $q_\theta(\mathbf{z}|\mathbf{x})$ . [Table 1](#) summarizes our results.



Table 1: MI Estimation on MNIST and CIFAR-10 with IWAE (with varying number of samples  $K$ ), and Multi-Sample AIS (with varying number of intermediate distributions  $T$ ). Bounds with a gap of less than 2 nats from the ground truth MI are in bold.

Method	Proposal	MNIST VAE2	MNIST VAE10	MNIST VAE100	MNIST GAN2	MNIST GAN10	MNIST GAN100
AIS ( $T=1$ )	$p(\mathbf{z})$	(0.00, 249.82)	(0.00, 1929.84)	(0.00, 5830.52)	(0.00, 726.27)	(0.00, 786.12)	(0.00, 861.38)
	$q(\mathbf{z} \mathbf{x})$	<b>(7.59, 9.24)</b>	(21.06, 63.00)	(34.49, 362.13)	(7.21, 19.13)	(3.67, 314.72)	(2.61, 513.33)
AIS ( $T=500$ )	$p(\mathbf{z})$	<b>(8.63, 9.12)</b>	(34.05, 39.09)	<b>(79.90, 95.17)</b>	<b>(9.21, 10.83)</b>	<b>(21.57, 22.47)</b>	<b>(25.86, 27.55)</b>
	$q(\mathbf{z} \mathbf{x})$	<b>(9.09, 9.09)</b>	<b>(34.16, 34.29)</b>	<b>(80.19, 82.34)</b>	<b>(10.69, 11.06)</b>	<b>(21.60, 23.06)</b>	<b>(25.58, 29.53)</b>
AIS ( $T=30K$ )	$p(\mathbf{z})$	<b>(8.98, 9.09)</b>	<b>(34.21, 34.21)</b>	<b>(80.78, 80.84)</b>	<b>(10.56, 10.81)</b>	<b>(21.97, 22.02)</b>	<b>(26.47, 26.52)</b>
	$q(\mathbf{z} \mathbf{x})$	<b>(9.09, 9.09)</b>	<b>(34.21, 34.21)</b>	<b>(80.77, 80.80)</b>	<b>(10.80, 10.81)</b>	<b>(22.01, 22.01)</b>	<b>(26.53, 26.54)</b>
IWAE ( $K=1$ )	$p(\mathbf{z})$	(0.00, 799.55)	(0.00, 3827.58)	(0.00, 11501.92)	(0.00, 1638.10)	(0.00, 1630.00)	(0.00, 1740.39)
	$q(\mathbf{z} \mathbf{x})$	<b>(8.63, 9.19)</b>	(25.20, <b>35.34</b> )	(44.54, 95.63)	(8.83, 17.58)	(4.23, 57.47)	(3.23, 260.87)
IWAE ( $K=1K$ )	$p(\mathbf{z})$	(6.81, 29.40)	(6.91, 1197.75)	(6.91, 4234.19)	(6.88, 121.89)	(6.91, 446.80)	(6.91, 494.73)
	$q(\mathbf{z} \mathbf{x})$	<b>(9.09, 9.10)</b>	(31.69, <b>34.24</b> )	(51.44, 85.30)	<b>(10.74, 11.40)</b>	(11.14, 52.73)	(10.14, 201.18)
IWAE ( $K=1M$ )	$p(\mathbf{z})$	<b>(9.09, 9.09)</b>	(13.82, 376.89)	(13.82, 2247.73)	<b>(10.76, 10.99)</b>	(13.81, 81.51)	(13.82, 114.01)
	$q(\mathbf{z} \mathbf{x})$	<b>(9.09, 9.09)</b>	<b>(34.10, 34.22)</b>	(58.35, 83.39)	<b>(10.81, 10.81)</b>	(17.76, 30.88)	(16.98, 58.04)

Method	Proposal	CIFAR GAN5	CIFAR GAN10	CIFAR GAN100
AIS $T=1$	$p(\mathbf{z})$	(0.00, 3601256.00)	(0.00, 4035635.75)	(0.00, 4853410.50)
	$q(\mathbf{z} \mathbf{x})$	(10.80, 157378.25)	(13.02, 758075.75)	(12.47, 2724562.25)
AIS $T=500$	$p(\mathbf{z})$	(18.37, 259.27)	(29.52, 33089.90)	(104.51, 63290.40)
	$q(\mathbf{z} \mathbf{x})$	(32.47, 69.54)	(48.16, 136.15)	(145.19, 2786.53)
AIS $T=100K$	$p(\mathbf{z})$	<b>(39.58, 41.06)</b>	<b>(71.87, 73.98)</b>	(480.26, 488.07)
	$q(\mathbf{z} \mathbf{x})$	<b>(39.22, 40.05)</b>	<b>(72.85, 73.54)</b>	(479.27, 484.84)
IWAE $K=1$	$p(\mathbf{z})$	(0.00, 7095384.00)	(0.00, 7765695.50)	(0.00, 9916102.00)
	$q(\mathbf{z} \mathbf{x})$	(14.53, <b>40.31</b> )	(17.45, 77.52)	(20.00, 5346.85)
IWAE $K=1K$	$p(\mathbf{z})$	(6.91, 1065552.25)	(6.91, 2044170.75)	(6.91, 2856714.50)
	$q(\mathbf{z} \mathbf{x})$	(21.43, <b>39.73</b> )	(24.06, <b>74.00</b> )	(26.98, 5283.13)
IWAE $K=1M$	$p(\mathbf{z})$	(13.82, 96698.10)	(13.82, 710511.63)	(13.82, 1903854.50)
	$q(\mathbf{z} \mathbf{x})$	(28.34, <b>39.71</b> )	(30.73, <b>73.36</b> )	(33.81, 5271.56)

**IWAE** As described in Sec. 2.3, IWAE bounds encompass a wide range of MI estimators. The  $K = 1$  bounds with learned  $q_\theta(\mathbf{z}|\mathbf{x})$  correspond to BA bounds, while for  $K > 1$  and  $p(\mathbf{z})$  as the proposal, we obtain Structured INFONCE. While the IWAE upper bound on MI, which uses the  $\log p(\mathbf{x})$  lower bound with independent sampling from  $q_\theta(\mathbf{z}|\mathbf{x})$ , is tight for certain models, we can see that the improvement of the IWAE lower bound on MI is limited to  $\log K$ , as expected from Prop. 2.1. In particular, exponentially large sample size is required to close the gap from the BA lower bound ( $K = 1$ ) to the true MI. For example, on CIFAR GAN100, at least  $e^{460}$  total samples are required to match the lower bound estimated by AIS. In App. B.3, we explicitly decompose  $I_{\text{IWAE}_L}(q_\theta, K)$  into an  $I_{\text{BA}_L}(q_\theta)$  term and a contrastive term to validate this logarithmic improvement with increasing  $K$ .

**Multi-Sample AIS** We evaluate Multi-Sample AIS with  $K = 48$  chains on MNIST and  $K = 12$  on CIFAR, and a varying number of intermediate distributions  $T$ . We show results for the Independent Multi-Sample AIS upper bound on MI and Coupled Reverse Multi-Sample AIS lower bound on MI in Table 1. Using large enough values of  $T$ , Multi-Sample AIS can tightly sandwich large values of ground truth MI for all models and datasets considered. This is in stark contrast to the exponential sample complexity required for the IWAE MI lower bound, and highlights that increasing  $T$  in Multi-Sample AIS is a practical way to reduce bias using additional computation. We provide runtime details in App. O.2.

### 5.3 ENERGY-BASED ESTIMATION OF MUTUAL INFORMATION

In this section, we evaluate the performance of our GIWAE and MINE-AIS methods, which assume access to a known marginal  $p(\mathbf{z})$  but not the conditional  $p(\mathbf{x}|\mathbf{z})$ . In Cor. 2.5, we have shown that for a fixed  $q_\theta(\mathbf{z}|\mathbf{x})$ , we have  $I_{\text{BA}_L}(q_\theta) \leq I_{\text{GIWAE}_L}(q_\theta, T_{\phi^*}, K) \leq I_{\text{IWAE}_L}(q_\theta, K) \leq I_{\text{BA}_L}(q_\theta) + \log K$ . Although we perform separate optimizations and obtain different  $q_\theta(\mathbf{z}|\mathbf{x})$  for each entry in Fig. 5a, we find that these relationships hold in almost all cases. We summarize the gaps in these bounds and their relationships in Fig. 5b.

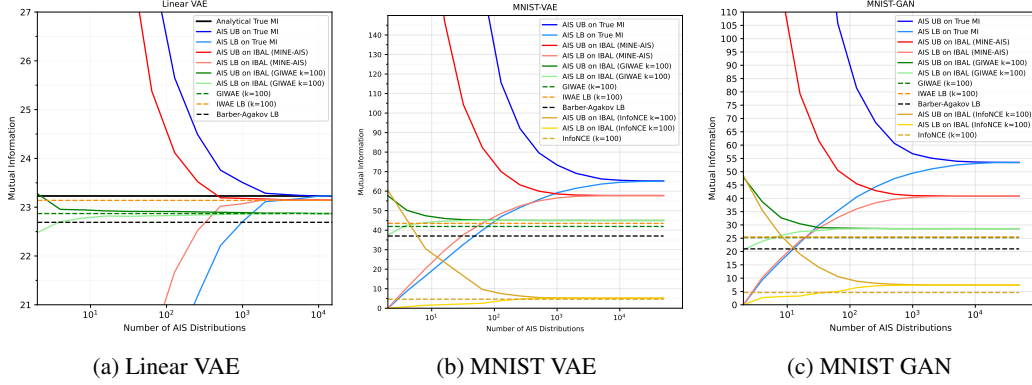


Figure 4: Estimating IBAL using Multi-Sample AIS for various methods of critic function training.

Input Used	Model	Bound		
		Linear VAE10	MNIST VAE20	MNIST GAN20
$p(\mathbf{x}, \mathbf{z})$	Analytical	23.23	N/A	N/A
	AIS Bound on True MI	(23.23, 23.23)	(65.11, 65.17)	(53.43, 53.50)
$p(\mathbf{x}, \mathbf{z})$ Joint Samples	IWAE LB ( $K = 1000$ )	20.53 + 2.66 = 23.19	38.21 + 6.90 = 45.11	20.97 + 6.91 = 27.88
	IWAE LB ( $K = 100$ )	21.64 + 1.50 = 23.14	38.86 + 4.61 = 43.47	20.86 + 4.60 = 25.46
	Structured InfoNCE LB ( $K = 1000$ )	6.91	6.91	6.91
	Structured InfoNCE LB ( $K = 100$ )	4.61	4.61	4.61
$p(\mathbf{z})$ Joint Samples	AIS Bound on IBAL (MINE-AIS)	(23.15, 23.15)	(57.72, 57.74)	(40.79, 40.79)
	AIS Bound on IBAL (GIWAE $K = 100$ )	(22.87, 22.87)	(44.97, 44.97)	(28.61, 28.62)
	AIS Bound on IBAL (InfoNCE $K = 100$ )	(11.38, 11.39)	(5.18, 5.18)	(7.42, 7.42)
	Generalized IWAE LB ( $K = 1000$ )	22.31 + 0.38 = 22.69	37.23 + 6.55 = 43.78	20.50 + 6.72 = 27.22
	Generalized IWAE LB ( $K = 100$ )	22.48 + 0.39 = 22.87	37.56 + 4.34 = 41.90	20.68 + 4.57 = 25.25
	Barber-Agakov LB ( $K = 1$ )	22.69	37.92	21.42
Joint Samples	InfoNCE LB ( $K = 1000$ )	6.91	6.91	6.91
	InfoNCE LB ( $K = 100$ )	4.61	4.61	4.61

Figure 5: (a) Comparison of energy-based bounds (GIWAE and MINE-AIS) with other MI bounds. (b) Visualizing the gaps of various energy-based lower bounds and their relationships.

**BA, IWAE, and GIWAE Bounds** Recall that  $I_{GIWAE_L}(q_\theta, T_\phi, K)$  (Eq. (11)) and  $I_{IWAE_L}(q_\theta, K)$  (Eq. (14)) can be decomposed into the sum of a BA lower bound and a contrastive term. We report the contribution of each term along with the overall lower bound in Fig. 5a. Despite the fact that GIWAE uses a learned  $T_\phi(\mathbf{x}, \mathbf{z})$  instead of the optimal critic in IWAE (Cor. 2.4), we observe that GIWAE can approach the performance of IWAE. We can also confirm that both bounds improve upon the BA lower bound. In all cases, (Structured) InfoNCE bounds, which use  $q_\theta(\mathbf{z}|\mathbf{x}) = p(\mathbf{z})$ , saturate to  $\log K$ .

We can further analyze the contribution of the contrastive term across different models. For the Linear VAE, the true posterior is in the Gaussian variational family and  $I_{BA_L}(q_\theta)$  is close to the analytical MI. In this case, the contrastive term provides much less than  $\log K$  improvement for GIWAE and IWAE, since even the optimal critic function cannot distinguish between  $q_\theta(\mathbf{z}|\mathbf{x})$  and  $p(\mathbf{z}|\mathbf{x})$ . As  $K$  increases, we learn a worse  $q_\theta$  in almost all cases, as measured by a lower BA term. This allows the contrastive term to achieve closer to its full potential  $\log K$ , resulting in a higher overall bound.<sup>3</sup> For more complex VAE and GAN posteriors, there is a reduced tradeoff between the terms. In these cases, the variational family is far enough from the true posterior (in reverse KL divergence) that either GIWAE or IWAE critic functions can approach  $\log K$  improvement without significantly lowering the BA term.

**MINE-AIS Bounds** We now discuss results for MINE-AIS, where we have used fixed standard Gaussian  $p(\mathbf{z})$  as the base variational distribution, energy-based training for  $T_\phi(\mathbf{x}, \mathbf{z})$ , and Multi-Sample AIS evaluation of  $IBAL(p(\mathbf{z}), T_\phi)$ . We can see in Fig. 5a that MINE-AIS improves over BA due to its flexible, energy-based variational family. To evaluate the quality of the learned  $T_\phi(\mathbf{x}, \mathbf{z})$ , we also compare the IBAL to the Multi-Sample AIS lower bound, which assumes access to  $p(\mathbf{x}|\mathbf{z})$  and corresponds to the optimal critic (Prop. 4.1). We find that MINE-AIS underestimates the ground truth MI by 11% and 24% on MNIST-VAE and MNIST-GAN, respectively.

<sup>3</sup>A similar observation can be made in training VAEs with the ELBO<sub>IWAE</sub> objective and a restricted variational family, where increasing  $K$  results in a worse  $q_\theta(\mathbf{z}|\mathbf{x})$  (in forward KL divergence) but a better overall bound.

We also observe that MINE-AIS outperforms GIWAE by 32% and 50% on MNIST-VAE and MNIST-GAN, respectively. We now investigate whether this improvement is due to a more costly Multi-Sample AIS evaluation or our energy-based training scheme for the critic  $T_\phi$ . In Fig. 4 and Fig. 5a, we use Multi-Sample AIS to evaluate the IBAL corresponding to  $(q_\theta, T_\phi)$ , which are learned by optimizing the GIWAE (with  $K = 100$ ) and INFONCE (with  $K = 100$  and  $q_\theta = p(\mathbf{z})$ ) lower bounds. As argued in Prop. L.2, the IBAL corresponds to the limiting behavior of GIWAE as  $K \rightarrow \infty$ . We observe that the AIS evaluation of the IBAL, corresponding to GIWAE or INFONCE critic functions, only marginally improves upon evaluation of the original GIWAE or INFONCE lower bounds. This indicates that the improvement of MINE-AIS over GIWAE or INFONCE can be primarily attributed to learning a better critic function using energy-based training.

Recall that the IWAE and Structured INFONCE critics use the true log importance weights  $T^*(\mathbf{x}, \mathbf{z}) = \log \frac{p(\mathbf{x}, \mathbf{z})}{q_\theta(\mathbf{z}|\mathbf{x})} + c(\mathbf{x})$  (Cor. 2.4), and with this optimal critic,  $\text{IBAL}(q_\theta, T^*) = I(\mathbf{x}; \mathbf{z})$  regardless of  $q_\theta(\mathbf{z}|\mathbf{x})$  (Prop. 4.1). We would thus expect Multi-Sample AIS evaluation of the  $\text{IBAL}(q_\theta, T_\phi)$  to tightly bound the true MI if the critic were optimal. We instead find that AIS evaluation for a learned GIWAE critic falls short of the true MI by 31% and 46% on MNIST-VAE and MNIST-GAN, respectively. This is despite the fact that the GIWAE critic came close to matching the performance of IWAE and saturating the contrastive term at  $\log K$  in the original objective. These observations highlight a further shortcoming of the contrastive bounds used in GIWAE and INFONCE: beyond their  $\log K$  limitations for evaluation (Cor. 2.5 and Cor. C.3), these bounds may not be conducive to learning the true log importance weights.

**Validation of Approximate Reverse Annealing for IBAL Lower Bound** As discussed in Sec. 4.2.2, obtaining a lower bound on the IBAL is intractable due to the need for exact samples from  $\pi_{\theta, \phi}(\mathbf{z}|\mathbf{x})$ . In Fig. 4, we confirm that our approximate reverse annealing procedure described in App. M.1 underestimates the IBAL for all MINE-AIS, GIWAE and INFONCE experiments, although we cannot mathematically guarantee this procedure provides a lower bound in general. With detailed discussion in App. M.1, we derive a sufficient condition under which our approximate reverse annealing procedure is guaranteed to provide a lower bound.

We can use our Multi-Sample AIS upper bound on the IBAL to validate the convergence of our estimation procedure, despite the fact that this quantity does not lower or upper bound the true MI in general. In other words, we can conclude that the true  $\text{IBAL}(q_\theta, T_\phi)$  has been obtained when its lower and upper bounds converge to the same estimate for a large number of intermediate distributions  $T$ .

**MINE-DV and MINE-F** We do not include results for MINE-DV and MINE-F, as they are highly unstable in large MI settings due to the difficulty of direct Monte Carlo estimation of  $\mathbb{E}_{p(\mathbf{x})p(\mathbf{z})} [e^{T_\phi(\mathbf{x}, \mathbf{z})}]$  (McAllester & Stratos, 2020). We expect Generalized MINE to suffer from the same challenges and instead recommend using MINE-AIS.

## 6 CONCLUSION

In this work, we have provided a unifying view of mutual information estimation from the perspective of importance sampling. We derived probabilistic interpretations of each bound, which shed light on the limitations of existing estimators and motivated our novel GIWAE, Multi-Sample AIS, and MINE-AIS bounds. When the conditional is not known, our GIWAE bounds highlight how variational bounds can complement contrastive learning to improve lower bounds on MI beyond known  $\log K$  limitations. When the full joint distribution is known, we show that our Multi-Sample AIS bounds can tightly estimate large values of MI without exponential sample complexity, and thus should be considered the gold standard for MI estimation in these settings. Finally, MINE-AIS extends Multi-Sample AIS evaluation to unknown conditional densities, and can be viewed as the infinite-sample behavior of GIWAE and existing contrastive bounds. Our MINE-AIS and Multi-Sample AIS methods highlight how MCMC techniques can be used to improve MI estimation when a single analytic marginal or conditional density is available.

## ACKNOWLEDGEMENTS

The authors thank Shengyang Sun, Guodong Zhang, Vaden Masrani, and Umang Gupta for helpful comments on drafts of this work. We also thank the anonymous reviewers whose comments greatly improved the presentation and encouraged us to derive several additional propositions. MG, RG and AM acknowledge support from the Canada CIFAR AI Chairs program.

## REFERENCES

- Alexander Alemi, Ben Poole, Ian Fischer, Joshua Dillon, Rif A Saurous, and Kevin Murphy. Fixing a broken ELBO. In *International Conference on Machine Learning*, pp. 159–168, 2018.
- Alexander A Alemi and Ian Fischer. GILBO: One metric to measure them all. In *Advances in Neural Information Processing Systems*, 2018.
- Alexander A Alemi, Ian Fischer, Joshua V Dillon, and Kevin Murphy. Deep variational information bottleneck. In *International Conference on Learning Representations*, 2017.
- Shun-Ichi Amari. Alpha-divergence is unique, belonging to both f-divergence and Bregman divergence classes. *IEEE Transactions on Information Theory*, 55(11):4925–4931, 2009.
- Michael Arbel, Liang Zhou, and Arthur Gretton. Generalized energy based models. In *International Conference on Learning Representations*, 2021.
- David Barber and Felix Agakov. The IM algorithm: A variational approach to information maximization. In *Proceedings of the 16th International Conference on Neural Information Processing Systems*, pp. 201–208, 2003.
- Mohamed Ishmael Belghazi, Aristide Baratin, Sai Rajeshwar, Sherjil Ozair, Yoshua Bengio, Aaron Courville, and Devon Hjelm. Mutual information neural estimation. In *International Conference on Machine Learning*, pp. 531–540. PMLR, 2018.
- Yuri Burda, Roger Grosse, and Ruslan Salakhutdinov. Accurate and conservative estimates of MRF log-likelihood using reverse annealing. In *Artificial Intelligence and Statistics*, pp. 102–110. PMLR, 2015.
- Yuri Burda, Roger B Grosse, and Ruslan Salakhutdinov. Importance weighted autoencoders. In *International Conference on Learning Representations*, 2016.
- Sourav Chatterjee, Persi Diaconis, et al. The sample size required in importance sampling. *The Annals of Applied Probability*, 28(2):1099–1135, 2018.
- Xi Chen, Yan Duan, Rein Houthoofd, John Schulman, Ilya Sutskever, and Pieter Abbeel. InfoGAN: Interpretable representation learning by information maximizing generative adversarial nets. In *Proceedings of the 30th International Conference on Neural Information Processing Systems*, pp. 2180–2188, 2016.
- Andrzej Cichocki and Shun-ichi Amari. Families of alpha-beta-and gamma-divergences: Flexible and robust measures of similarities. *Entropy*, 12(6):1532–1568, 2010.
- Kyle Cranmer, Johann Brehmer, and Gilles Louppe. The frontier of simulation-based inference. *Proceedings of the National Academy of Sciences*, 117(48):30055–30062, 2020.
- Chris Cremer, Quaid Morris, and David Duvenaud. Reinterpreting importance-weighted autoencoders. *arXiv preprint arXiv:1704.02916*, 2017.
- Amir Dembo and Ofer Zeitouni. *Large deviations techniques and applications*. Springer, 2009.
- Justin Domke and Daniel R Sheldon. Importance weighting and variational inference. In *Advances in neural information processing systems*, pp. 4470–4479, 2018.

- Arnaud Doucet, Will Sussman Grathwohl, Alexander G de G Matthews, and Heiko Strathmann. Annealed importance sampling meets score matching. In *ICLR Workshop on Deep Generative Models for Highly Structured Data*, 2022.
- Axel Finke. *On extended state-space constructions for Monte Carlo methods*. PhD thesis, University of Warwick, 2015.
- Roger B Grosse, Chris J Maddison, and Russ R Salakhutdinov. Annealing between distributions by averaging moments. *Advances in Neural Information Processing Systems*, 26, 2013.
- Roger B Grosse, Zoubin Ghahramani, and Ryan P Adams. Sandwiching the marginal likelihood using bidirectional monte carlo. *arXiv preprint arXiv:1511.02543*, 2015.
- Roger B Grosse, Siddharth Ancha, and Daniel M Roy. Measuring the reliability of MCMC inference with bidirectional Monte Carlo. In *Proceedings of the 30th International Conference on Neural Information Processing Systems*, pp. 2459–2467, 2016.
- Geoffrey E Hinton. Training products of experts by minimizing contrastive divergence. *Neural computation*, 14(8):1771–1800, 2002.
- Sicong Huang, Alireza Makhzani, Yanshuai Cao, and Roger Grosse. Evaluating lossy compression rates of deep generative models. In *International Conference on Machine Learning*. PMLR, 2020.
- Diederik P Kingma and Jimmy Ba. Adam: A method for stochastic optimization. *arXiv preprint arXiv:1412.6980*, 2014.
- Alex Krizhevsky. Learning multiple layers of features from tiny images. 2009.
- Dieterich Lawson, George Tucker, Bo Dai, and Rajesh Ranganath. Energy-inspired models: learning with sampler-induced distributions. In *Proceedings of the 33rd International Conference on Neural Information Processing Systems*, pp. 8501–8513, 2019.
- Yann LeCun, Léon Bottou, Yoshua Bengio, Patrick Haffner, et al. Gradient-based learning applied to document recognition. *Proceedings of the IEEE*, 86(11):2278–2324, 1998.
- Chris J Maddison, Dieterich Lawson, George Tucker, Nicolas Heess, Mohammad Norouzi, Andriy Mnih, Arnaud Doucet, and Yee Whye Teh. Filtering variational objectives. In *Proceedings of the 31st International Conference on Neural Information Processing Systems*, pp. 6576–6586, 2017.
- Alireza Makhzani, Jonathon Shlens, Navdeep Jaitly, Ian Goodfellow, and Brendan Frey. Adversarial autoencoders. *arXiv preprint arXiv:1511.05644*, 2015.
- David McAllester and Karl Stratos. Formal limitations on the measurement of mutual information. In *International Conference on Artificial Intelligence and Statistics*, pp. 875–884. PMLR, 2020.
- Shakir Mohamed and Danilo Jimenez Rezende. Variational information maximisation for intrinsically motivated reinforcement learning. *Advances in Neural Information Processing Systems*, 28:2125–2133, 2015.
- Radford M Neal. Annealed importance sampling. *Statistics and computing*, 11(2):125–139, 2001.
- Radford M Neal. MCMC using hamiltonian dynamics. *Handbook of Markov Chain Monte Carlo*, 2011.
- XuanLong Nguyen, Martin J Wainwright, and Michael I Jordan. Estimating divergence functionals and the likelihood ratio by convex risk minimization. *IEEE Transactions on Information Theory*, 56(11):5847–5861, 2010.
- Sebastian Nowozin, Botond Cseke, and Ryota Tomioka. f-GAN: Training generative neural samplers using variational divergence minimization. *Advances in Neural Information Processing Systems*, 29, 2016.
- Yury Polyanskiy and Yihong Wu. Information theory: From coding to learning, 2022.



- Ben Poole, Sherjil Ozair, Aaron Van Den Oord, Alex Alemi, and George Tucker. On variational bounds of mutual information. In *International Conference on Machine Learning*, 2019.
- Alec Radford, Luke Metz, and Soumith Chintala. Unsupervised representation learning with deep convolutional generative adversarial networks. *arXiv preprint arXiv:1511.06434*, 2015.
- Firas Rassoul-Agha and Timo Seppäläinen. *A course on large deviations with an introduction to Gibbs measures*, volume 162. American Mathematical Soc., 2015.
- Tim Salimans, Ian Goodfellow, Wojciech Zaremba, Vicki Cheung, Alec Radford, and Xi Chen. Improved techniques for training GANs. In *Advances in Neural Information Processing Systems*, pp. 2234–2242, 2016.
- Artem Sobolev. Thoughts on mutual information estimation: More estimators. *Blog post*, 2019. URL <http://artem.sobolev.name/posts/2019-08-10-thoughts-on-mutual-information-more-estimators.html>.
- Artem Sobolev and Dmitry P Vetrov. Importance weighted hierarchical variational inference. In *Advances in Neural Information Processing Systems*, volume 32, 2019.
- Jiaming Song and Stefano Ermon. Understanding the limitations of variational mutual information estimators. In *International Conference on Learning Representations*, 2019.
- Naftali Tishby, Fernando C Pereira, and William Bialek. The information bottleneck method. *arXiv preprint physics/0004057*, 2000.
- Aaron van den Oord, Yazhe Li, and Oriol Vinyals. Representation learning with contrastive predictive coding. *arXiv preprint arXiv:1807.03748*, 2018.
- Yuhuai Wu, Yuri Burda, Ruslan Salakhutdinov, and Roger Grosse. On the quantitative analysis of decoder-based generative models. In *International Conference on Learning Representations*, 2017.
- Shengjia Zhao, Jiaming Song, and Stefano Ermon. The information autoencoding family: A Lagrangian perspective on latent variable generative models. In *Proc. 34th Conference on Uncertainty in Artificial Intelligence*, 2018.

# Appendix

## Table of Contents

---

<b>A A General Approach for Deriving Extended State Space Bounds on Log Partition Functions</b>	<b>21</b>
<b>B Importance Weighted Autoencoder (IWAE)</b>	<b>22</b>
B.1 Probabilistic Interpretation and Bounds . . . . .	22
B.2 Proof of Logarithmic Improvement in $K$ for IWAE EUBO . . . . .	24
B.3 Experimental Results showing Logarithmic Improvement for $I_{\text{IWAE}_L}(q_\theta, K)$ . . . . .	25
B.4 Bias Reduction in $K$ for IWAE Lower Bound on $\log p(\mathbf{x})$ / Upper Bound on MI	26
B.5 Relationship with Structured InfoNCE . . . . .	26
<b>C Generalized IWAE</b>	<b>27</b>
C.1 Probabilistic Interpretation and Bounds . . . . .	27
C.2 GIWAE Upper Bound on MI Does Not Provide Benefit Over IWAE . . . . .	28
C.3 ELBO and EUBO are Special Cases of GIWAE Log Partition Function Bounds . . . . .	29
C.4 Proof of Relationship between IWAE and GIWAE Probabilistic Interpretations (Prop. 2.3) . . . . .	29
C.5 Proof of GIWAE Optimal Critic Function and Logarithmic Improvement (Cor. 2.4 and Cor. 2.5) . . . . .	31
C.6 Properties of InfoNCE . . . . .	32
<b>D Single-Sample AIS</b>	<b>32</b>
D.1 Proof of Prop. 3.1 (Complexity in $T$ for Single-Sample AIS) . . . . .	32
<b>E Independent Multi-Sample AIS</b>	<b>34</b>
E.1 Probabilistic Interpretation and Bounds . . . . .	34
E.2 Proof of Linear Bias Reduction in $T$ for IM-AIS . . . . .	34
E.3 Proof of Logarithmic Improvement of IM-AIS EUBO . . . . .	34
<b>F Reverse IWAE</b>	<b>35</b>
F.1 Probabilistic Interpretation and Bounds . . . . .	35
F.2 Improvement of RIWAE over ELBO and EUBO . . . . .	36
<b>G Independent Reverse Multi-Sample AIS</b>	<b>36</b>
G.1 Probabilistic Interpretation and Bounds . . . . .	36
G.2 Proof of Logarithmic Improvement in $K$ for Independent Reverse AIS . . . . .	37
<b>H Coupled Reverse Multi-Sample AIS</b>	<b>37</b>
H.1 Probabilistic Interpretation and Bounds . . . . .	37
H.2 Proof that CR-AIS Bounds Tighten with Increasing $K$ . . . . .	38
H.3 Proof of Logarithmic Improvement in $K$ for CR-AIS ELBO . . . . .	40
H.4 Linear Bias Reduction in $T$ for CR-AIS . . . . .	41
<b>I Comparison of Multi-Sample AIS Bounds</b>	<b>41</b>
<b>J Generalized Mutual Information Neural Estimation (GMINE)</b>	<b>41</b>
J.1 Probabilistic Interpretation of IBAL . . . . .	41
J.2 Probabilistic Interpretation of Generalized MINE-DV . . . . .	42

J.3	Probabilistic Interpretation of Generalized MINE-F . . . . .	44
<b>K</b>	<b>Conjugate Duality Interpretations</b>	<b>46</b>
K.1	Convex Analysis Background . . . . .	46
K.2	Conjugate Duality Interpretation of IBAL . . . . .	48
K.3	Conjugate Duality Interpretation of Generalized MINE-DV . . . . .	48
K.4	Conjugate Duality Interpretation of Generalized MINE-F . . . . .	49
K.5	Conjugate Duality Interpretation of GIWAE, IWAE, and InfoNCE . . . . .	50
<b>L</b>	<b>Properties of the IBAL</b>	<b>53</b>
L.1	Proofs for IBAL Optimal Critic Function (Prop. 4.1 and L.1) . . . . .	53
L.2	Proof of IBAL as Limiting Behavior of the GIWAE Objective as $K \rightarrow \infty$ (Prop. L.2)	54
L.3	Convergence of GIWAE SNIS Distribution to IBAL Energy-Based Posterior . . .	55
<b>M</b>	<b>MINE-AIS</b>	<b>56</b>
M.1	Multi-Sample AIS Evaluation of the IBAL . . . . .	56
<b>N</b>	<b>Applications to Mutual Information Estimation without Known Marginals</b>	<b>59</b>
N.1	BA Lower Bound . . . . .	59
N.2	GIWAE Lower Bound . . . . .	60
N.3	MINE-AIS / IBAL Lower Bound . . . . .	60
<b>O</b>	<b>Experimental Details</b>	<b>61</b>
O.1	Experiment Details of Sec. 5.2 . . . . .	61
O.2	Runtime Comparison . . . . .	62
O.3	Experiment Details for Energy-Based Bounds (Sec. 5.3) . . . . .	62
O.4	Analytical Solution of the Mutual Information on the Linear MNIST-VAE . . . .	63
O.5	Confidence Intervals for Multi-Sample AIS Experiments . . . . .	63

## A A GENERAL APPROACH FOR DERIVING EXTENDED STATE SPACE BOUNDS ON LOG PARTITION FUNCTIONS

In this section, we give a short proof that the gap in our general extended state space bounds from Sec. 2.1 corresponds to a forward or reverse KL divergence. We derive various upper and lower bounds on  $\log p(\mathbf{x})$  using this approach throughout the paper and appendix, and we provide a visual summary in Fig. 6.

First, we consider an extended state space target  $p_{\text{TGT}}(\mathbf{x}, \mathbf{z}_{\text{ext}})$  and proposal  $q_{\text{PROP}}(\mathbf{x}, \mathbf{z}_{\text{ext}})$  distributions. For all cases discussed in this work, we will choose our target and proposal distributions such that  $\log \frac{\mathcal{Z}_{\text{TGT}}(\mathbf{x})}{\mathcal{Z}_{\text{PROP}}(\mathbf{x})} = \log p(\mathbf{x})$ . For example, a common construction is to have  $\mathcal{Z}_{\text{TGT}}(\mathbf{x}) = \int p_{\text{TGT}}(\mathbf{x}, \mathbf{z}_{\text{ext}}) d\mathbf{z}_{\text{ext}} = p(\mathbf{x})$  and  $\mathcal{Z}_{\text{PROP}}(\mathbf{x}) = \int q_{\text{PROP}}(\mathbf{x}, \mathbf{z}_{\text{ext}}) d\mathbf{z}_{\text{ext}} = 1$ . Our ‘reverse’ importance sampling bounds App. F-G construct target and proposal such that  $\mathcal{Z}_{\text{TGT}}(\mathbf{x}) = p(\mathbf{x})^K$  and  $\mathcal{Z}_{\text{PROP}}(\mathbf{x}) = p(\mathbf{x})^{K-1}$ , which still yields  $\mathcal{Z}_{\text{TGT}}(\mathbf{x})/\mathcal{Z}_{\text{PROP}}(\mathbf{x}) = p(\mathbf{x})$ .

Each pair of extended state-space proposal and target distributions provides both an upper and lower bound on the log partition function. Taking the expected log ratio of unnormalized densities under either the proposal or target distribution, we have

$$\mathbb{E}_{q_{\text{PROP}}(\mathbf{z}_{\text{ext}}|\mathbf{x})} \left[ \log \frac{p_{\text{TGT}}(\mathbf{x}, \mathbf{z}_{\text{ext}})}{q_{\text{PROP}}(\mathbf{x}, \mathbf{z}_{\text{ext}})} \right] \leq \log \frac{\mathcal{Z}_{\text{TGT}}(\mathbf{x})}{\mathcal{Z}_{\text{PROP}}(\mathbf{x})} \leq \mathbb{E}_{p_{\text{TGT}}(\mathbf{z}_{\text{ext}}|\mathbf{x})} \left[ \log \frac{p_{\text{TGT}}(\mathbf{x}, \mathbf{z}_{\text{ext}})}{q_{\text{PROP}}(\mathbf{x}, \mathbf{z}_{\text{ext}})} \right]. \quad (34)$$

To confirm that these are indeed lower and upper bounds for any  $q_{\text{PROP}}$  and  $p_{\text{TGT}}$ , we can show that the gap in the lower bound in Eq. (34) is the forward KL divergence  $D_{\text{KL}}[q_{\text{PROP}}\|p_{\text{TGT}}]$ , and the gap in the upper bound is the reverse KL divergence,  $D_{\text{KL}}[p_{\text{TGT}}\|q_{\text{PROP}}]$

$$\mathbb{E}_{q_{\text{PROP}}(\mathbf{z}_{\text{ext}}|\mathbf{x})} \left[ \frac{p_{\text{TGT}}(\mathbf{x}, \mathbf{z}_{\text{ext}})}{q_{\text{PROP}}(\mathbf{x}, \mathbf{z}_{\text{ext}})} \right] = \log \frac{\mathcal{Z}_{\text{TGT}}(\mathbf{x})}{\mathcal{Z}_{\text{PROP}}(\mathbf{x})} - \underbrace{D_{\text{KL}}[q_{\text{PROP}}(\mathbf{z}_{\text{ext}}|\mathbf{x})\|p_{\text{TGT}}(\mathbf{z}_{\text{ext}}|\mathbf{x})]}_{\text{ELBO}(\mathbf{x}; q_{\text{PROP}}, p_{\text{TGT}})} \leq \log \frac{\mathcal{Z}_{\text{TGT}}(\mathbf{x})}{\mathcal{Z}_{\text{PROP}}(\mathbf{x})} \quad (35)$$

$$\mathbb{E}_{p_{\text{TGT}}(\mathbf{z}_{\text{ext}}|\mathbf{x})} \left[ \frac{p_{\text{TGT}}(\mathbf{x}, \mathbf{z}_{\text{ext}})}{q_{\text{PROP}}(\mathbf{x}, \mathbf{z}_{\text{ext}})} \right] = \log \frac{\mathcal{Z}_{\text{TGT}}(\mathbf{x})}{\mathcal{Z}_{\text{PROP}}(\mathbf{x})} + \underbrace{D_{\text{KL}}[p_{\text{TGT}}(\mathbf{z}_{\text{ext}}|\mathbf{x})\|q_{\text{PROP}}(\mathbf{z}_{\text{ext}}|\mathbf{x})]}_{\text{EUBO}(\mathbf{x}; q_{\text{PROP}}, p_{\text{TGT}})} \geq \log \frac{\mathcal{Z}_{\text{TGT}}(\mathbf{x})}{\mathcal{Z}_{\text{PROP}}(\mathbf{x})}. \quad (36)$$

Thus, the bounds in Eq. (34) directly generalize the standard ELBO ( $\log p(\mathbf{x}) - D_{\text{KL}}[q_{\theta}(\mathbf{z}|\mathbf{x})\|p(\mathbf{z}|\mathbf{x})]$ ) and EUBO ( $\log p(\mathbf{x}) + D_{\text{KL}}[p(\mathbf{z}|\mathbf{x})\|q_{\theta}(\mathbf{z}|\mathbf{x})]$ ), which appear as special cases when  $K = 1$ ,  $T = 1$ , the proposal distribution is  $q_{\text{PROP}}(\mathbf{z}|\mathbf{x}) = q_{\theta}(\mathbf{z}|\mathbf{x})$ , and the target distribution is  $p_{\text{TGT}}(\mathbf{z}|\mathbf{x}) = p(\mathbf{z}|\mathbf{x})$ . In what follows, our extended state space proposal or target distributions may include  $q_{\theta}(\mathbf{z}|\mathbf{x})$  as an initial or base variational distribution, with the posterior  $p(\mathbf{z}|\mathbf{x})$  often appearing within target distributions  $p_{\text{TGT}}(\mathbf{z}_{\text{ext}}|\mathbf{x})$ .

In Fig. 6, we summarize various extended state space proposal (third column) and target distributions (fourth column). We emphasize that the base variational distribution  $q_{\theta}(\mathbf{z}|\mathbf{x})$  (blue circles) and posterior distribution  $p(\mathbf{z}|\mathbf{x})$  (red circles) may be used multiple times, in either or both of the extended state space proposal and target distributions. Similarly, forward AIS chains (blue circles) starting from the initial distribution and the backward AIS chains (shown in red circles) starting from the posterior may be used repeatedly in both the proposal or target. In the next sections, we proceed to derive each of the bounds in Fig. 6 as special cases of this general approach, thus interpreting each importance sampling bound in terms of probabilistic inference in an extended state space.

## B IMPORTANCE WEIGHTED AUTOENCODER (IWAE)

### B.1 PROBABILISTIC INTERPRETATION AND BOUNDS

Consider a  $K$ -sample proposal distribution  $q_{\text{PROP}}^{\text{IWAE}}(\mathbf{z}^{(1:K)})$  using independent draws from an initial distribution  $q_{\theta}(\mathbf{z}|\mathbf{x})$ . The target distribution is defined as a uniform mixture of  $K$  components, where each component replaces the initial sample  $q_{\theta}(\mathbf{z}^{(k)}|\mathbf{x})$  in index  $k$  with a sample from the target distribution  $p(\mathbf{z}|\mathbf{x})$ .

$$q_{\text{PROP}}^{\text{IWAE}}(\mathbf{z}^{(1:K)}|\mathbf{x}) = \prod_{s=1}^K q_{\theta}(\mathbf{z}^{(s)}|\mathbf{x}), \quad p_{\text{TGT}}^{\text{IWAE}}(\mathbf{x}, \mathbf{z}^{(1:K)}) = \frac{1}{K} \sum_{s=1}^K p(\mathbf{x}, \mathbf{z}^{(s)}) \prod_{\substack{k=1 \\ k \neq s}}^K q_{\theta}(\mathbf{z}^{(k)}|\mathbf{x}). \quad (37)$$

Note that the normalizing constant of  $p_{\text{TGT}}^{\text{IWAE}}(\mathbf{x}, \mathbf{z}^{(1:K)})$ , or  $\int p_{\text{TGT}}^{\text{IWAE}}(\mathbf{x}, \mathbf{z}^{(1:K)}) d\mathbf{z}^{(1:K)}$ , equals  $p(\mathbf{x})$  since  $q_{\theta}(\mathbf{z}|\mathbf{x})$  is normalized and  $\int p(\mathbf{x}, \mathbf{z}) d\mathbf{z} = p(\mathbf{x})$ . To connect this with the IWAE bound, we show that the log importance ratio reduces to

$$\begin{aligned} \log \frac{p_{\text{TGT}}^{\text{IWAE}}(\mathbf{x}, \mathbf{z}^{(1:K)})}{q_{\text{PROP}}^{\text{IWAE}}(\mathbf{z}^{(1:K)}|\mathbf{x})} &= \log \frac{\frac{1}{K} \sum_{s=1}^K p(\mathbf{x}, \mathbf{z}^{(s)}) \prod_{\substack{k=1 \\ k \neq s}}^K q_{\theta}(\mathbf{z}^{(k)}|\mathbf{x})}{\prod_{k=1}^K q_{\theta}(\mathbf{z}^{(k)}|\mathbf{x})} \\ &= \log \frac{1}{K} \sum_{k=1}^K \frac{p(\mathbf{x}, \mathbf{z}^{(k)})}{q_{\theta}(\mathbf{z}^{(k)}|\mathbf{x})}. \end{aligned} \quad (38)$$

As in Eq. (34), we can obtain lower and upper bounds on  $\log p(\mathbf{x})$  by taking expectations under the proposal and target distributions, respectively.



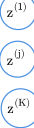
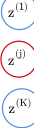
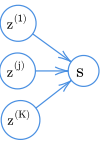
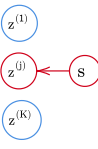

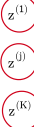


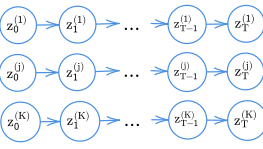
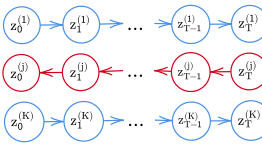
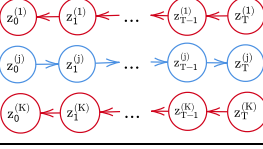
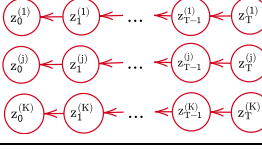
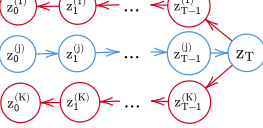
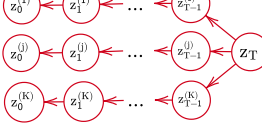
	Practicality	Extended State-Space Proposal Lower Bound on $\log p(\mathbf{x})$ (ELBO) Upper Bound on $I(\mathbf{x}; \mathbf{z})$	Extended State-Space Target Upper Bound on $\log p(\mathbf{x})$ (EUBO) Lower Bound on $I(\mathbf{x}; \mathbf{z})$
Simple IS	✓		
IWAE	✓		
Generalized IWAE	✓		
Reverse IWAE	✗		
Single-Sample AIS	✓		
Independent Multi-Sample AIS	✓		
Independent Reverse Multi-Sample AIS	✗		
Coupled Reverse Multi-Sample AIS	✓		

Figure 6: Comparison of the probabilistic extended state-space interpretations of different multi-sample bounds. Forward chains of AIS and variational distributions in IS / IWAE are colored in blue. Backward chains in AIS or posterior distributions in IS / IWAE are colored in red. Note that a lower bound on  $\log p(\mathbf{x})$ , translates to an upper bound on MI, and vice versa.

**Alternative Probabilistic Interpretation** We now present an alternative probabilistic interpretation of IWAE, which is similar to [Domke & Sheldon \(2018\)](#) and will be used as the foundation for our GIWAE bounds in [App. C](#). Consider the following extended state space target distribution,

$$p_{\text{TGT}}^{\text{IWAE}}(\mathbf{x}, \mathbf{z}^{(1:K)}, s) = \frac{1}{K} p(\mathbf{x}, \mathbf{z}^{(s)}) \prod_{\substack{k=1 \\ k \neq s}}^K q(\mathbf{z}^{(k)} | \mathbf{x}). \quad (39)$$



Note that marginalization over  $s$  leads to the IWAE mixture target in Eq. (4) or Eq. (37). We consider the extended state space proposal

$$q_{\text{PROP}}^{\text{IWAE}}(\mathbf{z}^{(1:K)}, s|\mathbf{x}) = \left( \prod_{k=1}^K q_{\theta}(\mathbf{z}^{(k)}|\mathbf{x}) \right) q_{\text{PROP}}^{\text{IWAE}}(s|\mathbf{z}^{(1:K)}, \mathbf{x}), \quad (40)$$

where we have defined  $q_{\text{PROP}}^{\text{IWAE}}(s|\mathbf{z}^{(1:K)}, \mathbf{x}) = \frac{p(\mathbf{x}, \mathbf{z}^{(s)})}{q_{\theta}(\mathbf{z}^{(s)}|\mathbf{x})} / \sum_{k=1}^K \frac{p(\mathbf{x}, \mathbf{z}^{(k)})}{q_{\theta}(\mathbf{z}^{(k)}|\mathbf{x})}$ .

As desired, the log importance weight match Eq. (38)

$$\log \frac{p_{\text{TGT}}^{\text{IWAE}}(\mathbf{x}, \mathbf{z}^{(1:K)}, s)}{q_{\text{PROP}}^{\text{IWAE}}(\mathbf{z}^{(1:K)}, s|\mathbf{x})} = \log \frac{\frac{1}{K} p(\mathbf{x}, \mathbf{z}^{(s)}) \prod_{\substack{k=1 \\ k \neq s}}^K q_{\theta}(\mathbf{z}^{(k)}|\mathbf{x})}{\prod_{k=1}^K q_{\theta}(\mathbf{z}^{(k)}|\mathbf{x}) \frac{\frac{p(\mathbf{x}, \mathbf{z}^{(s)})}{q_{\theta}(\mathbf{z}^{(s)}|\mathbf{x})}}{\sum_{k=1}^K \frac{p(\mathbf{x}, \mathbf{z}^{(k)})}{q_{\theta}(\mathbf{z}^{(k)}|\mathbf{x})}}} = \log \frac{1}{K} \sum_{k=1}^K \frac{p(\mathbf{x}, \mathbf{z}^{(k)})}{q_{\theta}(\mathbf{z}^{(k)}|\mathbf{x})}. \quad (41)$$

**Lower Bound on  $\log p(\mathbf{x})$  and Upper Bound on MI** Using the general approach in App. A, taking expectations under  $q_{\text{PROP}}^{\text{IWAE}}$  leads to a lower bound on  $\log p(\mathbf{x})$

$$\text{ELBO}_{\text{IWAE}}(\mathbf{x}; q_{\theta}, K) := \mathbb{E}_{\prod_{k=1}^K q_{\theta}(\mathbf{z}^{(k)}|\mathbf{x})} \left[ \log \frac{1}{K} \sum_{k=1}^K \frac{p(\mathbf{x}, \mathbf{z}^{(k)})}{q_{\theta}(\mathbf{z}^{(k)}|\mathbf{x})} \right]. \quad (42)$$

This corresponds to the following upper bound on MI for known  $p(\mathbf{x}|\mathbf{z})$

$$I(\mathbf{x}; \mathbf{z}) \leq I_{\text{IWAE}_U}(\mathbf{x}; q_{\theta}, K) = \mathbb{E}_{p(\mathbf{x}, \mathbf{z})} [\log p(\mathbf{x}|\mathbf{z})] - \mathbb{E}_{p(\mathbf{x})} [\text{ELBO}_{\text{IWAE}}(\mathbf{x}; q_{\theta}, K)] \quad (43)$$

$$= \mathbb{E}_{p(\mathbf{x}, \mathbf{z})} [\log p(\mathbf{x}|\mathbf{z})] - \mathbb{E}_{p(\mathbf{x})} \prod_{k=1}^K q_{\theta}(\mathbf{z}^{(k)}|\mathbf{x}) \left[ \log \frac{1}{K} \sum_{k=1}^K \frac{p(\mathbf{x}, \mathbf{z}^{(k)})}{q_{\theta}(\mathbf{z}^{(k)}|\mathbf{x})} \right] \quad (44)$$

**Upper Bound on  $\log p(\mathbf{x})$  and Lower Bound on MI** Similarly, with expectations under  $p_{\text{TGT}}^{\text{IWAE}}(\mathbf{z}^{(1:K)}|\mathbf{x})$ , we obtain an upper bound on  $\log p(\mathbf{x})$ . Since, for independent draws, the uniform mixture  $p_{\text{TGT}}^{\text{IWAE}}$  is invariant to index permutations, we may choose the target sample to be  $\mathbf{z}^{(1)}$  and obtain the upper bound of Sobolev & Vetrov (2019):

$$\text{EUBO}_{\text{IWAE}}(\mathbf{x}; q_{\theta}, K) := \mathbb{E}_{p(\mathbf{z}^{(1)}|\mathbf{x})} \prod_{k=2}^K q_{\theta}(\mathbf{z}^{(k)}|\mathbf{x}) \left[ \log \frac{1}{K} \sum_{i=1}^K \frac{p(\mathbf{x}, \mathbf{z}^{(i)})}{q(\mathbf{z}^{(i)}|\mathbf{x})} \right] \geq \log p(\mathbf{x}). \quad (45)$$

Translating this to a lower bound on MI with known  $p(\mathbf{x}|\mathbf{z})$ ,

$$I(\mathbf{x}; \mathbf{z}) \geq I_{\text{IWAE}_L}(\mathbf{x}; q_{\theta}, K) = \mathbb{E}_{p(\mathbf{x}, \mathbf{z})} [\log p(\mathbf{x}|\mathbf{z})] - \mathbb{E}_{p(\mathbf{x})} [\text{EUBO}_{\text{IWAE}}(\mathbf{x}; q_{\theta}, K)] \quad (46)$$

$$= \mathbb{E}_{p(\mathbf{x}, \mathbf{z})} [\log p(\mathbf{x}|\mathbf{z})] - \mathbb{E}_{p(\mathbf{x})p(\mathbf{z}^{(1)}|\mathbf{x})} \prod_{k=2}^K q_{\theta}(\mathbf{z}^{(k)}|\mathbf{x}) \left[ \log \frac{1}{K} \sum_{k=1}^K \frac{p(\mathbf{x}, \mathbf{z}^{(k)})}{q_{\theta}(\mathbf{z}^{(k)}|\mathbf{x})} \right]. \quad (47)$$

## B.2 PROOF OF LOGARITHMIC IMPROVEMENT IN $K$ FOR IWAE EUBO

We first recall results that IWAE bounds tighten with increasing  $K$ .

**Proposition B.1.** For given  $q_{\theta}(\mathbf{z}|\mathbf{x})$ ,  $\text{ELBO}_{\text{IWAE}}(\mathbf{x}; q_{\theta}, K+1) \geq \text{ELBO}_{\text{IWAE}}(\mathbf{x}; q_{\theta}, K)$  (Burda et al., 2016) and  $\text{EUBO}_{\text{IWAE}}(\mathbf{x}; q_{\theta}, K+1) \leq \text{EUBO}_{\text{IWAE}}(\mathbf{x}; q_{\theta}, K)$  (Sobolev & Vetrov, 2019).

**Proposition 2.1** (Improvement of IWAE with Increasing  $K$ ). Let  $p_{\text{TGT}}^{\text{IWAE}}(s|\mathbf{x}, \mathbf{z}^{(1:K)}) = \frac{p(\mathbf{x}, \mathbf{z}^{(s)})}{q_{\theta}(\mathbf{z}^{(s)}|\mathbf{x})} / \sum_{k=1}^K \frac{p(\mathbf{x}, \mathbf{z}^{(k)})}{q_{\theta}(\mathbf{z}^{(k)}|\mathbf{x})}$  denote the normalized importance weights and  $\mathcal{U}(s)$  indicate the uniform distribution over  $K$  discrete values. Then, we can characterize the improvement of  $\text{ELBO}_{\text{IWAE}}(\mathbf{x}; q_{\theta}, K)$  and  $\text{EUBO}_{\text{IWAE}}(\mathbf{x}; q_{\theta}, K)$  over  $\text{ELBO}(\mathbf{x}; q_{\theta})$  and  $\text{EUBO}(\mathbf{x}; q_{\theta})$  using KL diver-

gences, as follows

$$\text{ELBO}_{\text{IWAE}}(\mathbf{x}; q_\theta, K) = \text{ELBO}(\mathbf{x}; q_\theta) + \underbrace{\mathbb{E}_{q_{\text{PROP}}^{\text{IWAE}}(\mathbf{z}^{(1:K)}|\mathbf{x})} \left[ D_{\text{KL}}[\mathcal{U}(s) \| p_{\text{TGT}}^{\text{IWAE}}(s|\mathbf{z}^{(1:K)}, \mathbf{x})] \right]}_{0 \leq \text{KL of uniform from SNIS weights} \leq D_{\text{KL}}[q_\theta(\mathbf{z}|\mathbf{x}) \| p(\mathbf{z}|\mathbf{x})]}, \quad (6)$$

$$\text{EUBO}_{\text{IWAE}}(\mathbf{x}; q_\theta, K) = \text{EUBO}(\mathbf{x}; q_\theta) - \underbrace{\mathbb{E}_{p_{\text{TGT}}^{\text{IWAE}}(\mathbf{z}^{(1:K)}|\mathbf{x})} \left[ D_{\text{KL}}[p_{\text{TGT}}^{\text{IWAE}}(s|\mathbf{z}^{(1:K)}, \mathbf{x}) \| \mathcal{U}(s)] \right]}_{0 \leq \text{KL of SNIS weights from uniform} \leq \log K}. \quad (7)$$

*Proof.* We first note the single-sample  $\text{ELBO}(\mathbf{x}; q_\theta)$  and  $\text{EUBO}(\mathbf{x}; q_\theta)$  are special cases of  $\text{ELBO}_{\text{GIWAE}}(\mathbf{x}; q_\theta, T_\phi, K)$  and  $\text{EUBO}_{\text{GIWAE}}(\mathbf{x}; q_\theta, T_\phi, K)$  ([Lemma C.1](#)) with  $T_\phi = \text{const}$ . As a result, the gap between  $\text{ELBO}(\mathbf{x}; q_\theta)$  and  $\text{ELBO}_{\text{IWAE}}(\mathbf{x}; q_\theta, K)$ , for example, follows as a special case of the gap between  $\text{ELBO}_{\text{GIWAE}}(\mathbf{x}; q_\theta, T_\phi, K)$  and  $\text{ELBO}_{\text{IWAE}}(\mathbf{x}; q_\theta, K)$ , which we characterize in [Lemma C.2](#) ([App. C.4](#)). The result in [Prop. 2.1](#) follows directly.

We now justify the range of the KL divergences in [Eq. \(6\)](#) and [Eq. \(7\)](#) referenced in the underbraces.

*Improvement of  $\text{EUBO}_{\text{IWAE}}$ :* Note  $D_{\text{KL}}[p_{\text{TGT}}^{\text{GIWAE}}(s|\mathbf{z}^{(1:K)}, \mathbf{x}) \| \mathcal{U}(s)] = \log K - H(p_{\text{TGT}}^{\text{GIWAE}}(s|\mathbf{z}^{(1:K)}, \mathbf{x}))$  is bounded above by  $\log K$  since the entropy of a discrete random variable is nonnegative.

Thus, the improvement of  $\text{EUBO}_{\text{IWAE}}(\mathbf{x}; q_\theta, K)$  over  $\text{EUBO}(\mathbf{x}; q_\theta)$  is limited to  $\log K$ . We prove similar results in [Prop. 2.3](#) and [Cor. 2.5](#) ([App. C.4](#)), [Prop. E.2](#) ([App. E.3](#)) and [Prop. H.2](#) ([App. H.3](#)).

*Improvement of  $\text{ELBO}_{\text{IWAE}}$ :* On the other hand, the KL divergence  $D_{\text{KL}}[\mathcal{U}(s) \| p_{\text{TGT}}^{\text{GIWAE}}(s|\mathbf{z}^{(1:K)}, \mathbf{x})]$  is not limited by  $\log K$ . However, we do know that the improvement of  $\text{ELBO}_{\text{IWAE}}(\mathbf{x}; q_\theta, K)$  over  $\text{ELBO}(\mathbf{x}; q_\theta)$  will be limited by  $D_{\text{KL}}[q_\theta(\mathbf{z}|\mathbf{x}) \| p(\mathbf{z}|\mathbf{x})]$ , the gap of  $\text{ELBO}(\mathbf{x}; q_\theta)$ . □

[Prop. 2.1](#) shows that both IWAE upper and lower bounds on  $\log p(\mathbf{x})$  improve upon their single-sample counterparts, with the improvement of  $\text{EUBO}_{\text{IWAE}}(\mathbf{x}; q_\theta, K)$  over  $\text{EUBO}(\mathbf{x}; q_\theta)$  limited by  $\log K$ . [Cor. 2.2](#) follows directly by translating these results to bounds on MI.

**Corollary 2.2.** IWAE bounds on MI improve upon the BA bounds with the following relationships:

$$I_{\text{BAL}}(q_\theta) \leq I_{\text{IWAE}_L}(q_\theta, K) \leq I_{\text{BAL}}(q_\theta) + \log K, \quad I_{\text{IWAE}_U}(q_\theta, K) \leq I_{\text{BA}_U}(q_\theta). \quad (8)$$

*Proof.* Recall from [Sec. 1.1](#) and [Sec. 2.2](#) that  $I_{\text{BAL}}(q_\theta) = \mathbb{E}_{p(\mathbf{x}, \mathbf{z})}[\log p(\mathbf{x}|\mathbf{z})] - \mathbb{E}_{p(\mathbf{x})}[\text{EUBO}(\mathbf{x}; q_\theta)]$ , and  $I_{\text{IWAE}_L}(q_\theta, K) = \mathbb{E}_{p(\mathbf{x}, \mathbf{z})}[\log p(\mathbf{x}|\mathbf{z})] - \mathbb{E}_{p(\mathbf{x})}[\text{EUBO}_{\text{IWAE}}(\mathbf{x}; q_\theta, K)]$ . Using [Prop. 2.1](#), the fact that  $\text{EUBO}(\mathbf{x}; q_\theta) - \log K \leq \text{EUBO}_{\text{IWAE}}(\mathbf{x}; q_\theta, K)$  for any  $\mathbf{x}$  implies that

$$I_{\text{IWAE}_L}(q_\theta, K) - I_{\text{BAL}}(q_\theta) = \mathbb{E}_{p(\mathbf{x})}[\text{EUBO}(\mathbf{x}; q_\theta) - \text{EUBO}_{\text{IWAE}}(\mathbf{x}; q_\theta, K)] \leq \log K, \quad (48)$$

which results in  $I_{\text{IWAE}_L}(q_\theta, K) \leq I_{\text{BAL}}(q_\theta) + \log K$ , as desired.

$I_{\text{BAL}}(q_\theta) \leq I_{\text{IWAE}_L}(q_\theta, K)$  and  $I_{\text{IWAE}_U}(q_\theta, K) \leq I_{\text{BA}_U}(q_\theta)$  follow from the fact that IWAE bounds tighten with increasing  $K$  in [Prop. B.1](#). □

### B.3 EXPERIMENTAL RESULTS SHOWING LOGARITHMIC IMPROVEMENT FOR $I_{\text{IWAE}_L}(q_\theta, K)$

In [Sec. 2.4](#), we showed that IWAE is a special case of GIWAE, which decomposes into the sum of a variational BA lower bound and a  $K$ -sample contrastive term. This suggests that the IWAE lower bound on MI, which arises from an upper bound on  $\log p(\mathbf{x})$ , may be written as

$$I_{\text{IWAE}_L}(q_\theta, K) = \underbrace{\mathbb{E}_{p(\mathbf{x}, \mathbf{z})} \left[ \log \frac{q_\theta(\mathbf{z}|\mathbf{x})}{p(\mathbf{z})} \right]}_{I_{\text{BA}}(q)} + \underbrace{\mathbb{E}_{p(\mathbf{x})p(\mathbf{z}^{(1)}|\mathbf{x}) \prod_{k=2}^K q_\theta(\mathbf{z}^{(k)}|\mathbf{x})} \left[ \log \frac{p(\mathbf{x}, \mathbf{z}^{(1)})}{q_\theta(\mathbf{z}^{(1)}|\mathbf{x})} \frac{1}{K} \sum_{i=1}^K \frac{p(\mathbf{x}, \mathbf{z}^{(i)})}{q_\theta(\mathbf{z}^{(i)}|\mathbf{x})} \right]}_{0 \leq \text{contrastive term} \leq \log K}. \quad (49)$$

This way of writing  $I_{\text{IWAE}_L}(q_\theta, K)$  provides additional intuition for the result in [Prop. 2.1](#) and [Cor. 2.2](#). In particular, the improvement of  $I_{\text{IWAE}_L}(q_\theta, K)$  over  $I_{\text{BAL}}(q_\theta)$  is simply the contrastive term, which is limited to  $\log K$ .

Method	log $K$	Proposal	VAE2	VAE10	VAE100	GAN2	GAN10	GAN100
IWAE ( $K=1$ )	0	$p(\mathbf{z})$	0 + 0 = 0	0 + 0 = 0	0 + 0 = 0	0 + 0 = 0	0 + 0 = 0	0 + 0 = 0
		$q(\mathbf{z} \mathbf{x})$	8.63 + 0 = 8.63	25.20 + 0 = 25.20	44.54 + 0 = 44.54	8.83 + 0 = 8.83	4.23 + 0 = 4.23	3.23 + 0 = 3.23
IWAE ( $K=1K$ )	6.91	$p(\mathbf{z})$	0 + 6.81 = 6.81	0 + 6.91 = 6.91	0 + 6.91 = 6.91	0 + 6.88 = 6.88	0 + 6.91 = 6.91	0 + 6.91 = 6.91
		$q(\mathbf{z} \mathbf{x})$	7.29 + 1.8 = 9.09	25.20 + 6.49 = 31.69	44.54 + 6.90 = 51.44	7.82 + 2.92 = 10.74	4.23 + 6.91 = 11.14	3.23 + 6.91 = 10.14
IWAE ( $K=1M$ )	13.82	$p(\mathbf{z})$	0 + 9.09 = 9.09	0 + 13.82 = 13.82	0 + 13.82 = 13.82	0 + 10.76 = 10.76	0 + 13.81 = 13.81	0 + 13.82 = 13.82
		$q(\mathbf{z} \mathbf{x})$	3.78 + 5.31 = 9.09	25.20 + 8.90 = 34.10	44.54 + 13.81 = 58.35	6.02 + 4.79 = 10.81	4.23 + 13.53 = 17.76	3.17 + 13.81 = 16.98

Table 2: Decomposition of  $I_{\text{IWAE}_L}(q_\theta, K)$  into BA term and contrastive term ( $< \log K$ ) on MI estimation for VAE and GAN models trained on MNIST.

Method	log $K$	Proposal	GAN5	GAN10	GAN100
IWAE K=1	0	$p(\mathbf{z})$	0 + 0 = 0	0 + 0 = 0	0 + 0 = 0
		$q(\mathbf{z} \mathbf{x})$	14.53 + 0 = 14.53	17.45 + 0 = 17.45	20.00 + 0 = 20.00
IWAE K=1k	6.91	$p(\mathbf{z})$	0 + 6.91 = 6.91	0 + 6.91 = 6.91	0 + 6.91 = 6.91
		$q(\mathbf{z} \mathbf{x})$	14.53 + 6.90 = 21.43	16.68 + 6.9 = 23.58	20.07 + 6.91 = 26.98
IWAE K=1M	13.82	$p(\mathbf{z})$	0 + 13.82 = 13.82	0 + 13.82 = 13.82	0 + 13.82 = 13.82
		$q(\mathbf{z} \mathbf{x})$	14.53 + 13.81 = 28.34	16.92 + 13.81 = 30.73	20.00 + 13.81 = 33.81

Table 3: Decomposition of  $I_{\text{IWAE}_L}(q_\theta, K)$  into BA term and contrastive term ( $< \log K$ ) on MI estimation for GAN models trained on CIFAR-10.

Table 2 and Table 3 show the IWAE objective decomposition to the BA term and the contrastive term, on VAES and GANS trained MNIST and CIFAR-10 dataset. We can see that in all the experiments, the contribution of the contrastive term is always less than or equal to  $\log K$ .

For MNIST VAES and GANS with two dimensional latent spaces, the contrastive term may contribute notably less than  $\log K$ . In these cases, even the optimal critic function  $T^*(\mathbf{x}, \mathbf{z}) = \log \frac{p(\mathbf{x}, \mathbf{z})}{q_\theta(\mathbf{z}|\mathbf{x})} + c(\mathbf{x})$ , as used in IWAE, has difficulty distinguishing posterior and variational samples.

However, the contribution of the contrastive term is almost exactly  $\log K$  for higher dimensional VAE and GAN models, where the posterior  $p(\mathbf{z}|\mathbf{x})$  is more complex and is more easily distinguishable from the variational  $q_\theta(\mathbf{z}|\mathbf{x})$ . These results highlight the inherent exponential sample complexity of the IWAE lower bound on MI.

#### B.4 BIAS REDUCTION IN $K$ FOR IWAE LOWER BOUND ON $\log p(\mathbf{x})$ / UPPER BOUND ON MI

We have seen in App. B.2 Prop. 2.1 that the improvement of  $\text{EUBO}_{\text{IWAE}}(\mathbf{x}; q_\theta, K)$  and  $I_{\text{IWAE}_L}(\mathbf{x}; q_\theta, K)$  over the single-sample  $\text{EUBO}(\mathbf{x}; q_\theta)$  and  $I_{\text{BAL}}(\mathbf{x}; q_\theta)$  is limited by  $\log K$ . This suggests that exponential sample complexity in the gap of the EUBO,  $K \propto \exp\{D_{\text{KL}}[p(\mathbf{z}|\mathbf{x})\|q_\theta(\mathbf{z}|\mathbf{x})]\}$ , is required to obtain a tight lower bound.

The quantity  $D_{\text{KL}}[\mathcal{U}(s)\|p_{\text{TGT}}^{\text{IWAE}}(s|\mathbf{z}^{(1:K)}, \mathbf{x})]$ , which measures the improvement of the IWAE lower bound on  $\log p(\mathbf{x})$  over the ELBO, is not explicitly limited by  $\log K$ . However, Chatterjee et al. (2018) suggests that the same exponential sample complexity,  $K \propto \exp\{D_{\text{KL}}[p(\mathbf{z}|\mathbf{x})\|q_\theta(\mathbf{z}|\mathbf{x})]\}$ , is required for accurate importance sampling estimation with the proposal  $q_\theta(\mathbf{z}|\mathbf{x})$ . Maddison et al. (2017); Domke & Sheldon (2018) find that the bias of the IWAE lower bound in the limit of  $K \rightarrow \infty$  reduces at the rate of  $\mathcal{O}(\frac{1}{2K} \text{Var}[\frac{p(\mathbf{z}|\mathbf{x})}{q_\theta(\mathbf{z}|\mathbf{x})}])$ , although the  $\text{Var}[\frac{p(\mathbf{x}, \mathbf{z})}{q_\theta(\mathbf{z}|\mathbf{x})}]$  term is at least exponential in  $D_{\text{KL}}[p(\mathbf{z}|\mathbf{x})\|q_\theta(\mathbf{z}|\mathbf{x})]$  (Song & Ermon, 2019).

This exponential sample complexity for exact estimation of  $\log p(\mathbf{x})$  or  $I(\mathbf{x}, \mathbf{z})$  is usually impractical for complex target distributions and limited variational families, where  $D_{\text{KL}}[p(\mathbf{z}|\mathbf{x})\|q_\theta(\mathbf{z}|\mathbf{x})]$  may be large. This motivates our improved, Multi-Sample AIS proposals in Sec. 3.2, which achieve more favorable (linear) bias reduction by introducing MCMC transition kernels to bridge between  $q_\theta(\mathbf{z}|\mathbf{x})$  and  $p(\mathbf{z}|\mathbf{x})$ .

#### B.5 RELATIONSHIP WITH STRUCTURED INFONCE

We can recognize the Structured INFONCE upper and lower bounds for known  $p(\mathbf{x}|\mathbf{z})$  (Poole et al. (2019) Sec. 2.5) as simply applying the standard IWAE bounds, using the marginal  $p(\mathbf{z})$  in place of

the variational  $q_\theta(\mathbf{z}|\mathbf{x})$

$$\mathbb{E}_{p(\mathbf{x}, \mathbf{z}^{(1)}) \prod_{k=2}^K p(\mathbf{z}^{(k)})} \left[ \log \frac{p(\mathbf{x}|\mathbf{z}^{(1)})}{\frac{1}{K} \sum_{k=1}^K p(\mathbf{x}|\mathbf{z}^{(k)})} \right] \leq I(\mathbf{x}; \mathbf{z}) \leq \mathbb{E}_{p(\mathbf{x}) \prod_{k=1}^K p(\mathbf{z}^{(k)})} \left[ \log \frac{1}{\frac{1}{K} \sum_{k=1}^K p(\mathbf{x}|\mathbf{z}^{(k)})} \right] - H(\mathbf{x}|\mathbf{z}).$$

We refer to the lower bound as  $I_{S\text{-INFONCE}_L}(K)$  and the upper bound as  $I_{S\text{-INFONCE}_U}(K)$ . From [Cor. 2.2](#), we obtain an alternative proof that the Structured INFONCE lower bound is upper bounded by  $\log K$ . Since  $I_{\text{BAL}}(p(\mathbf{z})) \leq I_{\text{IWAE}_L}(p(\mathbf{z}), K) \leq I_{\text{BAL}}(p(\mathbf{z})) + \log K$  and the BA bound with a prior proposal equals 0 from [Eq. \(3\)](#), we have that  $0 \leq I_{S\text{-INFONCE}_L}(K) \leq \log K$ .

## C GENERALIZED IWAE

### C.1 PROBABILISTIC INTERPRETATION AND BOUNDS

To derive a probabilistic interpretation for GIWAE, our starting point is to further extend the state space of the IWAE target distribution in [Eq. \(4\)](#), using a uniform index variable  $p(s) = \frac{1}{K} \forall s$  that specifies which sample  $\mathbf{z}^{(k)}$  is drawn from the posterior  $p(\mathbf{z}|\mathbf{x})$ . This is shown in [Fig. 6](#), and leads to a joint distribution over  $(\mathbf{x}, \mathbf{z}^{(1:K)}, s)$  as

$$p_{\text{TGT}}^{\text{GIWAE}}(\mathbf{x}, \mathbf{z}^{(1:K)}, s) = \frac{1}{K} p(\mathbf{x}, \mathbf{z}^{(s)}) \prod_{\substack{k=1 \\ k \neq s}}^K q(\mathbf{z}^{(k)}|\mathbf{x}), \quad (50)$$

with marginalization over  $s$  leading to the mixture in [Eq. \(4\)](#). The posterior over the index variable  $s$ , which infers the ‘positive’ sample drawn from  $p(\mathbf{z}|\mathbf{x})$  given a set of samples  $\mathbf{z}^{(1:K)}$ , corresponds to the normalized importance weights

$$p_{\text{TGT}}^{\text{GIWAE}}(s|\mathbf{x}, \mathbf{z}^{(1:K)}) = \frac{\frac{p(\mathbf{x}, \mathbf{z}^{(s)})}{q_\theta(\mathbf{z}^{(s)}|\mathbf{x})}}{\sum_{k=1}^K \frac{p(\mathbf{x}, \mathbf{z}^{(k)})}{q_\theta(\mathbf{z}^{(k)}|\mathbf{x})}}, \quad (51)$$

which can be derived from  $p_{\text{TGT}}^{\text{GIWAE}}(s|\mathbf{x}, \mathbf{z}^{(1:K)}) = \frac{p_{\text{TGT}}^{\text{GIWAE}}(\mathbf{x}, \mathbf{z}^{(1:K)}, s)}{p_{\text{TGT}}^{\text{GIWAE}}(\mathbf{x}, \mathbf{z}^{(1:K)})} = \frac{\frac{1}{K} p(\mathbf{x}, \mathbf{z}^{(s)}) \prod_{k \neq s} q_\theta(\mathbf{z}^{(k)}|\mathbf{x})}{\frac{1}{K} \sum_{j=1}^K p(\mathbf{x}, \mathbf{z}^{(j)}) \prod_{k \neq j} q_\theta(\mathbf{z}^{(k)}|\mathbf{x})}$ .

For the GIWAE extended state space proposal distribution, we consider a categorical index variable  $q_{\text{PROP}}^{\text{GIWAE}}(s|\mathbf{z}^{(1:K)}, \mathbf{x})$  drawn according SNIS, with weights calculated using the critic function  $T_\phi$ .

$$q_{\text{PROP}}^{\text{GIWAE}}(\mathbf{z}^{(1:K)}, s|\mathbf{x}) = \left( \prod_{k=1}^K q_\theta(\mathbf{z}^{(k)}|\mathbf{x}) \right) q_{\text{PROP}}^{\text{GIWAE}}(s|\mathbf{z}^{(1:K)}, \mathbf{x}), \quad (52)$$

$$\text{where } q_{\text{PROP}}^{\text{GIWAE}}(s|\mathbf{z}^{(1:K)}, \mathbf{x}) = \frac{e^{T_\phi(\mathbf{x}, \mathbf{z}^{(s)})}}{\sum_{k=1}^K e^{T_\phi(\mathbf{x}, \mathbf{z}^{(k)})}}. \quad (53)$$

Similarly to [Lawson et al. \(2019\)](#), the variational SNIS distribution  $q_{\text{PROP}}^{\text{GIWAE}}(s|\mathbf{z}^{(1:K)}, \mathbf{x})$  is approximating the true SNIS distribution  $p_{\text{TGT}}^{\text{GIWAE}}(s|\mathbf{x}, \mathbf{z}^{(1:K)})$ . As we show in [App. C.4](#), the optimal critic function is  $T_\phi(\mathbf{x}, \mathbf{z}) = \log \frac{p(\mathbf{x}, \mathbf{z})}{q(\mathbf{z}|\mathbf{x})} + c(\mathbf{x})$ , which recovers the IWAE probabilistic interpretation (see [App. B.1](#)).

**Log Importance Ratio** To derive bounds on the log partition function, we first calculate the log unnormalized density ratio

$$\log \frac{p_{\text{TGT}}^{\text{GIWAE}}(\mathbf{z}^{(1:K)}, s, \mathbf{x})}{q_{\text{PROP}}^{\text{GIWAE}}(\mathbf{z}^{(1:K)}, s | \mathbf{x})} = \log \frac{\frac{1}{K} p(\mathbf{x}, \mathbf{z}^{(s)}) \prod_{\substack{k=1 \\ k \neq s}}^K q(\mathbf{z}^{(k)} | \mathbf{x})}{q(s | \mathbf{z}^{(1:K)}, \mathbf{x}) \prod_{k=1}^K q(\mathbf{z}^{(k)} | \mathbf{x})} \quad (54)$$

$$= \log \frac{1}{K} \frac{\sum_k e^{T(\mathbf{x}, \mathbf{z}^{(k)})} p(\mathbf{x}, \mathbf{z}^{(s)})}{e^{T(\mathbf{x}, \mathbf{z}^{(s)})} q(\mathbf{z}^{(s)} | \mathbf{x})} \quad (55)$$

$$= \log \frac{p(\mathbf{x}, \mathbf{z}^{(s)})}{q(\mathbf{z}^{(s)} | \mathbf{x})} - T(\mathbf{x}, \mathbf{z}^{(s)}) + \log \frac{1}{K} \sum_{k=1}^K e^{T(\mathbf{x}, \mathbf{z}^{(k)})}. \quad (56)$$

Taking the expectation of the log unnormalized density ratio under the proposal or target distribution yields a lower or upper bound, respectively, on  $\log p(\mathbf{x})$

$$\underbrace{\mathbb{E}_{q_{\text{PROP}}^{\text{GIWAE}}} \left[ \log \frac{p_{\text{TGT}}^{\text{GIWAE}}(\mathbf{z}^{(1:K)}, s, \mathbf{x})}{q_{\text{PROP}}^{\text{GIWAE}}(\mathbf{z}^{(1:K)}, s | \mathbf{x})} \right]}_{\text{ELBO}_{\text{GIWAE}}(\mathbf{x}; q_{\theta}, T_{\phi}, K)} \leq \log p(\mathbf{x}) \leq \underbrace{\mathbb{E}_{p_{\text{TGT}}^{\text{GIWAE}}} \left[ \log \frac{p_{\text{TGT}}^{\text{GIWAE}}(\mathbf{z}^{(1:K)}, s, \mathbf{x})}{q_{\text{PROP}}^{\text{GIWAE}}(\mathbf{z}^{(1:K)}, s | \mathbf{x})} \right]}_{\text{EUBO}_{\text{GIWAE}}(\mathbf{x}; q_{\theta}, T_{\phi}, K)}. \quad (57)$$

As in [Sec. 2.1](#) and [App. A](#), the gap in the lower and upper bounds can be derived as KL divergences in the extended state space.

**Upper Bound on  $\log p(\mathbf{x})$  and Lower Bound on MI** To derive an explicit form for the GIWAE upper bound on  $\log p(\mathbf{x})$ , we write

$$\begin{aligned} \text{EUBO}_{\text{GIWAE}}(q_{\theta}, T_{\phi}, K) &= \mathbb{E}_{p_{\text{TGT}}^{\text{GIWAE}}(\mathbf{z}^{(1:K)}, s | \mathbf{x})} \left[ \log \frac{p(\mathbf{x}, \mathbf{z}^{(s)})}{q(\mathbf{z}^{(s)} | \mathbf{x})} - T(\mathbf{x}, \mathbf{z}^{(s)}) + \log \frac{1}{K} \sum_{k=1}^K e^{T(\mathbf{x}, \mathbf{z}^{(k)})} \right] \\ &= \mathbb{E}_{p(\mathbf{z} | \mathbf{x})} \left[ \log \frac{p(\mathbf{x}, \mathbf{z})}{q(\mathbf{z} | \mathbf{x})} \right] - \mathbb{E}_{p(\mathbf{z}^{(1)} | \mathbf{x})} \prod_{k=2}^K q(\mathbf{z}^{(k)} | \mathbf{x}) \left[ \log \frac{e^{T(\mathbf{x}, \mathbf{z}^{(1)})}}{\frac{1}{K} \sum_{k=1}^K e^{T(\mathbf{x}, \mathbf{z}^{(k)})}} \right]. \end{aligned} \quad (58)$$

where, in the first term of the second line, we note that  $p_{\text{TGT}}^{\text{GIWAE}}(\mathbf{z}^{(1:K)}, s | \mathbf{x})$  specifies that  $\mathbf{z}^{(s)} \sim p(\mathbf{z} | \mathbf{x})$ . Since  $s \sim p(s) = \frac{1}{K}$  is sampled uniformly, we can assume  $s = 1$  in the second term due to permutation invariance.

Translating this into a lower bound on MI, we consider  $I(\mathbf{x}; \mathbf{z}) = -\mathbb{E}_{p(\mathbf{x})} [\log p(\mathbf{x})] - H(\mathbf{x} | \mathbf{z}) \geq -\mathbb{E}_{p(\mathbf{x})} [\text{EUBO}_{\text{GIWAE}}(q_{\theta}, T_{\phi}, K)] - H(\mathbf{x} | \mathbf{z})$ . Writing the conditional entropy term over the index  $s$ ,

$$I(\mathbf{x}; \mathbf{z}) \geq \mathbb{E}_{p(\mathbf{x}, \mathbf{z})} [\log p(\mathbf{x} | \mathbf{z})] \quad (59)$$

$$\begin{aligned} &- \left( \mathbb{E}_{p(\mathbf{x}) p(\mathbf{z} | \mathbf{x})} \left[ \log \frac{p(\mathbf{x}, \mathbf{z})}{q(\mathbf{z} | \mathbf{x})} \right] - \mathbb{E}_{p(\mathbf{x}) p(\mathbf{z}^{(1)} | \mathbf{x})} \prod_{k=2}^K q(\mathbf{z}^{(k)} | \mathbf{x}) \left[ \log \frac{e^{T_{\phi}(\mathbf{x}, \mathbf{z}^{(1)})}}{\frac{1}{K} \sum_{k=1}^K e^{T_{\phi}(\mathbf{x}, \mathbf{z}^{(k)})}} \right] \right) \\ &= \mathbb{E}_{p(\mathbf{x}, \mathbf{z})} \left[ \log \frac{q(\mathbf{z} | \mathbf{x})}{p(\mathbf{z})} \right] + \mathbb{E}_{p(\mathbf{x}) p(\mathbf{z}^{(1)} | \mathbf{x})} \prod_{k=2}^K q_{\theta}(\mathbf{z}^{(k)} | \mathbf{x}) \left[ \log \frac{e^{T_{\phi}(\mathbf{x}, \mathbf{z}^{(1)})}}{\frac{1}{K} \sum_{i=1}^K e^{T_{\phi}(\mathbf{x}, \mathbf{z}^{(i)})}} \right], \end{aligned} \quad (60)$$

which matches [Eq. \(11\)](#) from the main text.

## C.2 GIWAE UPPER BOUND ON MI DOES NOT PROVIDE BENEFIT OVER IWAE

To derive an explicit form for the GIWAE lower bound on  $\log p(\mathbf{x})$ ,

$$\text{ELBO}_{\text{GIWAE}}(\mathbf{x}; q_{\theta}, T_{\phi}, K) = \mathbb{E}_{q_{\text{PROP}}^{\text{GIWAE}}(\mathbf{z}^{(1:K)}, s | \mathbf{x})} \left[ \log \frac{p(\mathbf{x}, \mathbf{z}^{(s)})}{q(\mathbf{z}^{(s)} | \mathbf{x})} - T_{\phi}(\mathbf{x}, \mathbf{z}^{(s)}) + \log \frac{1}{K} \sum_{k=1}^K e^{T_{\phi}(\mathbf{x}, \mathbf{z}^{(k)})} \right] \quad (61)$$

Translating this to an upper bound on MI yields

$$I(\mathbf{x}; \mathbf{z}) \leq \mathbb{E}_{p(\mathbf{z}^{(s)}|\mathbf{x})} \left[ \log p(\mathbf{x}|\mathbf{z}^{(s)}) \right] - \left( \mathbb{E}_{\prod_{k=1}^K q(\mathbf{z}^{(k)}|\mathbf{x})} \left[ \sum_{s=1}^K \frac{e^{T_\phi(\mathbf{x}, \mathbf{z}^{(s)})}}{\sum_{k=1}^K e^{T_\phi(\mathbf{x}, \mathbf{z}^{(k)})}} \log \frac{p(\mathbf{x}, \mathbf{z}^{(s)})}{q(\mathbf{z}^{(s)}|\mathbf{x})} \right] \right. \\ \left. - \mathbb{E}_{q_{\text{PROP}}^{\text{GIWAE}}(\mathbf{z}^{(1:K)}, s|\mathbf{x})} \left[ \log \frac{e^{T(\mathbf{x}, \mathbf{z}^{(s)})}}{\frac{1}{K} \sum_{k=1}^K e^{T(\mathbf{x}, \mathbf{z}^{(k)})}} \right] \right) \quad (62)$$

Thus, in Eq. (62), knowledge of the full joint density is required to evaluate both the conditional entropy and  $\log \frac{p(\mathbf{x}, \mathbf{z}^{(s)})}{q(\mathbf{z}^{(s)}|\mathbf{x})}$  terms. If both  $p(\mathbf{z})$  and  $p(\mathbf{x}|\mathbf{z})$  are known, then we will show in Cor. 2.4 below that the optimal critic or negative energy function in GIWAE yields the true importance weights, and the resulting MI or log  $p(\mathbf{x})$  bounds matches the IWAE bounds.

We thus conclude that the GIWAE upper bound on MI and lower bound on  $\log p(\mathbf{x})$  does not provide any benefit over IWAE in practice. However,  $\text{ELBO}_{\text{GIWAE}}(\mathbf{x}; q_\theta, T_\phi, K)$  is still useful for analysis, as our proof of Lemma C.1 below allows us characterize the gap between  $\text{ELBO}_{\text{IWAE}}(\mathbf{x}; q_\theta, K)$  and  $\text{ELBO}(\mathbf{x}; q_\theta)$  in Prop. 2.1.

### C.3 ELBO AND EUBO ARE SPECIAL CASES OF GIWAE LOG PARTITION FUNCTION BOUNDS

**Lemma C.1.** *The single-sample ELBO and EUBO are special cases of GIWAE, with*

$$\begin{aligned} \text{ELBO}(\mathbf{x}; q_\theta) &= \text{ELBO}_{\text{GIWAE}}(\mathbf{x}; q_\theta, T_{\phi_0} = \text{const}, K), \\ \text{EUBO}(\mathbf{x}; q_\theta) &= \text{EUBO}_{\text{GIWAE}}(\mathbf{x}; q_\theta, T_{\phi_0} = \text{const}, K). \end{aligned}$$

In both cases, the SNIS sampling distribution (Eq. (53)) is uniform  $q_{\text{PROP}}^{\text{GIWAE}}(\mathbf{z}^{(1:K)}, s|\mathbf{x}) = \frac{1}{K} = \mathcal{U}(s)$ .

*Proof.* We consider the GIWAE probabilistic interpretation (App. C.1) for  $T_{\phi_0} = \text{const}$ . We refer to this extended state space proposal as  $q_{\text{PROP}}^{\text{BA}}$ , since it leads to  $I_{\text{BAL}}(q_\theta)$  and  $I_{\text{BAU}}(q_\theta)$  bounds on MI.

$$q_{\text{PROP}}^{\text{BA}}(\mathbf{z}^{(1:K)}, s|\mathbf{x}) = \left( \prod_{k=1}^K q_\theta(\mathbf{z}^{(k)}|\mathbf{x}) \right) q_{\text{PROP}}^{\text{BA}}(s|\mathbf{z}^{(1:K)}, \mathbf{x}), \quad (63)$$

$$\text{where } q_{\text{PROP}}^{\text{BA}}(s|\mathbf{z}^{(1:K)}, \mathbf{x}) = \frac{e^{T_{\phi_0}(\mathbf{x}, \mathbf{z}^{(s)})}}{\sum_{k=1}^K e^{T_{\phi_0}(\mathbf{x}, \mathbf{z}^{(k)})}} = \mathcal{U}(s) = \frac{1}{K}. \quad (64)$$

Note that the SNIS sampling distribution  $q_{\text{PROP}}^{\text{BA}}(s|\mathbf{z}^{(1:K)}, \mathbf{x})$  will be uniform, which matches  $p(s) = \frac{1}{K}$  in the GIWAE extended state space target distribution

$$p_{\text{TGT}}^{\text{GIWAE}}(\mathbf{z}^{(1:K)}, s|\mathbf{x}) = \frac{1}{K} p(\mathbf{z}^{(s)}|\mathbf{x}) \prod_{\substack{k=1 \\ k \neq s}}^K q_\theta(\mathbf{z}^{(k)}|\mathbf{x}) \quad (65)$$

Now, taking the log unnormalized importance weights, we obtain

$$\log \frac{p_{\text{TGT}}^{\text{GIWAE}}(\mathbf{z}^{(1:K)}, s|\mathbf{x})}{q_{\text{PROP}}^{\text{BA}}(\mathbf{z}^{(1:K)}, s|\mathbf{x})} = \log \frac{\frac{1}{K} p(\mathbf{z}^{(s)}|\mathbf{x}) \prod_{\substack{k=1 \\ k \neq s}}^K q_\theta(\mathbf{z}^{(k)}|\mathbf{x})}{\frac{1}{K} \prod_{k=1}^K q_\theta(\mathbf{z}^{(k)}|\mathbf{x})} = \log \frac{p(\mathbf{x}, \mathbf{z}^{(s)})}{q_\theta(\mathbf{z}^{(s)}|\mathbf{x})} \quad (66)$$

Taking expectations with respect to  $q_{\text{PROP}}^{\text{BA}}(\mathbf{z}^{(1:K)}, s|\mathbf{x})$  or  $p_{\text{TGT}}^{\text{GIWAE}}(\mathbf{z}^{(1:K)}, s|\mathbf{x})$  leads to  $\text{ELBO}(\mathbf{x}; q_\theta)$  and  $\text{EUBO}(\mathbf{x}; q_\theta)$  respectively, as in Sec. 2-2.2.  $\square$

### C.4 PROOF OF RELATIONSHIP BETWEEN IWAE AND GIWAE PROBABILISTIC INTERPRETATIONS (PROP. 2.3)

We first prove a lemma which relates both the GIWAE lower and upper bounds on  $\log p(\mathbf{x})$  to the respective IWAE bounds. From this lemma, Prop. 2.1 follows directly and relates the ELBO and EUBO (which are special cases of  $\text{ELBO}_{\text{GIWAE}}$  and  $\text{EUBO}_{\text{GIWAE}}$ ) to  $\text{ELBO}_{\text{IWAE}}$  and  $\text{EUBO}_{\text{IWAE}}$ .



**Lemma C.2.** *We can characterize the difference between IWAE and GIWAE bounds on  $\log p(\mathbf{x})$  using KL divergences between their respective SNIS distributions.*

$$\text{ELBO}_{\text{IWAE}}(\mathbf{x}; q_\theta, K) = \text{ELBO}_{\text{GIWAE}}(\mathbf{x}; q_\theta, T_\phi, K) + \mathbb{E}_{q_{\text{PROP}}^{\text{GIWAE}}(\mathbf{z}^{(1:K)}|\mathbf{x})} \left[ D_{\text{KL}}[q_{\text{PROP}}^{\text{GIWAE}}(s|\mathbf{z}^{(1:K)}, \mathbf{x}) \| p_{\text{TGT}}^{\text{IWAE}}(s|\mathbf{z}^{(1:K)}, \mathbf{x})] \right] \quad (67)$$

$$\text{EUBO}_{\text{IWAE}}(\mathbf{x}; q_\theta, K) = \text{EUBO}_{\text{GIWAE}}(\mathbf{x}; q_\theta, T_\phi, K) - \mathbb{E}_{p_{\text{TGT}}^{\text{IWAE}}(\mathbf{z}^{(1:K)}|\mathbf{x})} \left[ D_{\text{KL}}[p_{\text{TGT}}^{\text{IWAE}}(s|\mathbf{z}^{(1:K)}, \mathbf{x}) \| q_{\text{PROP}}^{\text{GIWAE}}(s|\mathbf{z}^{(1:K)}, \mathbf{x})] \right] \quad (68)$$

*Proof.* Recall from [Sec. 2.1](#) or [App. A](#) that the gap of the lower bound  $\text{ELBO}_{\text{GIWAE}}(\mathbf{x}; q_\theta, T_\phi, K)$  is  $D_{\text{KL}}[q_{\text{PROP}}^{\text{GIWAE}}(\mathbf{z}^{(1:K)}, s|\mathbf{x}) \| p_{\text{TGT}}^{\text{GIWAE}}(\mathbf{z}^{(1:K)}, s, \mathbf{x})]$ , while the gap of the upper bound  $\text{EUBO}_{\text{GIWAE}}(\mathbf{x}; q_\theta, T_\phi, K)$  is  $D_{\text{KL}}[p_{\text{TGT}}^{\text{GIWAE}}(\mathbf{z}^{(1:K)}, s|\mathbf{x}) \| q_{\text{PROP}}^{\text{GIWAE}}(\mathbf{z}^{(1:K)}, s|\mathbf{x})]$ . We will expand these KL divergences to reveal the relationship between the GIWAE bounds and IWAE bounds.

First, recall from [Eq. \(51\)](#) that the posterior over the index variable  $s$ , or target SNIS distribution, is

$$p_{\text{TGT}}^{\text{GIWAE}}(s|\mathbf{z}^{(1:K)}, \mathbf{x}) = \frac{p_{\text{TGT}}^{\text{GIWAE}}(\mathbf{z}^{(1:K)}, s, \mathbf{x})}{\sum_{s=1}^K p_{\text{TGT}}^{\text{GIWAE}}(\mathbf{z}^{(1:K)}, s, \mathbf{x})} = \frac{\frac{1}{K} p(\mathbf{x}, \mathbf{z}^{(s)}) \prod_{k=1, k \neq s}^K q_\theta(\mathbf{z}^{(k)}|\mathbf{x})}{\frac{1}{K} \sum_{s=1}^K p(\mathbf{x}, \mathbf{z}^{(s)}) \prod_{k=1, k \neq s}^K q_\theta(\mathbf{z}^{(k)}|\mathbf{x})} = \frac{\frac{p(\mathbf{x}, \mathbf{z}^{(s)})}{q(\mathbf{z}^{(s)}|\mathbf{x})}}{\sum_{s=1}^K \frac{p(\mathbf{x}, \mathbf{z}^{(s)})}{q(\mathbf{z}^{(s)}|\mathbf{x})}}.$$

The joint distribution then factorizes as  $p_{\text{TGT}}^{\text{GIWAE}}(\mathbf{z}^{(1:K)}, s, \mathbf{x}) = p_{\text{TGT}}^{\text{GIWAE}}(\mathbf{z}^{(1:K)}, \mathbf{x}) \cdot p_{\text{TGT}}^{\text{GIWAE}}(s|\mathbf{z}^{(1:K)}, \mathbf{x})$ .

*ELBO Case:* Using this factorization of  $p_{\text{TGT}}^{\text{GIWAE}}(\mathbf{z}^{(1:K)}, s, \mathbf{x})$ , we can rewrite the gap of  $\text{ELBO}_{\text{GIWAE}}(\mathbf{x}; q_\theta, T_\phi, K)$  as follows

$$\begin{aligned} & D_{\text{KL}}[q_{\text{PROP}}^{\text{GIWAE}}(\mathbf{z}^{(1:K)}, s|\mathbf{x}) \| p_{\text{TGT}}^{\text{GIWAE}}(\mathbf{z}^{(1:K)}, s|\mathbf{x})] \\ &= \mathbb{E}_{q_{\text{PROP}}^{\text{GIWAE}}(\mathbf{z}^{(1:K)}, s|\mathbf{x})} \left[ \log \frac{q_{\text{PROP}}^{\text{GIWAE}}(\mathbf{z}^{(1:K)}|\mathbf{x}) q_{\text{PROP}}^{\text{GIWAE}}(s|\mathbf{z}^{(1:K)}, \mathbf{x})}{p_{\text{TGT}}^{\text{GIWAE}}(\mathbf{z}^{(1:K)}|\mathbf{x}) p_{\text{TGT}}^{\text{GIWAE}}(s|\mathbf{z}^{(1:K)}, \mathbf{x})} \right] \\ &= D_{\text{KL}} \left[ \prod_{k=1}^K q_\theta(\mathbf{z}^{(k)}|\mathbf{x}) \middle\| \frac{1}{K} \sum_{s=1}^K p(\mathbf{z}^{(s)}|\mathbf{x}) \prod_{k=1, k \neq s}^K q_\theta(\mathbf{z}^{(k)}|\mathbf{x}) \right] + \mathbb{E}_{q_{\text{PROP}}^{\text{GIWAE}}} \left[ D_{\text{KL}}[q_{\text{PROP}}^{\text{GIWAE}}(s|\mathbf{z}^{(1:K)}, \mathbf{x}) \| p_{\text{TGT}}^{\text{GIWAE}}(s|\mathbf{z}^{(1:K)}, \mathbf{x})] \right] \\ &= D_{\text{KL}} \left[ q_{\text{PROP}}^{\text{IWAE}}(\mathbf{z}^{(1:K)}|\mathbf{x}) \middle\| p_{\text{TGT}}^{\text{IWAE}}(\mathbf{z}^{(1:K)}|\mathbf{x}) \right] + \mathbb{E}_{q_{\text{PROP}}^{\text{GIWAE}}} \left[ D_{\text{KL}}[q_{\text{PROP}}^{\text{GIWAE}}(s|\mathbf{z}^{(1:K)}, \mathbf{x}) \| p_{\text{TGT}}^{\text{GIWAE}}(s|\mathbf{z}^{(1:K)}, \mathbf{x})] \right], \end{aligned} \quad (70)$$

where we can recognize the first term as the gap in  $\text{ELBO}_{\text{IWAE}}(\mathbf{x}; q_\theta, K)$ . Noting that  $\text{ELBO}_{\text{IWAE}}(\mathbf{x}; q_\theta, K) - \text{ELBO}_{\text{GIWAE}}(\mathbf{x}; q_\theta, T_\phi, K) = D_{\text{KL}}[q_{\text{PROP}}^{\text{GIWAE}}(\mathbf{z}^{(1:K)}, s|\mathbf{x}) \| p_{\text{TGT}}^{\text{GIWAE}}(\mathbf{z}^{(1:K)}, s|\mathbf{x})] - D_{\text{KL}}[q_{\text{PROP}}^{\text{IWAE}}(\mathbf{z}^{(1:K)}|\mathbf{x}) \| p_{\text{TGT}}^{\text{IWAE}}(\mathbf{z}^{(1:K)}|\mathbf{x})]$ , we obtain [Eq. \(67\)](#), as desired

$$\text{ELBO}_{\text{IWAE}}(\mathbf{x}; q_\theta, K) = \text{ELBO}_{\text{GIWAE}}(\mathbf{x}; q_\theta, T_\phi, K) + \mathbb{E}_{q_{\text{PROP}}^{\text{GIWAE}}(\mathbf{z}^{(1:K)}|\mathbf{x})} \left[ D_{\text{KL}}[q_{\text{PROP}}^{\text{GIWAE}}(s|\mathbf{z}^{(1:K)}, \mathbf{x}) \| p_{\text{TGT}}^{\text{GIWAE}}(s|\mathbf{z}^{(1:K)}, \mathbf{x})] \right].$$

*EUBO Case:* For  $\text{ELBO}_{\text{GIWAE}}(\mathbf{x}; q_\theta, T_\phi, K)$ , the derivations follow in a similar fashion to [Eq. \(69\)](#)-[Eq. \(70\)](#), but using the reverse KL divergence and expectations under  $p_{\text{TGT}}^{\text{GIWAE}}(\mathbf{z}^{(1:K)}, s|\mathbf{x})$ .  $\square$

Translating [Lemma C.2](#) to a statement relating IWAE and GIWAE bounds on MI, we obtain the following proposition.

**Proposition 2.3** (Improvement of IWAE over GIWAE). *For a given  $q_\theta(\mathbf{z}|\mathbf{x})$ , the IWAE lower bound on MI is tighter than the GIWAE lower bound for any  $T_\phi(\mathbf{x}, \mathbf{z})$ . Their difference is the average KL divergence between the normalized importance weights  $p_{\text{TGT}}^{\text{GIWAE}}(s|\mathbf{z}^{(1:K)}, \mathbf{x})$  and the variational distribution  $q_{\text{PROP}}^{\text{GIWAE}}(s|\mathbf{z}^{(1:K)}, \mathbf{x})$  in [Eq. \(10\)](#),*

$$I_{\text{IWAE}_L}(q_\theta, K) = I_{\text{GIWAE}_L}(q_\theta, T_\phi, K) + \mathbb{E}_{p(\mathbf{x}) p_{\text{TGT}}^{\text{IWAE}}(\mathbf{z}^{(1:K)}|\mathbf{x})} \left[ D_{\text{KL}}[p_{\text{TGT}}^{\text{GIWAE}}(s|\mathbf{z}^{(1:K)}, \mathbf{x}) \| q_{\text{PROP}}^{\text{GIWAE}}(s|\mathbf{z}^{(1:K)}, \mathbf{x})] \right].$$

*Proof.* The result follows directly from [Lemma C.2](#). First, note that  $p_{\text{TGT}}^{\text{IWAE}}(\mathbf{x}, \mathbf{z}^{(1:K)}, s) = p_{\text{TGT}}^{\text{GIWAE}}(\mathbf{x}, \mathbf{z}^{(1:K)}, s)$ . Then, using the upper bounds on  $\log p(\mathbf{x})$  and taking outer expectations with respect to  $p(\mathbf{x})$ , we have

$$I_{\text{IWAE}_L}(q_\theta, K) - I_{\text{GIWAE}_L}(q_\theta, T_\phi, K) = -H(\mathbf{x}|\mathbf{z}) - \mathbb{E}_{p(\mathbf{x})} [\text{EUBO}_{\text{IWAE}}(\mathbf{x}; q_\theta, K)] \quad (71)$$

$$+ H(\mathbf{x}|\mathbf{z}) + \mathbb{E}_{p(\mathbf{x})} [\text{EUBO}_{\text{GIWAE}}(\mathbf{x}; q_\theta, T_\phi, K)]$$

$$= \mathbb{E}_{p(\mathbf{x}) p_{\text{TGT}}^{\text{IWAE}}(\mathbf{z}^{(1:K)}|\mathbf{x})} \left[ D_{\text{KL}}[p_{\text{TGT}}^{\text{IWAE}}(s|\mathbf{z}^{(1:K)}, \mathbf{x}) \| q_{\text{PROP}}^{\text{GIWAE}}(s|\mathbf{z}^{(1:K)}, \mathbf{x})] \right]. \quad (72)$$

□

### C.5 PROOF OF GIWAE OPTIMAL CRITIC FUNCTION AND LOGARITHMIC IMPROVEMENT (COR. 2.4 AND COR. 2.5)

We now prove Cor. 2.4 and Cor. 2.5 from the main text, with a corollary stating the results for the special case of INFONCE in App. C.6.

**Corollary 2.4** (Optimal GIWAE Critic Function yields IWAE). *For a given  $q_\theta(\mathbf{z}|\mathbf{x})$  and  $K > 1$ , the optimal GIWAE critic function is equal to the true log importance weight up to an arbitrary constant:  $T^*(\mathbf{x}, \mathbf{z}) = \log \frac{p(\mathbf{x}, \mathbf{z})}{q_\theta(\mathbf{z}|\mathbf{x})} + c(\mathbf{x})$ . With this choice of  $T^*(\mathbf{x}, \mathbf{z})$ , we have*

$$I_{\text{GIWAE}_L}(q_\theta, T^*, K) = I_{\text{IWAE}_L}(q_\theta, K). \quad (12)$$

*Proof.* Using Prop. 2.3, we can see that the gap in the GIWAE and IWAE bounds, which corresponds to the posterior KL divergence over the index variable  $s$ , will equal zero iff

$$q_{\text{PROP}}^{\text{GIWAE}}(s|\mathbf{z}^{(1:K)}, \mathbf{x}) = p_{\text{TGT}}^{\text{GIWAE}}(s|\mathbf{z}^{(1:K)}, \mathbf{x}) \implies \frac{e^{T(\mathbf{x}, \mathbf{z}^{(s)})}}{\sum_{k=1}^K e^{T(\mathbf{x}, \mathbf{z}^{(k)})}} = \frac{\frac{p(\mathbf{x}, \mathbf{z}^{(s)})}{q_\theta(\mathbf{z}^{(s)}|\mathbf{x})}}{\sum_{s=1}^K \frac{p(\mathbf{x}, \mathbf{z}^{(s)})}{q_\theta(\mathbf{z}^{(s)}|\mathbf{x})}} \quad (73)$$

This condition also ensures that the overall GIWAE proposal  $p_{\text{TGT}}^{\text{GIWAE}}(\mathbf{z}^{(1:K)}, s|\mathbf{x})$  (Eq. (50)) and target  $q_{\text{PROP}}^{\text{GIWAE}}(\mathbf{z}^{(1:K)}, s|\mathbf{x})$  (Eq. (52)) distributions match. We will show that any  $T(\mathbf{x}, \mathbf{z})$  which satisfies Eq. (73) has the form

$$T^*(\mathbf{x}, \mathbf{z}) = \log \frac{p(\mathbf{x}, \mathbf{z})}{q_\theta(\mathbf{z}|\mathbf{x})} + c(\mathbf{x}). \quad (74)$$

Let  $f(\mathbf{x}, \mathbf{z}) = \log \frac{p(\mathbf{x}, \mathbf{z})}{q_\theta(\mathbf{z}|\mathbf{x})} + g(\mathbf{x}, \mathbf{z})$ , which represents an arbitrary choice of critic function. We will show that  $g(\mathbf{x}, \mathbf{z})$  must be constant with respect to  $\mathbf{z}$

$$\begin{aligned} & \frac{e^{\log \frac{p(\mathbf{x}, \mathbf{z}^{(s)})}{q_\theta(\mathbf{z}^{(s)}|\mathbf{x})} + g(\mathbf{x}, \mathbf{z}^{(s)})}}{\sum_{k=1}^K e^{\log \frac{p(\mathbf{x}, \mathbf{z}^{(s)})}{q_\theta(\mathbf{z}^{(s)}|\mathbf{x})} + g(\mathbf{x}, \mathbf{z}^{(s)})}} = \frac{\frac{p(\mathbf{x}, \mathbf{z}^{(s)})}{q_\theta(\mathbf{z}^{(s)}|\mathbf{x})}}{\sum_{k=1}^K \frac{p(\mathbf{x}, \mathbf{z}^{(k)})}{q_\theta(\mathbf{z}^{(k)}|\mathbf{x})}} \\ \implies & e^{\log \frac{p(\mathbf{x}, \mathbf{z}^{(s)})}{q_\theta(\mathbf{z}^{(s)}|\mathbf{x})}} \cdot e^{g(\mathbf{x}, \mathbf{z}^{(s)})} \cdot \sum_{k=1}^K \frac{p(\mathbf{x}, \mathbf{z}^{(k)})}{q_\theta(\mathbf{z}^{(k)}|\mathbf{x})} = \frac{p(\mathbf{x}, \mathbf{z}^{(s)})}{q_\theta(\mathbf{z}^{(s)}|\mathbf{x})} \cdot \sum_{k=1}^K e^{\log \frac{p(\mathbf{x}, \mathbf{z}^{(k)})}{q_\theta(\mathbf{z}^{(k)}|\mathbf{x})} + g(\mathbf{x}, \mathbf{z}^{(k)})} \\ & \sum_{k=1}^K \frac{p(\mathbf{x}, \mathbf{z}^{(k)})}{q_\theta(\mathbf{z}^{(k)}|\mathbf{x})} \frac{p(\mathbf{x}, \mathbf{z}^{(s)})}{q_\theta(\mathbf{z}^{(s)}|\mathbf{x})} e^{g(\mathbf{x}, \mathbf{z}^{(s)})} = \sum_{k=1}^K \frac{p(\mathbf{x}, \mathbf{z}^{(k)})}{q_\theta(\mathbf{z}^{(k)}|\mathbf{x})} \frac{p(\mathbf{x}, \mathbf{z}^{(s)})}{q_\theta(\mathbf{z}^{(s)}|\mathbf{x})} e^{g(\mathbf{x}, \mathbf{z}^{(k)})} \\ \implies & g(\mathbf{x}, \mathbf{z}) = c(\mathbf{x}) \end{aligned}$$

where  $g(\mathbf{x}, \mathbf{z}) = c(\mathbf{x})$  is required in order to ensure that  $g(\mathbf{x}, \mathbf{z}^{(s)}) = g(\mathbf{x}, \mathbf{z}^{(k)})$  for arbitrary choices of  $\mathbf{z}$  samples.

This form for the optimal critic function  $T^*(\mathbf{x}, \mathbf{z})$  in Eq. (74) implies that learning  $T_\phi(\mathbf{x}, \mathbf{z})$  in GIWAE becomes unnecessary when the density ratio  $\frac{p(\mathbf{x}, \mathbf{z})}{q_\theta(\mathbf{z}|\mathbf{x})}$  is available in closed form, as is assumed in the IWAE bound.

For this choice of  $T^*(\mathbf{x}, \mathbf{z})$ , the value of the GIWAE objective matches the IWAE lower bound on MI.

$$\begin{aligned}
I_{\text{GIWAE}}(q_\theta, T^*, K) &= \mathbb{E}_{p(\mathbf{x}, \mathbf{z})} \left[ \log \frac{q(\mathbf{z}|\mathbf{x})}{p(\mathbf{z})} \right] + \mathbb{E}_{p(\mathbf{x}, \mathbf{z}^{(1)}) \prod_{k=2}^K q_\theta(\mathbf{z}^{(k)}|\mathbf{x})} \left[ \log \frac{e^{\log \frac{p(\mathbf{x}, \mathbf{z}^{(1)})}{q(\mathbf{z}^{(1)}|\mathbf{x})} \cdot e^{c(\mathbf{x})}}}{\frac{1}{K} \sum_{k=1}^K e^{\log \frac{p(\mathbf{x}, \mathbf{z}^{(k)})}{q_\theta(\mathbf{z}^{(k)}|\mathbf{x})} \cdot e^{c(\mathbf{x})}}} \right] \\
&= \mathbb{E}_{p(\mathbf{x}, \mathbf{z})} \left[ \log \frac{q(\mathbf{z}|\mathbf{x})}{p(\mathbf{z})} + \log \frac{p(\mathbf{x}, \mathbf{z})}{q(\mathbf{z}|\mathbf{x})} \right] - \mathbb{E}_{p(\mathbf{x}, \mathbf{z}^{(1)}) \prod_{k=2}^K q_\theta(\mathbf{z}^{(k)}|\mathbf{x})} \left[ \log \frac{1}{K} \sum_{i=1}^K \frac{p(\mathbf{x}, \mathbf{z}^{(i)})}{q_\theta(\mathbf{z}^{(i)}|\mathbf{x})} \right] \quad (75) \\
&= -H(\mathbf{x}|\mathbf{z}) + \left( -\mathbb{E}_{p(\mathbf{x})p(\mathbf{z}^{(s)}|\mathbf{x}) \prod_{k=2}^K q_\theta(\mathbf{z}^{(k)}|\mathbf{x})} \left[ \log \frac{1}{K} \sum_{i=1}^K \frac{p(\mathbf{x}, \mathbf{z}^{(i)})}{q_\theta(\mathbf{z}^{(i)}|\mathbf{x})} \right] \right) \\
&= I_{\text{IWAE}_L}(q_\theta, K).
\end{aligned}$$

The second term in Eq. (75) is exactly the negative of the IWAE upper bound on  $\log p(\mathbf{x})$  in Eq. (47). Combined with the entropy  $-H(\mathbf{x}|\mathbf{z})$ , we obtain the  $I_{\text{IWAE}_L}(q_\theta, K)$  lower bound on MI as desired.  $\square$

**Corollary 2.5** (Logarithmic Improvement of GIWAE). *Suppose the critic function  $T_\phi(\mathbf{x}, \mathbf{z})$  is parameterized by  $\phi$ , and  $\exists \phi_0$  s.t.  $\forall (\mathbf{x}, \mathbf{z})$ ,  $T_{\phi_0}(\mathbf{x}, \mathbf{z}) = \text{const}$ . For a given  $q_\theta(\mathbf{z}|\mathbf{x})$ , let  $T_{\phi^*}(\mathbf{x}, \mathbf{z})$  denote the critic function that maximizes the GIWAE lower bound. Using Cor. 2.2 and Cor. 2.4, we have*

$$I_{\text{BAL}}(q_\theta) \leq I_{\text{GIWAE}_L}(q_\theta, T_{\phi^*}, K) \leq I_{\text{IWAE}_L}(q_\theta, K) \leq I_{\text{BAL}}(q_\theta) + \log K. \quad (13)$$

*Proof.* We begin by showing that  $I_{\text{BAL}}(q_\theta) \leq I_{\text{GIWAE}_L}(q_\theta, T_{\phi^*}, K)$ . This follows from the assumption that there exists  $\phi_0$  in the parameter space of the neural network  $T_\phi$  such that  $T_{\phi_0} = \text{const}$ . With this  $\phi_0$ , we would have  $I_{\text{BAL}}(q_\theta) = I_{\text{GIWAE}_L}(q_\theta, T_{\phi_0}, K)$  as in Lemma C.1. Thus, the optimal  $\phi^*$  in the parameter space can only improve upon the BA bound.

Next, for any given  $\phi$  (including  $\phi^*$ ), we have  $I_{\text{GIWAE}_L}(q_\theta, T_\phi, K) \leq I_{\text{IWAE}_L}(q_\theta, K)$ , since IWAE uses the (unconstrained) optimal critic function  $T^* = \log \frac{p(\mathbf{x}, \mathbf{z})}{q_\theta(\mathbf{z}|\mathbf{x})} + c(\mathbf{x})$  (Cor. 2.4). The final inequality follows from Prop. 2.1, which shows that  $I_{\text{IWAE}_L}(q_\theta, K)$  improves by at most  $\log K$  over  $I_{\text{BAL}}(q_\theta)$ . These relationships are visualized in Fig. 5b.  $\square$

## C.6 PROPERTIES OF INFONCE

**Corollary C.3.** *Using the prior  $q_\theta(\mathbf{z}|\mathbf{x}) = p(\mathbf{z})$  as in INFONCE,*

(a) *For the optimal critic function, Cor. 2.4 implies  $T^*(\mathbf{x}, \mathbf{z}) = \log p(\mathbf{x}|\mathbf{z}) + c(\mathbf{x})$ , and*

$$I_{\text{GIWAE}_L}(p(\mathbf{z}), T^*, K) = I_{\text{INFONCE}_L}(T^*, K) = I_{\text{S-INFONCE}_L}(K). \quad (76)$$

(b) *For an arbitrary critic function  $T_\phi(\mathbf{x}, \mathbf{z})$ , Cor. 2.5 translates to*

$$0 \leq I_{\text{INFONCE}_L}(T_\phi, K) \leq I_{\text{S-INFONCE}_L}(K) \leq \log K. \quad (77)$$

For INFONCE, note that using the prior as the proposal does allow the critic to admit an efficient bi-linear implementation  $T_\phi(\mathbf{x}, \mathbf{z}) = f_{\phi_x}(\mathbf{x})^T f_{\phi_z}(\mathbf{z})$ , which requires only  $N + K$  forward passes instead of  $NK$  for GIWAE, where  $N$  is the batch size and  $K$  is the total number of positive and negative samples.

## D SINGLE-SAMPLE AIS

### D.1 PROOF OF PROP. 3.1 (COMPLEXITY IN $T$ FOR SINGLE-SAMPLE AIS)

In this section, we prove Prop. 3.1, which relates the sum of the gaps in the single-sample AIS upper and lower bounds to the symmetrized KL divergence between the endpoint distributions. We extend this result to IM-AIS in Cor. E.1 and CR-AIS in Cor. H.3.

**Proposition 3.1** (Complexity in  $T$ ). *Assuming perfect transitions and a geometric annealing path with linearly-spaced  $\{\beta_t\}_{t=1}^T$ , the gap of the AIS upper and lower bounds (Eq. (18)) reduces linearly with increasing  $T$ ,*

$$\text{EUBO}_{\text{AIS}}(\mathbf{x}; \pi_0, T) - \text{ELBO}_{\text{AIS}}(\mathbf{x}; \pi_0, T) = \frac{1}{T} \left( D_{\text{KL}}[\pi_T(\mathbf{z}|\mathbf{x}) \|\pi_0(\mathbf{z}|\mathbf{x})] + D_{\text{KL}}[\pi_0(\mathbf{z}|\mathbf{x}) \|\pi_T(\mathbf{z}|\mathbf{x})] \right). \quad (19)$$

Note that  $\text{EUBO}_{\text{AIS}}(\mathbf{x}; \pi_0, T) - \text{ELBO}_{\text{AIS}}(\mathbf{x}; \pi_0, T)$  on the left hand side also corresponds to the sum of the gaps  $D_{\text{KL}}[q_{\text{PROP}}^{\text{AIS}}(\mathbf{z}_{0:T}|\mathbf{x}) \|\pi_{\text{TGT}}^{\text{AIS}}(\mathbf{z}_{0:T}|\mathbf{x})] + D_{\text{KL}}[\pi_{\text{TGT}}^{\text{AIS}}(\mathbf{z}_{0:T}|\mathbf{x}) \|\pi_{\text{PROP}}^{\text{AIS}}(\mathbf{z}_{0:T}|\mathbf{x})]$ . This result translates to mutual information bounds as in Sec. 1.1.

In contrast to Grosse et al. (2013) Thm. 1, our linear bias reduction result holds for finite  $T$ .

*Proof.* For linear scheduling and perfect transitions, we simplify the difference in the single-sample upper and lower bounds as

$$\begin{aligned} \delta_L^{T,K=1} + \delta_U^{T,K=1} &= \text{EUBO}_{\text{AIS}}(\mathbf{x}; \pi_0, T) - \text{ELBO}_{\text{AIS}}(\mathbf{x}; \pi_0, T) \\ &= \mathbb{E}_{\mathbf{z}_{0:T} \sim p_{\text{TGT}}^{\text{AIS}}} \left[ \log \frac{p_{\text{TGT}}^{\text{AIS}}(\mathbf{x}, \mathbf{z}_{0:T})}{q_{\text{PROP}}^{\text{AIS}}(\mathbf{z}_{0:T}|\mathbf{x})} \right] - \mathbb{E}_{\mathbf{z}_{0:T} \sim q_{\text{PROP}}^{\text{AIS}}} \left[ \log \frac{p_{\text{TGT}}^{\text{AIS}}(\mathbf{x}, \mathbf{z}_{0:T})}{q_{\text{PROP}}^{\text{AIS}}(\mathbf{z}_{0:T}|\mathbf{x})} \right] \\ &= \mathbb{E}_{\mathbf{z}_{0:T} \sim p_{\text{TGT}}^{\text{AIS}}} \left[ \log \frac{\pi_T(\mathbf{x}, \mathbf{z}_T) \prod_{t=1}^T \tilde{\mathcal{T}}_t(\mathbf{z}_{t-1}|\mathbf{z}_t)}{\pi_0(\mathbf{z}_0|\mathbf{x}) \prod_{t=1}^T \mathcal{T}_t(\mathbf{z}_t|\mathbf{z}_{t-1})} \right] - \mathbb{E}_{\mathbf{z}_{0:T} \sim q_{\text{PROP}}^{\text{AIS}}} \left[ \log \frac{\pi_T(\mathbf{x}, \mathbf{z}_T) \prod_{t=1}^T \tilde{\mathcal{T}}_t(\mathbf{z}_{t-1}|\mathbf{z}_t)}{\pi_0(\mathbf{z}_0|\mathbf{x}) \prod_{t=1}^T \mathcal{T}_t(\mathbf{z}_t|\mathbf{z}_{t-1})} \right] \\ &= \mathbb{E}_{\mathbf{z}_{0:T} \sim p_{\text{TGT}}^{\text{AIS}}} \left[ \log \prod_{t=1}^T \left( \frac{\pi_T(\mathbf{x}, \mathbf{z}_t)}{\pi_0(\mathbf{z}_t|\mathbf{x})} \right)^{\beta_t - \beta_{t-1}} \right] - \mathbb{E}_{\mathbf{z}_{0:T} \sim q_{\text{PROP}}^{\text{AIS}}} \left[ \log \prod_{t=1}^T \left( \frac{\pi_T(\mathbf{x}, \mathbf{z}_t)}{\pi_0(\mathbf{z}_t|\mathbf{x})} \right)^{\beta_t - \beta_{t-1}} \right] \\ &= \mathbb{E}_{\mathbf{z}_{0:T} \sim p_{\text{TGT}}^{\text{AIS}}} \left[ \sum_{t=1}^T (\beta_t - \beta_{t-1}) \log \frac{\pi_T(\mathbf{x}, \mathbf{z}_t)}{\pi_0(\mathbf{z}_t|\mathbf{x})} \right] - \mathbb{E}_{\mathbf{z}_{0:T} \sim q_{\text{PROP}}^{\text{AIS}}} \left[ \sum_{t=1}^T (\beta_t - \beta_{t-1}) \log \frac{\pi_T(\mathbf{x}, \mathbf{z}_t)}{\pi_0(\mathbf{z}_t|\mathbf{x})} \right]. \quad (78) \\ &\stackrel{(1)}{=} \sum_{t=1}^T \mathbb{E}_{\pi_{\beta_t}(\mathbf{z})} \left[ (\beta_t - \beta_{t-1}) \log \frac{\pi_T(\mathbf{x}, \mathbf{z})}{\pi_0(\mathbf{z}|\mathbf{x})} \right] - \sum_{t=1}^T \mathbb{E}_{\pi_{\beta_{t-1}}(\mathbf{z})} \left[ (\beta_t - \beta_{t-1}) \log \frac{\pi_T(\mathbf{x}, \mathbf{z})}{\pi_0(\mathbf{z}|\mathbf{x})} \right] \\ &\stackrel{(2)}{=} \frac{1}{T} \mathbb{E}_{\pi_T(\mathbf{z})} \left[ \log \frac{\pi_T(\mathbf{x}, \mathbf{z})}{\pi_0(\mathbf{z}|\mathbf{x})} \right] - \frac{1}{T} \mathbb{E}_{\pi_0(\mathbf{z})} \left[ \log \frac{\pi_T(\mathbf{x}, \mathbf{z})}{\pi_0(\mathbf{z}|\mathbf{x})} \right] \\ &= \frac{1}{T} (D_{\text{KL}}(\pi_0 \|\pi_T) + D_{\text{KL}}(\pi_T \|\pi_0)), \end{aligned}$$

where in (2), we use the linear annealing schedule  $\beta_t - \beta_{t-1} = \frac{1}{T} \forall t$  and note that intermediate terms cancel in telescoping fashion. In (1), we have used the assumption of perfect transitions (PT), which is common in analysis of AIS (Neal, 2001; Grosse et al., 2013). In this case, the AIS proposal and target distributions have the following factorial form

$$\mathbf{z}_{0:T} \sim q_{\text{PROP}}^{\text{AIS}}(\mathbf{z}_{0:T}^{(1:K)}|\mathbf{x}) \stackrel{(\text{PT})}{=} \pi_0(\mathbf{z}_0) \prod_{t=1}^T \pi_{\beta_{t-1}}(\mathbf{z}_t), \quad (79)$$

$$\mathbf{z}_{0:T} \sim p_{\text{TGT}}^{\text{AIS}}(\mathbf{z}_{0:T}^{(1:K)}|\mathbf{x}) \stackrel{(\text{PT})}{=} \pi_T(\mathbf{z}_T) \prod_{t=1}^T \pi_{\beta_{t-1}}(\mathbf{z}_{t-1}). \quad (80)$$

In other words, for  $1 \leq t \leq T$ , perfect transitions results in independent, exact samples from  $\mathbf{z}_t \sim \pi_{\beta_{t-1}}(\mathbf{z})$  in the forward direction, and  $\mathbf{z}_t \sim \pi_{\beta_t}(\mathbf{z})$  in the reverse direction. Using the factorized structure of Eq. (79) and Eq. (80), the expectations over the extended state space simplify to a sum of expectations at each  $\mathbf{z}_t$ .

The above proves the proposition for the case of single sample AIS, but should also hold for our tighter multi-sample AIS bounds. We extend this result to Independent Multi-Sample AIS in App. E.2 below, and extend the result to Coupled Reverse Multi-Sample AIS in App. H.4.  $\square$

## E INDEPENDENT MULTI-SAMPLE AIS

### E.1 PROBABILISTIC INTERPRETATION AND BOUNDS

Our Independent Multi-Sample AIS (IM-AIS) are identical to the standard IWAE bounds in [App. B](#), but using AIS forward  $q_{\text{PROP}}^{\text{AIS}}(\mathbf{z}_{0:T}|\mathbf{x})$  and backward  $p_{\text{TGT}}^{\text{AIS}}(\mathbf{z}_{0:T}|\mathbf{x})$  chains of length  $T$  instead of the endpoint distributions only  $q_{\theta}(\mathbf{z}|\mathbf{x})$  and  $p(\mathbf{z}|\mathbf{x})$ .

In particular, we construct an extended state space proposal by running  $K$  independent AIS forward chains  $\mathbf{z}_{0:T}^{(k)} \sim q_{\text{PROP}}^{\text{AIS}}$  in parallel. As in the IWAE upper bound ([Eq. \(5\)](#)), the extended state space target involves selecting a single index  $s$  uniformly at random, and running a backward AIS chain  $\mathbf{z}_{0:T}^{(s)} \sim p_{\text{TGT}}^{\text{AIS}}$  starting from a true posterior sample  $\mathbf{z}_T \sim p(\mathbf{z}|\mathbf{x})$ . The remaining  $K - 1$  samples are obtained by running forward AIS chains, as visualized in [Fig. 2](#)

$$q_{\text{PROP}}^{\text{IM-AIS}}(\mathbf{z}_{0:T}^{(1:K)}|\mathbf{x}) := \prod_{k=1}^K q_{\text{PROP}}^{\text{AIS}}(\mathbf{z}_{0:T}^{(k)}|\mathbf{x}), \quad p_{\text{TGT}}^{\text{IM-AIS}}(\mathbf{x}, \mathbf{z}_{0:T}^{(1:K)}) := \frac{1}{K} \sum_{s=1}^K p_{\text{TGT}}^{\text{AIS}}(\mathbf{x}, \mathbf{z}_{0:T}^{(s)}) \prod_{\substack{k=1 \\ k \neq s}}^K q_{\text{PROP}}^{\text{AIS}}(\mathbf{z}_{0:T}^{(k)}|\mathbf{x}).$$

where  $q_{\text{PROP}}^{\text{AIS}}$  and  $p_{\text{TGT}}^{\text{AIS}}$  were defined in [Eq. \(17\)](#). Expanding the log unnormalized density ratio,

$$\log \frac{p_{\text{TGT}}^{\text{IM-AIS}}(\mathbf{x}, \mathbf{z}_{0:T}^{(1:K)})}{q_{\text{PROP}}^{\text{IM-AIS}}(\mathbf{z}_{0:T}^{(1:K)}|\mathbf{x})} = \log \frac{\frac{1}{K} \sum_{s=1}^K p_{\text{TGT}}^{\text{AIS}}(\mathbf{x}, \mathbf{z}_{0:T}^{(s)}) \prod_{\substack{k=1 \\ k \neq s}}^K q_{\text{PROP}}^{\text{AIS}}(\mathbf{z}_{0:T}^{(k)}|\mathbf{x})}{\prod_{k=1}^K q_{\text{PROP}}^{\text{AIS}}(\mathbf{z}_{0:T}^{(k)}|\mathbf{x})} \quad (81)$$

$$= \log \frac{1}{K} \sum_{k=1}^K \frac{p_{\text{TGT}}^{\text{AIS}}(\mathbf{x}, \mathbf{z}_{0:T}^{(k)})}{q_{\text{PROP}}^{\text{AIS}}(\mathbf{z}_{0:T}^{(k)}|\mathbf{x})} \quad (82)$$

which is similar to the IWAE ratio but involves AIS chains. Taking the expectation under the proposal and target as in [App. A](#) recovers the lower and upper bounds in [Eq. \(21\)](#). The gap in the lower bound is  $D_{\text{KL}}[q_{\text{PROP}}^{\text{IM-AIS}}(\mathbf{z}_{0:T}^{(1:K)}|\mathbf{x}) \| p_{\text{TGT}}^{\text{IM-AIS}}(\mathbf{z}_{0:T}^{(1:K)}|\mathbf{x})]$  and the gap in the upper bound is  $D_{\text{KL}}[p_{\text{TGT}}^{\text{IM-AIS}}(\mathbf{z}_{0:T}^{(1:K)}|\mathbf{x}) \| q_{\text{PROP}}^{\text{IM-AIS}}(\mathbf{z}_{0:T}^{(1:K)}|\mathbf{x})]$ .

### E.2 PROOF OF LINEAR BIAS REDUCTION IN $T$ FOR IM-AIS

**Corollary E.1** (Complexity in  $T$  for Independent Multi-Sample AIS Bound). *Assuming perfect transitions and a geometric annealing path with linearly-spaced  $\{\beta_t\}_{t=0}^T$ , the sum of the gaps in the Independent Multi-Sample AIS sandwich bounds on ML,  $I_{\text{IM-AIS}_U}(\pi_0, T) - I_{\text{IM-AIS}_L}(\pi_0, T)$ , reduces linearly with increasing  $T$ .*

*Proof.* Using identical proof techniques as for IWAE ([Burda et al. \(2016\)](#); [Sobolev & Vetrov \(2019\)](#), [Prop. B.1](#)), we can show that our Independent Multi-Sample AIS bounds  $\text{ELBO}_{\text{IM-AIS}}(\mathbf{x}; \pi_0, T, K - 1) \leq \text{ELBO}_{\text{IM-AIS}}(\mathbf{x}; \pi_0, T, K)$  and  $\text{EUBO}_{\text{IM-AIS}}(\mathbf{x}; \pi_0, T, K) \leq \text{EUBO}_{\text{IM-AIS}}(\mathbf{x}; \pi_0, T, K - 1)$  improve with increasing  $K$ . Thus, the bias of our multi-sample bounds is less than the bias of the single-sample bounds, so the inequality in [Eq. \(19\)](#) and linear bias reduction in [Prop. 3.1](#) also hold for Independent Multi-Sample AIS. We characterize this improvement in [Prop. E.2](#) below.  $\square$

### E.3 PROOF OF LOGARITHMIC IMPROVEMENT OF IM-AIS EUBO

**Proposition E.2** (Improvement of Independent Multi-Sample AIS over Single-Sample AIS).

Let  $p_{\text{TGT}}^{\text{IM-AIS}}(s|\mathbf{x}, \mathbf{z}_{0:T}^{(1:K)}) = \frac{p_{\text{TGT}}^{\text{AIS}}(\mathbf{x}, \mathbf{z}_{0:T}^{(s)})}{q_{\text{PROP}}^{\text{AIS}}(\mathbf{z}_{0:T}^{(s)}|\mathbf{x})} / \sum_{k=1}^K \frac{p_{\text{TGT}}^{\text{AIS}}(\mathbf{x}, \mathbf{z}_{0:T}^{(k)})}{q_{\text{PROP}}^{\text{AIS}}(\mathbf{z}_{0:T}^{(k)}|\mathbf{x})}$  denote the normalized importance weights over AIS chains, and let  $\mathcal{U}(s)$  indicate the uniform distribution over  $K$  discrete values. Then, we can characterize the improvement of the Independent Multi-Sample AIS bounds on  $\log p(\mathbf{x})$ ,  $\text{ELBO}_{\text{IM-AIS}}(\mathbf{x}; \pi_0, T, K)$  and  $\text{EUBO}_{\text{IM-AIS}}(\mathbf{x}; \pi_0, T, K)$ , over the single-sample AIS

bounds  $\text{ELBO}_{\text{AIS}}(\mathbf{x}; \pi_0, T)$  and  $\text{EUBO}_{\text{AIS}}(\mathbf{x}; \pi_0, T)$  using KL divergences, as follows

$$\begin{aligned} \text{ELBO}_{\text{IM-AIS}}(\mathbf{x}; \pi_0, T, K) &= \text{ELBO}_{\text{AIS}}(\mathbf{x}; \pi_0, T) + \underbrace{\mathbb{E}_{q_{\text{PROP}}^{\text{IM-AIS}}(\mathbf{z}_{0:T}^{(1:K)}|\mathbf{x})} \left[ D_{\text{KL}}[\mathcal{U}(s) \| p_{\text{TGT}}^{\text{IM-AIS}}(s|\mathbf{z}_{0:T}^{(1:K)}, \mathbf{x})] \right]}_{0 \leq \text{KL of uniform from SNIS weights} \leq D_{\text{KL}}[q_{\text{PROP}}^{\text{AIS}}(\mathbf{z}_{0:T}|\mathbf{x}) \| p_{\text{TGT}}^{\text{AIS}}(\mathbf{z}_{0:T}|\mathbf{x})]}, \quad (83) \\ \text{EUBO}_{\text{IM-AIS}}(\mathbf{x}; \pi_0, T, K) &= \text{EUBO}_{\text{AIS}}(\mathbf{x}; \pi_0, T) - \underbrace{\mathbb{E}_{p_{\text{TGT}}^{\text{IM-AIS}}(\mathbf{z}_{0:T}^{(1:K)}|\mathbf{x})} \left[ D_{\text{KL}}[p_{\text{TGT}}^{\text{IM-AIS}}(s|\mathbf{z}_{0:T}^{(1:K)}, \mathbf{x}) \| \mathcal{U}(s)] \right]}_{0 \leq \text{KL of SNIS weights from uniform} \leq \log K}. \quad (84) \end{aligned}$$

*Proof.* The result follows directly from [App. C.4 Prop. 2.3](#) by viewing Independent Multi-Sample AIS as IWAE with an AIS proposal as in [App. E.1](#). □

## F REVERSE IWAE

In this section, we propose Reverse IWAE (RIWAE), which is an impractical alternative to standard IWAE. However, we use this as the basis for our Independent Reverse ([App. G](#)) and Coupled Reverse Multi-Sample AIS bounds ([Sec. 3.3](#) and [App. H](#)).

### F.1 PROBABILISTIC INTERPRETATION AND BOUNDS

Similarly to simple reverse importance sampling,  $\frac{1}{p(\mathbf{x})} = \mathbb{E}_{p(\mathbf{z}|\mathbf{x})} \left[ \frac{q_{\theta}(\mathbf{z}|\mathbf{x})}{p(\mathbf{x}, \mathbf{z})} \right]$ , we consider  $K$  independent posterior samples in an extended state space target distribution. The proposal distribution for our importance sampling scheme is a mixture of  $K - 1$  posterior distributions and one variational distribution,

$$q_{\text{PROP}}^{\text{RIWAE}}(\mathbf{x}, \mathbf{z}^{(1:K)}) = \frac{1}{K} \sum_{s=1}^K q_{\theta}(\mathbf{z}^{(s)}|\mathbf{x}) \prod_{\substack{k=1 \\ k \neq s}}^K p(\mathbf{x}, \mathbf{z}^{(k)}), \quad p_{\text{TGT}}^{\text{RIWAE}}(\mathbf{x}, \mathbf{z}^{(1:K)}) = \prod_{k=1}^K p(\mathbf{x}, \mathbf{z}^{(k)}). \quad (85)$$

Note that we have normalization constants of  $\int p_{\text{TGT}}^{\text{RIWAE}}(\mathbf{x}, \mathbf{z}^{(1:K)}) d\mathbf{z}^{(1:K)} = p(\mathbf{x})^K$  and  $\int q_{\text{PROP}}^{\text{RIWAE}}(\mathbf{x}, \mathbf{z}^{(1:K)}) d\mathbf{z}^{(1:K)} = p(\mathbf{x})^{K-1}$  since the transition kernels of the reverse chains do not change the normalization.

We visualize this sampling scheme in [Fig. 6](#). Similarly to [Eq. \(38\)](#), the log unnormalized density ratio simplifies to

$$\log \frac{p_{\text{TGT}}^{\text{RIWAE}}(\mathbf{x}, \mathbf{z}^{(1:K)})}{q_{\text{PROP}}^{\text{RIWAE}}(\mathbf{x}, \mathbf{z}^{(1:K)})} = \log \frac{\prod_{k=1}^K p(\mathbf{x}, \mathbf{z}^{(k)})}{\frac{1}{K} \sum_{s=1}^K q_{\theta}(\mathbf{z}^{(s)}|\mathbf{x}) \prod_{\substack{k=1 \\ k \neq s}}^K p(\mathbf{x}, \mathbf{z}^{(k)})} \quad (86)$$

$$= -\log \frac{1}{K} \sum_{k=1}^K \frac{q_{\theta}(\mathbf{z}^{(k)}|\mathbf{x})}{p(\mathbf{x}, \mathbf{z}^{(k)})}. \quad (87)$$

Taking the expectation under the proposal and target distributions yield lower and upper bounds on  $\log p(\mathbf{x})$ . These translate to upper and lower bounds on  $\log p(\mathbf{x})$  which are different that standard IWAE bounds in [Eq. \(5\)](#),

$$\mathbb{E}_{q_{\theta}(\mathbf{z}^{(1)}|\mathbf{x}) \prod_{k=2}^K p(\mathbf{z}^{(k)}|\mathbf{x})} \left[ -\log \frac{1}{K} \sum_{k=1}^K \frac{q_{\theta}(\mathbf{z}^{(k)}|\mathbf{x})}{p(\mathbf{x}, \mathbf{z}^{(k)})} \right] \leq \log p(\mathbf{x}) \leq \mathbb{E}_{\prod_{k=1}^K p(\mathbf{z}^{(k)}|\mathbf{x})} \left[ -\log \frac{1}{K} \sum_{k=1}^K \frac{q_{\theta}(\mathbf{z}^{(k)}|\mathbf{x})}{p(\mathbf{x}, \mathbf{z}^{(k)})} \right].$$

Note these bounds are *impractical* as they would require more than one true posterior sample from  $p(\mathbf{z}|\mathbf{x})$ . However, we use them in [Sec. 3.3](#) and [App. H](#) to derive practical multi-sample reverse AIS bounds.



## F.2 IMPROVEMENT OF RIWAE OVER ELBO AND EUBO

**Proposition F.1** (Improvement of Reverse IWAE over ELBO and EUBO). *Let  $q_{\text{PROP}}^{\text{RIWAE}}(s|\mathbf{x}, \mathbf{z}^{(1:K)}) = \frac{q_{\theta}(\mathbf{z}^{(s)}|\mathbf{x})}{p(\mathbf{x}, \mathbf{z}^{(s)}|\mathbf{x})} / \sum_{k=1}^K \frac{q_{\theta}(\mathbf{z}^{(k)}|\mathbf{x})}{p(\mathbf{x}, \mathbf{z}^{(k)}|\mathbf{x})}$  denote the normalized reverse importance sampling weights, or the posterior over the index variable in Eq. (85). Let  $\mathcal{U}(s)$  indicate the uniform distribution over  $K$  discrete values. Then, we can characterize the improvement of the Reverse IWAE bounds on  $\log p(\mathbf{x})$ ,  $\text{ELBO}_{\text{RIWAE}}(\mathbf{x}; q_{\theta}, K)$  and  $\text{EUBO}_{\text{RIWAE}}(\mathbf{x}; q_{\theta}, K)$ , over the single-sample bounds  $\text{ELBO}(\mathbf{x}; q_{\theta})$  and  $\text{EUBO}(\mathbf{x}; q_{\theta})$  using KL divergences, as follows*

$$\text{ELBO}_{\text{RIWAE}}(\mathbf{x}; q_{\theta}, K) = \text{ELBO}(\mathbf{x}; q_{\theta}) + \underbrace{\mathbb{E}_{q_{\text{PROP}}^{\text{RIWAE}}(\mathbf{z}^{(1:K)}|\mathbf{x})} \left[ D_{\text{KL}}[q_{\text{PROP}}^{\text{RIWAE}}(s|\mathbf{x}, \mathbf{z}^{(1:K)}) || \mathcal{U}(s)] \right]}_{0 \leq \text{KL of uniform from SNIS weights} \leq \log K},$$

$$\text{EUBO}_{\text{RIWAE}}(\mathbf{x}; q_{\theta}, K) = \text{EUBO}(\mathbf{x}; q_{\theta}) - \underbrace{\mathbb{E}_{p_{\text{TGT}}^{\text{RIWAE}}(\mathbf{z}^{(1:K)}|\mathbf{x})} \left[ D_{\text{KL}}[\mathcal{U}(s) || q_{\text{PROP}}^{\text{RIWAE}}(s|\mathbf{x}, \mathbf{z}^{(1:K)})] \right]}_{0 \leq \text{KL of SNIS weights from uniform} \leq D_{\text{KL}}[p(\mathbf{z}|\mathbf{x}) || q_{\theta}(\mathbf{z}|\mathbf{x})]}.$$

*Proof.* The proof follows similarly as Prop. 2.1 or Lemma C.2.  $\square$

## G INDEPENDENT REVERSE MULTI-SAMPLE AIS

### G.1 PROBABILISTIC INTERPRETATION AND BOUNDS

In similar fashion to Reverse IWAE, we now use  $K$  independent reverse AIS chains to form an extended state space target distribution  $p_{\text{TGT}}^{\text{IR-AIS}}(\mathbf{z}_{0:T}^{(1:K)}, \mathbf{x})$ , and a mixture proposal distribution  $q_{\text{PROP}}^{\text{IR-AIS}}(\mathbf{z}_{0:T}^{(1:K)}, \mathbf{x})$  which includes a single forward AIS chain (see Fig. 2)

$$q_{\text{PROP}}^{\text{IR-AIS}}(\mathbf{x}, \mathbf{z}_{0:T}^{(1:K)}) = \frac{1}{K} \sum_{s=1}^K q_{\text{PROP}}^{\text{AIS}}(\mathbf{z}_{0:T}^{(s)}|\mathbf{x}) \prod_{\substack{k=1 \\ k \neq s}}^K p_{\text{TGT}}^{\text{AIS}}(\mathbf{x}, \mathbf{z}_{0:T}^{(k)}),$$

$$p_{\text{TGT}}^{\text{IR-AIS}}(\mathbf{x}, \mathbf{z}_{0:T}^{(1:K)}) = \prod_{k=1}^K p_{\text{TGT}}^{\text{AIS}}(\mathbf{x}, \mathbf{z}_{0:T}^{(k)}). \quad (88)$$

Similarly to Eq. (86)-(87), the log unnormalized density ratio becomes

$$\log \frac{p_{\text{TGT}}^{\text{IR-AIS}}(\mathbf{z}_{0:T}^{(1:K)}, \mathbf{x})}{q_{\text{PROP}}^{\text{IR-AIS}}(\mathbf{z}_{0:T}^{(1:K)}, \mathbf{x})} = \log \frac{\prod_{k=1}^K p_{\text{TGT}}^{\text{AIS}}(\mathbf{x}, \mathbf{z}_{0:T}^{(k)})}{\frac{1}{K} \sum_{k=1}^K q_{\text{PROP}}^{\text{AIS}}(\mathbf{z}_{0:T}^{(k)}|\mathbf{x}) \prod_{t=1}^T p_{\text{TGT}}^{\text{AIS}}(\mathbf{x}, \mathbf{z}_{0:T}^{(k)})} \quad (89)$$

$$= -\log \frac{1}{K} \sum_{k=1}^K \frac{q_{\text{PROP}}^{\text{AIS}}(\mathbf{z}_{0:T}^{(k)}, \mathbf{x})}{p_{\text{TGT}}^{\text{AIS}}(\mathbf{x}, \mathbf{z}_{0:T}^{(k)})}. \quad (90)$$

Taking expectations of the log unnormalized density ratio under the proposal and target, respectively, yield lower and upper bounds on  $\log p(\mathbf{x})$

$$\underbrace{\mathbb{E}_{\substack{\mathbf{z}_{0:T}^{(1)} \sim q_{\text{PROP}}^{\text{AIS}} \\ \mathbf{z}_{0:T}^{(2:K)} \sim p_{\text{TGT}}^{\text{AIS}}}} \left[ -\log \frac{1}{K} \sum_{k=1}^K \frac{q_{\text{PROP}}^{\text{AIS}}(\mathbf{z}_{0:T}^{(k)}|\mathbf{x})}{p_{\text{TGT}}^{\text{AIS}}(\mathbf{x}, \mathbf{z}_{0:T}^{(k)})} \right]}_{\text{ELBO}_{\text{IR-AIS}}(\mathbf{x}; \pi_0, K, T)} \leq \log p(\mathbf{x}) \leq \underbrace{\mathbb{E}_{\mathbf{z}_{0:T}^{(1:K)} \sim p_{\text{TGT}}^{\text{AIS}}} \left[ -\log \frac{1}{K} \sum_{k=1}^K \frac{q_{\text{PROP}}^{\text{AIS}}(\mathbf{z}_{0:T}^{(k)}|\mathbf{x})}{p_{\text{TGT}}^{\text{AIS}}(\mathbf{x}, \mathbf{z}_{0:T}^{(k)})} \right]}_{\text{EUBO}_{\text{IR-AIS}}(\mathbf{x}; \pi_0, K, T)}. \quad (91)$$

However, Independent Reverse Multi-Sample AIS may be impractical in common settings, since it is infeasible to have access to more than one true posterior sample.

## G.2 PROOF OF LOGARITHMIC IMPROVEMENT IN $K$ FOR INDEPENDENT REVERSE AIS

**Proposition G.1** (Improvement of Independent Reverse Multi-Sample AIS over Single-Sample AIS).

Let  $q_{\text{PROP}}^{\text{IR-AIS}}(s|\mathbf{x}, \mathbf{z}_{0:T}^{(1:K)}) = \frac{q_{\text{PROP}}^{\text{AIS}}(\mathbf{z}_{0:T}^{(s)}|\mathbf{x})}{p_{\text{TGT}}^{\text{AIS}}(\mathbf{x}, \mathbf{z}_{0:T}^{(s)})} / \sum_{k=1}^K \frac{q_{\text{PROP}}^{\text{AIS}}(\mathbf{z}_{0:T}^{(k)}|\mathbf{x})}{p_{\text{TGT}}^{\text{AIS}}(\mathbf{x}, \mathbf{z}_{0:T}^{(k)})}$  denote the normalized reverse importance sampling weights over AIS chains, and let  $\mathcal{U}(s)$  indicate the uniform distribution over  $K$  discrete values. Then, we can characterize the improvement of the Independent Reverse Multi-Sample AIS bounds on  $\log p(\mathbf{x})$ ,  $\text{ELBO}_{\text{IR-AIS}}(\mathbf{x}; \pi_0, K, T)$  and  $\text{EUBO}_{\text{IR-AIS}}(\mathbf{x}; \pi_0, K, T)$ , over the single-sample  $\text{ELBO}_{\text{AIS}}(\mathbf{x}; \pi_0, T)$  and  $\text{ELBO}_{\text{AIS}}(\mathbf{x}; \pi_0, T)$  using KL divergences, as follows

$$\begin{aligned} \text{ELBO}_{\text{IR-AIS}}(\mathbf{x}; \pi_0, K, T) &= \text{ELBO}_{\text{AIS}}(\mathbf{x}; \pi_0, T) + \underbrace{\mathbb{E}_{q_{\text{PROP}}^{\text{IR-AIS}}(\mathbf{z}_{0:T}^{(1:K)}|\mathbf{x})} \left[ D_{\text{KL}}[q_{\text{PROP}}^{\text{IR-AIS}}(s|\mathbf{x}, \mathbf{z}_{0:T}^{(1:K)}) || \mathcal{U}(s)] \right]}_{0 \leq \text{KL of uniform from SNIS weights} \leq \log K}, \\ \text{EUBO}_{\text{IR-AIS}}(\mathbf{x}; \pi_0, K, T) &= \text{EUBO}_{\text{AIS}}(\mathbf{x}; \pi_0, T) - \underbrace{\mathbb{E}_{p_{\text{TGT}}^{\text{IR-AIS}}(\mathbf{z}_{0:T}^{(1:K)}|\mathbf{x})} \left[ D_{\text{KL}}[\mathcal{U}(s) || q_{\text{PROP}}^{\text{IR-AIS}}(s|\mathbf{x}, \mathbf{z}_{0:T}^{(1:K)})] \right]}_{0 \leq \text{KL of SNIS weights from uniform} \leq D_{\text{KL}}[p_{\text{TGT}}^{\text{AIS}}(\mathbf{z}_{0:T}|\mathbf{x}) || q_{\text{PROP}}^{\text{AIS}}(\mathbf{z}_{0:T}|\mathbf{x})]}. \end{aligned}$$

*Proof.* The proof follows similarly as [Prop. 2.1](#) or [Lemma C.2](#).  $\square$

## H COUPLED REVERSE MULTI-SAMPLE AIS

### H.1 PROBABILISTIC INTERPRETATION AND BOUNDS

The Coupled Reverse Multi-Sample AIS extended state space target distribution in [Fig. 2](#) initializes  $K$  backward chains from a *single* target sample  $\mathbf{z}_T \sim \pi_T(\mathbf{z}|\mathbf{x})$ , which makes the bound useful in practical situations. We denote the remaining transitions as  $p_{\text{TGT}}^{\text{AIS}}(\mathbf{z}_{0:T-1}|\mathbf{z}_T, \mathbf{x})$ , since they are identical to standard AIS in [Eq. \(17\)](#). Thus, the CR-AIS extended state space target distribution is

$$p_{\text{TGT}}^{\text{CR-AIS}}(\mathbf{x}, \mathbf{z}_{0:T-1}, \mathbf{z}_T) = \pi_T(\mathbf{x}, \mathbf{z}_T) \prod_{k=1}^K p_{\text{TGT}}^{\text{AIS}}(\mathbf{z}_{0:T-1}^{(k)}|\mathbf{z}_T, \mathbf{x}). \quad (92)$$

The extended state space proposal is obtained by selecting an index  $s$  uniformly at random and running a single forward AIS chain. We then run  $K - 1$  backward chains, all starting from the last state of the selected forward chain,

$$q_{\text{PROP}}^{\text{CR-AIS}}(\mathbf{z}_{0:T-1}, \mathbf{z}_T|\mathbf{x}) := \frac{1}{K} \sum_{s=1}^K q_{\text{PROP}}^{\text{AIS}}(\mathbf{z}_{0:T-1}^{(s)}|\mathbf{z}_T|\mathbf{x}) \prod_{\substack{k=1 \\ k \neq s}}^K p_{\text{TGT}}^{\text{AIS}}(\mathbf{z}_{0:T-1}^{(k)}|\mathbf{z}_T, \mathbf{x}). \quad (93)$$

See [Fig. 2](#) or [Fig. 6](#) for a graphical model description.

We can construct log-partition bounds using the log ratio of unnormalized densities,

$$\log \frac{p_{\text{TGT}}^{\text{CR-AIS}}(\mathbf{z}_{0:T-1}, \mathbf{z}_T|\mathbf{x})}{q_{\text{PROP}}^{\text{CR-AIS}}(\mathbf{z}_{0:T-1}, \mathbf{z}_T|\mathbf{x})} = \log \frac{\pi_T(\mathbf{z}_T, \mathbf{x}) \prod_{k=1}^K p_{\text{TGT}}^{\text{AIS}}(\mathbf{z}_{0:T-1}^{(k)}|\mathbf{z}_T, \mathbf{x})}{\frac{1}{K} \sum_{s=1}^K q_{\text{PROP}}^{\text{AIS}}(\mathbf{z}_{0:T-1}^{(s)}|\mathbf{z}_T|\mathbf{x}) \prod_{\substack{k=1 \\ k \neq s}}^K p_{\text{TGT}}^{\text{AIS}}(\mathbf{z}_{0:T-1}^{(k)}|\mathbf{z}_T, \mathbf{x})} \quad (94)$$

$$= -\log \frac{1}{K} \sum_{k=1}^K \frac{q_{\text{PROP}}^{\text{AIS}}(\mathbf{z}_{0:T-1}^{(k)}|\mathbf{z}_T|\mathbf{x})}{p_{\text{TGT}}^{\text{AIS}}(\mathbf{z}_{0:T-1}^{(k)}|\mathbf{z}_T)\pi_T(\mathbf{z}_T, \mathbf{x})}. \quad (95)$$

Taking the expected log ratio under the proposal and target yields lower and upper bounds on  $\log p(\mathbf{x})$ ,

$$\begin{aligned} \text{ELBO}_{\text{CR-AIS}}(\mathbf{x}; \pi_0, K, T) &:= -\mathbb{E}_{\substack{\mathbf{z}_{0:T-1}, \mathbf{z}_T \sim q_{\text{PROP}}^{\text{AIS}}(\mathbf{z}_{0:T}|\mathbf{x}) \\ \mathbf{z}_{0:T-1} \sim p_{\text{TGT}}^{\text{AIS}}(\mathbf{z}_{0:T-1}|\mathbf{z}_T, \mathbf{x})}} \left[ \log \frac{1}{K} \sum_{k=1}^K \frac{q_{\text{PROP}}^{\text{AIS}}(\mathbf{z}_{0:T-1}^{(k)}, \mathbf{z}_T|\mathbf{x})}{p_{\text{TGT}}^{\text{AIS}}(\mathbf{x}, \mathbf{z}_{0:T-1}^{(k)}, \mathbf{z}_T)} \right] \leq \log p(\mathbf{x}) \\ \text{EUBO}_{\text{CR-AIS}}(\mathbf{x}; \pi_0, K, T) &:= -\mathbb{E}_{\substack{\mathbf{z}_T \sim \pi_T(\mathbf{z}_T|\mathbf{x}) \\ \mathbf{z}_{0:T-1}^{(1:K)} \sim p_{\text{TGT}}^{\text{AIS}}(\mathbf{z}_{0:T-1}|\mathbf{z}_T, \mathbf{x})}} \left[ \log \frac{1}{K} \sum_{k=1}^K \frac{q_{\text{PROP}}^{\text{AIS}}(\mathbf{z}_{0:T-1}^{(k)}, \mathbf{z}_T|\mathbf{x})}{p_{\text{TGT}}^{\text{AIS}}(\mathbf{x}, \mathbf{z}_{0:T-1}^{(k)}, \mathbf{z}_T)} \right] \geq \log p(\mathbf{x}). \end{aligned}$$

## H.2 PROOF THAT CR-AIS BOUNDS TIGHTEN WITH INCREASING $K$

In this section, we prove that Coupled Reverse Multi-Sample AIS bounds get tighter with increasing  $K$ . Our proof provides an alternative perspective to [Burda et al. \(2016\)](#); [Sobolev & Vetrov \(2019\)](#) for showing the monotonic improvement of IWAE or Independent Multi-Sample AIS with  $K$ . We will also characterize the improvement of CR-AIS bounds over single-sample AIS bounds in [Prop. H.2](#), as a direct consequence of this lemma.

**Lemma H.1** (CR-AIS Bounds Tighten with Increasing  $K$ ). *Coupled Reverse Multi-Sample AIS bounds get tighter with increasing number of samples  $K$ . In other words, for any  $K > 1$ ,*

$$\text{ELBO}_{\text{CR-AIS}}(\mathbf{x}; \pi_0, T, K-1) \leq \text{ELBO}_{\text{CR-AIS}}(\mathbf{x}; \pi_0, T, K) \leq \log p(\mathbf{x}), \quad (96)$$

$$\text{EUBO}_{\text{CR-AIS}}(\mathbf{x}; \pi_0, T, K-1) \geq \text{EUBO}_{\text{CR-AIS}}(\mathbf{x}; \pi_0, T, K) \geq \log p(\mathbf{x}). \quad (97)$$

*Proof.* Our proof will proceed by introducing an additional set of  $M$  index variables  $s_{1:M}$  into the  $K$ -sample probabilistic interpretation of CR-AIS in [Eq. \(92\)-\(93\)](#), with  $M < K$ . We will show that the KL divergence in this *joint* state space (including  $s_{1:M}$ ) is equal to the gap of the  $M$ -sample  $\text{ELBO}_{\text{CR-AIS}}(\mathbf{x}; \pi_0, T, M)$  or  $\text{EUBO}_{\text{CR-AIS}}(\mathbf{x}; \pi_0, T, M)$ . We then show that marginalizing over  $s_{1:M}$  yields the gap of the  $K$ -sample  $\text{ELBO}_{\text{CR-AIS}}(\mathbf{x}; \pi_0, T, K)$  or  $\text{EUBO}_{\text{CR-AIS}}(\mathbf{x}; \pi_0, T, K)$ . Since marginalization cannot increase the KL divergence, we will have shown that for any  $M < K$ ,  $D_{\text{KL}}[q_{\text{PROP}}^{\text{CR-AIS}}(\mathbf{z}_{0:T-1}^{(1:K)}, \mathbf{z}_T|\mathbf{x}) \| p_{\text{TGT}}^{\text{CR-AIS}}(\mathbf{z}_{0:T-1}^{(1:K)}, \mathbf{z}_T|\mathbf{x})] \leq D_{\text{KL}}[q_{\text{PROP}}^{\text{CR-AIS}}(\mathbf{z}_{0:T-1}^{(1:M)}, \mathbf{z}_T|\mathbf{x}) \| p_{\text{TGT}}^{\text{CR-AIS}}(\mathbf{z}_{0:T-1}^{(1:M)}, \mathbf{z}_T|\mathbf{x})]$  and thus  $\text{ELBO}_{\text{CR-AIS}}(\mathbf{x}; \pi_0, T, M) \leq \text{ELBO}_{\text{CR-AIS}}(\mathbf{x}; \pi_0, T, K)$ . Identical reasoning holds for the  $\text{EUBO}_{\text{CR-AIS}}$ .

**Sub-Sampling Probabilistic Interpretation** Let  $\mathcal{U}(s_1, \dots, s_M)$  indicate the probability of drawing  $M < K$  sample indices uniformly without replacement (i.e. each  $s_m$  is distinct). In the CR-AIS target distribution, there is no distinction between the indices  $\{s_{1:M}\}$  and  $k \notin \{s_{1:M}\}$  after drawing  $\mathbf{z}_T \sim \pi_T(\mathbf{x}, \mathbf{z})$ . We can write

$$p_{\text{TGT}}^{\text{CR-AIS}}(\mathbf{x}, s_{1:M}, \mathbf{z}_{0:T-1}^{(1:K)}, \mathbf{z}_T) = \mathcal{U}(s_1, \dots, s_M) \cdot \pi_T(\mathbf{x}, \mathbf{z}_T) \prod_{k=1}^K p_{\text{TGT}}^{\text{AIS}}(\mathbf{z}_{0:T-1}^{(k)}|\mathbf{z}_T, \mathbf{x}) \quad (98)$$

which, after marginalization over  $s_{1:M}$ , clearly matches  $p_{\text{TGT}}^{\text{CR-AIS}}(\mathbf{x}, \mathbf{z}_{0:T-1}^{(1:K)}, \mathbf{z}_T)$ .

We also draw  $s_{1:M} \sim \mathcal{U}(s_1, \dots, s_M)$  for the extended state space proposal. Next, we select an index  $m$  uniformly at random from  $\{1, \dots, M\}$ , which is used to specify which chain  $\mathbf{z}_{0:T-1}^{(s_m)}$  is run in the forward direction to obtain  $\mathbf{z}_T$ , as in [Eq. \(93\)](#). After marginalizing over  $m$ , we obtain the following mixture proposal distribution

$$\begin{aligned} q_{\text{PROP}}^{\text{CR-AIS}}(s_{1:M}, \mathbf{z}_{0:T-1}^{(1:K)}, \mathbf{z}_T|\mathbf{x}) &:= \mathcal{U}(s_1, \dots, s_M) \cdot \left( \frac{1}{M} \sum_{m=1}^M q_{\text{PROP}}^{\text{AIS}}(\mathbf{z}_{0:T-1}^{(s_m)}, \mathbf{z}_T|\mathbf{x}) \prod_{\substack{j=1 \\ j \neq m}}^M p_{\text{TGT}}^{\text{AIS}}(\mathbf{z}_{0:T-1}^{(s_j)}|\mathbf{z}_T, \mathbf{x}) \right) \\ &\cdot \prod_{\substack{k=1 \\ k \notin \{s_{1:M}\}}}^K p_{\text{TGT}}^{\text{AIS}}(\mathbf{z}_{0:T-1}^{(k)}|\mathbf{z}_T, \mathbf{x}). \quad (99) \end{aligned}$$

We will consider marginalizing over  $s_{1:M}$  below, but first write the KL divergence in the extended state space which includes  $s_{1:M}$ . For example, the forward KL divergence matches the gap of the  $M$ -sample  $\text{ELBO}_{\text{CR-AIS}}(\mathbf{x}; \pi_0, T, M)$ ,

$$D_{\text{KL}}[q_{\text{PROP}}^{\text{CR-AIS}}(s_{1:M}, \mathbf{z}_{0:T-1}^{(1:K)}, \mathbf{z}_T | \mathbf{x}) \| p_{\text{TGT}}^{\text{CR-AIS}}(s_{1:M}, \mathbf{z}_{0:T-1}^{(1:K)}, \mathbf{z}_T | \mathbf{x})] \quad (100)$$

$$\begin{aligned} &= \mathbb{E}_{q_{\text{PROP}}^{\text{CR-AIS}}} \left[ \log \frac{\cancel{\mathcal{U}(s_{1:M})} \cdot \left( \frac{1}{M} \sum_{m=1}^M q_{\text{PROP}}^{\text{AIS}}(\mathbf{z}_{0:T-1}^{(s_m)}, \mathbf{z}_T | \mathbf{x}) \prod_{\substack{j=1 \\ j \neq m}}^M p_{\text{TGT}}^{\text{AIS}}(\mathbf{z}_{0:T-1}^{(s_j)} | \mathbf{z}_T, \mathbf{x}) \right) \cdot \prod_{\substack{k=1 \\ k \notin \{s_{1:M}\}}}^K p_{\text{TGT}}^{\text{AIS}}(\mathbf{z}_{0:T-1}^{(k)} | \mathbf{z}_T, \mathbf{x})}{\cancel{\mathcal{U}(s_{1:M})} \cdot \pi_T(\mathbf{x}, \mathbf{z}_T) \prod_{k \in \{s_{1:M}\}} p_{\text{TGT}}^{\text{AIS}}(\mathbf{z}_{0:T-1}^{(k)} | \mathbf{z}_T, \mathbf{x}) \prod_{\substack{k=1 \\ k \notin \{s_{1:M}\}}}^K p_{\text{TGT}}^{\text{AIS}}(\mathbf{z}_{0:T-1}^{(k)} | \mathbf{z}_T, \mathbf{x})} \right] \\ &= D_{\text{KL}}[q_{\text{PROP}}^{\text{CR-AIS}}(\mathbf{z}_{0:T-1}^{(1:M)}, \mathbf{z}_T | \mathbf{x}) \| p_{\text{TGT}}^{\text{CR-AIS}}(\mathbf{z}_{0:T-1}^{(1:M)}, \mathbf{z}_T | \mathbf{x})], \end{aligned} \quad (101)$$

which matches the  $M$ -sample probabilistic interpretation of CR-AIS from [App. H.1](#). Identical reasoning holds for the case of  $\text{EUBO}_{\text{CR-AIS}}(\mathbf{x}; \pi_0, T, K) \leq \text{EUBO}_{\text{CR-AIS}}(\mathbf{x}; \pi_0, T, M)$  using the reverse KL divergence.

**Marginalization over  $s_{1:M}$**  We have already seen from [Eq. \(98\)](#) that the marginal  $\sum_{s_{1:M}} p_{\text{TGT}}^{\text{CR-AIS}}(\mathbf{x}, s_{1:M}, \mathbf{z}_{0:T-1}^{(1:K)}, \mathbf{z}_T)$  matches the  $K$ -sample target distribution  $p_{\text{TGT}}^{\text{CR-AIS}}(\mathbf{x}, \mathbf{z}_{0:T-1}^{(1:K)}, \mathbf{z}_T)$ .

We would now like to marginalize over  $s_{1:M}$  in  $q_{\text{PROP}}^{\text{CR-AIS}}(s_{1:M}, \mathbf{z}_{0:T-1}^{(1:K)}, \mathbf{z}_T | \mathbf{x})$ . Combining the two product terms in [Eq. \(99\)](#),

$$\sum_{s_{1:M}} q_{\text{PROP}}^{\text{CR-AIS}}(s_{1:M}, \mathbf{z}_{0:T-1}^{(1:K)}, \mathbf{z}_T | \mathbf{x}) = \mathbb{E}_{\mathcal{U}(s_{1:M})} \left[ \frac{1}{M} \sum_{m=1}^M q_{\text{PROP}}^{\text{AIS}}(\mathbf{z}_{0:T-1}^{(s_m)}, \mathbf{z}_T | \mathbf{x}) \prod_{\substack{k=1 \\ k \neq s_m}}^K p_{\text{TGT}}^{\text{AIS}}(\mathbf{z}_{0:T-1}^{(k)} | \mathbf{z}_T, \mathbf{x}) \right] \quad (102)$$

$$= \frac{1}{M} \sum_{m=1}^M \mathbb{E}_{\mathcal{U}(s_{1:M})} \left[ q_{\text{PROP}}^{\text{AIS}}(\mathbf{z}_{0:T-1}^{(s_m)}, \mathbf{z}_T | \mathbf{x}) \prod_{\substack{k=1 \\ k \neq s_m}}^K p_{\text{TGT}}^{\text{AIS}}(\mathbf{z}_{0:T-1}^{(k)} | \mathbf{z}_T, \mathbf{x}) \right] \quad (103)$$

$$\stackrel{(1)}{=} \frac{1}{M} \sum_{m=1}^M \mathbb{E}_{\mathcal{U}(s_m)} \left[ q_{\text{PROP}}^{\text{AIS}}(\mathbf{z}_{0:T-1}^{(s_m)}, \mathbf{z}_T | \mathbf{x}) \prod_{\substack{k=1 \\ k \neq s_m}}^K p_{\text{TGT}}^{\text{AIS}}(\mathbf{z}_{0:T-1}^{(k)} | \mathbf{z}_T, \mathbf{x}) \right] \quad (104)$$

$$\stackrel{(2)}{=} \frac{1}{M} \sum_{m=1}^M \frac{1}{K} \sum_{j=1}^K \left[ q_{\text{PROP}}^{\text{AIS}}(\mathbf{z}_{0:T-1}^{(j)}, \mathbf{z}_T | \mathbf{x}) \prod_{\substack{k=1 \\ k \neq j}}^K p_{\text{TGT}}^{\text{AIS}}(\mathbf{z}_{0:T-1}^{(k)} | \mathbf{z}_T, \mathbf{x}) \right] \quad (105)$$

$$= \frac{1}{K} \sum_{j=1}^K \left[ q_{\text{PROP}}^{\text{AIS}}(\mathbf{z}_{0:T-1}^{(j)}, \mathbf{z}_T | \mathbf{x}) \prod_{\substack{k=1 \\ k \neq j}}^K p_{\text{TGT}}^{\text{AIS}}(\mathbf{z}_{0:T-1}^{(k)} | \mathbf{z}_T, \mathbf{x}) \right] \quad (106)$$

where in (1), we can write the marginal  $\mathcal{U}(s_m)$  since the terms inside expectation do not explicitly depend on the other indices in  $s_{1:M}$ . In (2), we use the fact that the marginal over any  $s_m$  is uniform.

Thus, we have shown that the marginal distributions match the standard  $K$ -sample target and proposal distributions of CR-AIS, with

$$D_{\text{KL}} \left[ \sum_{s_{1:M}} q_{\text{PROP}}^{\text{CR-AIS}}(s_{1:M}, \mathbf{z}_{0:T-1}^{(1:K)}, \mathbf{z}_T | \mathbf{x}) \| \sum_{s_{1:M}} p_{\text{TGT}}^{\text{CR-AIS}}(s_{1:M}, \mathbf{z}_{0:T-1}^{(1:K)}, \mathbf{z}_T | \mathbf{x}) \right] = \underbrace{D_{\text{KL}}[q_{\text{PROP}}^{\text{CR-AIS}}(\mathbf{z}_{0:T-1}^{(1:K)}, \mathbf{z}_T | \mathbf{x}) \| p_{\text{TGT}}^{\text{CR-AIS}}(\mathbf{z}_{0:T-1}^{(1:K)}, \mathbf{z}_T | \mathbf{x})]}_{\text{gap of ELBO}_{\text{CR-AIS}}(\mathbf{x}; \pi_0, T, K)}$$

and similar reasoning for the EUBO using the reverse KL divergence.

**Conclusion of Proof** Since marginalization can not increase the KL divergence, we have

$$\underbrace{D_{\text{KL}}[q_{\text{PROP}}^{\text{CR-AIS}}(\mathbf{z}_{0:T-1}^{(1:K)}, \mathbf{z}_T | \mathbf{x}) \| p_{\text{TGT}}^{\text{CR-AIS}}(\mathbf{z}_{0:T-1}^{(1:K)}, \mathbf{z}_T | \mathbf{x})]}_{\text{gap of ELBO}_{\text{CR-AIS}}(\mathbf{x}; \pi_0, T, K)} \leq \underbrace{D_{\text{KL}}[q_{\text{PROP}}^{\text{CR-AIS}}(s_{1:M}, \mathbf{z}_{0:T-1}^{(1:K)}, \mathbf{z}_T | \mathbf{x}) \| p_{\text{TGT}}^{\text{CR-AIS}}(s_{1:M}, \mathbf{z}_{0:T-1}^{(1:K)}, \mathbf{z}_T | \mathbf{x})]}_{\text{gap of ELBO}_{\text{CR-AIS}}(\mathbf{x}; \pi_0, T, M) \text{ (Eq. (101))}}. \quad (107)$$

This shows that  $\text{ELBO}_{\text{CR-AIS}}(\mathbf{x}; \pi_0, T, K)$  is tighter than  $\text{ELBO}_{\text{CR-AIS}}(\mathbf{x}; \pi_0, T, M)$ , with  $\text{ELBO}_{\text{CR-AIS}}(\mathbf{x}; \pi_0, T, K) \geq \text{ELBO}_{\text{CR-AIS}}(\mathbf{x}; \pi_0, T, M)$ . Identical reasoning holds for the case of  $\text{EUBO}_{\text{CR-AIS}}(\mathbf{x}; \pi_0, T, K) \leq \text{EUBO}_{\text{CR-AIS}}(\mathbf{x}; \pi_0, T, M)$  using the reverse KL divergence. Choosing  $M = K - 1$  proves that the bounds tighten as  $K$  increases, as desired.  $\square$

**Characterizing the Improvement of  $K$ -Sample over  $M$ -Sample CR-AIS** Note that we can explicitly write the gap of the inequality Eq. (107) using the chain rule for joint probability, for example  $q_{\text{PROP}}^{\text{CR-AIS}}(s_{1:M}, \mathbf{z}_{0:T-1}^{(1:K)}, \mathbf{z}_T | \mathbf{x}) = q_{\text{PROP}}^{\text{CR-AIS}}(\mathbf{z}_{0:T-1}^{(1:K)}, \mathbf{z}_T | \mathbf{x}) q_{\text{PROP}}^{\text{CR-AIS}}(s_{1:M} | \mathbf{z}_{0:T-1}^{(1:K)}, \mathbf{z}_T, \mathbf{x})$ .

The gap in Eq. (107) also corresponds to the gap between  $\text{ELBO}_{\text{CR-AIS}}(\mathbf{x}; \pi_0, T, K)$  and  $\text{ELBO}_{\text{CR-AIS}}(\mathbf{x}; \pi_0, T, M)$ , so we can write

$$\begin{aligned} & \text{ELBO}_{\text{CR-AIS}}(\mathbf{x}; \pi_0, T, K) - \text{ELBO}_{\text{CR-AIS}}(\mathbf{x}; \pi_0, T, M) \\ &= D_{\text{KL}}[q_{\text{PROP}}^{\text{CR-AIS}}(s_{1:M} | \mathbf{z}_{0:T-1}^{(1:K)}, \mathbf{z}_T, \mathbf{x}) \| p_{\text{TGT}}^{\text{CR-AIS}}(s_{1:M} | \mathbf{z}_{0:T-1}^{(1:K)}, \mathbf{z}_T, \mathbf{x})]. \end{aligned} \quad (108)$$

Below, we analyze the posterior over the index variable for  $M = 1$  as a special case. This allows us to characterize the gap between  $\text{ELBO}_{\text{CR-AIS}}(\mathbf{x}; \pi_0, T, K)$  and the single-sample  $\text{ELBO}_{\text{AIS}}(\mathbf{x}; \pi_0, T) = \text{ELBO}_{\text{CR-AIS}}(\mathbf{x}; \pi_0, T, K = 1)$ .

### H.3 PROOF OF LOGARITHMIC IMPROVEMENT IN $K$ FOR CR-AIS ELBO

**Proposition H.2** (Improvement of Coupled Reverse Multi-Sample AIS over Single-Sample AIS). *Let*

$$q_{\text{PROP}}^{\text{CR-AIS}}(s | \mathbf{x}, \mathbf{z}_{0:T-1}^{(1:K)}, \mathbf{z}_T) = \frac{q_{\text{PROP}}^{\text{AIS}}(\mathbf{z}_{0:T-1}^{(s)}, \mathbf{z}_T | \mathbf{x})}{p_{\text{TGT}}^{\text{AIS}}(\mathbf{x}, \mathbf{z}_{0:T-1}^{(s)} | \mathbf{z}_T)} = \frac{K}{\sum_{k=1}^K} \frac{q_{\text{PROP}}^{\text{AIS}}(\mathbf{z}_{0:T-1}^{(k)}, \mathbf{z}_T | \mathbf{x})}{p_{\text{TGT}}^{\text{AIS}}(\mathbf{x}, \mathbf{z}_{0:T-1}^{(k)} | \mathbf{z}_T)} \quad (109)$$

denote the normalized importance weights over the AIS chains used in Coupled Reverse Multi-Sample AIS, and let  $\mathcal{U}(s)$  indicate the uniform distribution over  $K$  discrete values. Then, we can characterize the improvement of the Coupled Reverse Multi-Sample AIS bounds on  $\log p(\mathbf{x})$ ,  $\text{ELBO}_{\text{CR-AIS}}(\mathbf{x}; \pi_0, T, K)$  and  $\text{EUBO}_{\text{CR-AIS}}(\mathbf{x}; \pi_0, T, K)$ , over the single-sample AIS bounds  $\text{ELBO}_{\text{AIS}}(\mathbf{x}; \pi_0, T)$  and  $\text{EUBO}_{\text{AIS}}(\mathbf{x}; \pi_0, T)$  using KL divergences, as follows

$$\begin{aligned} \text{ELBO}_{\text{CR-AIS}}(\mathbf{x}; \pi_0, T, K) &= \text{ELBO}_{\text{AIS}}(\mathbf{x}; \pi_0, T) + \underbrace{\mathbb{E}_{q_{\text{PROP}}^{\text{CR-AIS}}(\mathbf{z}_{0:T-1}^{(1:K)}, \mathbf{z}_T | \mathbf{x})} \left[ D_{\text{KL}}[q_{\text{PROP}}^{\text{CR-AIS}}(s | \mathbf{x}, \mathbf{z}_{0:T-1}^{(1:K)}, \mathbf{z}_T) \| \mathcal{U}(s)] \right]}_{0 \leq \text{KL of uniform from SNIS weights} \leq \log K}, \\ \text{EUBO}_{\text{CR-AIS}}(\mathbf{x}; \pi_0, T, K) &= \text{EUBO}_{\text{AIS}}(\mathbf{x}; \pi_0, T) - \underbrace{\mathbb{E}_{p_{\text{TGT}}^{\text{CR-AIS}}(\mathbf{z}_{0:T-1}^{(1:K)}, \mathbf{z}_T | \mathbf{x})} \left[ D_{\text{KL}}[\mathcal{U}(s) \| q_{\text{PROP}}^{\text{CR-AIS}}(s | \mathbf{x}, \mathbf{z}_{0:T-1}^{(1:K)}, \mathbf{z}_T)] \right]}_{0 \leq \text{KL of SNIS weights from uniform} \leq D_{\text{KL}}[p_{\text{TGT}}^{\text{AIS}}(\mathbf{z}_{0:T} | \mathbf{x}) \| q_{\text{PROP}}^{\text{AIS}}(\mathbf{z}_{0:T} | \mathbf{x})}]. \end{aligned}$$

*Proof.* Using  $M = 1$  in Eq. (108) above, we obtain

$$\begin{aligned} & \text{ELBO}_{\text{CR-AIS}}(\mathbf{x}; \pi_0, T, K) - \text{ELBO}_{\text{AIS}}(\mathbf{x}; \pi_0, T, M = 1) \\ &= D_{\text{KL}}[q_{\text{PROP}}^{\text{CR-AIS}}(s | \mathbf{z}_{0:T-1}^{(1:K)}, \mathbf{z}_T, \mathbf{x}) \| p_{\text{TGT}}^{\text{CR-AIS}}(s | \mathbf{z}_{0:T-1}^{(1:K)}, \mathbf{z}_T, \mathbf{x})] \end{aligned} \quad (110)$$

From Eq. (99), we can write the posterior over the index variable as

$$q_{\text{PROP}}^{\text{CR-AIS}}(s | \mathbf{z}_{0:T-1}^{(1:K)}, \mathbf{z}_T, \mathbf{x}) = \frac{q_{\text{PROP}}^{\text{AIS}}(\mathbf{z}_{0:T-1}^{(s)}, \mathbf{z}_T | \mathbf{x})}{p_{\text{TGT}}^{\text{AIS}}(\mathbf{x}, \mathbf{z}_{0:T-1}^{(s)} | \mathbf{z}_T)} = \frac{K}{\sum_{k=1}^K} \frac{q_{\text{PROP}}^{\text{AIS}}(\mathbf{z}_{0:T-1}^{(k)}, \mathbf{z}_T | \mathbf{x})}{p_{\text{TGT}}^{\text{AIS}}(\mathbf{x}, \mathbf{z}_{0:T-1}^{(k)} | \mathbf{z}_T)} \quad (111)$$

For the target distribution in Eq. (98), all  $K$  samples are drawn from  $p_{\text{TGT}}^{\text{AIS}}(\mathbf{z}_{0:T-1}^{(k)} | \mathbf{x}, \mathbf{z}_T) \pi(\mathbf{x}, \mathbf{z}_T)$  and the posterior  $p_{\text{TGT}}^{\text{CR-AIS}}(s | \mathbf{z}_{0:T-1}^{(1:K)}, \mathbf{z}_T, \mathbf{x}) = \mathcal{U}(s)$  is uniform.

Thus, we can characterize the improvement of the  $K$ -sample CR-AIS ELBO over its single-chain AIS

$$\text{ELBO}_{\text{CR-AIS}}(\mathbf{x}; \pi_0, T, K) - \text{ELBO}_{\text{AIS}}(\mathbf{x}; \pi_0, T) = \mathbb{E}_{q_{\text{PROP}}^{\text{CR-AIS}}(\mathbf{z}_{0:T-1}^{(1:K)}, \mathbf{z}_T | \mathbf{x})} \left[ D_{\text{KL}}[q_{\text{PROP}}^{\text{CR-AIS}}(s | \mathbf{x}, \mathbf{z}_{0:T-1}^{(1:K)}, \mathbf{z}_T) \| \mathcal{U}(s)] \right] \quad (112)$$

The proof follows identically for the EUBO.

For the ELBO, the KL divergence with the uniform distribution in the second argument is bounded above by  $\log K$ . For the EUBO, the improvement of CR-AIS is limited by the gap in the single-chain  $\text{EUBO}_{\text{AIS}}(\mathbf{x}; \pi_0, T)$ , which corresponds to  $D_{\text{KL}}[p_{\text{TGT}}^{\text{AIS}}(\mathbf{z}_{0:T} | \mathbf{x}) \| q_{\text{PROP}}^{\text{AIS}}(\mathbf{z}_{0:T} | \mathbf{x})]$ .  $\square$

#### H.4 LINEAR BIAS REDUCTION IN $T$ FOR CR-AIS

**Corollary H.3** (Complexity in  $T$  for Coupled Reverse Multi-Sample AIS Bound). *Assuming perfect transitions and a geometric annealing path with linearly-spaced  $\{\beta_t\}_{t=0}^T$ , the sum of the gaps in the Coupled Reverse Multi-Sample AIS sandwich bounds on MI,  $I_{\text{CR-AIS}_U}(\pi_0, K, T) - I_{\text{CR-AIS}_L}(\pi_0, K, T)$ , reduces linearly with increasing  $T$ .*

*Proof.* Since we have shown in Prop. H.2 that  $\text{ELBO}_{\text{CR-AIS}}(\pi_0, K, T)$  and  $\text{EUBO}_{\text{CR-AIS}}(\pi_0, K, T)$  are tighter than  $\text{ELBO}_{\text{AIS}}(\pi_0, T)$  and  $\text{EUBO}_{\text{AIS}}(\pi_0, T)$ , the bias in the CR-AIS sandwich bounds  $\text{EUBO}_{\text{CR-AIS}}(\pi_0, K, T) - \text{ELBO}_{\text{CR-AIS}}(\pi_0, K, T)$  will be less than that of single-sample AIS. Thus, Eq. (19) will hold with an inequality, and CR-AIS will inherit the linear bias reduction under perfect transitions and linear scheduling from Prop. 3.1 (see App. D.1).  $\square$

## I COMPARISON OF MULTI-SAMPLE AIS BOUNDS

In this section, we provide more extensive results for the experiments of Sec. 5.1. In Fig. 7, we compare the performance of our various Multi-Sample AIS bounds for different values of  $K$  and  $T$ . We consider MI estimation of Linear VAE, MNIST-VAE, and MNIST-GAN.

## J GENERALIZED MUTUAL INFORMATION NEURAL ESTIMATION (GMINE)

In this section, we provide probabilistic interpretations for the MINE lower bounds on MI from Belghazi et al. (2018), which allows us to derive novel *Generalized* MINE bounds. In a similar spirit to GIWAE, Generalized MINE uses a base variational distribution  $q_\theta(\mathbf{z}|\mathbf{x})$  to tighten the MINE-DV or MINE-F bound and can be evaluated when  $p(\mathbf{z})$  is available.

See Fig. 8 for a summary of Generalized MINE bounds and their relationships. We discuss probabilistic interpretations in this section, and provide complementary interpretations in terms of conjugate dual representations of the KL divergence in App. K.

We begin by deriving a probabilistic interpretation for the IBAL lower bound in Sec. 4, which we will show is closely related to the probabilistic interpretations of MINE. Our MINE-AIS method is designed to optimize and evaluate the IBAL lower bound on MI, with detailed discussion in Sec. 4 and App. M.

### J.1 PROBABILISTIC INTERPRETATION OF IBAL

For an energy-based posterior approximation

$$\pi_{\theta, \phi}(\mathbf{z}|\mathbf{x}) := \frac{1}{\mathcal{Z}_{\theta, \phi}(\mathbf{x})} q_\theta(\mathbf{z}|\mathbf{x}) e^{T_\phi(\mathbf{x}, \mathbf{z})}, \quad \text{where } \mathcal{Z}_{\theta, \phi}(\mathbf{x}) = \mathbb{E}_{q_\theta(\mathbf{z}|\mathbf{x})} [e^{T_\phi(\mathbf{x}, \mathbf{z})}], \quad (113)$$

we consider the BA lower bound on MI,

$$\begin{aligned} I_{\text{BAL}}(\pi_{\theta, \phi}) &= I(\mathbf{x}, \mathbf{z}) - \mathbb{E}_{p(\mathbf{x})} [D_{\text{KL}}[p(\mathbf{z}|\mathbf{x})||\pi_{\theta, \phi}(\mathbf{z}|\mathbf{x})]] \\ &= \mathbb{E}_{p(\mathbf{x}, \mathbf{z})} \left[ \log \frac{p(\mathbf{x}, \mathbf{z})}{p(\mathbf{x})p(\mathbf{z})} \right] - \mathbb{E}_{p(\mathbf{x}, \mathbf{z})} [\log p(\mathbf{z}|\mathbf{x})] + \mathbb{E}_{p(\mathbf{x}, \mathbf{z})} [T(\mathbf{x}, \mathbf{z})] - \mathbb{E}_{p(\mathbf{x}, \mathbf{z})} [\log \mathcal{Z}_{\theta, \phi}] \\ &= \mathbb{E}_{p(\mathbf{x}, \mathbf{z})} \left[ \log \frac{q_\theta(\mathbf{z}|\mathbf{x})}{p(\mathbf{z})} \right] + \mathbb{E}_{p(\mathbf{x}, \mathbf{z})} [T_\phi(\mathbf{x}, \mathbf{z})] - \mathbb{E}_{p(\mathbf{x})} [\log \mathcal{Z}_{\theta, \phi}(\mathbf{x})] \\ &= \underbrace{\mathbb{E}_{p(\mathbf{x}, \mathbf{z})} \left[ \log \frac{q_\theta(\mathbf{z}|\mathbf{x})}{p(\mathbf{z})} \right]}_{I_{\text{BAL}}(q_\theta)} + \underbrace{\mathbb{E}_{p(\mathbf{x}, \mathbf{z})} \left[ \log \frac{e^{T_\phi(\mathbf{x}, \mathbf{z})}}{\mathbb{E}_{q_\theta(\mathbf{z}|\mathbf{x})} [e^{T_\phi(\mathbf{x}, \mathbf{z})}]} \right]}_{\text{contrastive term}} \\ &=: \text{IBAL}(q_\theta, T_\phi), \end{aligned} \quad (114)$$

where the gap in the mutual information bound is  $\mathbb{E}_{p(\mathbf{x})} [D_{\text{KL}}[p(\mathbf{z}|\mathbf{x})||\pi_{\theta, \phi}(\mathbf{z}|\mathbf{x})]]$ . Note that  $\text{IBAL}(q_\theta, T_\phi)$  includes  $I_{\text{BAL}}(q_\theta)$  as one of its terms, where we refer to  $q_\theta(\mathbf{z}|\mathbf{x})$  as the base varia-



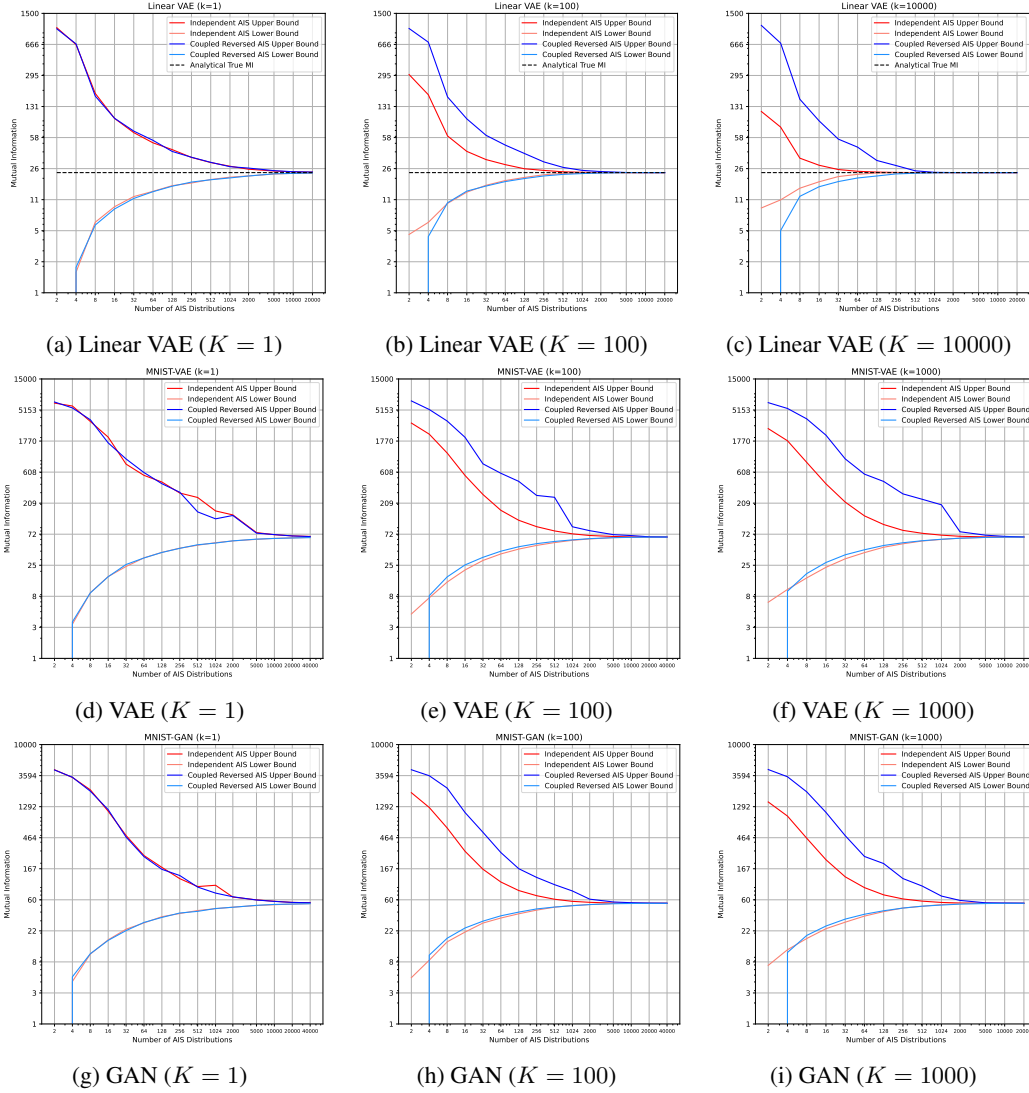


Figure 7: Comparing Multi-Sample AIS sandwich bounds and evaluating the effect of  $K$  and  $T$  for MI estimation in deep generative models.

tional distribution. We visualize relationships between various energy-based bounds in Fig. 5b and Fig. 8.

**Proposition 4.1.** For a given  $q_\theta(\mathbf{z}|\mathbf{x})$ , the optimal IBAL critic function equals the log importance weights up to a constant  $T^*(\mathbf{x}, \mathbf{z}) = \log \frac{p(\mathbf{x}, \mathbf{z})}{q_\theta(\mathbf{z}|\mathbf{x})} + c(\mathbf{x})$ . For this  $T^*$ , we have  $\text{IBAL}(q_\theta, T^*) = I(\mathbf{x}; \mathbf{z})$ .

See App. L.1 for the proof.

## J.2 PROBABILISTIC INTERPRETATION OF GENERALIZED MINE-DV

We can interpret the MINE-DV bound of Belghazi et al. (2018) as arising from an energy-based variational approximation  $\pi_{\theta, \phi}(\mathbf{x}, \mathbf{z})$  of the full joint distribution  $p(\mathbf{x}, \mathbf{z})$  as follows

$$\pi_{\theta, \phi}(\mathbf{x}, \mathbf{z}) := \frac{1}{\mathcal{Z}} p(\mathbf{x}) q_\theta(\mathbf{z}|\mathbf{x}) e^{T_\phi(\mathbf{x}, \mathbf{z})}, \quad \text{where } \mathcal{Z} = \mathbb{E}_{p(\mathbf{x}) q_\theta(\mathbf{z}|\mathbf{x})} \left[ e^{T_\phi(\mathbf{x}, \mathbf{z})} \right], \quad (115)$$

$q_\theta(\mathbf{z}|\mathbf{x})$  is a base variational distribution, and  $T_\phi$  is a critic or negative energy function.

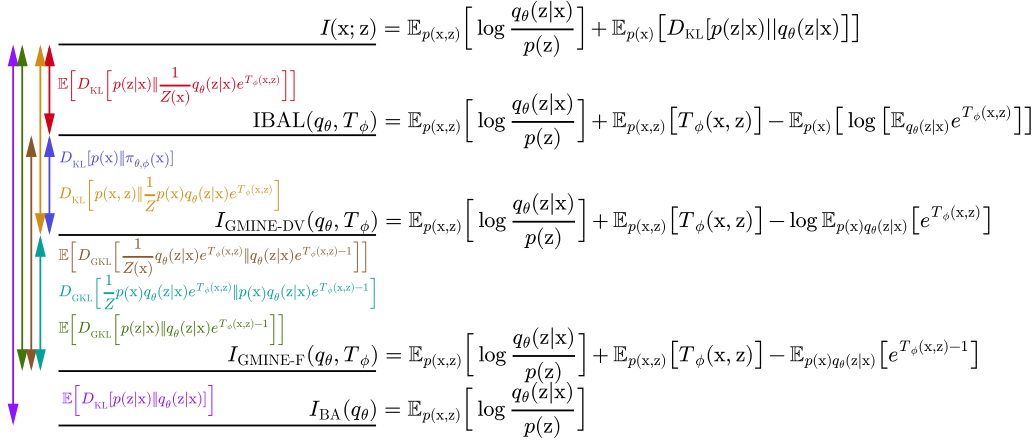


Figure 8: Generalized Energy Based Bounds. Arrows indicate the gaps in each MI lower bound or its relationship to other lower bounds.  $D_{\text{GKL}}[\cdot|\cdot]$  represents the *generalized* KL divergence between two unnormalized densities (see App. J.3). All bounds are written in terms of a base variational distribution  $q_\theta(\mathbf{z}|\mathbf{x})$ , which may be chosen to be the marginal  $p(\mathbf{z})$  as in MINE-DV and MINE-F.

Note that for the induced marginal  $\pi_{\theta,\phi}(\mathbf{x}) := \int \pi_{\theta,\phi}(\mathbf{x}, \mathbf{z}) d\mathbf{z} \neq p(\mathbf{x})$  due to the contribution of the critic function. Instead, we have

$$\pi_{\theta,\phi}(\mathbf{x}) = \frac{1}{\mathcal{Z}} p(\mathbf{x}) \mathcal{Z}(\mathbf{x}), \quad (116)$$

where  $\mathcal{Z}(\mathbf{x}) = \int q(\mathbf{z}|\mathbf{x}) e^{T_\phi(\mathbf{x},\mathbf{z})} d\mathbf{z}$  and  $\mathcal{Z} = \int p(\mathbf{x}) q(\mathbf{z}|\mathbf{x}) e^{T_\phi(\mathbf{x},\mathbf{z})} d\mathbf{x} d\mathbf{z} = \mathbb{E}_{p(\mathbf{x})}[\mathcal{Z}(\mathbf{x})]$ .

Subtracting the joint KL divergence  $D_{\text{KL}}[p(\mathbf{x}, \mathbf{z})|\pi_{\theta,\phi}(\mathbf{x}, \mathbf{z})]$  from  $I(\mathbf{x}; \mathbf{z})$ , we obtain the *Generalized* MINE-DV lower bound on MI

$$I(\mathbf{x}; \mathbf{z}) \geq I(\mathbf{x}; \mathbf{z}) - D_{\text{KL}}\left[p(\mathbf{x}, \mathbf{z}) \left\| \frac{1}{\mathcal{Z}} p(\mathbf{x}) q_\theta(\mathbf{z}|\mathbf{x}) e^{T_\phi(\mathbf{x},\mathbf{z})} \right\| \right] \quad (117)$$

$$\begin{aligned} &= \mathbb{E}_{p(\mathbf{x},\mathbf{z})} \left[ \log \frac{q_\theta(\mathbf{z}|\mathbf{x})}{p(\mathbf{z})} \right] + \mathbb{E}_{p(\mathbf{x},\mathbf{z})} [T_\phi(\mathbf{x}, \mathbf{z})] - \log \mathbb{E}_{p(\mathbf{x})q_\theta(\mathbf{z}|\mathbf{x})} [e^{T_\phi(\mathbf{x},\mathbf{z})}] \\ &=: I_{\text{GMINE-DV}}(q_\theta, T_\phi). \end{aligned} \quad (118)$$

By construction, Eq. (117) shows that the gap in Generalized MINE-DV is  $D_{\text{KL}}[p(\mathbf{x}, \mathbf{z})|\frac{1}{\mathcal{Z}}p(\mathbf{x})q_\theta(\mathbf{z}|\mathbf{x})e^{T_\phi(\mathbf{x},\mathbf{z})}]$ , which has a probabilistic interpretation in terms of the approximate joint distribution  $\pi_{\theta,\phi}(\mathbf{x}, \mathbf{z})$ .

**Relationship with MINE-DV** For  $q_\theta(\mathbf{z}|\mathbf{x}) = p(\mathbf{z})$ , we obtain the MINE-DV bound (Belghazi et al., 2018; Poole et al., 2019) as a special case with  $I_{\text{MINE-DV}}(T_\phi) = I_{\text{GMINE-DV}}(p(\mathbf{z}), T_\phi)$ . In particular, the joint base distribution in Eq. (115) corresponds to the product of marginals  $p(\mathbf{x})p(\mathbf{z})$ . Our probabilistic interpretation shows that the gap in MINE-DV corresponds to  $D_{\text{KL}}[p(\mathbf{x}, \mathbf{z})|\frac{1}{\mathcal{Z}}p(\mathbf{x})p(\mathbf{z})e^{T_\phi(\mathbf{x},\mathbf{z})}]$ .

We expect that the Generalized MINE, with a learned variational distribution  $q_\theta(\mathbf{z}|\mathbf{x})$ , to obtain tighter bounds than MINE-DV. We can guarantee that  $I_{\text{GMINE-DV}}(q_\theta^*, T_\phi) \geq I_{\text{MINE-DV}}(T_\phi)$  for the optimal  $q_\theta^*$  with a given  $T_\phi$ , so long as  $p(\mathbf{z})$  is in the variational family (i.e.,  $\exists \theta_0$  such that  $q_{\theta_0}(\mathbf{z}|\mathbf{x}) = p(\mathbf{z})$ ).

**Relationship with BA Bound** Choosing a constant critic function  $T_{\phi_0}(\mathbf{x}, \mathbf{z}) = \text{const}$ , we can see that  $\pi_{\theta,\phi_0}(\mathbf{x}, \mathbf{z}) = p(\mathbf{x})q_\theta(\mathbf{z}|\mathbf{x})$  and  $I_{\text{GMINE-DV}}(q_\theta, T_{\phi_0} = \text{const}) = I_{\text{BAL}}(q_\theta)$  for a given  $q_\theta(\mathbf{z}|\mathbf{x})$ .

**Optimal Critic Function** For a given  $q_\theta(\mathbf{z}|\mathbf{x})$ , the optimal critic function of Generalized MINE-DV corresponds to the log importance weight between the target  $p(\mathbf{x}, \mathbf{z})$  and the joint base distribution  $p(\mathbf{x})q_\theta(\mathbf{z}|\mathbf{x})$ , plus a constant

$$T^*(\mathbf{x}, \mathbf{z}) = \log \frac{p(\mathbf{x}, \mathbf{z})}{p(\mathbf{x})q_\theta(\mathbf{z}|\mathbf{x})} + c. \quad (119)$$

For the optimal critic function associated with a given  $q_\theta(\mathbf{z}|\mathbf{x})$ , we have  $I_{\text{MINE-DV}}(q_\theta, T^*) = I(\mathbf{x}; \mathbf{z})$ .

**Relationship with IBAL** We can use our probabilistic interpretation to show that the IBAL is tighter than Generalized MINE-DV, with  $\text{IBAL}(q_\theta, T_\phi) \geq I_{\text{GMINE-DV}}(q_\theta, T_\phi)$ . Subtracting the gaps in the bounds in Eq. (114) and Eq. (117),

$$\begin{aligned} \text{IBAL}(q_\theta, T_\phi) &= I_{\text{GMINE-DV}}(q_\theta, T_\phi) + \underbrace{D_{\text{KL}}[p(\mathbf{x}, \mathbf{z}) \|\pi_{\theta, \phi}(\mathbf{x}, \mathbf{z})]}_{\text{gap in GMINE-DV}(q_\theta, T_\phi)} - \underbrace{\mathbb{E}_{p(\mathbf{x})} [D_{\text{KL}}[p(\mathbf{z}|\mathbf{x}) \|\pi_{\theta, \phi}(\mathbf{z}|\mathbf{x})]]}_{\text{gap in IBAL}(q_\theta, T_\phi)} \\ &= I_{\text{GMINE-DV}}(q_\theta, T_\phi) + \mathbb{E}_{p(\mathbf{x})} \left[ \log \frac{p(\mathbf{x})}{\pi_{\theta, \phi}(\mathbf{x})} \right] \end{aligned} \quad (120)$$

$$= I_{\text{GMINE-DV}}(q_\theta, T_\phi) + D_{\text{KL}}[p(\mathbf{x}) \|\pi_{\theta, \phi}(\mathbf{x})] \quad (121)$$

$$\geq I_{\text{GMINE-DV}}(q_\theta, T_\phi). \quad (122)$$

We see that the difference between  $\text{IBAL}(q_\theta, T_\phi)$  and  $I_{\text{GMINE-DV}}(q_\theta, T_\phi)$  corresponds to a marginal KL divergence in the  $\mathbf{x}$  space, where  $\pi_{\theta, \phi}(\mathbf{x})$  is defined in Eq. (116).

As in Poole et al. (2019), we can also interpret the gap between the  $\text{IBAL}(q_\theta, T_\phi)$  and  $I_{\text{GMINE-DV}}(q_\theta, T_\phi)$  as an application of Jensen’s inequality, with

$$D_{\text{KL}}[p(\mathbf{x}) \|\pi_{\theta, \phi}(\mathbf{x})] = D_{\text{KL}} \left[ p(\mathbf{x}) \left\| \frac{1}{\mathcal{Z}} p(\mathbf{x}) \mathcal{Z}(\mathbf{x}) \right. \right] \quad (123)$$

$$= \log \mathcal{Z} - \mathbb{E}_{p(\mathbf{x})} [\log \mathcal{Z}(\mathbf{x})] \quad (124)$$

$$= \log \mathbb{E}_{p(\mathbf{x})} [\mathcal{Z}(\mathbf{x})] - \mathbb{E}_{p(\mathbf{x})} [\log \mathcal{Z}(\mathbf{x})], \quad (125)$$

since  $\log \mathbb{E}_{p(\mathbf{x})} [\mathcal{Z}(\mathbf{x})] \geq \mathbb{E}_{p(\mathbf{x})} [\log \mathcal{Z}(\mathbf{x})]$ .

### J.3 PROBABILISTIC INTERPRETATION OF GENERALIZED MINE-F

The BA lower bound and its corresponding EUBO upper bound on  $\log p(\mathbf{x})$  are derived using a KL divergence between the true and approximate posterior, which are normalized conditional distributions over  $\mathbf{z}$  given  $\mathbf{x}$ . In this section, we interpret the MINE-F bound (Belghazi et al., 2018) as arising from a generalized notion of the KL divergence between possibly *unnormalized* density functions. In particular, our probabilistic interpretation will involve an unnormalized  $\tilde{\pi}_{\theta, \phi}(\mathbf{z}|\mathbf{x})$  which seeks to approximate the true (normalized) posterior  $p(\mathbf{z}|\mathbf{x})$ .

**Generalized KL Divergence (GKL)** First, we state the definition of the *generalized* KL divergence, which takes unnormalized measures as input arguments and corresponds to the limiting behavior of the  $\alpha$ -divergence (Cichocki & Amari (2010))

$$D_{\text{GKL}}[\tilde{r}(\mathbf{z}) \|\tilde{s}(\mathbf{z})] = \int \tilde{r}(\mathbf{z}) \log \frac{\tilde{r}(\mathbf{z})}{\tilde{s}(\mathbf{z})} d\mathbf{z} - \int \tilde{r}(\mathbf{z}) d\mathbf{z} + \int \tilde{s}(\mathbf{z}) d\mathbf{z}. \quad (126)$$

As in the case of the standard KL divergence, this quantity is nonnegative, convex in either argument, and vanishes for  $\tilde{r}(\mathbf{z}) = \tilde{s}(\mathbf{z})$ . It is also a member of both the family of Bregman divergences and  $f$ -divergences (Amari, 2009). If  $r(\mathbf{z})$  and  $s(\mathbf{z})$  are normalized, then  $D_{\text{GKL}}[r(\mathbf{z}) \|\tilde{s}(\mathbf{z})] = D_{\text{KL}}[r(\mathbf{z}) \|\tilde{s}(\mathbf{z})]$ . Finally, if  $r(\mathbf{z})$  is normalized and  $\tilde{s}(\mathbf{z})$  is unnormalized, one can easily confirm that

$$\begin{aligned} D_{\text{GKL}}[r(\mathbf{z}) \|\tilde{s}(\mathbf{z})] &= D_{\text{KL}}[r(\mathbf{z}) \|\tilde{s}(\mathbf{z})] + D_{\text{GKL}}[\tilde{s}(\mathbf{z})] \\ &\geq D_{\text{KL}}[r(\mathbf{z}) \|\tilde{s}(\mathbf{z})]. \end{aligned} \quad (127)$$

**Generalized EUBO (GEUBO)** Since the Generalized KL divergence is always nonnegative, we define a Generalized EUBO by adding the Generalized KL divergence between the normalized true posterior and an unnormalized approximate posterior  $\tilde{\pi}(\mathbf{z}|\mathbf{x})$ .

$$\text{GEUBO}(\mathbf{x}; \tilde{\pi}) := \log p(\mathbf{x}) + D_{\text{GKL}}[p(\mathbf{z}|\mathbf{x}) \|\tilde{\pi}(\mathbf{z}|\mathbf{x})] \quad (128)$$

$$= \mathbb{E}_{p(\mathbf{z}|\mathbf{x})} \left[ \log \frac{p(\mathbf{x}, \mathbf{z})}{\tilde{\pi}(\mathbf{z}|\mathbf{x})} \right] - 1 + \mathcal{Z}_{\tilde{\pi}}(\mathbf{x}), \quad (129)$$

where we define  $\mathcal{Z}_{\tilde{\pi}}(\mathbf{x}) := \int \tilde{\pi}(\mathbf{z}|\mathbf{x}) d\mathbf{z}$ . In general, we have  $\text{EUBO}(\mathbf{x}; \pi) \leq \text{GEUBO}(\mathbf{x}; \tilde{\pi})$  where  $\pi$  is the normalized distribution of  $\tilde{\pi}$ , with equality if  $\tilde{\pi}$  is normalized.

**Generalized BA (GBA)** Using the Generalized EUBO in place of  $\log p(\mathbf{x})$ , we obtain the following lower bound on MI, which we denote as the Generalized BA lower bound

$$\begin{aligned} I(\mathbf{x}; \mathbf{z}) &\geq I(\mathbf{x}; \mathbf{z}) - \mathbb{E}_{p(\mathbf{x})} [D_{\text{GKL}}[p(\mathbf{z}|\mathbf{x}) \|\tilde{\pi}(\mathbf{z}|\mathbf{x})]] \\ &= \mathbb{E}_{p(\mathbf{x}, \mathbf{z})} \left[ \log \frac{\tilde{\pi}(\mathbf{z}|\mathbf{x})}{p(\mathbf{z})} \right] + 1 - \mathbb{E}_{p(\mathbf{x})} [\mathcal{Z}_{\tilde{\pi}}(\mathbf{x})] \\ &=: I_{\text{GBA}_L}(\tilde{\pi}). \end{aligned} \quad (130)$$

**Generalized MINE-F (GMINE-F)** We now consider an unnormalized, energy-based approximation to the true posterior, involving a base variational distribution  $q_\theta(\mathbf{z}|\mathbf{x})$  and a learned critic function  $T_\phi(\mathbf{x}, \mathbf{z})$

$$\tilde{\pi}_{\theta, \phi}(\mathbf{z}|\mathbf{x}) := q_\theta(\mathbf{z}|\mathbf{x}) e^{T_\phi(\mathbf{x}, \mathbf{z}) - 1}. \quad (131)$$

Using this unnormalized approximate posterior in the GBA lower bound in Eq. (130), we obtain the *Generalized* MINE-F lower bound

$$I(\mathbf{x}; \mathbf{z}) \geq I(\mathbf{x}; \mathbf{z}) - \mathbb{E}_{p(\mathbf{x})} [D_{\text{GKL}}[p(\mathbf{z}|\mathbf{x}) \|\tilde{\pi}_{\theta, \phi}(\mathbf{z}|\mathbf{x})]] \quad (132)$$

$$= \mathbb{E}_{p(\mathbf{x}, \mathbf{z})} \left[ \log \frac{q_\theta(\mathbf{z}|\mathbf{x})}{p(\mathbf{z})} \right] + \mathbb{E}_{p(\mathbf{x}, \mathbf{z})} [T_\phi(\mathbf{x}, \mathbf{z})] - \mathbb{E}_{p(\mathbf{x}) q_\theta(\mathbf{z}|\mathbf{x})} \left[ e^{T_\phi(\mathbf{x}, \mathbf{z}) - 1} \right] \quad (133)$$

$$=: I_{\text{GMINE-F}}(q_\theta, T_\phi). \quad (134)$$

By construction, we can see that the gap in  $I_{\text{GMINE-F}}(q_\theta, T_\phi)$  is equal to the Generalized KL divergence  $\mathbb{E}_{p(\mathbf{x})} [D_{\text{GKL}}[p(\mathbf{z}|\mathbf{x}) \|\tilde{\pi}_{\theta, \phi}(\mathbf{z}|\mathbf{x})]]$  in Eq. (132). As in the case of MINE-DV, we obtain the standard MINE-F lower bound  $I_{\text{MINE-F}}(T_\phi) = I_{\text{GMINE-F}}(p(\mathbf{z}), T_\phi)$  when using the marginal  $p(\mathbf{z})$  as the proposal.

**Optimal Critic Function** The optimal critic function of Generalized MINE-F is  $T^*(\mathbf{x}, \mathbf{z}) = 1 + \log \frac{p(\mathbf{x}, \mathbf{z})}{p(\mathbf{x})q(\mathbf{z}|\mathbf{x})}$  (Poole et al., 2019). In this case, we obtain  $I_{\text{GMINE-F}}(q_\theta, T^*) = I(\mathbf{x}; \mathbf{z})$  in Eq. (133).

**Relationship with IBAL** We would now like to relate the gap in  $I_{\text{GMINE-F}}(q_\theta, T_\phi)$  to the gap in  $I_{\text{IBAL}}(q_\theta, T_\phi)$ . First, note that the normalized distribution corresponding to  $\tilde{\pi}_{\theta, \phi}(\mathbf{z}|\mathbf{x}) = q_\theta(\mathbf{z}|\mathbf{x}) e^{T_\phi(\mathbf{x}, \mathbf{z}) - 1}$  matches the the energy-based posterior in the IBAL,  $\pi_{\theta, \phi}(\mathbf{z}|\mathbf{x}) = \frac{1}{\mathcal{Z}(\mathbf{x})} q_\theta(\mathbf{z}|\mathbf{x}) e^{T_\phi(\mathbf{x}, \mathbf{z})}$ . Using Eq. (127), we have

$$\mathbb{E}_{p(\mathbf{x})} [D_{\text{GKL}}[p(\mathbf{z}|\mathbf{x}) \|\tilde{\pi}_{\theta, \phi}(\mathbf{z}|\mathbf{x})]] = \mathbb{E}_{p(\mathbf{x})} [D_{\text{KL}}[p(\mathbf{z}|\mathbf{x}) \|\pi_{\theta, \phi}(\mathbf{z}|\mathbf{x})]] + \mathbb{E}_{p(\mathbf{x})} [D_{\text{GKL}}[\pi_{\theta, \phi}(\mathbf{z}|\mathbf{x}) \|\tilde{\pi}_{\theta, \phi}(\mathbf{z}|\mathbf{x})]].$$

and substituting in the definition of each term

$$\begin{aligned} \underbrace{\mathbb{E}_{p(\mathbf{x})} \left[ D_{\text{GKL}} \left[ p(\mathbf{z}|\mathbf{x}) \left\| q_\theta(\mathbf{z}|\mathbf{x}) e^{T_\phi(\mathbf{x}, \mathbf{z}) - 1} \right\| \right] \right]}_{\text{gap of GMINE-F}} &= \underbrace{\mathbb{E}_{p(\mathbf{x})} \left[ D_{\text{KL}} \left[ p(\mathbf{z}|\mathbf{x}) \left\| \frac{1}{\mathcal{Z}(\mathbf{x})} q_\theta(\mathbf{z}|\mathbf{x}) e^{T_\phi(\mathbf{x}, \mathbf{z})} \right\| \right] \right]}_{\text{gap of IBAL}} \\ &\quad + \underbrace{\mathbb{E}_{p(\mathbf{x})} \left[ D_{\text{GKL}} \left[ \frac{1}{\mathcal{Z}(\mathbf{x})} q_\theta(\mathbf{z}|\mathbf{x}) e^{T_\phi(\mathbf{x}, \mathbf{z})} \left\| q_\theta(\mathbf{z}|\mathbf{x}) e^{T_\phi(\mathbf{x}, \mathbf{z}) - 1} \right\| \right] \right]}_{\geq 0}, \end{aligned} \quad (135)$$

where the final term  $D_{\text{GKL}}[\pi_{\theta, \phi}(\mathbf{z}|\mathbf{x}) \|\tilde{\pi}_{\theta, \phi}(\mathbf{z}|\mathbf{x})] \geq 0$  is nonnegative because it is a generalized KL divergence. Thus, we have

$$\text{IBAL}(q_\theta, T_\phi) = I_{\text{GMINE-F}}(q_\theta, T_\phi) + \mathbb{E}_{p(\mathbf{x})} [D_{\text{GKL}}[\pi_{\theta, \phi}(\mathbf{z}|\mathbf{x}) \|\tilde{\pi}_{\theta, \phi}(\mathbf{z}|\mathbf{x})]] \geq I_{\text{GMINE-F}}(q_\theta, T_\phi). \quad (136)$$

Alternatively, Poole et al. (2019) use the inequality  $\log u \leq u - 1$  to show that

$$D_{\text{GKL}}[\pi_{\theta, \phi}(\mathbf{z}|\mathbf{x}) \|\tilde{\pi}_{\theta, \phi}(\mathbf{z}|\mathbf{x})] = \mathbb{E}_{p(\mathbf{x})} [\mathcal{Z}(\mathbf{x}) - 1 - \log \mathcal{Z}(\mathbf{x})] \geq 0.$$

We visualize the relationship between IBAL and Generalized MINE-F in Fig. 8.

**Relationship with Generalized MINE-DV** To characterize the gap between Generalized MINE-DV and Generalized MINE-F, we can again use the equality from Eq. (127), but this time using divergences over joint distributions.

$$\begin{aligned}
D_{\text{GKL}} \left[ p(\mathbf{x}, \mathbf{z}) \middle\| \tilde{\pi}_{\theta, \phi}(\mathbf{x}, \mathbf{z}) \right] &= D_{\text{KL}} \left[ p(\mathbf{x}, \mathbf{z}) \middle\| \pi_{\theta, \phi}(\mathbf{x}, \mathbf{z}) \right] + D_{\text{GKL}} \left[ \pi_{\theta, \phi}(\mathbf{x}, \mathbf{z}) \middle\| \tilde{\pi}_{\theta, \phi}(\mathbf{x}, \mathbf{z}) \right] \\
\underbrace{D_{\text{GKL}} \left[ p(\mathbf{x}, \mathbf{z}) \middle\| p(\mathbf{x})q_{\theta}(\mathbf{z}|\mathbf{x})e^{T_{\phi}(\mathbf{x}, \mathbf{z})-1} \right]}_{\text{gap in GMINE-F}} &= \underbrace{D_{\text{KL}} \left[ p(\mathbf{x}, \mathbf{z}) \middle\| \frac{1}{Z} p(\mathbf{x})q_{\theta}(\mathbf{z}|\mathbf{x})e^{T_{\phi}(\mathbf{x}, \mathbf{z})} \right]}_{\text{gap in GMINE-DV}} \\
&\quad + \underbrace{D_{\text{GKL}} \left[ \frac{1}{Z} p(\mathbf{x})q_{\theta}(\mathbf{z}|\mathbf{x})e^{T_{\phi}(\mathbf{x}, \mathbf{z})} \middle\| p(\mathbf{x})q_{\theta}(\mathbf{z}|\mathbf{x})e^{T_{\phi}(\mathbf{x}, \mathbf{z})-1} \right]}_{\geq 0}.
\end{aligned} \tag{137}$$

In this case, we have  $D_{\text{GKL}} \left[ \frac{1}{Z} p(\mathbf{x})q_{\theta}(\mathbf{z}|\mathbf{x})e^{T_{\phi}(\mathbf{x}, \mathbf{z})} \middle\| p(\mathbf{x})q_{\theta}(\mathbf{z}|\mathbf{x})e^{T_{\phi}(\mathbf{x}, \mathbf{z})-1} \right] \geq 0$ . Thus, Generalized MINE-DV is tighter than Generalized MINE-F (see Fig. 8), which generalizes the finding in Poole et al. (2019) that standard MINE-DV is tighter than standard MINE-F.

## K CONJUGATE DUALITY INTERPRETATIONS

In this section, we interpret the energy-based MI lower bounds in MINE-AIS, Generalized MINE-DV, Generalized MINE-F, GIWAE, IWAE, and INFONCE from the perspective of conjugate duality. In particular, we highlight that the critic or negative energy function in the above bounds arises as a dual variable in the convex conjugate representation of the KL divergence. In all cases, the KL divergence of interest corresponds to the gap in the BA lower bound

$$I(\mathbf{x}; \mathbf{z}) = \mathbb{E}_{p(\mathbf{x}, \mathbf{z})} \left[ \log \frac{q_{\theta}(\mathbf{z}|\mathbf{x})}{p(\mathbf{z})} \right] + \mathbb{E}_{p(\mathbf{x})} [D_{\text{KL}}[p(\mathbf{z}|\mathbf{x}) \| q_{\theta}(\mathbf{z}|\mathbf{x})]]. \tag{138}$$

For  $q_{\theta}(\mathbf{z}|\mathbf{x}) = p(\mathbf{z})$ , the BA lower bound term is 0 and our derivations correspond to taking dual representation of MI directly, e.g.  $\mathbb{E}_{p(\mathbf{x})} [D_{\text{KL}}[p(\mathbf{z}|\mathbf{x}) \| p(\mathbf{z})]]$ , as in Belghazi et al. (2018).

Our conjugate duality interpretations are complementary to our probabilistic interpretations, with either approach equally valid for deriving lower bounds and characterizing their gaps.

### K.1 CONVEX ANALYSIS BACKGROUND

Suppose  $(X, \Sigma)$  is a measurable space,  $B(\Sigma)$  is the space of bounded measurable functions  $u : X \rightarrow \mathbb{R}$ , and  $\mathcal{M}(X)$ ,  $\mathcal{M}_+(X)$ ,  $\mathcal{P}(X)$  are the space of finite signed measures, finite positive measures, and probability measures, respectively. Consider the following dual pairing between  $\mathcal{M}(X)$  and  $B(\Sigma)$

$$\langle \pi, u \rangle := \int_X u d\pi, \quad \forall \pi \in \mathcal{M}(X), \quad \forall u \in B(\Sigma). \tag{139}$$

The conjugate function of  $\Omega : \mathcal{M}(X) \rightarrow (-\infty, +\infty]$ , denoted by  $\Omega^* : B(\Sigma) \rightarrow (-\infty, +\infty]$ , and the biconjugate function, denoted by  $\Omega^{**} : \mathcal{M}(X) \rightarrow (-\infty, +\infty]$ , are obtained by

$$\Omega^*(u) := \sup_{\pi \in \mathcal{M}(X)} \{ \langle \pi, u \rangle - \Omega(\pi) \}, \quad \forall u \in B(\Sigma), \tag{140}$$

$$\Omega^{**}(\pi) := \sup_{u \in B(\Sigma)} \{ \langle \pi, u \rangle - \Omega^*(u) \}, \quad \forall \pi \in \mathcal{M}(X). \tag{141}$$

If  $\Omega$  is a convex and lower-semicontinuous function, we have  $\Omega = \Omega^{**}$ . The pair of  $(\pi, u)$  are in dual correspondence iff  $u \in \partial\Omega(\pi)$ , where  $\partial$  denotes the subdifferential mapping. Note that the duality mapping between  $(\pi, u)$  could generally be a multi-valued mapping. However, it can be shown that  $(\pi, u)$  are in dual correspondence or  $u \in \partial\Omega(\pi)$  iff  $\Omega(\pi) + \Omega^*(u) = \langle \pi, u \rangle$  (see Eq. (143) below).

Suppose  $\pi_1, \pi_2 \in \mathcal{M}(X)$ , and  $(\pi_1, u_1)$  are in dual correspondence. Using the subdifferential  $u_1$ , we can define the Bregman divergence generated by a convex function  $\Omega$  as follows

$$D_{\Omega}^{u_1}(\pi_2, \pi_1) = \Omega(\pi_2) - \Omega(\pi_1) - \langle \pi_2 - \pi_1, u_1 \rangle. \tag{142}$$

This Bregman divergence can be used to characterize the gap of Fenchel-Young inequality

$$\begin{aligned}
\Omega(\pi_2) + \Omega^*(u_1) &= \langle \pi_2, u_1 \rangle + D_{\Omega}^{u_1}(\pi_2, \pi_1) \\
&\geq \langle \pi_2, u_1 \rangle, \quad \forall \pi_1, \pi_2 \in \mathcal{M}(X), \forall u_1 \in \partial\Omega(\pi_1).
\end{aligned} \tag{143}$$

The Fenchel-Young inequality is tight iff  $(\pi_2, u_1)$  are in dual correspondence.

### K.1.1 DUAL OF KL DIVERGENCE

The KL divergence from a reference measure  $m \in \mathcal{P}(X)$  is denoted by  $\Omega_m = D_{\text{KL}}[\cdot \| m] : \mathcal{M}(X) \rightarrow (-\infty, +\infty]$  and defined as

$$\Omega_m^*(\pi) = D_{\text{KL}}[\pi \| m] := \begin{cases} \langle \pi, \log \frac{d\pi}{dm} \rangle & \pi \ll m, \pi \in \mathcal{P}(X), \\ +\infty & \text{otherwise.} \end{cases} \quad (144)$$

The conjugate function of the KL divergence,  $\Omega_m^* : B(\Sigma) \rightarrow (-\infty, +\infty]$  is

$$\Omega_m^*(u) = \log \int e^u dm. \quad (145)$$

See Dembo & Zeitouni (2009, Lemma 6.2.13) or Rassoul-Agha & Seppäläinen (2015, Theorem 5.4) for proof. Furthermore, the pair of  $(\pi, u)$  are in dual correspondence if

$$\pi = \frac{me^u}{\int e^u dm} \iff u = \log \frac{d\pi}{dm} + c, \quad (146)$$

where  $c$  is an arbitrary constant.

Suppose  $\pi_1, \pi_2 \in \mathcal{M}(X)$ , and that  $(\pi_1, u_1)$  and  $(\pi_2, u_2)$  are in dual correspondence. Then, the Bregman divergence generated by the KL divergence is the KL divergence:

$$D_{D_{\text{KL}}[\cdot \| m]}^{u_1}(\pi_2, \pi_1) = \left\langle \pi_2, \log \frac{d\pi_2}{d\pi_1} \right\rangle \quad (147)$$

$$= D_{\text{KL}}[\pi_2 \| \pi_1]. \quad (148)$$

This Bregman divergence characterizes the gap of Fenchel-Young inequality as follows

$$\begin{aligned} D_{\text{KL}}[\pi_2 \| m] &= \langle \pi_2, u_1 \rangle - \log \int e^{u_1} dm + D_{\text{KL}}[\pi_2 \| \pi_1] \\ &\geq \langle \pi_2, u_1 \rangle - \log \int e^{u_1} dm. \end{aligned} \quad (149)$$

### K.1.2 DUAL OF GENERALIZED KL DIVERGENCE

The Generalized KL (GKL) divergence from a reference measure  $m \in \mathcal{M}_+(X)$ , is denoted by  $\Omega_m = D_{\text{GKL}}[\cdot \| m] : \mathcal{M}(X) \rightarrow (-\infty, +\infty]$ , and defined as

$$\Omega_m(\pi) = D_{\text{GKL}}[\pi \| m] := \begin{cases} \langle \pi, \log \frac{d\pi}{dm} \rangle - \pi(X) + m(X) & \pi \ll m, \pi \in \mathcal{M}_+(X), \\ +\infty & \text{otherwise.} \end{cases} \quad (150)$$

Note that unlike the KL divergence, the GKL divergence could output finite values for non-probability measures. However, for probability measures, it is equal to the KL divergence.

The conjugate function of the Generalized KL divergence,  $\Omega_m^* : B(\Sigma) \rightarrow (-\infty, +\infty]$  is

$$\Omega_m^*(u) = \int e^u dm - m(X). \quad (151)$$

See Polyanskiy & Wu (2022, Theorem 7.24) for proof. Furthermore, the pair of  $(\pi, u)$  are in dual correspondence if

$$d\pi = e^u dm \iff u = \log \frac{d\pi}{dm}. \quad (152)$$

Suppose  $\pi_1, \pi_2 \in \mathcal{M}(X)$ , and that  $(\pi_1, u_1)$  and  $(\pi_2, u_2)$  are in dual correspondence. Then, the Bregman divergence generated by the GKL divergence is the GKL divergence,

$$D_{D_{\text{GKL}}[\cdot \| m]}^{u_1}(\pi_2, \pi_1) = \left\langle \pi_2, \log \frac{d\pi_2}{d\pi_1} \right\rangle - \pi_2(X) + \pi_1(X) \quad (153)$$

$$= D_{\text{GKL}}[\pi_2 \| \pi_1]. \quad (154)$$

This Bregman divergence characterizes the gap of Fenchel-Young inequality as follows

$$\begin{aligned} D_{\text{GKL}}[\pi_2 \| m] &= \langle \pi_2, u_1 \rangle - \int e^{u_1} dm + m(X) + D_{\text{GKL}}[\pi_2 \| \pi_1] \\ &\geq \langle \pi_2, u_1 \rangle - \int e^{u_1} dm + m(X). \end{aligned} \quad (155)$$



## K.2 CONJUGATE DUALITY INTERPRETATION OF IBAL

To obtain an alternative derivation of  $\text{IBAL}(q_\theta, T_\phi)$ , we consider the *conditional* KL divergence function from a reference probability density  $q_\theta(\mathbf{z}|\mathbf{x})$  (with respect to the Lebesgue measure),

$$\Omega(\pi) = D_{\text{KL}}[\pi(\mathbf{z}|\mathbf{x})\|q_\theta(\mathbf{z}|\mathbf{x})], \quad (156)$$

which is a convex, lower semi-continuous function of  $\pi$ . To derive its conjugate  $\Omega^*(T)$ , note that our optimization is implicitly restricted to normalized distributions by the definition in Eq. (144)

$$\Omega^*(T) := \sup_{\pi(\mathbf{z}|\mathbf{x})} \int \pi(\mathbf{z}|\mathbf{x})T(\mathbf{x}, \mathbf{z})d\mathbf{z} - \Omega(\pi) = \log \int q_\theta(\mathbf{z}|\mathbf{x})e^{T(\mathbf{x}, \mathbf{z})} d\mathbf{z}. \quad (157)$$

As in Eq. (146), the dual correspondence between  $\pi_T$  and  $T_\pi$  is given by

$$\pi_T(\mathbf{z}|\mathbf{x}) = \frac{1}{\mathcal{Z}(\mathbf{x}; T)} q_\theta(\mathbf{z}|\mathbf{x})e^{T(\mathbf{x}, \mathbf{z})} \iff T_\pi(\mathbf{x}, \mathbf{z}) := \log \frac{\pi(\mathbf{z}|\mathbf{x})}{q_\theta(\mathbf{z}|\mathbf{x})} + c(\mathbf{x}), \quad (158)$$

where  $c(\mathbf{x})$  is an arbitrary constant function in  $\mathbf{x}$ .

We leverage this duality to estimate the KL divergence  $\Omega(p(\mathbf{z}|\mathbf{x})) = D_{\text{KL}}[p(\mathbf{z}|\mathbf{x})\|q_\theta(\mathbf{z}|\mathbf{x})]$  from  $q_\theta(\mathbf{z}|\mathbf{x})$  to the true posterior  $p(\mathbf{z}|\mathbf{x})$ . In particular, plugging into Eq. (141) for the (convex, lower-semicontinuous) KL divergence suggests the following variational representation

$$D_{\text{KL}}[p(\mathbf{z}|\mathbf{x})\|q_\theta(\mathbf{z}|\mathbf{x})] = \sup_{T(\mathbf{x}, \mathbf{z})} \int p(\mathbf{z}|\mathbf{x})T(\mathbf{x}, \mathbf{z})d\mathbf{z} - \log \int q_\theta(\mathbf{z}|\mathbf{x})e^{T(\mathbf{x}, \mathbf{z})} d\mathbf{z}. \quad (159)$$

For a suboptimal  $T_\pi(\mathbf{x}, \mathbf{z})$ , which is in dual correspondence with  $\pi_T(\mathbf{z}|\mathbf{x})$  instead of the desired posterior  $p(\mathbf{z}|\mathbf{x})$ , we can use Eq. (149) to obtain a lower bound on  $D_{\text{KL}}[p(\mathbf{z}|\mathbf{x})\|q_\theta(\mathbf{z}|\mathbf{x})]$ . To characterize the gap in this inequality, one can confirm using Eq. (147) that the Bregman divergence generated by the KL divergence is also the KL divergence  $D_{D_{\text{KL}}[\cdot\|\cdot]}[p, \pi] = D_{\text{KL}}[p\|\pi]$ . Thus, we have

$$D_{\text{KL}}[p(\mathbf{z}|\mathbf{x})\|q_\theta(\mathbf{z}|\mathbf{x})] = \int p(\mathbf{z}|\mathbf{x})T(\mathbf{x}, \mathbf{z})d\mathbf{z} - \log \mathbb{E}_{q_\theta(\mathbf{z}|\mathbf{x})} [e^{T(\mathbf{x}, \mathbf{z})}] + D_{\text{KL}}[p(\mathbf{z}|\mathbf{x})\|\pi_T(\mathbf{z}|\mathbf{x})]. \quad (160)$$

Finally, the  $\text{IBAL}(q_\theta, T_\phi)$  uses this variational representation of the gap in the BA lower bound,  $\mathbb{E}_{p(\mathbf{x})} [D_{\text{KL}}[p(\mathbf{z}|\mathbf{x})\|q_\theta(\mathbf{z}|\mathbf{x})]]$ , to obtain a tighter bound on MI. In particular, for any learned critic function  $T(\mathbf{x}, \mathbf{z})$ , we can use Eq. (160) to derive the IBAL and its gap,

$$\begin{aligned} I(\mathbf{x}; \mathbf{z}) &= \underbrace{\mathbb{E}_{p(\mathbf{x}, \mathbf{z})} \left[ \log \frac{q_\theta(\mathbf{z}|\mathbf{x})}{p(\mathbf{z})} \right]}_{\text{IBAL}(q_\theta)} + \mathbb{E}_{p(\mathbf{x})} [D_{\text{KL}}[p(\mathbf{z}|\mathbf{x})\|q_\theta(\mathbf{z}|\mathbf{x})]] \\ &= \underbrace{\mathbb{E}_{p(\mathbf{x}, \mathbf{z})} \left[ \log \frac{q_\theta(\mathbf{z}|\mathbf{x})}{p(\mathbf{z})} \right]}_{\text{IBAL}(q_\theta, T_\phi)} + \mathbb{E}_{p(\mathbf{x})} \left[ \mathbb{E}_{p(\mathbf{z}|\mathbf{x})} [T(\mathbf{x}, \mathbf{z})] - \log \mathbb{E}_{q_\theta(\mathbf{z}|\mathbf{x})} [e^{T(\mathbf{x}, \mathbf{z})}] \right] + \mathbb{E}_{p(\mathbf{x})} [D_{\text{KL}}[p(\mathbf{z}|\mathbf{x})\|\pi_T(\mathbf{z}|\mathbf{x})]]. \end{aligned} \quad (161)$$

The optimal critic function  $T^*(\mathbf{x}, \mathbf{z})$  provides the maximizing argument in Eq. (159) and is in dual correspondence with the true posterior  $p(\mathbf{z}|\mathbf{x})$ . In particular, we have  $\pi_{T^*}(\mathbf{z}|\mathbf{x}) = p(\mathbf{z}|\mathbf{x})$ , resulting in  $I(\mathbf{x}; \mathbf{z}) = \text{IBAL}(q_\theta, T^*)$ .

## K.3 CONJUGATE DUALITY INTERPRETATION OF GENERALIZED MINE-DV

To obtain a conjugate duality interpretation of (Generalized) MINE-DV, we consider the dual representation of the KL divergence over *joint* distributions. Choosing  $\pi_0(\mathbf{x}, \mathbf{z}) = p(\mathbf{x})q_\theta(\mathbf{z}|\mathbf{x})$  as the reference density, the KL divergence is a convex function of the first argument

$$\Omega(\pi) = D_{\text{KL}}[\pi(\mathbf{x}, \mathbf{z})\|p(\mathbf{x})q_\theta(\mathbf{z}|\mathbf{x})]. \quad (162)$$

This KL divergence matches the gap in the BA bound  $\mathbb{E}_{p(\mathbf{x})} [D_{\text{KL}}[p(\mathbf{z}|\mathbf{x})\|q_\theta(\mathbf{z}|\mathbf{x})]] = D_{\text{KL}}[p(\mathbf{x}, \mathbf{z})\|p(\mathbf{x})q_\theta(\mathbf{z}|\mathbf{x})]$  after noting the marginal distribution of both  $p(\mathbf{x}, \mathbf{z})$  and  $p(\mathbf{x})q_\theta(\mathbf{z}|\mathbf{x})$  is  $p(\mathbf{x})$ . However, the duality associated with  $\Omega(\cdot) = D_{\text{KL}}[\cdot\|\pi_0(\mathbf{x}, \mathbf{z})]$  holds for arbitrary joint distributions, and we will see that using this divergence leads to looser bound on MI than in App. K.2.

As in Eq. (145), the conjugate function is

$$\Omega^*(T) := \sup_{\pi(\mathbf{x}, \mathbf{z})} \int \pi(\mathbf{x}, \mathbf{z}) T(\mathbf{x}, \mathbf{z}) d\mathbf{x} d\mathbf{z} - \Omega(\pi(\mathbf{x}, \mathbf{z})) = \log \mathbb{E}_{p(\mathbf{x}) q_\theta(\mathbf{z}|\mathbf{x})} \left[ e^{T(\mathbf{x}, \mathbf{z})} \right], \quad (163)$$

where we have used  $p(\mathbf{x}) q_\theta(\mathbf{z}|\mathbf{x})$  as the reference density in the definition Eq. (144). Note that the expectation over  $p(\mathbf{x})$  now appears inside the log in  $\Omega^*(T)$ , compared with the conjugate for the conditional KL divergence in Eq. (157). We have the following dual correspondence

$$\pi_T(\mathbf{x}, \mathbf{z}) := \frac{1}{\mathcal{Z}(T)} p(\mathbf{x}) q_\theta(\mathbf{z}|\mathbf{x}) e^{T(\mathbf{x}, \mathbf{z})} \iff T_\pi(\mathbf{x}, \mathbf{z}) = \log \frac{\pi(\mathbf{x}, \mathbf{z})}{p(\mathbf{x}) q_\theta(\mathbf{z}|\mathbf{x})} + c, \quad (164)$$

where  $c$  is an arbitrary constant.

Finally, we use Eq. (141) to write the dual representation of joint KL divergence as

$$D_{\text{KL}}[p(\mathbf{x}, \mathbf{z}) \| p(\mathbf{x}) q_\theta(\mathbf{z}|\mathbf{x})] = \sup_{T(\mathbf{x}, \mathbf{z})} \int p(\mathbf{x}, \mathbf{z}) T(\mathbf{x}, \mathbf{z}) d\mathbf{x} d\mathbf{z} - \log \mathbb{E}_{p(\mathbf{x}) q_\theta(\mathbf{z}|\mathbf{x})} \left[ e^{T(\mathbf{x}, \mathbf{z})} \right]. \quad (165)$$

As in the previous section and Eq. (149), a suboptimal  $T(\mathbf{x}, \mathbf{z})$ , which is in dual correspondence with  $\pi_T(\mathbf{z}|\mathbf{x})$  instead of the desired posterior  $p(\mathbf{z}|\mathbf{x})$ , yields a lower bound on  $D_{\text{KL}}[p(\mathbf{x}, \mathbf{z}) \| p(\mathbf{x}) q_\theta(\mathbf{z}|\mathbf{x})]$ , with the gap equal to the Bregman divergence (or KL divergence)

$$D_{\text{KL}}[p(\mathbf{x}, \mathbf{z}) \| p(\mathbf{x}) q_\theta(\mathbf{z}|\mathbf{x})] = \int p(\mathbf{x}, \mathbf{z}) T(\mathbf{x}, \mathbf{z}) d\mathbf{x} d\mathbf{z} - \log \mathbb{E}_{p(\mathbf{x}) q_\theta(\mathbf{z}|\mathbf{x})} \left[ e^{T(\mathbf{x}, \mathbf{z})} \right] + D_{\text{KL}}[p(\mathbf{x}, \mathbf{z}) \| \pi_T(\mathbf{x}, \mathbf{z})]. \quad (166)$$

The Generalized MINE-DV bound  $I_{\text{GMINE-DV}}(q_\theta, T_\phi)$  uses this variational representation of the gap in the BA lower bound to obtain a tighter bound on MI. For a learned critic  $T(\mathbf{x}, \mathbf{z})$ , we can use Eq. (166) to write

$$\begin{aligned} I(\mathbf{x}; \mathbf{z}) &= \underbrace{\mathbb{E}_{p(\mathbf{x}, \mathbf{z})} \left[ \log \frac{q_\theta(\mathbf{z}|\mathbf{x})}{p(\mathbf{z})} \right]}_{I_{\text{BAL}}(q_\theta)} + \mathbb{E}_{p(\mathbf{x})} [D_{\text{KL}}[p(\mathbf{z}|\mathbf{x}) \| q_\theta(\mathbf{z}|\mathbf{x})]] \\ &= \underbrace{\mathbb{E}_{p(\mathbf{x}, \mathbf{z})} \left[ \log \frac{q_\theta(\mathbf{z}|\mathbf{x})}{p(\mathbf{z})} \right] + \mathbb{E}_{p(\mathbf{x}) p(\mathbf{z}|\mathbf{x})} [T(\mathbf{x}, \mathbf{z}) - \log \mathbb{E}_{p(\mathbf{x}) q_\theta(\mathbf{z}|\mathbf{x})} \left[ e^{T(\mathbf{x}, \mathbf{z})} \right]]}_{I_{\text{GMINE-DV}}(q_\theta, T_\phi)} + D_{\text{KL}}[p(\mathbf{x}) p(\mathbf{z}|\mathbf{x}) \| \pi_T(\mathbf{x}, \mathbf{z})] \end{aligned} \quad (167)$$

As noted in App. J.2, the Generalized MINE-DV bound is looser than the IBAL.

#### K.4 CONJUGATE DUALITY INTERPRETATION OF GENERALIZED MINE-F

Nguyen et al. (2010) consider the conjugate duality associated with the family of  $f$ -divergences, of which the KL divergence is a special case. We will show that this dual representation corresponds to taking the conjugate function of the Generalized KL divergence, which can take unnormalized densities as input (see the definition in Eq. (150)),

$$\Omega(\tilde{\pi}) = D_{\text{GKL}}[\tilde{\pi}(\mathbf{z}|\mathbf{x}) \| \tilde{q}_\theta(\mathbf{z}|\mathbf{x})]. \quad (168)$$

To calculate the conjugate, we do not need to restrict to normalized distributions and obtain, as in Eq. (151),

$$\begin{aligned} \Omega^*(T') &:= \sup_{\tilde{\pi}(\mathbf{z}|\mathbf{x})} \int \tilde{\pi}(\mathbf{z}|\mathbf{x}) T'(\mathbf{x}, \mathbf{z}) d\mathbf{z} - D_{\text{GKL}}[\tilde{\pi}(\mathbf{z}|\mathbf{x}) \| \tilde{q}_\theta(\mathbf{z}|\mathbf{x})] \\ &= \int \tilde{q}_\theta(\mathbf{z}|\mathbf{x}) e^{T'(\mathbf{x}, \mathbf{z})} d\mathbf{z} - \int \tilde{q}_\theta(\mathbf{z}|\mathbf{x}) d\mathbf{z} \end{aligned} \quad (169)$$

Solving for the optimizing argument or writing the dual correspondence in Eq. (152), we obtain

$$\tilde{\pi}_{T'}(\mathbf{z}|\mathbf{x}) = \tilde{q}_\theta(\mathbf{z}|\mathbf{x}) e^{T'(\mathbf{x}, \mathbf{z})} \iff T'_\pi(\mathbf{x}, \mathbf{z}) = \log \frac{\tilde{\pi}(\mathbf{z}|\mathbf{x})}{\tilde{q}_\theta(\mathbf{z}|\mathbf{x})}. \quad (170)$$

The dual representation of the Generalized KL divergence now matches Nguyen et al. (2010),

$$D_{\text{GKL}}[\tilde{p}(\mathbf{z}|\mathbf{x}) \| \tilde{q}(\mathbf{z}|\mathbf{x})] = \sup_{T'(\mathbf{x}, \mathbf{z})} \int \tilde{p}(\mathbf{z}|\mathbf{x}) T'(\mathbf{x}, \mathbf{z}) d\mathbf{z} - \int \tilde{q}(\mathbf{z}|\mathbf{x}) e^{T'(\mathbf{x}, \mathbf{z})} d\mathbf{z} + \int \tilde{q}(\mathbf{z}|\mathbf{x}) d\mathbf{z}. \quad (171)$$

We now consider the reparameterization  $T'(\mathbf{x}, \mathbf{z}) = T(\mathbf{x}, \mathbf{z}) - 1$ . Assuming a normalized  $\tilde{q}(\mathbf{z}|\mathbf{x}) = q(\mathbf{z}|\mathbf{x})$  and  $\tilde{p}(\mathbf{z}|\mathbf{x}) = p(\mathbf{z}|\mathbf{x})$ , and noting that  $D_{\text{GKL}}[p(\mathbf{z}|\mathbf{x})\|q_\theta(\mathbf{z}|\mathbf{x})] = D_{\text{KL}}[p(\mathbf{z}|\mathbf{x})\|q_\theta(\mathbf{z}|\mathbf{x})]$  for normalized distributions, we obtain

$$D_{\text{KL}}[p(\mathbf{z}|\mathbf{x})\|q_\theta(\mathbf{z}|\mathbf{x})] = \sup_{T(\mathbf{x}, \mathbf{z})} \int p(\mathbf{z}|\mathbf{x})T(\mathbf{x}, \mathbf{z})d\mathbf{z} - \int q_\theta(\mathbf{z}|\mathbf{x})e^{T(\mathbf{x}, \mathbf{z})-1}d\mathbf{z}, \quad (172)$$

which matches dual representation of the KL divergence found in [Belghazi et al. \(2018\)](#); [Nowozin et al. \(2016\)](#).

For a suboptimal  $T_\pi(\mathbf{x}, \mathbf{z})$  which is in dual correspondence with  $\pi_T(\mathbf{z}|\mathbf{x})$  instead of the desired posterior  $p(\mathbf{z}|\mathbf{x})$ , we can use [Eq. \(155\)](#) to obtain a lower bound on  $D_{\text{GKL}}[p(\mathbf{z}|\mathbf{x})\|q_\theta(\mathbf{z}|\mathbf{x})] = D_{\text{KL}}[p(\mathbf{z}|\mathbf{x})\|q_\theta(\mathbf{z}|\mathbf{x})]$ . To characterize the gap of this lower bound, note from [Eq. \(153\)](#) that the Bregman divergence generated by the Generalized KL divergence is also the Generalized KL divergence  $D_{D_{\text{GKL}}[\cdot|\tilde{q}]}[\tilde{p}|\tilde{\pi}] = D_{\text{GKL}}[\tilde{p}|\tilde{\pi}]$ . Thus, we have

$$D_{\text{KL}}[p(\mathbf{z}|\mathbf{x})\|q_\theta(\mathbf{z}|\mathbf{x})] = \int p(\mathbf{z}|\mathbf{x})T(\mathbf{x}, \mathbf{z})d\mathbf{z} - \int q_\theta(\mathbf{z}|\mathbf{x})e^{T(\mathbf{x}, \mathbf{z})-1}d\mathbf{z} + D_{\text{GKL}}[p(\mathbf{z}|\mathbf{x})\|q_\theta(\mathbf{z}|\mathbf{x})e^{T(\mathbf{x}, \mathbf{z})-1}]. \quad (173)$$

Finally, we obtain the Generalized MINE-F bound by evaluating the dual representation of the Generalized KL divergence for normalized  $p(\mathbf{z}|\mathbf{x})$  and  $q_\theta(\mathbf{z}|\mathbf{x})$ . In particular,  $I_{\text{GMINE-F}}(q_\theta, T_\phi)$  uses the critic function  $T_\phi$  to tighten the gap in  $I_{\text{BAL}}(q_\theta)$  via the dual optimization in [Eq. \(173\)](#),

$$\begin{aligned} I(\mathbf{x}; \mathbf{z}) &= \underbrace{\mathbb{E}_{p(\mathbf{x}, \mathbf{z})} \left[ \log \frac{q_\theta(\mathbf{z}|\mathbf{x})}{p(\mathbf{z})} \right]}_{I_{\text{BAL}}(q_\theta)} + \mathbb{E}_{p(\mathbf{x})} [D_{\text{KL}}[p(\mathbf{z}|\mathbf{x})\|q_\theta(\mathbf{z}|\mathbf{x})]] \quad (174) \\ &= \underbrace{\mathbb{E}_{p(\mathbf{x}, \mathbf{z})} \left[ \log \frac{q_\theta(\mathbf{z}|\mathbf{x})}{p(\mathbf{z})} \right] + \mathbb{E}_{p(\mathbf{x})} \left[ \mathbb{E}_{p(\mathbf{z}|\mathbf{x})} [T(\mathbf{x}, \mathbf{z})] - \mathbb{E}_{q_\theta(\mathbf{z}|\mathbf{x})} [e^{T(\mathbf{x}, \mathbf{z})-1}] \right]}_{I_{\text{GMINE-F}}(q_\theta, T_\phi)} + \mathbb{E}_{p(\mathbf{x})} [D_{\text{GKL}}[p(\mathbf{z}|\mathbf{x})\|\tilde{\pi}_{T-1}(\mathbf{z}|\mathbf{x})]]. \end{aligned} \quad (175)$$

The optimal critic function is the dual variable of the true posterior  $p(\mathbf{z}|\mathbf{x})$ , which can be found using [Eq. \(170\)](#) as  $T(\mathbf{x}, \mathbf{z}) = 1 + \log \frac{p(\mathbf{z}|\mathbf{x})}{q_\theta(\mathbf{z}|\mathbf{x})}$ . With this optimal critic, the Generalized MINE-F bound is tight.

## K.5 CONJUGATE DUALITY INTERPRETATION OF GIWAE, IWAE, AND INFONCE

In this section, we use conjugate duality to derive the GIWAE, IWAE, and INFO-NCE bounds on mutual information and characterize their gaps. Our approach extends that of [Poole et al. \(2019\)](#), where the MINE-F dual representation ([App. K.4](#)) was used to derive INFO-NCE. We provide an alternative derivation using the dual representation associated with the conditional KL divergence and IBAL in [App. K.2](#). For either dual representation, GIWAE, IWAE, and INFO-NCE arise from limiting the family of the critic functions  $T_\phi$  in order to eliminate the intractable log partition function term.

We start from the decomposition of  $I(\mathbf{x}; \mathbf{z})$  into  $I_{\text{BAL}}(q_\theta)$  and its gap

$$I(\mathbf{x}; \mathbf{z}) = \underbrace{\mathbb{E}_{p(\mathbf{x}, \mathbf{z})} \left[ \log \frac{q_\theta(\mathbf{z}|\mathbf{x})}{p(\mathbf{z})} \right]}_{I_{\text{BAL}}(q_\theta)} + \mathbb{E}_{p(\mathbf{x})} [D_{\text{KL}}[p(\mathbf{z}|\mathbf{x})\|q_\theta(\mathbf{z}|\mathbf{x})]]. \quad (176)$$

We will focus on the dual representation of the normalized, conditional KL divergence  $\Omega(\cdot) = D_{\text{KL}}[\cdot\|q_\theta(\mathbf{z}|\mathbf{x})]$ , as in [App. K.2](#).

**Multi-Sample IBAL** Consider extending the state space of the posterior or target distribution  $p(\mathbf{z}|\mathbf{x})$ , by using an additional  $K - 1$  samples from a base variational distribution  $q_\theta(\mathbf{z}|\mathbf{x})$  to construct

$$p_{\text{TGT}}(\mathbf{z}^{(1:K)}, s|\mathbf{x}) := \mathcal{U}(s)p(\mathbf{z}^{(s)}|\mathbf{x}) \prod_{\substack{k=1 \\ k \neq s}}^K q_\theta(\mathbf{z}^{(k)}|\mathbf{x}), \quad (177)$$

where  $s$  is an index variable  $s \sim \mathcal{U}(s)$  drawn uniformly at random from  $1 \leq s \leq K$ , which specifies the index of the posterior sample  $p(\mathbf{z}|\mathbf{x})$ . We similarly expand the state space of the base variational distribution to write

$$q_{\text{PROP}}(\mathbf{z}^{(1:K)}, s|\mathbf{x}) := \mathcal{U}(s) \prod_{k=1}^K q_{\theta}(\mathbf{z}^{(k)}|\mathbf{x}). \quad (178)$$

It can be easily verified that this construction does not change the value of the KL divergence

$$\begin{aligned} D_{\text{KL}}[p_{\text{TGT}}(\mathbf{z}^{(1:K)}, s|\mathbf{x}) \| q_{\text{PROP}}(\mathbf{z}^{(1:K)}, s|\mathbf{x})] &= \mathbb{E}_{p_{\text{TGT}}(\mathbf{z}^{(1:K)}, s|\mathbf{x})} \left[ \log \frac{p_{\text{TGT}}(\mathbf{z}^{(1:K)}, s|\mathbf{x})}{q_{\text{PROP}}(\mathbf{z}^{(1:K)}, s|\mathbf{x})} \right] \\ &= \mathbb{E}_{p_{\text{TGT}}(\mathbf{z}^{(1:K)}, s|\mathbf{x})} \left[ \log \frac{\mathcal{U}(s)p(\mathbf{z}^{(s)}|\mathbf{x}) \prod_{k \neq s} q_{\theta}(\mathbf{z}^{(k)}|\mathbf{x})}{\mathcal{U}(s) \prod_{k=1}^K q_{\theta}(\mathbf{z}^{(k)}|\mathbf{x})} \right] \\ &= \mathbb{E}_{\mathcal{U}(s)p(\mathbf{z}^{(s)}|\mathbf{x})} \left[ \log \frac{p(\mathbf{z}^{(s)}|\mathbf{x})}{q_{\theta}(\mathbf{z}^{(s)}|\mathbf{x})} \right] \\ &= \mathbb{E}_{p(\mathbf{z}|\mathbf{x})} \left[ \log \frac{p(\mathbf{z}|\mathbf{x})}{q_{\theta}(\mathbf{z}|\mathbf{x})} \right] \\ &= D_{\text{KL}}[p(\mathbf{z}|\mathbf{x}) \| q_{\theta}(\mathbf{z}|\mathbf{x})]. \end{aligned}$$

Consider the convex function

$$\Omega(\cdot) := D_{\text{KL}}[\cdot \| q_{\text{PROP}}(\mathbf{z}^{(1:K)}, s|\mathbf{x})], \quad (179)$$

where the primal variable is a distribution in the extended-state space of  $(\mathbf{z}^{(1:K)}, s)$ , and the dual variable is a critic function  $\mathcal{T}(\mathbf{x}, \mathbf{z}^{(1:K)}, s)$ . We derive a conjugate optimization in similar fashion to [App. K.2](#), but now over the extended state space. For this  $\Omega(\cdot)$ , the conjugate function  $\Omega^*(\mathcal{T})$  takes a log-mean-exp form analogous to [Eq. \(145\)](#)<sup>4</sup>. We can write the variational representation of  $\Omega(p_{\text{TGT}})$  as

$$\Omega(p_{\text{TGT}}) = \sup_{\mathcal{T}} \int \sum_{s=1}^K p_{\text{TGT}}(\mathbf{z}^{(1:K)}, s|\mathbf{x}) \mathcal{T}(\mathbf{x}, \mathbf{z}^{(1:K)}, s) d\mathbf{z}^{(1:K)} - \log \mathbb{E}_{q_{\text{PROP}}(\mathbf{z}^{(1:K)}, s|\mathbf{x})} \left[ e^{\mathcal{T}(\mathbf{x}, \mathbf{z}^{(1:K)}, s)} \right]. \quad (180)$$

For a particular choice of  $\mathcal{T}(\mathbf{x}, \mathbf{z}^{(1:K)}, s)$ , we can use [Eq. \(180\)](#) to obtain a lower bound on the KL divergence  $D_{\text{KL}}[p(\mathbf{z}|\mathbf{x}) \| q_{\theta}(\mathbf{z}|\mathbf{x})]$  (as in [Eq. \(149\)](#)). This lower bound translates to the *Multi-Sample* IBAL lower bound on MI,  $I_{\text{MS-IBAL}}(q_{\theta}, \mathcal{T})$  via [Eq. \(176\)](#).

$$\begin{aligned} I(\mathbf{x}; \mathbf{z}) &\geq \mathbb{E}_{p(\mathbf{x}, \mathbf{z})} \left[ \log \frac{q_{\theta}(\mathbf{z}|\mathbf{x})}{p(\mathbf{z})} \right] + \mathbb{E}_{p(\mathbf{x})} \left[ \mathbb{E}_{p_{\text{TGT}}(\mathbf{z}^{(1:K)}, s|\mathbf{x})} [\mathcal{T}(\mathbf{x}, \mathbf{z}^{(1:K)}, s)] - \log \underbrace{\mathbb{E}_{q_{\text{PROP}}(\mathbf{z}^{(1:K)}, s|\mathbf{x})} [e^{\mathcal{T}(\mathbf{x}, \mathbf{z}^{(1:K)}, s)}]}_{\mathcal{Z}(\mathbf{x}; \mathcal{T})} \right] \\ &=: I_{\text{MS-IBAL}}(q_{\theta}, \mathcal{T}), \end{aligned} \quad (181)$$

where  $\mathcal{Z}(\mathbf{x}; \mathcal{T})$  is the normalization constant of the dual distribution  $\pi_{\mathcal{T}}(\mathbf{z}^{(1:K)}, s|\mathbf{x})$  corresponding to  $\mathcal{T}$ ,

$$\pi_{\mathcal{T}}(\mathbf{z}^{(1:K)}, s|\mathbf{x}) = \frac{1}{\mathcal{Z}(\mathbf{x}; \mathcal{T})} q_{\text{PROP}}(\mathbf{z}^{(1:K)}, s|\mathbf{x}) e^{\mathcal{T}(\mathbf{x}, \mathbf{z}^{(1:K)}, s)}. \quad (182)$$

As in [Eq. \(149\)](#), we can write the gap of  $I_{\text{MS-IBAL}}(q_{\theta}, \mathcal{T})$  as a Bregman divergence or KL divergence

$$I(\mathbf{x}; \mathbf{z}) = I_{\text{MS-IBAL}}(q_{\theta}, \mathcal{T}) + \mathbb{E}_{p(\mathbf{x})} \left[ D_{\text{KL}}[p_{\text{TGT}}(\mathbf{z}^{(1:K)}, s|\mathbf{x}) \| \pi_{\mathcal{T}}(\mathbf{z}^{(1:K)}, s|\mathbf{x})] \right]. \quad (183)$$

The optimal  $K$ -sample energy function in [Eq. \(180\)](#) should result in  $\pi_{\mathcal{T}^*}(\mathbf{z}^{(1:K)}, s|\mathbf{x}) = p_{\text{TGT}}(\mathbf{z}^{(1:K)}, s|\mathbf{x})$ . Using similar reasoning as in [App. C.5](#) or [App. L.1](#), this occurs for  $\mathcal{T}^*(\mathbf{x}, \mathbf{z}^{(1:K)}, s) = \log \frac{p(\mathbf{z}^{(s)}|\mathbf{x})}{q_{\theta}(\mathbf{z}^{(s)}|\mathbf{x})} + c(\mathbf{x})$ , for which we have  $I(\mathbf{x}; \mathbf{z}) = I_{\text{MS-IBAL}}(q_{\theta}, \mathcal{T}^*)$ .

<sup>4</sup>We consider the conjugate with restriction to normalized distributions as in [App. K.1.1](#).

**GIWAE is a Multi-Sample IBAL with a Restricted Function Family** Although extending the state space did not change the value of the KL divergence or alter the optimal critic function, it does allow us to consider a restricted class of multi-sample energy functions that yield tractable, low variance estimators. In particular, GIWAE and INFO-NCE arise from choosing a restricted family of functions  $\mathcal{T}_{\text{GIWAE}}(\mathbf{x}, \mathbf{z}^{(1:K)}, s)$ , under which the problematic  $\log \mathcal{Z}(\mathbf{x}; \mathcal{T})$  term evaluates to 0. This function family is defined as

$$\mathcal{T}_{\text{GIWAE}}(\mathbf{x}, \mathbf{z}^{(1:K)}, s) := \log \frac{e^{T_\phi(\mathbf{x}, \mathbf{z}^{(s)})}}{\frac{1}{K} \sum_{k=1}^K e^{T_\phi(\mathbf{x}, \mathbf{z}^{(k)})}}, \quad (184)$$

where  $\mathcal{T}_{\text{GIWAE}}(\mathbf{x}, \mathbf{z}^{(1:K)}, s)$  is specified by an arbitrary single-sample critic function  $T_\phi(\mathbf{x}, \mathbf{z})$ . We can now see that  $\log \mathcal{Z}(\mathbf{x}; \mathcal{T}_{\text{GIWAE}}) = 0$ ,

$$\log \mathcal{Z}(\mathbf{x}; \mathcal{T}_{\text{GIWAE}}) = \log \mathbb{E}_{q_{\text{PROP}}(\mathbf{z}^{(1:K)}, s | \mathbf{x})} \left[ e^{\mathcal{T}_{\text{GIWAE}}(\mathbf{x}, \mathbf{z}^{(1:K)}, s)} \right] = \log \mathbb{E}_{\mathcal{U}(s) \prod_{k=1}^K q_\theta(\mathbf{z}^{(k)} | \mathbf{x})} \left[ \frac{e^{T_\phi(\mathbf{x}, \mathbf{z}^{(s)})}}{\frac{1}{K} \sum_{k=1}^K e^{T_\phi(\mathbf{x}, \mathbf{z}^{(k)})}} \right] = 0,$$

using the fact that  $\mathbf{z}^{(1:K)} \sim \prod_{k=1}^K q_\theta(\mathbf{z}^{(k)} | \mathbf{x})$  is invariant to re-indexing. With this simplification,  $I_{\text{MS-IBAL}}(q_\theta, \mathcal{T}_{\text{GIWAE}})$  recovers the GIWAE lower bound on MI

$$I(\mathbf{x}; \mathbf{z}) \geq I_{\text{MS-IBAL}}(q_\theta, \mathcal{T}_{\text{GIWAE}}) \quad (185)$$

$$= \mathbb{E}_{p(\mathbf{x}, \mathbf{z})} \left[ \log \frac{q_\theta(\mathbf{z} | \mathbf{x})}{p(\mathbf{z})} \right] + \mathbb{E}_{\frac{1}{K} p(\mathbf{x}) p(\mathbf{z}^{(s)} | \mathbf{x}) \prod_{\substack{k \neq s \\ k=1}}^K q_\theta(\mathbf{z}^{(k)} | \mathbf{x})} \left[ \log \frac{e^{T_\phi(\mathbf{x}, \mathbf{z}^{(s)})}}{\frac{1}{K} \sum_{k=1}^K e^{T_\phi(\mathbf{x}, \mathbf{z}^{(k)})}} \right] \quad (186)$$

$$= \mathbb{E}_{p(\mathbf{x}, \mathbf{z})} \left[ \log \frac{q_\theta(\mathbf{z} | \mathbf{x})}{p(\mathbf{z})} \right] + \mathbb{E}_{p(\mathbf{x}) p(\mathbf{z}^{(1)} | \mathbf{x}) \prod_{k=2}^K q_\theta(\mathbf{z}^{(k)} | \mathbf{x})} \left[ \log \frac{e^{T_\phi(\mathbf{x}, \mathbf{z}^{(1)})}}{\frac{1}{K} \sum_{k=1}^K e^{T_\phi(\mathbf{x}, \mathbf{z}^{(k)})}} \right] \quad (187)$$

$$= I_{\text{GIWAE}}(q_\theta, T_\phi, K).$$

Finally, we can use [Eq. \(183\)](#) to recover the probabilistic interpretation of GIWAE and the gap in the lower bound on MI. As we saw above, the dual distribution  $\pi_{\mathcal{T}_{\text{GIWAE}}}(\mathbf{z}^{(1:K)}, s | \mathbf{x})$  is normalized with  $\mathcal{Z}(\mathbf{x}; \mathcal{T}_{\text{GIWAE}}) = 1$ . In particular, we can write

$$\pi_{\mathcal{T}_{\text{GIWAE}}}(\mathbf{z}^{(1:K)}, s | \mathbf{x}) = \frac{1}{\mathcal{Z}(\mathbf{x}; \mathcal{T}_{\text{GIWAE}})} q_{\text{PROP}}(\mathbf{z}^{(1:K)}, s | \mathbf{x}) e^{\mathcal{T}_{\text{GIWAE}}(\mathbf{x}, \mathbf{z}^{(1:K)}, s)} \quad (188)$$

$$= \frac{1}{\mathcal{Z}(\mathbf{x}; \mathcal{T}_{\text{GIWAE}})} \mathcal{U}(s) \prod_{k=1}^K q_\theta(\mathbf{z}^{(k)} | \mathbf{x}) \frac{e^{T_\phi(\mathbf{x}, \mathbf{z}^{(s)})}}{\frac{1}{K} \sum_{k=1}^K e^{T_\phi(\mathbf{x}, \mathbf{z}^{(k)})}} \quad (189)$$

$$= \prod_{k=1}^K q_\theta(\mathbf{z}^{(k)} | \mathbf{x}) \frac{e^{T_\phi(\mathbf{x}, \mathbf{z}^{(s)})}}{\sum_{k=1}^K e^{T_\phi(\mathbf{x}, \mathbf{z}^{(k)})}} \quad (190)$$

which recovers  $q_{\text{PROP}}^{\text{GIWAE}}(\mathbf{z}^{(1:K)}, s | \mathbf{x})$  from the probabilistic interpretation of GIWAE in [Eq. \(52\)](#) or [App. C.1](#). We can write the gap of  $I_{\text{GIWAE}}(q_\theta, T_\phi, K) = I_{\text{MS-IBAL}}(q_\theta, \mathcal{T}_{\text{GIWAE}})$  as the Bregman divergence or KL divergence as in [Eq. \(149\)](#)

$$I(\mathbf{x}; \mathbf{z}) = I_{\text{MS-IBAL}}(q_\theta, \mathcal{T}_{\text{GIWAE}}) + \mathbb{E}_{p(\mathbf{x})} \left[ D_{\text{KL}} \left[ p_{\text{TGT}}(\mathbf{z}^{(1:K)}, s | \mathbf{x}) \| \pi_{\mathcal{T}_{\text{GIWAE}}}(\mathbf{z}^{(1:K)}, s | \mathbf{x}) \right] \right], \quad (191)$$

which matches the reverse KL divergence  $\mathbb{E}_{p(\mathbf{x})} \left[ D_{\text{KL}} \left[ p_{\text{TGT}}^{\text{GIWAE}}(\mathbf{z}^{(1:K)}, s | \mathbf{x}) \| q_{\text{PROP}}^{\text{GIWAE}}(\mathbf{z}^{(1:K)}, s | \mathbf{x}) \right] \right]$  derived from the probabilistic approach in [App. C.1](#). Recall that INFO-NCE is a special case of GIWAE with  $q_\theta(\mathbf{z} | \mathbf{x}) = p(\mathbf{z})$  ([Sec. 2.4](#)).

**Conjugate Duality Interpretation of IWAE** We can gain alternative perspective on IWAE from this conjugate duality interpretation. In particular, IWAE is a special case of GIWAE, where the optimal single-sample critic function  $T^*(\mathbf{x}, \mathbf{z}) = \log \frac{p(\mathbf{x}, \mathbf{z})}{q_\theta(\mathbf{z}|\mathbf{x})} + c(\mathbf{x})$  (see Sec. 2.4) is used in Eq. (184) to construct the optimal multi-sample function  $\mathcal{T}_{\text{IWAE}}$  from within the GIWAE restricted multi-sample function family. Thus, we have  $I_{\text{MS-IBAL}}(q_\theta, \mathcal{T}_{\text{IWAE}}) = I_{\text{IWAE}}(q_\theta, K)$ .

Although IWAE uses the optimal critic function, the restriction to the function family in Eq. (184) is necessary to obtain a tractable bound on the KL divergence  $D_{\text{KL}}[p(\mathbf{z}|\mathbf{x})\|q_\theta(\mathbf{z}|\mathbf{x})]$  and mutual information. Without the restricted function family, the intractable log partition term in Eq. (180) would require MCMC methods such as AIS for accurate estimation, as we saw for the single-sample IBAL in Sec. 4.

## L PROPERTIES OF THE IBAL

Our MINE-AIS method in Sec. 4 and App. M optimizes the *Implicit Barber Agakov* lower bound (IBAL) on MI from Eq. (27). We first recall the probabilistic interpretation of the IBAL bound from App. J.1. For a posterior approximation with a learned negative energy function  $T_\phi$  and base variational distribution  $q_\theta(\mathbf{z}|\mathbf{x})$ ,

$$\pi_{\theta, \phi}(\mathbf{z}|\mathbf{x}) = \frac{1}{\mathcal{Z}_{\theta, \phi}(\mathbf{x})} q_\theta(\mathbf{z}|\mathbf{x}) e^{T_\phi(\mathbf{x}, \mathbf{z})}, \quad \text{where } \mathcal{Z}_{\theta, \phi}(\mathbf{x}) = \mathbb{E}_{q_\theta(\mathbf{z}|\mathbf{x})} \left[ e^{T_\phi(\mathbf{x}, \mathbf{z})} \right], \quad (192)$$

we consider the BA lower bound on MI,

$$I(\mathbf{x}, \mathbf{z}) \geq I_{\text{BAL}}(\pi_{\theta, \phi}) \quad (193)$$

$$= I(\mathbf{x}, \mathbf{z}) - \mathbb{E}_{p(\mathbf{x})} [D_{\text{KL}}[p(\mathbf{z}|\mathbf{x})\|\pi_{\theta, \phi}(\mathbf{z}|\mathbf{x})]] \quad (194)$$

$$= \underbrace{\mathbb{E}_{p(\mathbf{x}, \mathbf{z})} \left[ \log \frac{q_\theta(\mathbf{z}|\mathbf{x})}{p(\mathbf{z})} \right]}_{I_{\text{BAL}}(q_\theta)} + \underbrace{\mathbb{E}_{p(\mathbf{x}, \mathbf{z})} \left[ \log \frac{e^{T_\phi(\mathbf{x}, \mathbf{z})}}{\mathbb{E}_{q_\theta(\mathbf{z}|\mathbf{x})} [e^{T_\phi(\mathbf{x}, \mathbf{z})}]} \right]}_{\text{contrastive term}} \quad (195)$$

$$=: \text{IBAL}(q_\theta, T_\phi). \quad (196)$$

The gap of this lower bound on mutual information is  $\mathbb{E}_{p(\mathbf{x})} [D_{\text{KL}}[p(\mathbf{z}|\mathbf{x})\|\pi_{\theta, \phi}(\mathbf{z}|\mathbf{x})]]$ , as in Sec. 2.2.

### L.1 PROOFS FOR IBAL OPTIMAL CRITIC FUNCTION (PROP. 4.1 AND L.1)

**Proposition 4.1.** *For a given  $q_\theta(\mathbf{z}|\mathbf{x})$ , the optimal IBAL critic function equals the log importance weights up to a constant  $T^*(\mathbf{x}, \mathbf{z}) = \log \frac{p(\mathbf{x}, \mathbf{z})}{q_\theta(\mathbf{z}|\mathbf{x})} + c(\mathbf{x})$ . For this  $T^*$ , we have  $\text{IBAL}(q_\theta, T^*) = I(\mathbf{x}; \mathbf{z})$ .*

*Proof.* Recall that the gap in  $\text{IBAL}(q_\theta, T_{\phi^*})$  is  $\mathbb{E}_{p(\mathbf{x})} [D_{\text{KL}}[p(\mathbf{z}|\mathbf{x})\|\pi_{\theta, \phi}(\mathbf{z}|\mathbf{x})]] = I(\mathbf{x}; \mathbf{z}) - \text{IBAL}(q_\theta, T_{\phi^*})$ . This implies that the bound will be tight iff  $p(\mathbf{z}|\mathbf{x}) = \pi_{\theta, \phi}(\mathbf{z}|\mathbf{x}) \propto p(\mathbf{x}, \mathbf{z})$ . We can easily show that the true log importance weights (plus a constant) satisfy this property

$$\pi_{\theta, \phi}(\mathbf{z}|\mathbf{x}) = \frac{1}{\mathcal{Z}_{\theta, \phi}(\mathbf{x})} q_\theta(\mathbf{z}|\mathbf{x}) e^{\log \frac{p(\mathbf{x}, \mathbf{z})}{q_\theta(\mathbf{z}|\mathbf{x})} + c(\mathbf{x})} = \frac{e^{c(\mathbf{x})}}{\mathcal{Z}_{\theta, \phi}(\mathbf{x})} p(\mathbf{x}, \mathbf{z}) = p(\mathbf{z}|\mathbf{x}), \quad (197)$$

where  $e^{c(\mathbf{x})}$  is absorbed into the normalization constant. Conversely, using  $g(\mathbf{x}, \mathbf{z})$  which depends on  $\mathbf{z}$  in  $T(\mathbf{x}, \mathbf{z}) = \log \frac{p(\mathbf{x}, \mathbf{z})}{q_\theta(\mathbf{z}|\mathbf{x})} + g(\mathbf{x}, \mathbf{z})$  would change the density over  $\mathbf{z}$  to no longer match  $p(\mathbf{z}|\mathbf{x})$ .

At this value, the IBAL is exactly equal to  $I(\mathbf{x}; \mathbf{z})$

$$\begin{aligned} \text{IBAL}(q_\theta, T^*) &= \mathbb{E}_{p(\mathbf{x}, \mathbf{z})} \left[ \log \frac{q_\theta(\mathbf{z}|\mathbf{x})}{p(\mathbf{z})} \right] + \mathbb{E}_{p(\mathbf{x}, \mathbf{z})} [T_\phi(\mathbf{x}, \mathbf{z})] - \mathbb{E}_{p(\mathbf{x})} [\log \mathcal{Z}_{\theta, \phi}(\mathbf{x})] \\ &= \mathbb{E}_{p(\mathbf{x}, \mathbf{z})} \left[ \log \frac{q_\theta(\mathbf{z}|\mathbf{x})}{p(\mathbf{z})} \right] + \mathbb{E}_{p(\mathbf{x}, \mathbf{z})} \left[ \log \frac{p(\mathbf{x}, \mathbf{z})}{q_\theta(\mathbf{z}|\mathbf{x})} + \log c(\mathbf{x}) \right] - \mathbb{E}_{p(\mathbf{x})} \left[ \log \mathbb{E}_{q_\theta(\mathbf{z}|\mathbf{x})} \frac{p(\mathbf{x}, \mathbf{z})}{q_\theta(\mathbf{z}|\mathbf{x})} + \log c(\mathbf{x}) \right] \\ &= \mathbb{E}_{p(\mathbf{x}, \mathbf{z})} \left[ \log \frac{p(\mathbf{x}, \mathbf{z})}{p(\mathbf{z})p(\mathbf{x})} \right] = I(\mathbf{x}; \mathbf{z}). \end{aligned}$$

□

**Proposition L.1.** Suppose the critic function  $T_\phi(\mathbf{x}, \mathbf{z})$  is parameterized by  $\phi$ , and that  $\exists \phi_0$  s.t.  $T_{\phi_0}(\mathbf{x}, \mathbf{z}) = \text{const}$ . For a given  $q_\theta(\mathbf{z}|\mathbf{x})$ , let  $T_{\phi^*}(\mathbf{x}, \mathbf{z})$  denote the critic function that maximizes  $\text{IBAL}(q_\theta, T_\phi)$ . Then,

$$I_{\text{BAL}}(q_\theta) \leq \text{IBAL}(q_\theta, T_{\phi^*}) \leq I(\mathbf{x}; \mathbf{z}) = I_{\text{BAL}}(q_\theta) + \mathbb{E}_{p(\mathbf{x})} [D_{\text{KL}}[p(\mathbf{z}|\mathbf{x}) \| q_\theta(\mathbf{z}|\mathbf{x})]]. \quad (198)$$

In particular, the contrastive term in Eq. (27) is upper bounded by  $\mathbb{E}_{p(\mathbf{x})} [D_{\text{KL}}[p(\mathbf{z}|\mathbf{x}) \| q_\theta(\mathbf{z}|\mathbf{x})]]$ .

*Proof.* The BA bound is a special case of the  $\text{IBAL}(q_\theta, T_\phi)$  with constant  $T_{\phi_0} = c$  and the contrastive term equal to 0. Since  $\phi_0$  is a possible parameterization, we can only improve upon  $I_{\text{BAL}}(q_\theta)$  by learning  $T_\phi$ . The parameterized family of  $T_\phi$  may not be expressive enough to match the true log importance weights, so  $\text{IBAL}(q_\theta, T_{\phi^*}) \leq \text{IBAL}(q_\theta, T^*) = I(\mathbf{x}; \mathbf{z})$  using Prop. 4.1.  $\square$

## L.2 PROOF OF IBAL AS LIMITING BEHAVIOR OF THE GIWAE OBJECTIVE AS $K \rightarrow \infty$ (PROP. L.2)

**Proposition L.2** (IBAL as Limiting Behavior of GIWAE). For given  $q_\theta(\mathbf{z}|\mathbf{x})$  and  $T_\phi(\mathbf{x}, \mathbf{z})$ , we have

$$\lim_{K \rightarrow \infty} I_{\text{GIWAE}_L}(q_\theta, T_\phi, K) = \text{IBAL}(q_\theta, T_\phi). \quad (199)$$

*Proof.* Comparing the form of  $I_{\text{GIWAE}_L}(q_\theta, T_\phi, K)$  to the  $\text{IBAL}(q_\theta, T_\phi)$  for a fixed  $q_\theta$  and  $T_\phi$ ,

$$I_{\text{GIWAE}}(q_\theta, T_\phi, K) = \mathbb{E}_{p(\mathbf{x}, \mathbf{z})} \left[ \log \frac{q(\mathbf{z}|\mathbf{x})}{p(\mathbf{z})} \right] + \mathbb{E}_{p(\mathbf{x}, \mathbf{z}^{(1)}) \prod_{k=2}^K q_\theta(\mathbf{z}^{(k)}|\mathbf{x})} \left[ \log \frac{e^{T_\phi(\mathbf{x}, \mathbf{z}^{(1)})}}{\frac{1}{K} \sum_{i=1}^K e^{T_\phi(\mathbf{x}, \mathbf{z}^{(i)})}} \right]$$

$$\text{IBAL}(q_\theta, T_\phi) = \mathbb{E}_{p(\mathbf{x}, \mathbf{z})} \left[ \log \frac{q_\theta(\mathbf{z}|\mathbf{x})}{p(\mathbf{z})} \right] + \mathbb{E}_{p(\mathbf{x}, \mathbf{z})} \left[ \log \frac{e^{T_\phi(\mathbf{x}, \mathbf{z})}}{\mathbb{E}_{q_\theta(\mathbf{z}|\mathbf{x})} [e^{T_\phi(\mathbf{x}, \mathbf{z})}]} \right].$$

we can see that both bounds include the same first term  $I_{\text{BAL}}(q_\theta)$  and the same numerator of the contrastive term. To prove the proposition, we can thus focus on characterizing the limiting behavior of the denominator

$$\forall \mathbf{x}: \lim_{K \rightarrow \infty} \mathbb{E}_{p(\mathbf{z}^{(1)}|\mathbf{x}) \prod_{k=2}^K q_\theta(\mathbf{z}^{(k)}|\mathbf{x})} \left[ \log \frac{1}{K} \sum_{k=1}^K e^{T_\phi(\mathbf{x}, \mathbf{z})} \right] = \underbrace{\log \mathbb{E}_{q_\theta(\mathbf{z}|\mathbf{x})} [e^{T_\phi(\mathbf{x}, \mathbf{z})}]}_{= \log \mathcal{Z}_{\theta, \phi}(\mathbf{x})}, \quad (200)$$

where we introduce the notation  $\log \mathcal{Z}_{\text{GIWAE}}(\mathbf{x}, K)$  for convenience and the right hand side is the log partition function for the IBAL energy-based posterior  $\pi_{\theta, \phi}(\mathbf{z}|\mathbf{x})$ . Intuitively, we expect Eq. (200) to hold since the contribution of the single posterior sample  $p(\mathbf{z}|\mathbf{x})$  in the GIWAE expectation will vanish as  $K \rightarrow \infty$ .

More formally, we consider the sequence of values  $\log \mathcal{Z}_{\text{GIWAE}}(\mathbf{x}, K)$  as a function of  $K$ . We derive lower and upper bounds on the value of  $\log \mathcal{Z}_{\text{GIWAE}}(\mathbf{x}, K)$  for fixed  $K$  and show that each of these sequences of lower and upper bounds converge to  $\log \mathcal{Z}_{\theta, \phi}(\mathbf{x})$  in the limit as  $K \rightarrow \infty$ . Using the squeeze theorem for sequences, this is sufficient to demonstrate the claim that  $\lim_{K \rightarrow \infty} \log \mathcal{Z}_{\text{GIWAE}}(\mathbf{x}, K) = \log \mathcal{Z}_{\theta, \phi}(\mathbf{x})$  in Eq. (200). Since the other terms in  $I_{\text{GIWAE}_L}(q_\theta, T_\phi, K)$  and  $\text{IBAL}(q_\theta, T_\phi)$  are identical, this is sufficient to prove the proposition.

*Lower Bound on  $\log \mathcal{Z}_{\text{GIWAE}}(\mathbf{x}, K)$ :* We rely on the fact that the exponential function  $e^{T_\phi(\mathbf{x}, \mathbf{z})} \geq 0$  to simply ignore the contribution of the  $p(\mathbf{z}|\mathbf{x})$  term.

$$\log \mathcal{Z}_{\text{GIWAE}}(\mathbf{x}, K) = \mathbb{E}_{p(\mathbf{z}^{(1)}|\mathbf{x}) \prod_{k=2}^K q_\theta(\mathbf{z}^{(k)}|\mathbf{x})} \left[ \log \sum_{k=1}^K e^{T_\phi(\mathbf{x}, \mathbf{z}^{(k)})} \right] - \log K \quad (201)$$

$$\stackrel{(1)}{\geq} \mathbb{E}_{\prod_{k=2}^K q_\theta(\mathbf{z}^{(k)}|\mathbf{x})} \left[ \log \sum_{k=2}^K e^{T_\phi(\mathbf{x}, \mathbf{z}^{(k)})} \right] - \log K \quad (202)$$

$$= \mathbb{E}_{\prod_{k=2}^K q_\theta(\mathbf{z}^{(k)}|\mathbf{x})} \left[ \log \frac{1}{K-1} \sum_{k=2}^K e^{T_\phi(\mathbf{x}, \mathbf{z}^{(k)})} \right] + \log \frac{K-1}{K} \quad (203)$$

$$=: \text{LB}(\mathbf{x}; K), \quad (204)$$



where in (1), we obtain a lower bound by ignoring the contribution of the positive sample from  $p(\mathbf{z}|\mathbf{x})$ . The first term is the  $k$ -sample IWAE lower bound with the proposal  $q_\theta(\mathbf{z})$  and target  $\pi_{\theta,\phi}(\mathbf{x}, \mathbf{z})$ :  $\mathbb{E}_{q_\theta(\mathbf{z}^{1:K})}[\log \frac{1}{K} \sum_k \frac{\pi_{\theta,\phi}(\mathbf{x}, \mathbf{z}^{(k)})}{q_\theta(\mathbf{z}^{(k)}|\mathbf{x})}]$ , and thus converges to  $\log \mathcal{Z}_{\theta,\phi}$  as  $K \rightarrow \infty$ . As  $K \rightarrow \infty$ , we also have  $\log \frac{K-1}{K} \rightarrow 0$ , so that the limit of their sum is

$$\lim_{K \rightarrow \infty} \text{LB}(\mathbf{x}; K) = \log \mathbb{E}_{q_\theta(\mathbf{z}|\mathbf{x})} \left[ e^{T_\phi(\mathbf{x}, \mathbf{z})} \right] = \log \mathcal{Z}_{\theta,\phi}(\mathbf{x}). \quad (205)$$

*Upper Bound on  $\log \mathcal{Z}_{\text{GIWAE}}(\mathbf{x}, K)$ :* To upper bound  $\log \mathcal{Z}_{\text{GIWAE}}(\mathbf{x}, K)$ , we separately consider terms arising from  $p(\mathbf{z}|\mathbf{x})$  samples and  $q_\theta(\mathbf{z}|\mathbf{x})$  samples. Noting that  $p_{\text{TGT}}^{\text{GIWAE}}(\mathbf{z}^{(1:K)}, s|\mathbf{x})$  in Eq. (39) is invariant to the index  $s$ , we can assume  $\mathbf{z}^{(1)} \sim p(\mathbf{z}|\mathbf{x})$  and write

$$\begin{aligned} \log \mathcal{Z}_{\text{GIWAE}}(\mathbf{x}, K) &= \mathbb{E}_{p(\mathbf{z}^{(1)}|\mathbf{x}) \prod_{k=2}^K q_\theta(\mathbf{z}^{(k)}|\mathbf{x})} \left[ \log \left( \frac{1}{K} e^{T_\phi(\mathbf{x}, \mathbf{z}^{(1)})} + \frac{1}{K} \sum_{k=2}^K e^{T_\phi(\mathbf{x}, \mathbf{z}^{(k)})} \right) \right] \\ &= \mathbb{E}_{p(\mathbf{z}^{(1)}|\mathbf{x}) \prod_{k=2}^K q_\theta(\mathbf{z}^{(k)}|\mathbf{x})} \left[ \log \left( \frac{1}{K} e^{T_\phi(\mathbf{x}, \mathbf{z}^{(1)})} + \frac{K-1}{K} \cdot \frac{1}{K-1} \sum_{k=2}^K e^{T_\phi(\mathbf{x}, \mathbf{z}^{(k)})} \right) \right] \\ &\leq \log \left( \frac{1}{K} \mathbb{E}_{p(\mathbf{z}^{(1)}|\mathbf{x})} \left[ e^{T_\phi(\mathbf{x}, \mathbf{z}^{(1)})} \right] + \mathbb{E}_{\prod_{k=2}^K q_\theta(\mathbf{z}^{(k)}|\mathbf{x})} \left[ \frac{K-1}{K} \cdot \frac{1}{K-1} \sum_{k=2}^K e^{T_\phi(\mathbf{x}, \mathbf{z}^{(k)})} \right] \right) \\ &= \log \left( \frac{1}{K} \mathbb{E}_{p(\mathbf{z}^{(1)}|\mathbf{x})} \left[ e^{T_\phi(\mathbf{x}, \mathbf{z}^{(1)})} \right] + \frac{K-1}{K} \cdot \frac{1}{K-1} \sum_{k=2}^K \mathbb{E}_{q_\theta(\mathbf{z}^{(k)}|\mathbf{x})} \left[ e^{T_\phi(\mathbf{x}, \mathbf{z}^{(k)})} \right] \right) \\ &= \log \left( \frac{1}{K} \mathbb{E}_{p(\mathbf{z}^{(1)}|\mathbf{x})} \left[ e^{T_\phi(\mathbf{x}, \mathbf{z}^{(1)})} \right] + \frac{K-1}{K} \mathcal{Z}_{\theta,\phi}(\mathbf{x}) \right) \end{aligned} \quad (206)$$

$$=: \text{UB}(\mathbf{x}; K). \quad (207)$$

Since  $\log(u)$  is a continuous function, we know that  $\lim_{K \rightarrow \infty} \log(f(K)) = \log \lim_{K \rightarrow \infty} f(K)$ . We thus reason about the limiting behavior of the terms inside the logarithm in Eq. (206). As  $K \rightarrow \infty$ , we have  $\frac{1}{K} \rightarrow 0$ , and thus the first term inside the log goes to 0. For the second term, we also have  $\frac{K-1}{K} \rightarrow 1$ . Thus, we have

$$\lim_{K \rightarrow \infty} \text{UB}(\mathbf{x}; K) = \log \mathbb{E}_{q_\theta(\mathbf{z}|\mathbf{x})} \left[ e^{T_\phi(\mathbf{x}, \mathbf{z})} \right] = \log \mathcal{Z}_{\theta,\phi}(\mathbf{x}). \quad (208)$$

As reasoned above, the convergence of the sequence of both upper and lower bounds to  $\log \mathcal{Z}_{\theta,\phi}(\mathbf{x})$  implies that  $\lim_{K \rightarrow \infty} \log \mathcal{Z}_{\text{GIWAE}}(\mathbf{x}, K) = \log \mathcal{Z}_{\theta,\phi}(\mathbf{x})$ . By the reasoning surrounding Eq. (200), this implies  $\lim_{K \rightarrow \infty} I_{\text{GIWAE}_L}(q_\theta, T_\phi) = \text{IBAL}(q_\theta, T_\phi)$  as desired.  $\square$

### L.3 CONVERGENCE OF GIWAE SNIS DISTRIBUTION TO IBAL ENERGY-BASED POSTERIOR

In this section, we consider the marginal SNIS distribution of GIWAE, which is induced by sampling  $K$  times from  $q_\theta(\mathbf{z}|\mathbf{x})$  and returning the sample in index  $s$  with probability  $q_{\text{PROP}}^{\text{GIWAE}}(s|\mathbf{x}, \mathbf{z}^{(1:K)}) \propto e^{T_\phi(\mathbf{x}, \mathbf{z}^{(s)})}$ . As  $K \rightarrow \infty$ , we show that this distribution converges to the single-sample energy-based posterior approximation underlying the IBAL and MINE-AIS. A similar observation is made in Sec. 3.2 of Lawson et al. (2019). This result regarding the probabilistic interpretations of GIWAE and the IBAL is complementary to the result in Prop. L.2 regarding the limiting behavior of the bounds.

**Proposition L.3.** *Define the marginal SNIS distribution of GIWAE,  $q_{\text{PROP}}^{\text{GIWAE}}(\mathbf{z}|\mathbf{x}; K)$ , using the following sampling procedure*

1. Sample from  $s, \mathbf{z}^{(1:K)} \sim q_{\text{PROP}}^{\text{GIWAE}}(s, \mathbf{z}^{(1:K)}|\mathbf{x})$  according to Eq. (52)
2. Return  $\mathbf{z} = \mathbf{z}^{(s)}$ .

*Then, as  $K \rightarrow \infty$ , the KL divergence (in either direction) between the marginal SNIS distribution of GIWAE and the energy-based variational distribution of IBAL,  $\pi_{\theta,\phi}(\mathbf{z}|\mathbf{x}) \propto q_\theta(\mathbf{z}|\mathbf{x})e^{T_\phi(\mathbf{x}, \mathbf{z})}$ , goes to*

zero.

$$\lim_{K \rightarrow \infty} D_{\text{KL}}[q_{\text{PROP}}^{\text{GIWAE}}(\mathbf{z}|\mathbf{x}; K) \|\pi_{\theta, \phi}(\mathbf{z}|\mathbf{x})] = 0$$

and  $\lim_{K \rightarrow \infty} D_{\text{KL}}[\pi_{\theta, \phi}(\mathbf{z}|\mathbf{x}) \| q_{\text{PROP}}^{\text{GIWAE}}(\mathbf{z}|\mathbf{x}; K)] = 0.$

*Proof.* To prove the proposition, we consider a mixture target distribution similar to the case of IWAE. However, in this case, we take a single sample from  $\pi_{\theta, \phi}(\mathbf{z}|\mathbf{x})$  instead of  $p(\mathbf{z}|\mathbf{x})$

$$p_{\text{TGT}}^{\text{GIWAE}, \pi}(s, \mathbf{z}^{(1:K)}, \mathbf{x}) = \frac{1}{K} \pi_{\theta, \phi}(\mathbf{z}^{(s)}|\mathbf{x}) \prod_{\substack{k=1 \\ k \neq s}}^K q_{\theta}(\mathbf{z}^{(s)}|\mathbf{x}). \quad (209)$$

Note that the probabilistic interpretations  $q_{\text{PROP}}^{\text{GIWAE}}(s, \mathbf{z}^{(1:K)}|\mathbf{x})$  and  $p_{\text{TGT}}^{\text{GIWAE}, \pi}(s, \mathbf{z}^{(1:K)}, \mathbf{x})$  exactly match the IWAE proposal and target distributions in [App. B.1](#) where, in the target distribution, the posterior  $p(\mathbf{z}|\mathbf{x})$  has been replaced by  $\pi_{\theta, \phi}(\mathbf{z}|\mathbf{x})$ . Thus, we can analyze the KL divergences  $D_{\text{KL}}[q_{\text{PROP}}^{\text{GIWAE}}(s, \mathbf{z}^{(1:K)}|\mathbf{x}) \| p_{\text{TGT}}^{\text{GIWAE}, \pi}(s, \mathbf{z}^{(1:K)}|\mathbf{x})]$  and  $D_{\text{KL}}[p_{\text{TGT}}^{\text{GIWAE}, \pi}(s, \mathbf{z}^{(1:K)}|\mathbf{x}) \| q_{\text{PROP}}^{\text{GIWAE}}(s, \mathbf{z}^{(1:K)}|\mathbf{x})]$  using techniques from previous work on IWAE. Following similar arguments as in [Domke & Sheldon \(2018\)](#) (Thm 2) and [Cremer et al. \(2017\)](#), these extended state space KL divergences upper bound the KL divergence between the marginal SNIS distribution and energy-based target, e.g.  $D_{\text{KL}}[q_{\text{PROP}}^{\text{GIWAE}}(\mathbf{z}|\mathbf{x}; K) \|\pi_{\theta, \phi}(\mathbf{z}|\mathbf{x})] \leq D_{\text{KL}}[q_{\text{PROP}}^{\text{GIWAE}}(s, \mathbf{z}^{(1:K)}|\mathbf{x}) \| p_{\text{TGT}}^{\text{GIWAE}, \pi}(s, \mathbf{z}^{(1:K)}|\mathbf{x})]$ . As  $K \rightarrow \infty$ ,  $D_{\text{KL}}[q_{\text{PROP}}^{\text{GIWAE}}(s, \mathbf{z}^{(1:K)}|\mathbf{x}) \| p_{\text{TGT}}^{\text{GIWAE}, \pi}(s, \mathbf{z}^{(1:K)}|\mathbf{x})] \rightarrow 0$  since it is an instance of the IWAE gap. Thus, the KL divergence  $D_{\text{KL}}[q_{\text{PROP}}^{\text{GIWAE}}(\mathbf{z}|\mathbf{x}; K) \|\pi_{\theta, \phi}(\mathbf{z}|\mathbf{x})]$  also vanishes. Similar reasoning applies for the reverse KL divergence.  $\square$

## M MINE-AIS

### M.1 MULTI-SAMPLE AIS EVALUATION OF THE IBAL

After training the variational base distribution  $q_{\theta}(\mathbf{z}|\mathbf{x})$  and the critic function  $T_{\phi}(\mathbf{x}, \mathbf{z})$  using the MINE-AIS training procedure above, we still need to evaluate the IBAL lower bound on MI,  $\text{IBAL}(q_{\theta}, T_{\phi})$ . We can easily upper bound  $\text{IBAL}(q_{\theta}, T_{\phi})$  using a Multi-Sample AIS lower bound on  $\log \mathcal{Z}_{\theta, \phi}(\mathbf{x})$  with expectations under the forward sampling procedure  $q_{\text{PROP}}^{\text{AIS}}(\mathbf{z}_{0:T}|\mathbf{x})$ . However, an upper bound on  $\text{IBAL}(q_{\theta}, T_{\phi})$  is not guaranteed to preserve a lower bound on MI.

In order to obtain a lower bound on the IBAL, we would need to obtain an upper bound on  $\log \mathcal{Z}_{\theta, \phi}(\mathbf{x}) = \log \mathbb{E}_{q_{\theta}(\mathbf{z}|\mathbf{x})} [e^{T_{\phi}(\mathbf{x}, \mathbf{z})}]$ , the log partition function of  $\pi_{\theta, \phi}(\mathbf{z}|\mathbf{x})$ . However, considering this to be the target distribution  $\pi_T(\mathbf{z}|\mathbf{x})$  in Multi-Sample AIS, we would require exact samples from  $\pi_{\theta, \phi}(\mathbf{z}|\mathbf{x})$  to guarantee an upper bound on  $\log \mathcal{Z}_{\theta, \phi}(\mathbf{x})$ . Since these samples are unavailable, we demonstrate conditions under which we can preserve an upper bound on  $\log \mathcal{Z}_{\theta, \phi}(\mathbf{x})$  (and lower bound on  $\text{IBAL}(q_{\theta}, T_{\phi})$ ) by sampling from  $p(\mathbf{z}|\mathbf{x})$  instead of  $\pi_{\theta, \phi}(\mathbf{z}|\mathbf{x})$  to initialize our backward annealing chains in [Prop. M.1](#) below.

Using the single sample AIS bounds to estimate  $\log \mathcal{Z}_{\theta, \phi}(\mathbf{x})$ , we have the following extended state space proposal and target distributions,

$$p_{\text{TGT}}^{\text{AIS}, \pi}(\mathbf{z}_{0:T}|\mathbf{x}) := \pi_{\theta, \phi}(\mathbf{z}_T|\mathbf{x}) \prod_{t=1}^T \tilde{\mathcal{T}}_t(\mathbf{z}_{t-1}|\mathbf{z}_t), \quad q_{\text{PROP}}^{\text{AIS}, \pi}(\mathbf{z}_{0:T}|\mathbf{x}) := q_{\theta}(\mathbf{z}_0|\mathbf{x}) \prod_{t=1}^T \mathcal{T}_t(\mathbf{z}_t|\mathbf{z}_{t-1}). \quad (210)$$

We emphasize that in  $p_{\text{TGT}}^{\text{AIS}, \pi}$ ,  $q_{\text{PROP}}^{\text{AIS}, \pi}$ , the transition kernels and intermediate densities are based on the critic  $T_{\phi}(\mathbf{x}, \mathbf{z})$  and energy-based posterior  $\pi_{\theta, \phi}(\mathbf{z}|\mathbf{x})$  whose log partition function we seek to estimate. Recall from [Sec. 2.1](#) that taking the expected log importance weights under  $p_{\text{TGT}}^{\text{AIS}, \pi}(\mathbf{z}_{0:T}|\mathbf{x})$  yields an upper bound on  $\log \mathcal{Z}_{\theta, \phi}(\mathbf{x})$ . However, since it is difficult to draw exact samples from  $\pi_{\theta, \phi}(\mathbf{z}|\mathbf{x})$  to initialize backward annealing chains and sample from  $p_{\text{TGT}}^{\text{AIS}, \pi}(\mathbf{z}_{0:T}|\mathbf{x})$ , we instead consider sampling from the posterior  $p(\mathbf{z}|\mathbf{x})$ . Using the same transition kernels  $\tilde{\mathcal{T}}_t$  as above, we first define the conditional distribution  $p_{\text{TGT}}^{\text{AIS}, \pi}(\mathbf{z}_{0:T-1}|\mathbf{x}, \mathbf{z}_T)$  of the backward chain for a given  $\mathbf{z}_T$

$$p_{\text{TGT}}^{\text{AIS}, \pi}(\mathbf{z}_{0:T-1}|\mathbf{x}, \mathbf{z}_T) := \prod_{t=1}^T \tilde{\mathcal{T}}_t(\mathbf{z}_{t-1}|\mathbf{z}_t). \quad (211)$$

Using this notation, the target distribution in Eq. (210) can also be rewritten as  $p_{\text{TGT}}^{\text{AIS},\pi}(\mathbf{z}_{0:T}|\mathbf{x}) = \pi_{\theta,\phi}(\mathbf{z}_T|\mathbf{x})p_{\text{TGT}}^{\text{AIS},\pi}(\mathbf{z}_{0:T-1}|\mathbf{x}, \mathbf{z}_T)$ .

We now define an *approximate* extended state space target distribution in which backward chains are initialized with samples from  $\mathbf{z}_T \sim p(\mathbf{z}|\mathbf{x})$ ,

$$p_{\text{TGT}}^{\text{APPROX}}(\mathbf{z}_{0:T}|\mathbf{x}) := p(\mathbf{z}_T|\mathbf{x}) \prod_{t=1}^T \tilde{\mathcal{T}}_t(\mathbf{z}_{t-1}|\mathbf{z}_t) = p(\mathbf{z}_T|\mathbf{x})p_{\text{TGT}}^{\text{AIS},\pi}(\mathbf{z}_{0:T-1}|\mathbf{x}, \mathbf{z}_T). \quad (212)$$

In the following proposition, we characterize the conditions under which sampling from  $p_{\text{TGT}}^{\text{APPROX}}(\mathbf{z}_{0:T}|\mathbf{x})$  preserves an upper bound on  $\log \mathcal{Z}_{\theta,\phi}(\mathbf{x})$ .

**Proposition M.1.** *Define the AIS marginal distribution  $q_{\text{PROP}}^{\text{AIS},\pi}(\mathbf{z}_T|\mathbf{x})$  over the final state in the extended state space proposal as  $q_{\text{PROP}}^{\text{AIS},\pi}(\mathbf{z}_T|\mathbf{x}) := \int q_{\text{PROP}}^{\text{AIS},\pi}(\mathbf{z}_{0:T}|\mathbf{x})d\mathbf{z}_{0:T-1}$ . If we have*

$$D_{\text{KL}}[p(\mathbf{z}_T|\mathbf{x})\|q_{\text{PROP}}^{\text{AIS},\pi}(\mathbf{z}_T|\mathbf{x})] \geq D_{\text{KL}}[p(\mathbf{z}_T|\mathbf{x})\|\pi_{\theta,\phi}(\mathbf{z}_T|\mathbf{x})], \quad (213)$$

*then initializing the backward AIS chain using  $\mathbf{z}_T \sim p(\mathbf{z}|\mathbf{x})$  (i.e., sampling under  $p_{\text{TGT}}^{\text{APPROX}}(\mathbf{z}_{0:T}|\mathbf{x})$ ), yields an upper bound on  $\log \mathcal{Z}_{\theta,\phi}(\mathbf{x})$ ,*

$$\mathbb{E}_{p_{\text{TGT}}^{\text{APPROX}}(\mathbf{z}_{0:T}|\mathbf{x})} \left[ \log \frac{p_{\text{TGT}}^{\text{AIS},\pi}(\mathbf{x}, \mathbf{z}_{0:T})}{q_{\text{PROP}}^{\text{AIS},\pi}(\mathbf{z}_{0:T}|\mathbf{x})} \right] \geq \log \mathcal{Z}_{\theta,\phi}(\mathbf{x}). \quad (214)$$

*Proof.* We begin by writing several definitions, which will allow us to factorize the extended state space proposal  $q_{\text{PROP}}^{\text{AIS},\pi}(\mathbf{z}_{0:T}|\mathbf{x})$  in the time-reversed direction. This factorization will include the final AIS marginal  $q_{\text{PROP}}^{\text{AIS},\pi}(\mathbf{z}_T|\mathbf{x})$ .

Starting from Eq. (210), the forward transitions  $q_{\text{PROP}}^{\text{AIS},\pi}(\mathbf{z}_{0:T}|\mathbf{x}) = q_{\theta}(\mathbf{z}_0|\mathbf{x}) \prod_{t=1}^T \mathcal{T}_t(\mathbf{z}_t|\mathbf{z}_{t-1})$  induce the marginal distributions  $q_{\text{PROP}}^{\text{AIS},\pi}(\mathbf{z}_t|\mathbf{x})$  at each step. The forward transitions and marginals induce a *posterior* kernel  $\tilde{\mathcal{T}}_t^q(\mathbf{z}_{t-1}|\mathbf{z}_t)$ , which allows us to rewrite  $q_{\text{PROP}}^{\text{AIS},\pi}(\mathbf{z}_{0:T}|\mathbf{x})$  using a reverse factorization

$$q_{\text{PROP}}^{\text{AIS},\pi}(\mathbf{z}_{0:T}|\mathbf{x}) = q_{\text{PROP}}^{\text{AIS},\pi}(\mathbf{z}_T|\mathbf{x}) \prod_{t=1}^T \tilde{\mathcal{T}}_t^q(\mathbf{z}_{t-1}|\mathbf{z}_t), \quad (215)$$

$$\text{where } \tilde{\mathcal{T}}_t^q(\mathbf{z}_{t-1}|\mathbf{z}_t) = \frac{q_{\text{PROP}}^{\text{AIS},\pi}(\mathbf{z}_{t-1}|\mathbf{x})\mathcal{T}_t(\mathbf{z}_t|\mathbf{z}_{t-1})}{q_{\text{PROP}}^{\text{AIS},\pi}(\mathbf{z}_t|\mathbf{x})}. \quad (216)$$

The posterior reverse transitions  $\tilde{\mathcal{T}}_t^q(\mathbf{z}_{t-1}|\mathbf{z}_t)$  are intractable in practice, and cannot be simplified to match the kernels in the target distribution  $p_{\text{TGT}}^{\text{AIS},\pi}(\mathbf{z}_{0:T-1}|\mathbf{x}, \mathbf{z}_T) = \prod_{t=1}^T \tilde{\mathcal{T}}_t(\mathbf{z}_{t-1}|\mathbf{z}_t)$  using the invariance or detailed balance conditions. Doucet et al. (2022) provide a promising approach using score matching to approximate these posterior transitions  $\tilde{\mathcal{T}}_t^q(\mathbf{z}_{t-1}|\mathbf{z}_t)$ .

Finally, we write the posterior reverse process conditioned on a particular  $\mathbf{z}_T$  as

$$q_{\text{PROP}}^{\text{AIS},\pi}(\mathbf{z}_{0:T-1}|\mathbf{x}, \mathbf{z}_T) := \prod_{t=1}^T \tilde{\mathcal{T}}_t^q(\mathbf{z}_{t-1}|\mathbf{z}_t). \quad (217)$$

With the goal of upper bounding  $\log \mathcal{Z}_{\theta,\phi}(\mathbf{x}) = \int q_{\theta}(\mathbf{z}|\mathbf{x})e^{T\phi(\mathbf{x},\mathbf{z})}d\mathbf{z}$ , we consider the log importance weights with expectations under the target distribution  $p_{\text{TGT}}^{\text{APPROX}}(\mathbf{z}_{0:T}|\mathbf{x}) = p(\mathbf{z}_T|\mathbf{x})p_{\text{TGT}}^{\text{AIS},\pi}(\mathbf{z}_{0:T-1}|\mathbf{x}, \mathbf{z}_T)$ , as in Eq. (214).

Using the above notation, we have

$$\mathbb{E}_{p_{\text{TGT}}^{\text{APPROX}}(\mathbf{z}_{0:T}|\mathbf{x})} \left[ \log \frac{p_{\text{TGT}}^{\text{AIS},\pi}(\mathbf{x}, \mathbf{z}_{0:T})}{q_{\text{PROP}}^{\text{AIS},\pi}(\mathbf{z}_{0:T}|\mathbf{x})} \right] = \log \mathcal{Z}_{\theta,\phi}(\mathbf{x}) + \mathbb{E}_{p_{\text{TGT}}^{\text{APPROX}}(\mathbf{z}_{0:T}|\mathbf{x})} \left[ \log \frac{p_{\text{TGT}}^{\text{AIS},\pi}(\mathbf{z}_{0:T}|\mathbf{x})}{q_{\text{PROP}}^{\text{AIS},\pi}(\mathbf{z}_{0:T}|\mathbf{x})} \right] \quad (218)$$

$$= \log \mathcal{Z}_{\theta,\phi}(\mathbf{x}) + \mathbb{E}_{p_{\text{TGT}}^{\text{APPROX}}(\mathbf{z}_{0:T}|\mathbf{x})} \left[ \log \frac{\pi_{\theta,\phi}(\mathbf{z}_T|\mathbf{x}) p_{\text{TGT}}^{\text{AIS},\pi}(\mathbf{z}_{0:T-1}|\mathbf{x}, \mathbf{z}_T) p(\mathbf{z}_T|\mathbf{x})}{q_{\text{PROP}}^{\text{AIS},\pi}(\mathbf{z}_T|\mathbf{x}) q_{\text{PROP}}^{\text{AIS},\pi}(\mathbf{z}_{0:T-1}|\mathbf{x}, \mathbf{z}_T) p(\mathbf{z}_T|\mathbf{x})} \right] \quad (219)$$

$$= \log \mathcal{Z}_{\theta,\phi}(\mathbf{x}) + D_{\text{KL}}[p(\mathbf{z}_T|\mathbf{x}) \| q_{\text{PROP}}^{\text{AIS},\pi}(\mathbf{z}_T|\mathbf{x})] - D_{\text{KL}}[p(\mathbf{z}_T|\mathbf{x}) \| \pi_{\theta,\phi}(\mathbf{z}_T|\mathbf{x})] \quad (220)$$

$$+ \mathbb{E}_{p(\mathbf{z}_T|\mathbf{x})} [D_{\text{KL}}[p_{\text{TGT}}^{\text{AIS},\pi}(\mathbf{z}_{0:T-1}|\mathbf{x}, \mathbf{z}_T) \| q_{\text{PROP}}^{\text{AIS},\pi}(\mathbf{z}_{0:T-1}|\mathbf{x}, \mathbf{z}_T)]]$$

The intractable KL divergence  $D_{\text{KL}}[p_{\text{TGT}}^{\text{AIS},\pi}(\mathbf{z}_{0:T-1}|\mathbf{x}, \mathbf{z}_T) \| q_{\text{PROP}}^{\text{AIS},\pi}(\mathbf{z}_{0:T-1}|\mathbf{x}, \mathbf{z}_T)]$  compares the reverse kernels in the target distribution  $\tilde{\mathcal{T}}_t(\mathbf{z}_{t-1}|\mathbf{z}_t)$  against the posterior  $\tilde{\mathcal{T}}_t^q(\mathbf{z}_{t-1}|\mathbf{z}_t)$ . Ignoring this nonnegative term, we can lower bound the expectation on the LHS

$$\mathbb{E}_{p_{\text{TGT}}^{\text{APPROX}}} \left[ \log \frac{p_{\text{TGT}}^{\text{AIS},\pi}(\mathbf{x}, \mathbf{z}_{0:T})}{q_{\text{PROP}}^{\text{AIS},\pi}(\mathbf{z}_{0:T}|\mathbf{x})} \right] \geq \log \mathcal{Z}_{\theta,\phi}(\mathbf{x}) + D_{\text{KL}}[p(\mathbf{z}_T|\mathbf{x}) \| q_{\text{PROP}}^{\text{AIS},\pi}(\mathbf{z}_T|\mathbf{x})] - D_{\text{KL}}[p(\mathbf{z}_T|\mathbf{x}) \| \pi_{\theta,\phi}(\mathbf{z}_T|\mathbf{x})].$$

Finally, under the assumption of the proposition that  $D_{\text{KL}}[p(\mathbf{z}_T|\mathbf{x}) \| q_{\text{PROP}}^{\text{AIS},\pi}(\mathbf{z}_T|\mathbf{x})] \geq D_{\text{KL}}[p(\mathbf{z}_T|\mathbf{x}) \| \pi_{\theta,\phi}(\mathbf{z}_T|\mathbf{x})]$ , we have the desired result.  $\square$

**KL Divergence Condition** In [Prop. M.1](#), we have shown that we can preserve an upper bound on  $\log \mathcal{Z}_{\theta,\phi}(\mathbf{x})$  by initializing the reverse chain using a posterior sample, under a condition on the KL divergence,

$$D_{\text{KL}}[p(\mathbf{z}_T|\mathbf{x}) \| q_{\text{PROP}}^{\text{AIS},\pi}(\mathbf{z}_T|\mathbf{x})] \geq D_{\text{KL}}[p(\mathbf{z}_T|\mathbf{x}) \| \pi_{\theta,\phi}(\mathbf{z}_T|\mathbf{x})]. \quad (221)$$

While we cannot guarantee this condition, we intuitively expect [Eq. \(221\)](#) to hold in practice since  $\pi_{\theta,\phi}(\mathbf{z}|\mathbf{x})$  has been directly trained to match  $p(\mathbf{z}|\mathbf{x})$ . By contrast,  $q_{\text{PROP}}^{\text{AIS},\pi}(\mathbf{z}_T|\mathbf{x})$  is the final state of an AIS procedure, which approximates  $\pi_{\theta,\phi}(\mathbf{z}|\mathbf{x})$  and does not have access to information about  $p(\mathbf{z}|\mathbf{x})$ . [Burda et al. \(2015\)](#) use a similar approach for lower bounding the log likelihood in EBMs, but give an example of a Restricted Boltzmann Machines (RBM) model (in their [Sec. 5](#)) in which [Eq. \(221\)](#) does not hold.

As desired, we find in our experiments in [Fig. 4](#) that our approximate reverse annealing procedure underestimates the IBAL in all of the MINE-AIS, GIWAE and INFONCE experiments, for all numbers of intermediate distributions  $T$ .

**T = 1 Special Case** For  $T = 1$ , we have  $q_{\text{PROP}}^{\text{AIS},\pi}(\mathbf{z}_1|\mathbf{x}) = q_{\theta}(\mathbf{z}_1|\mathbf{x})$ . In particular, [Prop. M.1](#) will provide an upper bound on  $\log \mathcal{Z}_{\theta,\phi}(\mathbf{x})$  if

$$D_{\text{KL}}[p(\mathbf{z}|\mathbf{x}) \| q_{\theta}(\mathbf{z}|\mathbf{x})] \geq D_{\text{KL}}[p(\mathbf{z}|\mathbf{x}) \| \pi_{\theta,\phi}(\mathbf{z}|\mathbf{x})]. \quad (222)$$

This condition is guaranteed under the assumptions of [Prop. L.1](#), where  $\text{IBAL}(q_{\theta}, T_{\phi^*}) = I_{\text{BAL}}(\pi_{\theta,\phi^*})$  improves upon  $I_{\text{BAL}}(q_{\theta})$  for an energy function  $T_{\phi^*}(\mathbf{x}, \mathbf{z})$  which has been trained to maximize the IBAL. In [Eq. \(222\)](#) the KL divergence on the left-hand side corresponds to the gap in the BA lower bound, which is larger than the gap in the IBAL on the right-hand side. We can further show that the lower bound on  $\text{IBAL}(q_{\theta}, T_{\phi})$  resulting from [Prop. M.1](#) with  $T = 1$  is the BA lower bound,

$$\begin{aligned} \text{IBAL}(q_{\theta}, T_{\phi}) &= \mathbb{E}_{p(\mathbf{x}, \mathbf{z})} \left[ \log \frac{q_{\theta}(\mathbf{z}|\mathbf{x})}{p(\mathbf{z})} \right] + \mathbb{E}_{p(\mathbf{x}, \mathbf{z})} [T_{\phi}(\mathbf{x}, \mathbf{z})] - \mathbb{E}_{p(\mathbf{x})} [\log \mathcal{Z}_{\theta,\phi}(\mathbf{x})] \\ &\geq \mathbb{E}_{p(\mathbf{x}, \mathbf{z})} \left[ \log \frac{q_{\theta}(\mathbf{z}|\mathbf{x})}{p(\mathbf{z})} \right] + \mathbb{E}_{p(\mathbf{x}, \mathbf{z})} [T_{\phi}(\mathbf{x}, \mathbf{z})] - \mathbb{E}_{p_{\text{TGT}}^{\text{APPROX}}} \left[ \log \frac{p_{\text{TGT}}^{\text{AIS},\pi}(\mathbf{x}, \mathbf{z}_{0:T})}{q_{\text{PROP}}^{\text{AIS},\pi}(\mathbf{z}_{0:T}|\mathbf{x})} \right] \\ &= \mathbb{E}_{p(\mathbf{x}, \mathbf{z})} \left[ \log \frac{q_{\theta}(\mathbf{z}|\mathbf{x})}{p(\mathbf{z})} \right] + \mathbb{E}_{p(\mathbf{x}, \mathbf{z})} [T_{\phi}(\mathbf{x}, \mathbf{z})] - \mathbb{E}_{p(\mathbf{x}, \mathbf{z})} \left[ \log \frac{q_{\theta}(\mathbf{z}|\mathbf{x}) e^{T_{\phi}(\mathbf{x}, \mathbf{z})}}{q_{\theta}(\mathbf{z}|\mathbf{x})} \right] \\ &= \mathbb{E}_{p(\mathbf{x}, \mathbf{z})} \left[ \log \frac{q_{\theta}(\mathbf{z}|\mathbf{x})}{p(\mathbf{z})} \right] + \mathbb{E}_{p(\mathbf{x}, \mathbf{z})} [T_{\phi}(\mathbf{x}, \mathbf{z})] - \mathbb{E}_{p(\mathbf{x}, \mathbf{z})} [T_{\phi}(\mathbf{x}, \mathbf{z})] \\ &= I_{\text{BAL}}(q_{\theta}). \end{aligned}$$

We can confirm this in Fig. 4, where for  $T = 1$ , the approximate lower bounds on  $\text{IBAL}(q_\theta, T_\phi)$  begin from the appropriate BA lower bound. For example, in the case of IBAL evaluation for GIWAE ( $K = 100$ ), the light green curve starts from the BA lower bound term reported in the decomposition of the GIWAE ( $K = 100$ ) lower bound in Fig. 5a. Using more intermediate distributions ( $T > 1$ ) for the AIS approximate bound in Prop. M.1, the estimates in Fig. 4 approach the true value of  $\text{IBAL}(q_\theta, T_\phi)$  in all cases.

## N APPLICATIONS TO MUTUAL INFORMATION ESTIMATION WITHOUT KNOWN MARGINALS

While the focus in of our work is evaluating the mutual information  $I(\mathbf{x}; \mathbf{z})$  in settings where at least a single marginal is available, we are often interested in estimating or optimizing the mutual information where no marginal distribution is available. A natural setting where no marginal distribution is available is representation learning where the goal is to maximize the mutual information between the data distribution  $q_{\text{data}}(\mathbf{x})$  and the representation induced by a stochastic mapping  $q_\psi(\mathbf{z}|\mathbf{x})$  parameterized by  $\psi$ ,

$$I(\mathbf{x}; \mathbf{z}) = \mathbb{E}_{q_{\text{data}}(\mathbf{x})q_\psi(\mathbf{z}|\mathbf{x})} \left[ \log \frac{q_\psi(\mathbf{x}, \mathbf{z})}{q_{\text{data}}(\mathbf{x})q_\psi(\mathbf{z})} \right] = \mathbb{E}_{q_{\text{data}}(\mathbf{x})q_\psi(\mathbf{z}|\mathbf{x})} \left[ \log \frac{q_\psi(\mathbf{x}|\mathbf{z})}{q_{\text{data}}(\mathbf{x})} \right] \quad (223)$$

where  $q_\psi(\mathbf{z}) = \int q_{\text{data}}(\mathbf{x})q_\psi(\mathbf{z}|\mathbf{x})d\mathbf{x}$  represents the ‘‘aggregated posterior’’ (Makhzani et al., 2015) or induced marginal distribution over  $\mathbf{z}$ .

### N.1 BA LOWER BOUND

Using the notation of Eq. (223), we can write the BA lower bound as

$$I(\mathbf{x}; \mathbf{z}) \geq I(\mathbf{x}; \mathbf{z}) - \underbrace{\mathbb{E}_{q_\psi(\mathbf{z})} \left[ D_{\text{KL}}[q_\psi(\mathbf{x}|\mathbf{z})||p_\theta(\mathbf{x}|\mathbf{z})] \right]}_{\text{gap}} \quad (224)$$

$$= \mathbb{E}_{q_{\text{data}}(\mathbf{x})} \mathbb{E}_{q_\psi(\mathbf{z}|\mathbf{x})} \left[ \log \frac{p_\theta(\mathbf{x}|\mathbf{z})}{q_{\text{data}}(\mathbf{x})} \right] \quad (225)$$

$$= \mathbb{E}_{q_{\text{data}}(\mathbf{x})} \underbrace{\mathbb{E}_{q_\psi(\mathbf{z}|\mathbf{x})} \left[ \log p_\theta(\mathbf{x}|\mathbf{z}) \right]}_{\text{negative reconstruction loss of } \mathbf{x}} + \underbrace{H_{\text{data}}(\mathbf{x})}_{\text{constant}} \quad (226)$$

$$=: I_{\text{BAL}}(p_\theta(\mathbf{x}|\mathbf{z}))$$

where  $p_\theta(\mathbf{x}|\mathbf{z})$  is a variational distribution, parameterized by  $\theta$ , that tries to match to the *inverse encoding distribution*  $q_\psi(\mathbf{x}|\mathbf{z}) \propto q_{\text{data}}(\mathbf{x})q_\psi(\mathbf{z}|\mathbf{x})$ . The first term in Eq. (225) can be interpreted as the reconstruction term, and the second term is the entropy of the data distribution, which is constant.

**Evaluating MI up to a Constant** Note that the gradient of  $I_{\text{BAL}}(p_\theta(\mathbf{x}|\mathbf{z}))$  with respect to the parameters  $\theta$  does not depend on the marginal  $q_{\text{data}}(\mathbf{x})$ , and thus we may still optimize the variational distribution when the data distribution is unknown. We can then use the resulting  $p_\theta(\mathbf{x}|\mathbf{z})$  to estimate the BA lower bound on mutual information *up to a constant*,  $H_{\text{data}}(\mathbf{x})$ . This is useful in comparing the MI induced by two different representations  $q_{\psi_1}(\mathbf{z}|\mathbf{x})$  and  $q_{\psi_2}(\mathbf{z}|\mathbf{x})$  of the same data distribution.

**Optimizing MI with the BA Lower Bound** The BA lower bound is also amenable to backpropagation through the parameters of the encoding distribution  $q_\psi(\mathbf{z}|\mathbf{x})$ , even when analytic marginal densities for  $q_{\text{data}}(\mathbf{x})$  or  $q_\psi(\mathbf{z})$  are not available.

Maximization of the BA lower bound appears in various settings, including in representation learning (Alemi et al., 2017, 2018), reinforcement learning (Mohamed & Rezende, 2015), improving interpretability in GANs (Chen et al., 2016), and variational information bottleneck methods (Tishby et al., 2000; Alemi et al., 2017, 2018).

## N.2 GIWAE LOWER BOUND

In this section, we discuss the applicability of our GIWAE lower bound in mutual information maximization settings. Rewriting the GIWAE lower bound in Eq. (11) for the case of estimating  $I(\mathbf{x}; \mathbf{z})$  in Eq. (223), we have

$$\begin{aligned}
 I(\mathbf{x}; \mathbf{z}) &\geq \underbrace{\mathbb{E}_{q_{\text{data}}(\mathbf{x})q_{\psi}(\mathbf{z}|\mathbf{x})} [\log p_{\theta}(\mathbf{x}|\mathbf{z})]}_{\text{negative reconstruction loss of } \mathbf{x}} + \underbrace{H_{\text{data}}(\mathbf{x})}_{\text{constant}} + \underbrace{\mathbb{E}_{q_{\psi}(\mathbf{x}, \mathbf{z}) \prod_{k=2}^K p_{\theta}(\mathbf{x}^{(k)}|\mathbf{z})} \left[ \log \frac{e^{T_{\phi}(\mathbf{x}, \mathbf{z})}}{\frac{1}{K}(e^{T_{\phi}(\mathbf{x}, \mathbf{z})} + \sum_{k=2}^K e^{T_{\phi}(\mathbf{x}^{(k)}, \mathbf{z})})} \right]}_{\text{contrastive term } \leq \log K} \\
 &=: I_{\text{GIWAE}_L}(p_{\theta}(\mathbf{x}|\mathbf{z}), T_{\phi}, K)
 \end{aligned} \tag{227}$$

Note that we can use a single joint sample from  $q_{\text{data}}(\mathbf{x})q_{\psi}(\mathbf{z}|\mathbf{x}) = q_{\psi}(\mathbf{z})q_{\psi}(\mathbf{x}|\mathbf{z})$  to obtain a positive sample from the inverse encoding distribution  $\mathbf{x} \sim q_{\psi}(\mathbf{x}|\mathbf{z})$  for a particular  $\mathbf{z} \sim q_{\psi}(\mathbf{z})$ , in a similar fashion to our ancestral sampling in Sec. 1.1. For a given  $\mathbf{z}$ , the negative samples correspond to  $K - 1$  samples from the stochastic decoder  $\mathbf{x}^{(2:K)} \sim p_{\theta}(\mathbf{x}|\mathbf{z})$ .

From the importance sampling perspective, we can view the GIWAE lower bound as corresponding to an upper bound on the ‘‘log partition function’’  $\log q_{\psi}(\mathbf{z})$  for a particular  $\mathbf{z} \sim q_{\psi}(\mathbf{z})$ . The contrastive term in Eq. (227) arises from SNIS sampling of a single  $\mathbf{x}^{(s)}$  in the extended state space proposal, with  $q_{\text{PROP}}^{\text{GIWAE}}(s|\mathbf{z}, \mathbf{x}^{(1:K)}) = e^{T_{\phi}(\mathbf{x}^{(s)}, \mathbf{z})} / \sum_{k=1}^K e^{T_{\phi}(\mathbf{x}^{(k)}, \mathbf{z})}$ .

Finally, we note that optimization over the energy function  $T_{\phi}(\mathbf{x}, \mathbf{z})$  improves upon  $I_{\text{BAL}}(p_{\theta}(\mathbf{x}|\mathbf{z}))$  in Eq. (225) by at most  $\log K$  nats using the contrastive term.

**Evaluating MI up to a Constant** Similar to the BA bound, the GIWAE lower bound can be used to evaluate the mutual information up to the constant data entropy when  $q_{\text{data}}(\mathbf{x})$  is unknown. This may be useful in comparing the MI induced by two different representations  $q_{\psi_1}(\mathbf{z}|\mathbf{x})$  and  $q_{\psi_2}(\mathbf{z}|\mathbf{x})$  of the same data distribution. Note that the reconstruction and contrastive terms in Eq. (227) depend on samples from  $q_{\text{data}}(\mathbf{x})$  and not the density. Thus, our ability to take gradients with respect to the parameters of the variational distribution  $p_{\theta}(\mathbf{x}|\mathbf{z})$  or energy function  $T_{\phi}(\mathbf{x}, \mathbf{z})$  are not affected by the fact that the marginal distribution is unknown.

**Optimizing MI with the GIWAE Lower Bound** The GIWAE lower bound may also be used for mutual information maximization with respect to the parameters of  $q_{\psi}(\mathbf{z}|\mathbf{x})$ , since each term in Eq. (227) is amenable to backpropagation. Since GIWAE generalizes both the BA and INFO-NCE lower bounds, it can be used as a drop-in replacement for either of these bounds for optimizing MI (e.g., see van den Oord et al. (2018)).

## N.3 MINE-AIS / IBAL LOWER BOUND

Recall that MINE-AIS estimation would involve an energy based variational approximation to the inverse encoding distribution  $q_{\psi}(\mathbf{x}|\mathbf{z})$ ,

$$\pi_{\theta, \phi}(\mathbf{x}|\mathbf{z}) = \frac{1}{\mathcal{Z}(\mathbf{z})} p_{\theta}(\mathbf{x}|\mathbf{z}) e^{T_{\phi}(\mathbf{x}, \mathbf{z})}. \tag{228}$$

Note that IBAL lower bound on  $I(\mathbf{x}; \mathbf{z})$  involves an intractable log partition function term  $\mathbb{E}_{q_{\psi}(\mathbf{z})} [\log \mathcal{Z}(\mathbf{z})] = \mathbb{E}_{q_{\psi}(\mathbf{z})} [\log \mathbb{E}_{p_{\theta}(\mathbf{x}|\mathbf{z})} [e^{T_{\phi}(\mathbf{x}, \mathbf{z})}]]$ .

$$\begin{aligned}
 I(\mathbf{x}; \mathbf{z}) &\geq \underbrace{\mathbb{E}_{q_{\text{data}}(\mathbf{x})} \mathbb{E}_{q_{\psi}(\mathbf{z}|\mathbf{x})} [\log p_{\theta}(\mathbf{x}|\mathbf{z})]}_{\text{negative reconstruction loss of } \mathbf{x}} + \underbrace{H_{\text{data}}(\mathbf{x})}_{\text{constant}} + \underbrace{\mathbb{E}_{q_{\psi}(\mathbf{x}, \mathbf{z})} \left[ \log \frac{e^{T_{\phi}(\mathbf{x}, \mathbf{z})}}{\mathbb{E}_{p_{\theta}(\mathbf{x}|\mathbf{z})} [e^{T_{\phi}(\mathbf{x}, \mathbf{z})}]} \right]}_{\text{contrastive term } \leq \mathbb{E}_{q_{\psi}(\mathbf{z})} [D_{\text{KL}}[q_{\psi}(\mathbf{x}|\mathbf{z}) \| p_{\theta}(\mathbf{x}|\mathbf{z})]]} \\
 &=: \text{IBAL}(p_{\theta}(\mathbf{x}|\mathbf{z}), T_{\phi})
 \end{aligned} \tag{229}$$

where the term in the denominator is the partition function  $\mathcal{Z}(\mathbf{z}) = \mathbb{E}_{p_{\theta}(\mathbf{x}|\mathbf{z})} [e^{T_{\phi}(\mathbf{x}, \mathbf{z})}]$ .

When taking gradients as in Eq. (31)-(32), we obtain

$$\frac{\partial}{\partial \theta} \text{IBAL}(p_\theta, T_\phi) = \mathbb{E}_{q_{\text{data}}(\mathbf{x})q_\psi(\mathbf{z}|\mathbf{x})} \left[ \frac{\partial}{\partial \theta} \log p_\theta(\mathbf{x}|\mathbf{z}) \right] - \mathbb{E}_{q_\psi(\mathbf{z})\pi_{\theta,\phi}(\mathbf{x}|\mathbf{z})} \left[ \frac{\partial}{\partial \theta} \log p_\theta(\mathbf{x}|\mathbf{z}) \right], \quad (230)$$

$$\frac{\partial}{\partial \phi} \text{IBAL}(p_\theta, T_\phi) = \mathbb{E}_{q_{\text{data}}(\mathbf{x})q_\psi(\mathbf{z}|\mathbf{x})} \left[ \frac{\partial}{\partial \phi} T_\phi(\mathbf{x}, \mathbf{z}) \right] - \mathbb{E}_{q_\psi(\mathbf{z})\pi_{\theta,\phi}(\mathbf{x}|\mathbf{z})} \left[ \frac{\partial}{\partial \phi} T_\phi(\mathbf{x}, \mathbf{z}) \right]. \quad (231)$$

To obtain approximate negative samples from  $\pi_{\theta,\phi}(\mathbf{x}|\mathbf{z})$  for a given  $\mathbf{z}$ , we can use MCMC transition kernels since the unnormalized target density  $\tilde{\pi}_{\theta,\phi}(\mathbf{x}|\mathbf{z}) = p_\theta(\mathbf{x}|\mathbf{z})e^{T_\phi(\mathbf{x},\mathbf{z})}$  is tractable.

**Evaluating MI up to a Constant** Since only samples from  $q_{\text{data}}(\mathbf{x})$  are required for the MINE-AIS training procedure in Eq. (230)-(231), we can learn the base variational distribution  $p_\theta(\mathbf{x}|\mathbf{z})$  and energy function  $T_\phi(\mathbf{x}, \mathbf{z})$  in cases when the marginal distribution  $q_{\text{data}}(\mathbf{x})$  is unknown.

As in the case of GIWAE and BA lower bounds above, we can also evaluate the IBAL lower bound in Eq. (229) up to a constant. As in the main text, this involves using multi-sample AIS techniques to bound the intractable log partition function term  $\log \mathcal{Z}(\mathbf{z}) = \log \mathbb{E}_{p_\theta(\mathbf{x}|\mathbf{z})} [e^{T_\phi(\mathbf{x},\mathbf{z})}]$ .

**Optimizing MI with the MINE-AIS Lower Bound** If we are interested in optimizing the MINE-AIS lower bound with respect to the parameters of a stochastic encoder  $q_\psi(\mathbf{z}|\mathbf{x})$ , we would need to backpropagate through the Multi-Sample AIS procedure used to estimate the  $\log \mathcal{Z}(\mathbf{z})$  term, but computing the gradients are intractable. We thus conclude that, among our proposed methods, GIWAE is the most directly applicable in settings of MI for representation learning.

## O EXPERIMENTAL DETAILS

### O.1 EXPERIMENT DETAILS OF SEC. 5.2

In this section, we provide the experiment details used in Sec. 5.2. For more details, see the public Github repository, [https://github.com/huangcong/ais\\_mi\\_estimation](https://github.com/huangcong/ais_mi_estimation).

#### O.1.1 DATASETS AND MODELS

We used MNIST (LeCun et al., 1998) and CIFAR-10 (Krizhevsky, 2009) datasets in our experiments.

**Real-Valued MNIST** For the VAE experiments on the real-valued MNIST dataset (Table 1), the encoder’s architecture is 784 – 1024 – 1024 – 1024 –  $z$ , where  $z$  is the latent code size shown in the row header of Table 1. The decoder architecture is the reverse of the encoder architecture. The decoder variance is learned scalar.

For the GAN experiments on MNIST (Table 1), we used the same decoder architecture as our VAEs. In order to stabilize the training dynamics, we used the gradient penalty (GP) (Salimans et al., 2016).

The network was trained for 300 epochs with the learning rate of 0.0001 using the Adam optimizer (Kingma & Ba, 2014), and the checkpoint with the best validation loss was used for the evaluation.

**CIFAR-10** For the CIFAR-10 experiments (Table 1), we experimented with a smaller version of DCGAN (Radford et al., 2015) (see the public code). The number at the end of each model name in Table 1 indicates the latent code size.

#### O.1.2 EXPERIMENT DETAILS OF SEC. 5.2

For the AIS temperature schedule, We used sigmoid schedules as used in Wu et al. (2017). The step size of HMC was adaptively tuned to achieve an average acceptance probability of 65% as suggested in Neal (2001). For all MNIST experiments in Table 1, we evaluated on a single batch size of 128 simulated data. For all CIFAR experiments in Table 1 we used a single batch of 32 simulated data. All experiments are run on on Tesla P100 or Quadro RTX 6000 or Tesla T4 GPUs.



## O.2 RUNTIME COMPARISON

We benchmarked the runtime on Tesla P100 GPUs. For MNIST, it took about 35 minutes to run IWAE with  $K = 1M$ , about 8 hours to run AIS with  $T = 30K$ . For CIFAR, it took about 45 minutes to run IWAE with  $K = 1M$ , and about 12 hours for the AIS with  $T = 100K$ .

In Fig. 9, we evaluate the tradeoff between runtime and bound tightness for evaluating the generative MI for VAE and GAN models with 100-dimensional latent codes trained on the MNIST dataset. We compare IWAE and multi-sample AIS evaluation, with the same experimental settings as in App. O.1.2 and an initial distribution  $q_\theta(\mathbf{z}|\mathbf{x})$ . We plot wall clock time on the  $x$ -axis, where increasing runtime reflects increasing  $K$  for IWAE and increasing  $T$  for AIS.

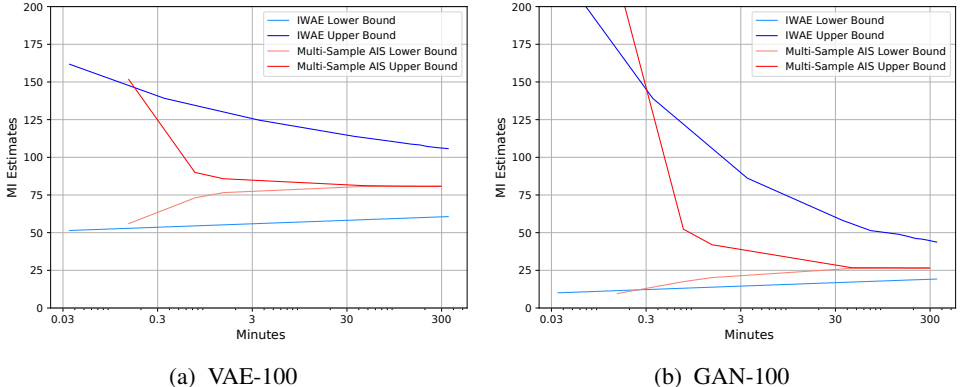


Figure 9: Runtime vs. Bound Tightness for VAE (left) and GAN (right) models on MNIST.

## O.3 EXPERIMENT DETAILS FOR ENERGY-BASED BOUNDS (SEC. 5.3)

**Models and Data** The linear VAE model has a Gaussian prior  $\mathbf{z} \sim \mathcal{N}(0, I)$  with the dimension of 10. The dimension of the output  $\mathbf{x}$  is 100. The weights are sampled randomly from a Gaussian distribution with the standard deviation of 1, and the standard deviation of the Gaussian observation noise at the output is 1. The MNIST-VAE20, is a VAE model that is trained on the real-valued MNIST dataset. It has a Gaussian prior  $\mathbf{z} \sim \mathcal{N}(0, I)$  with the dimension of 20. The decoder has one layer of ReLU non-linearity of size 1000, followed by a linear layer that predicts the mean of a Gaussian observation model with the fixed standard deviation of 0.1. MNIST-GAN20 decoder uses one layer of ReLU non-linearity of size 1000 followed by a sigmoid layer that predicts the mean of a Gaussian observation model with the fixed standard deviation of 0.1. In all the experiments, we use a fixed batch of 100 data points.

**BA, IWAE and GIWAE** For the BA bound,  $q_\theta(\mathbf{z}|\mathbf{x})$  is parameterized using a neural network that predicts the mean and log-std of a diagonal Gaussian distribution. The neural network has two layers of ReLU non-linearity of size 2000. The IWAE experiments used the same architecture for  $q_\theta(\mathbf{z}|\mathbf{x})$ . The GIWAE experiments, in addition to  $q_\theta(\mathbf{z}|\mathbf{x})$  with the same architecture, used a critic function  $T_\phi(\mathbf{x}, \mathbf{z})$  that is parameterized by a neural network that concatenates  $(\mathbf{x}, \mathbf{z})$  and pass them through two layers of ReLU non-linearity of size 2000, followed by a linear layer that outputs a scalar value. The parameters of  $q_\theta(\mathbf{z}|\mathbf{x})$  and  $T_\phi(\mathbf{x}, \mathbf{z})$  are trained jointly.

**Multi-Sample AIS** For the Multi-Sample AIS bounds, for all models, we used up to  $K = 1000$  chains (see Fig. 7), and up to  $T = 50K$  intermediate distributions with linear schedule (see Fig. 7 and Fig. 4). We used HMC as the AIS kernel, with  $\epsilon = 0.02$  and  $L = 20$  leap frog steps.

**MINE-AIS** For the training of the MINE-AIS, we used a critic function  $T_\phi(\mathbf{x}, \mathbf{z})$  that is parameterized by a neural network that concatenates  $(\mathbf{x}, \mathbf{z})$  and pass them through three layers of ReLU non-linearity of size 2000, followed by a linear layer that outputs a scalar value. We chose the Gaussian prior  $\mathcal{N}(0, I)$  as the base distribution  $q_\theta(\mathbf{z}|\mathbf{x})$ . In order to take a sample from  $\pi_{\theta, \phi}(\mathbf{z}|\mathbf{x})$ , we used the HMC method that is initialized with a true posterior  $p(\mathbf{z}|\mathbf{x})$  sample, with  $M = 10$  iterations each with  $L = 20$  leapfrog steps. For the step size of HMC, we used  $\epsilon = 0.05$  for the linear VAE model

and  $\epsilon = 0.02$  for the MNIST-VAE20 and MNIST-GAN20. For the evaluation of MINE-AIS, we used Multi-Sample AIS with the same parameters as the AIS evaluation experiments described above.

#### O.4 ANALYTICAL SOLUTION OF THE MUTUAL INFORMATION ON THE LINEAR MNIST-VAE

In order to verify our implementations, we have derived the MI analytically for the linear VAEs and verified that it matches the MI estimated by AIS. For simplicity, we assume a fixed identity covariance matrix  $\mathbf{I}$  at the output of the conditional likelihood of the linear VAE decoder, i.e., the decoder of the VAE is simply:  $\mathbf{x} = \mathbf{W}\mathbf{z} + \mathbf{b} + \epsilon$ , where  $\mathbf{x}$  is the observation,  $\mathbf{z}$  is the latent code vector  $\mathbf{z} \sim \mathcal{N}(\mathbf{0}, \mathbf{I})$ ,  $\mathbf{W}$  is the decoder weight matrix and  $\mathbf{b}$  is the bias. The observation noise of the decoder is  $\epsilon \sim \mathcal{N}(\mathbf{0}, \mathbf{I})$ . It is easily shown that the conditional likelihood is  $p(\mathbf{x}|\mathbf{z}) = \mathcal{N}(\mathbf{x}|\mathbf{W}\mathbf{z} + \mathbf{b}, \mathbf{I})$  and thus we can solve for the marginal

$$p(\mathbf{x}) = \mathcal{N}(\mathbf{x}|\boldsymbol{\mu}_{\mathbf{x}} = \mathbf{b}, \boldsymbol{\Sigma}_{\mathbf{x}} = \mathbf{I} + \mathbf{W}\mathbf{W}^{\top}). \quad (232)$$

The differential entropy of  $\mathbf{x}$  is:

$$H(\mathbf{x}) = \frac{k}{2} + \frac{k}{2} \log(2\pi) + \frac{1}{2} \log(\det \boldsymbol{\Sigma}_{\mathbf{x}}), \quad (233)$$

where  $k$  is the dimension of the observation. The conditional entropy is

$$H(\mathbf{x}|\mathbf{z}) = \frac{k}{2} + \frac{k}{2} \log(2\pi) + \frac{1}{2} \log(\det \mathbf{I}) \quad (234)$$

$$= \frac{k}{2} + \frac{k}{2} \log(2\pi). \quad (235)$$

Thus, the mutual information is

$$I(\mathbf{x}; \mathbf{z}) = H(\mathbf{x}) - H(\mathbf{x}|\mathbf{z}) \quad (236)$$

$$= \frac{1}{2} \log(\det \boldsymbol{\Sigma}_{\mathbf{x}}). \quad (237)$$

#### O.5 CONFIDENCE INTERVALS FOR MULTI-SAMPLE AIS EXPERIMENTS

Table 4 and Table 5 provides the 95% confidence intervals for the AIS results reported in Table 1. The confidence intervals were computed over confidence interval over 8 batches each with 16 data points for MNIST; and over 8 batches 4 data points for CIFAR.

Method	Proposal		VAE2	VAE10	VAE100	GAN2	GAN10	GAN100
AIS T=1	$p(\mathbf{z})$	UB	(213.54, 286.11)	(1849.03, 2010.66)	(5564.53, 6096.51)	(665.25, 787.30)	(745.68, 826.55)	(795.81, 926.94)
		LB	(0.00, 0.00)	(0.00, 0.00)	(0.00, 0.00)	(0.00, 0.00)	(0.00, 0.00)	(0.00, 0.00)
	$q(\mathbf{z} \mathbf{x})$	UB	(8.77, 9.72)	(59.34, 66.66)	(345.45, 378.80)	(5.32, 32.95)	(293.60, 335.83)	(482.40, 544.26)
		LB	(7.47, 7.71)	(60.09, 66.61)	(32.46, 36.52)	(7.01, 7.41)	(3.41, 3.94)	(2.40, 2.83)
AIS T=500	$p(\mathbf{z})$	UB	(8.78, 9.45)	(38.61, 39.57)	(92.32, 98.03)	(10.52, 11.13)	(21.91, 23.04)	(26.89, 28.22)
		LB	(8.31, 8.95)	(33.69, 34.41)	(77.77, 82.02)	(8.89, 9.53)	(21.18, 21.96)	(25.36, 26.36)
	$q(\mathbf{z} \mathbf{x})$	UB	(8.77, 9.41)	(33.94, 34.63)	(79.96, 84.71)	(10.51, 11.07)	(22.53, 23.58)	(28.82, 30.24)
		LB	(8.78, 9.40)	(33.80, 34.53)	(78.01, 82.37)	(10.40, 10.98)	(21.19, 22.00)	(25.09, 26.06)
AIS T=30K	$p(\mathbf{z})$	UB	(8.74, 9.39)	(33.82, 34.60)	(78.62, 83.07)	(10.51, 11.11)	(21.54, 22.50)	(25.97, 27.07)
		LB	(8.65, 9.28)	(33.86, 34.56)	(78.51, 83.05)	(10.23, 10.88)	(21.50, 22.45)	(25.96, 26.98)
	$q(\mathbf{z} \mathbf{x})$	UB	(8.77, 9.40)	(33.85, 34.58)	(78.56, 83.03)	(10.52, 11.10)	(21.54, 22.47)	(26.01, 27.07)
		LB	(8.77, 9.41)	(33.86, 34.56)	(78.52, 83.02)	(10.51, 11.09)	(21.55, 22.48)	(26.02, 27.03)
IWAE K=1	$p(\mathbf{z})$	UB	(735.94, 863.16)	(3628.86, 4026.29)	(10705.98, 12297.86)	(1543.54, 1732.65)	(1556.00, 1704.00)	(1680.50, 1800.28)
		LB	(0.00, 0.00)	(0.00, 0.00)	(0.00, 0.00)	(0.00, 0.00)	(0.00, 0.00)	(0.00, 0.00)
	$q(\mathbf{z} \mathbf{x})$	UB	(8.83, 9.56)	(34.82, 35.86)	(92.82, 98.44)	(5.71, 29.45)	(38.80, 76.14)	(243.34, 278.41)
		LB	(8.47, 8.79)	(24.54, 25.86)	(41.53, 47.54)	(8.57, 9.10)	(3.85, 4.61)	(2.94, 3.52)
IWAE K=1K	$p(\mathbf{z})$	UB	(24.32, 34.49)	(1132.54, 1262.97)	(3987.51, 4480.86)	(101.75, 142.03)	(430.40, 463.19)	(462.95, 526.51)
		LB	(6.74, 6.87)	(6.91, 6.91)	(6.91, 6.91)	(6.84, 6.93)	(6.91, 6.91)	(6.91, 6.91)
	$q(\mathbf{z} \mathbf{x})$	UB	(8.78, 9.41)	(33.87, 34.61)	(83.15, 87.46)	(10.06, 12.74)	(34.11, 71.36)	(182.82, 219.55)
		LB	(8.79, 9.39)	(31.08, 32.30)	(48.44, 54.45)	(10.46, 11.02)	(10.75, 11.52)	(9.84, 10.43)
IWAE K=1M	$p(\mathbf{z})$	UB	(8.76, 9.43)	(352.91, 400.87)	(2078.30, 2417.17)	(10.62, 11.36)	(71.93, 91.09)	(100.27, 127.75)
		LB	(8.77, 9.41)	(13.82, 13.82)	(13.82, 13.82)	(10.50, 11.03)	(13.79, 13.82)	(13.82, 13.82)
	$q(\mathbf{z} \mathbf{x})$	UB	(8.77, 9.40)	(33.87, 34.57)	(81.42, 85.36)	(10.53, 11.10)	(28.51, 33.26)	(52.41, 63.68)
		LB	(8.78, 9.41)	(33.67, 34.53)	(55.35, 61.36)	(10.53, 11.10)	(17.31, 18.21)	(16.63, 17.32)

Table 4: Confidence intervals of AIS and IWAE estimates of MI on MNIST. UB stands for Upper Bound, and LB stands for Lower Bound.

Model	Proposal		GAN5	GAN10	GAN100
AIS (T=1)	$p(\mathbf{z})$	UB	(2875853.34, 4326658.66)	(3593559.12, 4477712.38)	(4038603.09, 5668217.91)
		LB	(0.00, 0.00)	(0.00, 0.00)	(0.00, 0.00)
	$q(\mathbf{z} \mathbf{x})$	UB	(30896.74, 54151.34)	(241342.62, 566015.82)	(1874938.58, 2881576.42)
		LB	(13.24, 14.64)	(15.70, 18.89)	(18.41, 21.93)
AIS (T=500)	$p(\mathbf{z})$	UB	(205.11, 313.44)	(24683.10, 41496.70)	(25453.02, 101127.79)
		LB	(17.44, 19.30)	(28.41, 30.63)	(98.37, 110.65)
	$q(\mathbf{z} \mathbf{x})$	UB	(59.40, 79.68)	(116.02, 156.28)	(1603.13, 3969.92)
		LB	(31.63, 33.30)	(45.45, 50.88)	(134.35, 156.02)
AIS (T=100K)	$p(\mathbf{z})$	UB	(40.55, 41.57)	(72.17, 75.80)	(479.04, 497.10)
		LB	(39.01, 40.15)	(70.19, 73.55)	(470.05, 490.47)
	$q(\mathbf{z} \mathbf{x})$	UB	(39.55, 40.56)	(71.87, 75.22)	(475.07, 494.61)
		LB	(38.64, 39.80)	(71.35, 74.75)	(468.64, 489.89)
IWAE (K=1)	$p(\mathbf{z})$	UB	(6115557.66, 8075210.34)	(6019901.15, 9511489.86)	(7339411.95, 12492792.05)
		LB	(0.00, 0.00)	(0.00, 0.00)	(0.00, 0.00)
	$q(\mathbf{z} \mathbf{x})$	UB	(39.68, 40.95)	(75.00, 80.03)	(-1810.70, 12504.41)
		LB	(14.15, 14.90)	(16.28, 18.62)	(18.39, 21.60)
IWAE (K=1K)	$p(\mathbf{z})$	UB	(921258.02, 1209846.48)	(1673333.03, 2415008.47)	(2181660.84, 3531768.16)
		LB	(6.91, 6.91)	(6.91, 6.91)	(6.91, 6.91)
	$q(\mathbf{z} \mathbf{x})$	UB	(39.40, 40.06)	(72.31, 75.68)	(-1872.12, 12438.39)
		LB	(21.05, 21.81)	(22.18, 24.99)	(25.32, 28.64)
IWAE (K=1M)	$p(\mathbf{z})$	UB	(76776.88, 116619.32)	(582880.62, 838142.63)	(1479829.44, 2327879.56)
		LB	(13.82, 13.82)	(13.82, 13.82)	(13.82, 13.82)
	$q(\mathbf{z} \mathbf{x})$	UB	(39.26, 40.17)	(71.63, 75.08)	(-1883.22, 12426.34)
		LB	(27.96, 28.72)	(29.86, 31.60)	(32.21, 35.42)

Table 5: Confidence intervals of AIS and IWAE estimates of MI on CIFAR. UB stands for Upper Bound, and LB stands for Lower Bound.